HUNTING THE HUNTERS

WILDLIFE MONITORING SYSTEM

EYUEL DEBEBE AYELE

Propositions

accompanying the thesis

Hunting the Hunters
Wildlife Monitoring System

by

Eyuel D. Ayele

1. Wildlife monitoring solutions are useless unless the demand for wildlife products is ultimately eradicated (Chapter 2 and 3).
2. Herd mobility aware communication networks significantly improve the energy consumption efficiency (Chapter 4 to 7).
3. Utilizing short-range opportunistic networks provide a fine-grained movement information for monitoring wildlife (Chapter 8).
4. The effect of the poaching crisis is not addressed sufficiently, because of the stunning and often misleading wildlife images.
5. The difference between poaching and hunting is one of permission.
6. The recipe to ignoring peer pressure is feeling confident in what you do.
7. The researcher has to do the research first. If he/she doesn't know about something, then has to ask the right people who do.
8. Doing research is like making sure to enter the correct destination address into a navigation system.
9. Curiosity did not kill the cat; worrying about the research did.

These propositions are regarded as opposable and defendable, and have been approved as such by the prof. dr. ir. P. J. M. Havinga (Paul).

HUNTING THE HUNTERS

Wildlife Monitoring System

Eyuel Debebe Ayele

HUNTING THE HUNTERS

Wildlife Monitoring System

DISSERTATION

to obtain
the degree of doctor at the Universiteit Twente,
on the authority of the rector magnificus,
Prof.dr. T.T.M. Palstra,
on account of the decision of the Doctorate Board
to be publicly defended
on Wednesday 29 April 2020 at 14.45 uur

by

Eyuel Debebe Ayele
born on May 18, 1985
in Jigjiga, Ethiopia

This dissertation has been approved by:

supervisor
Prof. dr. P.J.M. Havinga

Cover design: Ipskamp Printing Enschede
Printed by: Ipskamp Printing Enschede
Lay-out:
ISBN: 978-90-365-5003-1
DOI: 10.3990/1.9789036550031

Graduation Committee:

Chairman / secretary	prof.dr. J.N. Kok
supervisor:	prof.dr.ir. P.J.M. Havinga
:	
Committee Members	prof.dr. J.L. van den Berg prof.dr. A.D. Nelson prof. dr. ir. M.J. Bentum prof. dr. E. Ethiopia Nigussie

Dedicated to my wife
Barsenet T. Wube

"So many of our dreams first seem impossible, then they seem improbable, and then, when we summon the will, they soon become inevitable."

— Christopher Reeve.

Abstract

DURING the last decades, there has been a dramatic rise in number of illegal animal poaching incidents. Wildlife Monitoring Systems (WMSs) are emerging as a solution to help reduce poaching incidents by monitoring the activities of wild animals. The technological advances in low-power wireless networks have paved the way to exploit their potential for utilizing in wireless based WMS. One of the fundamental difficulties for utilizing existing wireless based WMS is the lack of full network connectivity provision due to the sparsely con-specific mobility behaviour of wild animals. Unlike static network applications, where the proximity among sensor nodes is fixed, wild animals often show signs of movement which alters the spatial proximity between neighbouring sensor nodes.

To address this challenge, this thesis deals with leveraging short-rage radio and low-power wide area networks to provide a communication network architecture that is energy-efficient, reliable, and has a low latency. We present a single-hop, multi-hop, and opportunistic multi-hop hybrid tree network architecture for WMS.

Moreover, in wildlife monitoring applications, WMS often has to deal with frequent herd mobility. We address this issue by applying a herd-movement adaptive scheme. The particular focus of this technique is to have a strategy to adapt to the movement pattern of animals to make the communication network more efficient. We developed a mobility state driven data advertising control scheme based on an unsupervised learning algorithm. In addition, we implement a managed data dissemination scheme with controlling and prioritizing data replication function. In contrast to existing forwarding algorithms, it optimally makes data forwarding decisions by utilizing locally accessible information. Hence, the proposed algorithm adapts to dynamic network topology caused by the inherent sporadic connectivity among mobile herd of animals.

Finally, the application of WMS communication network is demonstrated for inferring movement of an animal from the received signal information. This is introduced by using short-range radio for proximity and relative ranging as an alternative approach for the current use of GPS to examine the mobility interaction between wild animals. The developed animal movement analysis framework helps to infer how animal population density changes due to certain natural disturbances and how the animals interact to one another.

Samenvatting

IN DE laatste decennia was er een dramatische stijging van het aantal illegale stroperij-incidenten. Wildlife Monitoring Systemen (WMS) zijn in opkomst als oplossing om stroperij-incidenten te helpen verminderen door de activiteiten van wilde dieren te monitoren. De technologische vooruitgang op het gebied van draadloze netwerken met een laag stroomverbruik heeft de weg vrijgemaakt voor het benutten van hun potentieel voor het gebruik van draadloze WMS. Een van de belangrijkste problemen bij het gebruik van bestaande draadloze WMS is het gebrek aan volledige netwerkverbindingen als gevolg van het schaarse soortelijk mobiliteitsgedrag van wilde dieren.

In tegenstelling tot statische netwerktoepassingen, waar de nabijheid tussen sensor knooppunten is gefixeerd, vertonen wilde dieren vaak tekenen van beweging die de ruimtelijke nabijheid tussen naburige sensor knooppunten verandert. Om deze uitdaging aan te gaan, behandeld deze dissertatie het gebruik van radio- en low-power breedbandnetwerken voor een communicatienetwerk architectuur die energiezuinig en betrouwbaar is en een lage latency heeft. We presenteren een single-hop, multi-hop, en opportunistische multi-hop hybride boom netwerkarchitectuur voor WMS. Bovendien heeft WMS in natuur monitoring toepassingen vaak te maken met frequente mobiliteit van kuddes. We pakken dit probleem aan door het toepassen van een kudde-beweging adaptief communicatieschema. De focus van deze techniek is om een strategie te hebben welke zich aanpast aan het bewegingspatroon van de dieren om het communicatienetwerk efficiënter te maken. We ontwikkelden een data adverteer controleschema die is aangedreven door de actuele mobiliteit-status van een kudde. Dit schema is gebaseerd op een onbeheerd leeralgoritme

Daarnaast implementeren we een gemanagede data disseminatie schema met controle en prioritering van data replicatie functie. In tegenstelling tot bestaande doorsturen algoritmen maakt het optimaal gebruik van lokaal toegankelijke informatie om data door te sturen. Vandaar dat de voorgestelde algoritmen zich aanpassen naar dynamische netwerktopologie veroorzaakt door de inherente sporadische connectiviteit tussen mobiele kudde dieren. Tot slot wordt de toepassing van WMS-communicatienetwerk gedemonstreerd voor het afleiden van beweging van een dier uit de ontvangen signaalinformatie. Dit gebeurt door het gebruik van korte afstand radio voor het bepalen van nabijheid tussen dieren als een alternatief voor het gebruik van GPS zodat de mobiele interactie tussen wilde dieren in kaart kan worden gebracht. Het ontwikkelde kader voor bewegingsanalyse van dieren helpt om af te leiden hoe de populatiedichtheid van dieren verandert als gevolg van bepaalde natuurlijke verstoringen en hoe de dieren op elkaar inwerken.

ማጠቃለያ

በአለፉት አስርት ዓመታት ውስጥ በሕገ-ወጥ መንገድ የእንስሳት እርባታ ክስተቶች ቁጥር አስገራሚ እድገት ታይቷል ። የዱር እንስሳት ቁጥጥር ሥርዓቶች (WMSs) የዱር እንስሳትን እንቅስቃሴ በመቆጣጠር የአደን እንስሳትን አደጋ ለመቀነስ የሚረዱ እንደ መፍትሄ ሆነው ብቅ አሉ ።
በአነስተኛ ኃይል አልባ ገመድ አልባ አውታረ መረቦች ውስጥ ያሉት የቴክኖሎጅካዊ ዕድገቶች ሽቦ አልባ በተመሰረተው WMS ውስጥ የመጠቀም አቅማቸውን እንዲጠቀሙ መንገድ አደረጉ ። ሽቦ አልባ መሠረት ያደረገ WMSን ለመጠቀም መሰረታዊ ከሆኑ ችግሮች መካከል አንዱ በእንስሳው ልዩ በሆነ የእንቅስቃሴ ባህሪ ምክንያት የሙሉ አውታረ መረብ ግንኙነት አቅርቦት አለመኖር ነው ። በሴንቲሜትሪ አንጓዎች መካከል ያለው ቅርበት የሚቆይበት የማይለዋወጥ የአውታረ መረብ ትግበራዎች በተቃራኒ የዱር እንስሳት ብዙውን ጊዜ በአጎራባች ዳሳሽ መስኮች መካከል ያለውን የቦታ ርቀት የሚቀይር የመንቀሳቀስ ምልክቶችን ያሳያሉ ።

ይህንን ተፈታታኝ ሁኔታ ለመቋቋም ይህ ፅንሰ-ሀሳብ ኃይል ቆጣቢ ፣ አስተማማኝ እና ዝቅተኛ መዘግየት ያለው የግንኙነት አውታረ መረብ ሥነ-ሕንፃን ለማቅረብ የአጭር-ቁጣ ሬዲዮ እና ዝቅተኛ ኃይል ሰፊ አካባቢ አውታረ መረቦችን ይመለከታል። ለWMS ነጠላ-ሆፕ ፣ ባለብዙ-ሆፕ ፣ እና አጋጣሚአችን ያገናዘበ ባለብዙ-ድምር የዛፍ መረብ ንድፍ አቅርበናል ። በተጨማሪም ፣ በዱር እንስሳት ቁጥጥር አፕሊኬሽኖች ውስጥ WMS ብዙውን ጊዜ በተደጋጋሚ መንጋ እንቅስቃሴን ይመለከታል ። የኩበት መንቀሳቀሻ መላመድ ዘዴን በመተግበር ይህንን ችግር እንቀርባለን ። የዚህ ዘዴ ልዩ ትኩረት የግንኙነት ኔትወርክ ይበልጥ ቀልጣፋ ለማድረግ ከእንስሶቻቸው እንቅስቃሴ ጋር መላመድ የሚያስችል ስልት ሊኖረው ይገባል ። ቁጥጥር ባልተደረገ የመማር ስልተ-ቀመር መሠረት የመንቀሳቀስ ሁኔታን የሚነዳ የውሂብ ማስታወቂያ ቁጥጥር መርሃግብር አዳብረን። በተጨማሪም ፣ የመረጃ አተገባበር ተግባርን በመቆጣጠር እና ቅድሚያ በመስጠት የተቀናጀ የውሂብ ስርጭት አሰራጭ መርሃግብር እንተገብራለን። ከነባር ማስተላለፍ ስልተ ቀመሮች በተቃራኒው ፣ በአከባቢው ተደራሽ የሆኑ መረጃዎችን በመጠቀም የሀሳብ ማስተላለፍ ውሳኔዎችን በተሻለ ሁኔታ ያደርጋል ። ስለሆነም የታቀደው ስልተ ቀመር በተንቀሳቃሽ የእንስሳ መንጋዎች መካከል በተፈጥሯዊ ድንገተኛ ትስስር ምክንያት ከተለዋዋጭ የአውታረ መረብ ቶፖሎጂ ጋር ይጣጣማል።

በመጨረሻም ፣ የ WMS የግንኙነት አውታረ መረብ ትግበራ ከተቀበለው የምልክት መረጃ የእንስሳ እንቅስቃሴን ለማንቀሳቀስ ታይቷል ። ይህ በአጭር ርቀት ሬዲዮን ቅርብ ለቅርብነት እና አንጻራዊ ለሆነ ወቅታዊ የ GPS አጠቃቀምን እንደ አማራጭ አቀራረብ በመጠቀም በዱር እንስሳት መካከል ያለውን የመንቀሳቀስ ግንኙነት ለመመርመር ነው ። የዳበረው የእንስሳ እንቅስቃሴ ትንተና ማዕቀፍ በተወሰኑ የተፈጥሮ ረብሻዎች ምክንያት የእንስሳት ብዛት ምን ያህል እንደሚቀያየር ለማወቅ እና እንስሳት እርስ በእርሱ እንዴት እንደሚገናኙ ለማወቅ ይረዳል ።

Acknowledgements

Pursuing this PhD has been a truly life-changing experience for me and it would not have been conceivable to manage without the help and direction that I got from numerous individuals. Throughout the composition of this dissertation, I have received so much help. First of all I would like to mention my deepest gratitude to my promoters Dr. Nirvana Meratnia and Prof. Paul Havinga for helping conduct the research on this particular topic. Their inspiration, knowledge, and patience have given me more strength. I would also like to express my special appreciation and gratitude, in particular, to Prof. Paul Havinga in formulating the research topic and methodology. I would like to thank Dr. Nirvana for empowering my research and for enabling me to develop as a research scientist. Your constructive criticism and recommendation on my research has been invaluable.

I would like to acknowledge my colleagues Jacob and Fatjon for their magnificent joint effort. You bolstered me incredibly and were continually ready to support me. Thank you all for your fantastic collaboration and for the majority of the open doors I received to conduct my research and further my dissertation. Every one of you has been there to support me in gathering information for my PhD dissertation. Extraordinary gratitude to my family for their advice and thoughtful help. Words can not express that I am so appreciative to my wife Barsenet Wube for the constant support you have gave. You are consistently there for me. Thank you for supporting me for everything, and particularly I cannot thank you enough for empowering me throughout this experience.

Additionally, to all in the PS research group, it was an extraordinary experience in my four years of research. A debt of gratitude is in order for all your supports. Special thanks to our secretary Nicole Baveld for her out-most help throughout my work in PS research group. And finally, above all else, I would like to express my gratitude toward God almighty for giving me the capacity, strength, and knowledge the chance to take on this beautiful journey to fruitful completion. Without his gifts, this accomplishment would not have been conceivable.

Contents

List of Figures

List of Tables

List of Abbreviations

WMS	**W**ildlife **M**onitoring **S**ystem
WSN	**W**ireless **S**ensor **N**etwork
AB	**A**nimal **B**roadcaster
AS	**A**nimal **S**canner
LG	**L**ong-range **G**ateway
LoRa	**L**ong-range **R**adio
LoRaWAN	**L**ong-range **R**adio **W**ide **A**rea **N**etwork
LPWAN	**L**ow **P**ower **W**ide **A**rea **N**etwork
BLE	**B**luetooth **L**ow **E**nergy
RFID	**R**adio **F**requency **ID**entification
DSP	**D**igital **S**ignal **P**rocessor
MBS	**M**obile **B**iological **S**ensor
PTTs	**P**latform **T**ransmitter **T**erminals
LOS	**L**ine of **S**ight
MAC	**M**edium **A**ccess **C**ontrol
TDMA	**T**ime **D**ivision **M**ultiple **A**ccess
DD	**D**irect **D**elivery
FC	**F**irst **C**ontact
SnW	**S**pray and **W**ait
CBR	**C**ontact **B**ased **R**outing
DF	**D**elegation **F**orwarding
CSMA	**C**arrier **S**ense **M**ultiple **A**ccess
HAMA	**h**erd-movement **a**daptive **M**AC protocol
SOM	**S**elf **O**ganizing **M**ap
SM	**S**tationary **m**ode
BOM	**B**eacon **O**n **M**otion
MANER	**M**anaged **D**ata **D**issemination **S**cheme
NMI	**N**ormalized **M**utual **I**nformation
MAD	**M**ean **A**bsolute **D**eviation

List of Nomenclature

BW	bandwidth
SF	spreading factor
CR	coding rate
$n_{preamble}$	number of preambles
CRC	coding rate correction
DR	data rate
f_{LoRa}	LoRa Carrier freq.
f_{BLE}	BLE Carrier freq.
$\sigma_{\psi_{dB}}$	log-normal shadowing
γ	path-loss exponent
h_t	LG antenna height [m]
$Cov(C)$	coverage area probability
P_{Tx}	transmit power
P_{RxBLE}	BLE receiver power
P_{RxLoRa}	LoRa receiver power
d_c	critical range
d_0	BLE near-field range
n	number of nodes
PL_{BLE}	packet for BLE
$BLEDR$	BLE data rate
PL_{BLE}	packet for LoRa
x	resync. period
m	number of resync period
t	simulation duration
T^{+}_{BC}	beacon data broadcasting interval
T^{+}_{sw}	beacon data scanning window
T^{+}_{sc}	beacon data scanning interval
$T^{+}_{s,min}$	recommended minimum broadcast interval
t_{pol}	length of transmitter's polling preamble
t_{tx}	time interval needed to complete transmitting a packet
t_a	active state duration
$T_{cp,i}$	control period
N	regeneration cycles
$Ti_{s,i}$	estimated sleep-time
$X^{(r)}$	idle-time for the rth regeneration cycle
K_i	mean buffer size
λ^{-1}	inter-packet interval
S_n	packet transmission time of the nth packet
W_n	waiting time of the nth packet

ToA	time-on-air
$T^{+}_{sl,BOM}$	advertising interval for the BOM states
$T^{+}_{sl,SM}$	advertising interval for the SM states
T^{+}_{BC}	advertising interval for the conventional states
WL	optimal window length of detecting activity
ρ	proportion AB node is in BOM
I_{tx}	transmit current consumption
Ti	training instances
LS	lattice size
SR	sampling rate
C^{n}	data cluster
TPR	true positive rate
FDR	false detection rate
$x_i(t)$	X coordinate of node i at time t
$y_i(t)$	Y coordinate of node i at time t
$V(t)$	velocity vector of node i at time t in relative to the previous time frame t'
$v_i(t) = \|V_i(t)\|$	speed of node i at time t in relative to the previous time slot
$\theta_i(t)\|$	angle made by velocity vector of node i at time t with the $X - axis$
$a_i(t)$	acceleration vector of node i at time t
$E_{i,j}(t)$	euclidean distance between nodes i and j at time t
$RD(A(t), B(t'))$	relative direction (RD)
$SR(A(t), B(t'))$	speed ratio (SR) between two vectors A(t) and B(t')
R	maximum transmission range of a mobile node
N	number of mobile nodes
$G = (v, E)$	graph network: a graph $G = (v, E)$
V	graph nodes
E	graph edges
$X(i, j, t)$	an indicator a value 1 iff there is a link nodes i and j at time t
$D_s(i, j, t)$	average degree of spatial dependence
$LD(i, j, t, t')$	average link duration

Chapter 1

Introduction

CURRENTLY, *Wild animals, rhinos and elephants in particular, are facing an ever increasing poaching crisis. One of the solutions proposed for this crisis is a proper wireless sensor network based wildlife monitoring system (WMS) to help with the animal protection. A WMS enables wireless sensor devices to communicate for animal activity monitoring effort. In this chapter, we present the main characteristics and technical requirements of a WMS. Moreover, the research objective, hypothesis and an overview of the thesis organization is also discussed in this chapter.*

1.1 Introduction

Between the year 1900 and 2018, roughly 90 % of African elephants have disappeared [7]. Throughout 2016, every 8 hours one rhino was killed for its horn in South Africa alone [7]. Moreover, an elephant is currently being killed every 20 minutes each day [8, 1]. These magnificent animals are shown in Figure 1.1. The poaching statistics totals to 1054 rhino deaths in a population of roughly 25,000 [1, 8, 7] and 27,000 elephant deaths in a population of roughly 377,000 [9]. Figure 1.2 shows overall number of poached rhinos per year. Due to increased protection efforts the number of rhino poaching incidents are decreasing once again, although the losses are still extremely high [10]. If poaching is not halted soon, the existing rhino population will not be able to procreate rapidly enough and will start to diminish once more.

(A) *White Rhinoceros*

(B) *African Elephants*

FIGURE 1.1: *White Rhinoceros and African Elephants in their natural habitats [1]*

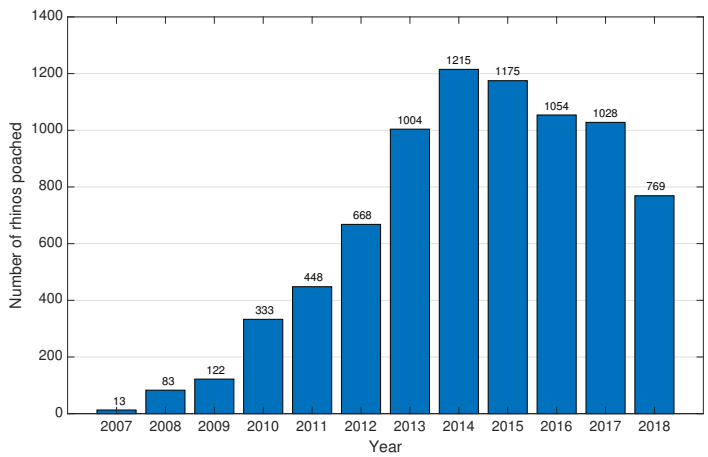

FIGURE 1.2: *Number of poached rhinos in South Africa, adopted from the data published by the South African Department of Environmental Affairs(2016) [1]*

The belief that rhinoceros horn has medicinal power together with increasing wealth of the population, fuel the demand for rhino horn and ivory in Asian countries such as Viet Nam and China [1, 7]. While high profits can be generated from poaching, the risk that is involved with poaching is often relatively low compared to drug trafficking. Therefore, the trade of ivory and rhinoceros horn unfortunately remains a lucrative business for criminal syndicates [10]. Unfortunately, poaching is not limited to rhinos and elephants; amongst other species, tigers and pangolins are also heavily threatened by poaching for their skin, bones, and scales. Ultimately, the best solution to poaching is the eradication of demand for rhino horn, ivory, and other wildlife products [11]. Until the demand has successfully been eradicated it remains critically important to protect the ever more fragile wildlife populations against poachers.

One of the promising solutions to protect wild animals against poaching is to introduce a wireless wildlife monitoring system (WMS). As part of a WMS, sensor collars can be deployed to monitor the animals' activities. Because the activities are seen as an indication of the presence of poachers, since wild animals are naturally known to react to the presence of poachers [12]. Several efforts have been made to develop wireless sensor network (WSN) based WMS, where a wireless technologies are utilized by forming multi-hop mesh/ad-hoc networks [13, 14]. While making some progress in terms of energy efficiency, existing wireless technologies are still not suitable for applications such as wildlife monitoring due to high latency and low connectivity coverage to monitor large areas [13, 14].

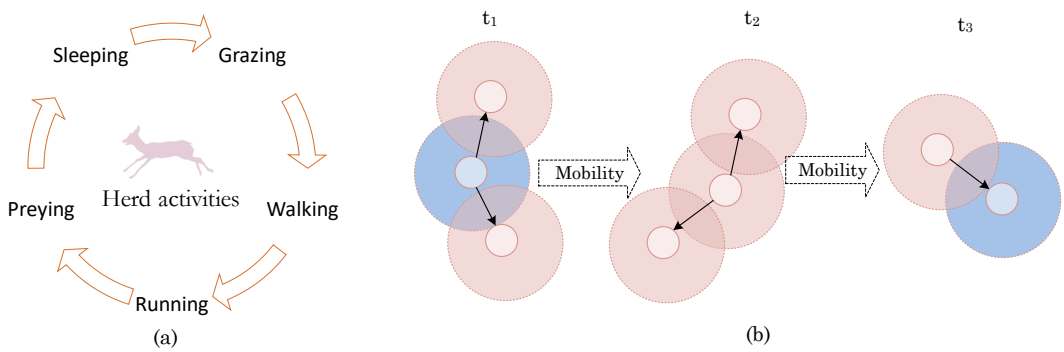

FIGURE 1.3: *A day in the wild: (a) typical animal movements, (b) Impact of movement on wireless link example.*

One of the main challenges in realizing wireless technology based solutions for wildlife monitoring is that wild animals often depict a sparsely mobile and conspecific behaviour, e.g. grazing, pursuing a prey or running from danger such as illegal hunters or poachers (Figure 1.3) [15, 16]. Thus unlike static network applications, where the proximity among sensor nodes is fixed, sensor nodes often show a level of movement which changes the spacial proximity between neighboring nodes. Consequently, leading to lack of full network connectivity, where node mobility highly impacts the wireless communication links substantially, making the wireless monitoring technique less efficient interms of energy consumption, reliability, and latency.

Moreover, it is also a challenge to support heterogeneous network services, such as localization, proximity inference, and data pre-processing; with sensor nodes (e.g. accelerometer and gyroscope, etc) are deployed on collars to monitor animal activities [13, 17, 18]. In addition, often contradicting requirements such as (i) high energy efficiency, (ii) high reliability, and (iii) low latency are expected to be satisfied in a WMS deployment for fine-grained monitoring. Hence, a mechanism to control the trade-off between the WMS requirements (e.g. energy consumption, reliability, and latency) is necessary, which may not be practically achievable by using a single category of wireless solution alone. Although a few works have been conducted to address this issue by proposing a wireless network architecture for WMS [19], none of them provides a real-time (fine-grained) animal monitoring. This is mainly because they often ignore the tremendous benefits of collaborative sensing among mobile nodes.

Therefore, in this thesis we present a hybrid (dual) interface based wireless sensor network for WMS that exploits short-range and long-range wireless technologies. The main focus of this thesis is to provide a wireless communication system for a sparsely con-specific (clustered) mobile animals, while ensuring high energy-efficiency, high reliability and low latency.

The rest of this chapter is organized as follows: Section 1.2 describes the device components of a typical WMS network. Section 1.3 details the functional requirements of a WMS. The research objectives and hypothesis will be presented in Section 1.4. The contribution of this thesis is summarized in Section 1.5. Section 1.6 and Section 1.7 respectively presents the animal mobility data-sets and the performance metrics used in this thesis work. Finally, the organisation of the thesis is provided in Section 1.8.

1.2 WMS Network Architecture

Figure 1.4 shows a typical example of a WMS network architecture that we adapted in this thesis work, illustrating herds of mobile wireless sensor networks integrated with a long-range backbone network [20]. This network architecture useful in case of wildlife monitoring, where sensors are collared for monitoring the behaviour and movement of animals. As shown in Figure 1.4, there are mainly three device types in a typical WMS: (i) animal broadcaster (AB), (ii) animal scanner (AS), and (iii) long-range gateway (LG). Each of them are explained as follows:

- **Animal broadcaster (AB)** are the physical end-devices consisting of sensors which are able to measure and send data to AS nodes. They are typically small in size with embedded radio and sensor modules. Their number depends on the population of animals in the habitat area. These sensor nodes could be deployed as collars worn by animals, thus they are often mobile.
- **Animal scanner (AS)** are data scanner nodes, which listen for AB nodes' data in the surrounding area. AS nodes could have a dual interface, i.e. they utilize

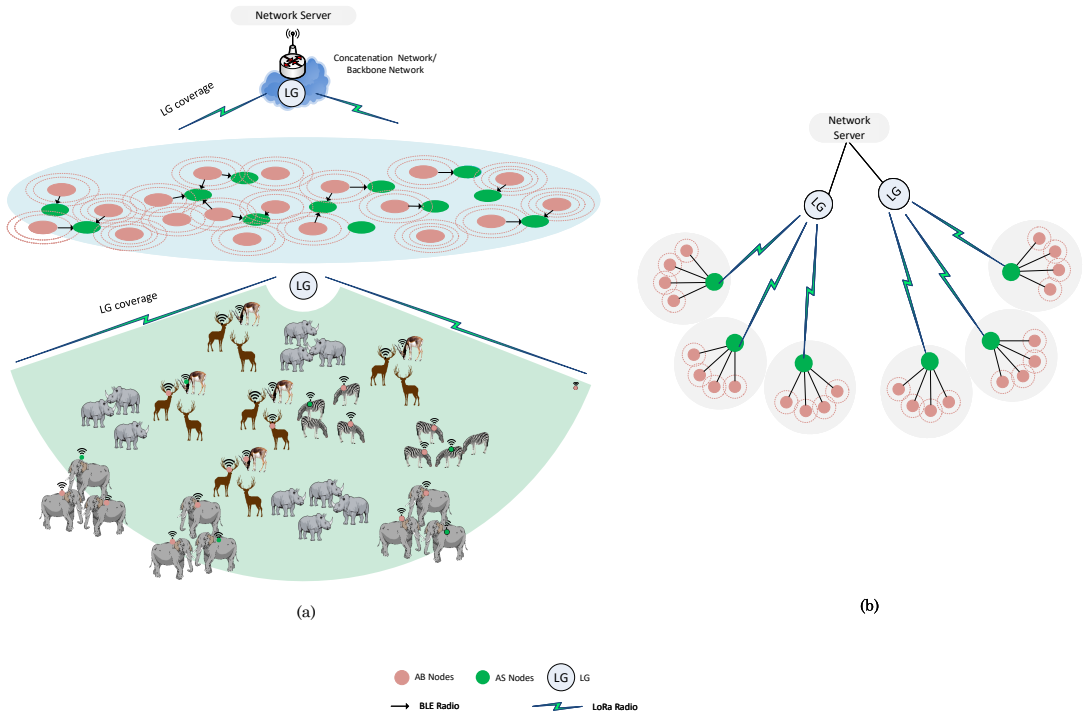

FIGURE 1.4: *A WMS typical example. (a) network architectures, (b) Hierarchical network layout. Device types are: (i) AS- Animal Scanner, (ii) AB- Animal Broadcaster, and (iii) LG- Long-range Gateway.*

short-range and long-range radios. To reduce the total network communication overhead of transmitted packets, AS nodes periodically coordinate communication and prune incoming data from AB nodes before forwarding to the data collection center. These devices are also mobile since they could be deployed on animals as well. They are fewer in terms of number compared to AB nodes, but more powerful in computational power.

- **Long-range gateway (LG)** is responsible for relaying data to the network server. The gateway communicates with AS nodes, but do not directly communicate with the AB nodes. They are usually mounted on elevated location to increase their coverage.
- **Network server** executes the management and operation application to process the incoming data from LG. Animal and poacher activity monitoring and real-time event mapping services could be provided in this WMS component.

1.3 Requirements of wireless sensor based WMS

Generally, it is difficult to develop a generic wireless sensor network based monitoring system satisfying all the WMS application requirements. Every requirement has its own specific design challenges. However, unlike conventional wireless sensor

network monitoring systems, WMS poses a mixed and often conflicting set of requirements due to its inherent challenges such as network topology dynamics and sparse connectivity. In this section, we describe the requirements of WMS:

- **Energy efficiency**: In WMS, sensor nodes are placed on animals or in the field unattended for months or years. Most of the wildlife habitat locations are geographically very remote. Thus, a WMS could be isolated from power lines and rely solely on battery and possibly also energy harvesting technologies. Therefore, each device should be able to efficiently manage its energy supply in order to maximize the total WMS life-time in the long-run.
- **Reliability**: Reliability in wireless sensor based MWS corresponds to the packet delivery probability, i.e. *the ratio of successfully delivered data to receiver nodes to total number of data transmitted by sender nodes*. WMS solutions need to have a relatively higher reliability to provide a consistence data delivery service.
- **Latency**: In a WMS a data should be sent in real-time (fine-grained) manner, i.e. with low latency as soon as the data is sensed. The latency in WMS is measured by *the difference between the time a data is sent from the source nodes and time it is delivered at the destination nodes*. For WMS a high response time or a low end-to-end latency is required. The end-to-end latency needed for effective wildlife monitoring should be in the range of several milliseconds to few seconds. Especially, in highly mobile animal state, within few milliseconds is required to capture the movement pattern of animals.
- **Long-range coverage**: Wildlife conservation areas are very large, e.g. a typical national park is approximately 100 km long, and has an average width of 50 km [15]. Hence, WMS needs to provide a full coverage of the protected field. In order to address coverage problem, WMS could leverage long range radio to cover the animal habitats efficiently.
- **Scalability**: The typical population size of a herd could range from 10s to 100s [13, 14]. Hence, the WMS should be able to accommodate a growing number of additional sensor collars joining the WMS. Scalability could be achieved by means of hardware and software techniques. When the WMS is scaled up by introducing new WMS devices, the system should seamlessly integrate new WMS devices with no or little manual modification.
- **Robustness**: A WSM should endure various technical and environmental deployment factors. Problems in a WMS can occur at any point between the generated event and monitoring process. For instance, the destruction of individual WMS components should not lead to a complete failure of the overall WMS.

Even though it is practically difficult to satisfy all these requirements without any compromise, a WMS should attempt to comply with the most important wireless communication network parameters such as low energy consumption, low latency, and high reliability.

1.4 Research objective and hypothesis

Based on the outlined WMS requirements and characteristics of wild animals, several wireless technologies may be good candidates for WMS design. However, challenges associated with WMS, mainly the node dynamics (mobility) and the sparsely con-specific living behaviour of animals, substantially limits the adaptation of existing wireless solutions.

The prime research objective of this thesis is, therefore, to provide a network communication network architecture that ensures high energy-efficiency, high reliability, and low latency, while addressing the WMS challenges such as a sparsely conspecific (clustered) and mobile animals. Furthermore, we demonstrate how WMS communication network architecture could be utilized in inferring the movement patterns of animals.

This research objective can be sub-divided into various specific research issues related to design of inter- and intra-cluster communication technique, handling the effect of node mobility and herd clustering for wildlife monitoring applications. To this end, in this thesis we aim to address the following research questions:

Research question 1: To what extent can combining inter- and intra-cluster communication provide an efficient wireless communication network architecture ensuring high energy-efficiency, high reliability, and low latency for wildlife monitoring?

Research question 2: Can the effect of sporadic animal movement be utilized for optimal communication network architecture design while achieving the network requirements?

Research question 3: How to address the lack of full network connectivity by leveraging the animals' conspecific or clustering behaviour?

1.4.1 Research hypothesis

We tackle the outlined research questions, with the following accompanying hypothesis.

To answer research question 1,
Hypothesis 1 (H1): A hybrid tree network topology, which is a combination of inter-cluster with short-range (BLE) and intra-cluster with long-range (LoRa) wireless link, is more optimal than simple star network topology based on short-range or long-range only wireless communication.

To answer research question 2,
Hypothesis 2 (H2): A light-weight single-hop based communication network architecture will significantly reduce the energy consumption of end-nodes while at the same time achieving very low latency and high reliability for WMS.

We also addressed other alternative approaches to address the research question 2, such as

Hypothesis 3 (H3): A multi-hop network with a data traffic adaptiveness for the wildlife monitoring.

Hypothesis 4 (H4): Movement adaptiveness could be complemented with beacon transmission mode, where the sensor nodes would be aware of the nodes' mobility states by utilizing real sensor data such as accelerometer.

To answer research question 3,
Hypothesis 5 (H5): It is possible to implement an opportunistic multi-hop network network architecture with a data replication scheme to control and prioritize data dissemination in WMS. Hence, the communication routing algorithm will adapt to dynamic network topology due to the inherent lack of full-connectivity between herd of animals.

1.5 Thesis contributions

In the light of the aforementioned research challenges, the main contributions of the thesis work are detailed as follows:

Contribution 1: Leveraging BLE and LoRa radio for WMS

In this contribution, we present an analyses and comparison of a hybrid tree network topologies to conventional star network topology for WMS. We demonstrate that hybrid network topologies such as single-hop, multi-hop, and opportunistic multi-hop, are more optimal than the conventional star network topology for WMS application. Hence, we discuss an analytical model to investigate the performance of hybrid tree based networks in terms of energy consumption under a wildlife monitoring use-case. This contribution appeared in [21]:

> [21] *E. D. Ayele and K. Das and N. Meratnia and P. J. M. Havinga, Leveraging BLE and LoRa in IoT network for wildlife monitoring system (WMS), In IEEE proceedings of IEEE 4th World Forum on Internet of Things (WF-IoT), pages 342–348, Singapore, Feb. 2018.*

Contribution 2: Single-hop communication with hybrid tree network

In this contribution, we present design and implementation of asynchronous dual interface network. We evaluate performance of the WMS protocol in comparison with conventional opportunistic systems under actual animal movement scenarios. This contribution appeared in [22]:

> [22]*E. D. Ayele and N. Meratnia and P. J. M. Havinga, Asynchronous dual radio opportunistic beacon network protocol for wildlife monitoring system, 2019 10th IFIP International Conference on New Technologies, Mobility and Security, Gran Canaria, Spain, July 2019, pp. 1-7.*

Contribution 3: Multi-hop communication with hybrid tree network
In this contribution, a herd-movement driven asynchronous duty-cycling communication protocol suitable for mobile sensor nodes is presented. The protocol is

demonstrated to adapt to the specific animal movement patterns to make the wireless communication more energy-efficient and reliable. This contribution has appeared in [23].

> [23] *E. D. Ayele and N. Meratnia and P. J. M. Havinga, HAMA: A Herd-Movement Adaptive MAC Protocol for Wireless Sensor Networks, In proceedings of the 8th IFIP International Conference on New Technologies, Mobility and Security (NTMS), Larnaca, Cyprus, Nov 2016, pages 1–7.*

Contribution 4: Opportunistic multi-hop communication in hybrid tree network
Conventional multi-hop communication, often perform poorly in scenarios where the communication path is intermittent due to node mobility. While making some progress in energy efficiency aspect, these protocols still suffer from high latency mainly due to node mobility. To overcome this problem, in this contribution, we first explore the existing opportunistic multi-hop communication protocols that are the recent evolution of the traditional wireless sensor networks (WSN).

In addition, we present an optimized opportunistic multi-hop protocol utilized to provide communication facilities among devices in sparse and mobile network scenarios, as in WMS applications. The features that makes opportunistic multi-hop communication suitable for WMS scenario are (i) there is no network topology limitation, because node mobility is supported and (ii) intermediate nodes utilize a simple store-carry-and-forward (SCF) scheme for data dissemination with out relying on routing tables. This minimizes data latency while avoiding deterioration in data reliability. This contributions have appeared in [24, 25].

> [24] *E. D. Ayele and N. Meratnia and P. J. M. Havinga, Towards a New Opportunistic Network for Wildlife Monitoring System, In IEEE proceedings of 9th IFIP International Conference on New Technologies, Mobility and Security (NTMS), pages 1–5, Nov 2018, Paris, French.*
>
> [25] *E. D. Ayele and N. Meratnia and P. J. M. Havinga, MANER: Managed Data Dissemination Scheme for LoRa IoT Enabled Wildlife Monitoring System (WMS), In IEEE proceedings of 9th IFIP International Conference on New Technologies, Mobility and Security (NTMS),pages 1–7, Nov 2018, Paris, French.*

Contribution 5: Animal spatial social network analysis

In this contribution, the application of BLE radio based WMS network architecture for inferring animal social behaviour is discussed. Proximity and relative ranging is as an alternative solution to the existing application of GPS and proximity sensors for studying animal movement behaviours. This contribution appears in [26]:

> [26] *H. Coen, Inferring animal social interaction using proximity based on BLE network,Essay (Master), EEMCS: Electrical Engineering, Mathematics and Computer Science, August 2018.*
> [Under review] *E. D. Ayele and H. Coen and N. Meratnia and P. J. M. Havinga, Animal Spatial Social Network Analysis Through Utilizing LoRa and BLE, ACM Transactions on Internet of Things (TIOT), 2019.*

1.6 Mobility models and datasets

We have utilized the following mobility data-sets for simulation in different chapters of this thesis. In our evaluation and simulations, animals are assumed to be mobile, hence, we introduce four mobility models ($M_1 = ZebraNet$, $M_2 = Nomadic$, $M_3 = Pursue$, $M_4 = RandomWayPoint(RWP)$) for group (herd) movement.

- ZebraNet (M_1) project movement dataset of animal movement traces collected from real-world ZebraNet deployments [27]. The data contained in this data set are movement traces collected from two real-world ZebraNet deployments at Sweetwaters Game Reserve near Nanyuki, Kenya [27]. The first deployment was in January 2004 and the second deployment was during summer of 2005. The data offer detailed animal position information using UTM format. The GPS was sampled every 10min during a foraging activity. In this mobility scenario, animals also show a conspecifics living behaviour, thus there exits 'herding' or clustering behaviour to some degree.
- BonnMotion [28] mobility scenario generator is used to generate standard mobility dataset. We generated mobility models M_2, M_3, and M_4 using BonnMotion tool [**aschenbruck2010bonnmotion**], where mobile nodes move with mobility trajectory and are set to move at random speed range of [10,30 km/h] with max-pause = 5s. M_2, M_3, and M_4 movement models are used as an input mobility scenarios with actual coordinate data tupils $(nID, x, y, time)$. The $M_2 = nomadic$ model represents groups of mobile nodes that collectively move from one point to another [29, 30]. Within each cluster or group of mobile nodes, individual animals maintain their own personal proximity where they move in random ways. The herd would move from one location of interest to another together; however, the animals within the herd would roam around a within the cluster individually with leaving the cluster. As the name implies, the $M_3 = pursue$ mobility model represents mobile nodes tracking a particular target node [29, 30]. For example, this model could represent predators or poachers attempting to catch a prey animal.

As the main aim of this thesis work would be to investigate and develop the WMS communication network architecture by emulating wildlife movement pattern. In the following chapters, with respect to the specific goal of that chapter we use a slight variation of the mobility models, for example, in terms of number of nodes, node speed, area, etc. Hence, unless otherwise mentioned, in all these mobility patterns, 50 mobile nodes are allowed to move in an area of 1000mx1000m for a time period 8000 time-frames. For nomadic, we used 5 groups of 10 nodes each moving independently of each other and in an overlapping fashion. For pursue, the 50 mobile nodes were placed in a similar way as nomadic model, and two extra pursuing nodes are introduced randomly to emulate predatory distressing behavior. Their movement was controlled as per the specifications of each models. If a pursing node moves beyond the boundary of the defined area, it is re-inserted at the beginning position in a randomly chosen coordinate in the area. Table 1.1 summarizes the mobility data-sets used in each chapter.

TABLE 1.1: *Mobility data-sets used per chapter. n/a=not applicable*

	ZebraNet (M_1)	BonnMotion (M_2)	BonnMotion (M_3)	BonnMotion (M_4)
Chapter 5	✓	n/a	n/a	n/a
Chapter 6.2	✓	n/a	n/a	✓
Chapter 6.3	n/a	n/a	n/a	n/a
Chapter 7	✓	n/a	n/a	✓
Chapter 8.2	✓	n/a	/a	n/a
Chapter 8.3	n/a	✓	✓	✓

1.7 Main performance metrics

Three metrics are used to evaluate the communication network performance for WMS approaches in this thesis, they are outlined as follows:

- Average reliability (D_e) is a measure of the ratio of number of packets successfully received by a long-range gateway (LG) to number of AB packets transmitted. We record the number of packets received at the LG node and the total number of AB data sent.
- End-to-End latency (ℓ), average latency of a transmitted AB packet defines the ratio of the time when the AB data is transmitted to the time when it is received at LG node. The simulator records the time when a packet is received at the LG node and the time when it is sent to determine the ℓ.
- Average energy consumption (E), is a function of average energy consumption of all nodes in the network.

1.8 Thesis organization

The rest of this thesis is organized as follows: In Chapter 2, the state-of-the-art works related to wireless wildlife monitoring is discussed. Chapter 3 presents the existing multi-hop and opportunistic network protocols for wildlife monitoring. Chapter 6 further describes leveraging BLE and LoRa radio for WMS. Single-hop communication with hybrid tree network is discussed in Chapter 5. Chapter 4 details a multi-hop communication with hybrid tree network. Chapter 7 presents opportunistic multi-hop communication in hybrid tree network. Chapter 8 elucidates the application of the proposed WMS network for inferring the spatial social movement of wild animals. Finally, Chapter 9 concludes the thesis with concluding remarks while outlining future works.

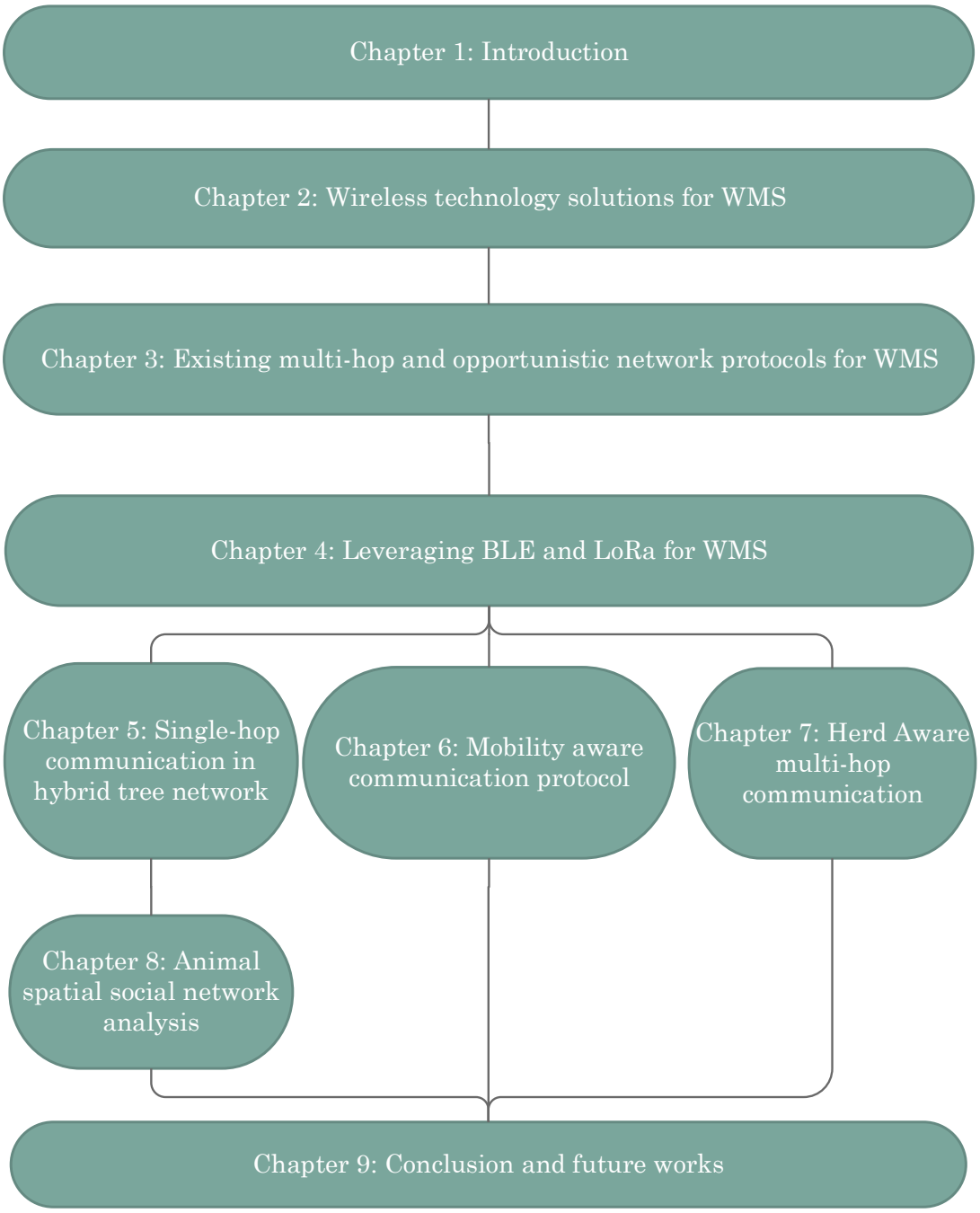

FIGURE 1.5: *Thesis organization structure*

Chapter 2

Wireless Wildlife Monitoring Systems (WMSs) - Literature Review

---

THIS *chapter, we review the existing wireless technology based wildlife monitoring solutions that help in the conservation of endangered species from extinction. We also present the challenges for providing an effective WMS solutions. Finally, we outline the open research challenges and concluding remarks.*

Part of this chapter has appeared in:
[31] Jacob Kamminga, Eyuel D. Ayele, Nirvana Meratnia, and Paul Havinga, "Poaching Detection Technologies—A Survey," Sensors (Basel). 2018 May; Vol 18(5).
Author Contributions: Jacob Kamminga and Eyuel D. Ayele conceived and designed the survey; J.K. and E.A. executed the survey; J.K. and E.A. wrote the paper; and N.M. and P.H. supervised the project.

2.1 Introduction

In general, animals are monitored either by logging their location, e.g. using GPS tags, or by recording their movement passing through a specific location [32, 33]. The reviewed works in this chapter use various movement monitoring approaches such as *GPS tagging, ultrasonic, seismic, camera traps, acoustic fixed arrays, mark-recapture, etc.* [31, 34, 35, 36, 37]. In this section, we provide an overview of these techniques that are utilized for animal activity monitoring along with their pros and cons. In the following subsection, we discuss their utilization in the existing state-of-the-art-works in detail.

The camera traps are motion sensitive cameras placed in the area of interest, offering a non-invasive way of monitoring [33]. Camera traps can operate for weeks unattended. The photos taken by camera traps are not only used to capture the presence of animals, but also their behaviour. Camera traps can also be used to determine the local animal density, which becomes more valuable when data is gathered over years or across different sites. Disadvantage of camera traps are the limited live data transmission, requiring a larger battery or a solar panel. Moreover, camera traps only capture animals that are in front of the camera, lacking the panorama view of surrounding animals [33].

The advantage of the acoustic fixed arrays [34, 38] is that they are non-invasive, making use of microphones placed in the environment to study animals. They allow biologists to localize animals based on where arrays are placed in their natural habitat, providing spatial context for monitoring and measuring animal movement. Multiple animals can be studied simultaneously while human observers are absent from the area. Acoustic monitoring is suitable for monitoring long periods, over nights, and in thick vegetation, where visual tracking is often difficult [34, 38]. The cons of acoustic monitoring is that it cannot be used for silent animals, and it requires microphones to be positioned near to the target animals to collect correct recordings [34, 38]. Moreover, spatial acoustic monitoring requires precise coordination of the recordings from each microphone, requiring that the clock of the microphones to be regularly synchronized on a millisecond level. Some researchers found a solution to this problem by using kilometres of cable to connect microphones to a central recorder, increasing the amount of labour to set this up [34, 38].

Using the mark-recapture approaches, animals are captured and marked with coloured metal bands, ear tags or toe clips and released again to their natural habitat, making it possible to identify the animals at a later point in time when they are re-captured or re-sighted [35]. The method makes it possible to gather information about characteristics of individuals (such as age or sex) and population changes over time. Disadvantages of this approach are that tags can get lost and animals disappear and could be hard to re-catch. More importantly, this approach does not provide much information about the animal behavioural patterns [35].

GPS gives the absolute coordinates of a mobile node, but it is expensive and energy consuming [39, 40]. It also suffers from frequent satellite disconnections in indoor environments. RFID is a technology that employs radio frequency signals to exchange data between a reader and an electronic tag attached to an object for the

purpose of identification and tracking. RFID readers could be located strategically in the field [41, 42, 43, 44]. One of its drawbacks is the relative short communication range (1 to 2 m) and the inhibition to future extensions.

Ultrasonic sensors can sense signals beyond the frequency range that humans can hear. Main applications for ultrasonic sensors are sonar, industrial materials testing, and medical imaging [16]. Sonar is used for ranging and underwater detection of targets with a technique similar to radar, but the emitted energy comes in the form of ultrasonic sound signals. Ultrasonic sensors are capable of detecting most objects that have sufficient acoustic reflectively. They are less affected by condensing moisture than photoelectric sensors. However, sound absorbing materials, such as rubber, cloth, foam and foliage absorb the sound and are hard to detect. Therefore it becomes easy to hide from ultrasonic sensors and they don't have a practical use in detection of poachers. They have not been used in any of the reviewed works of this survey.

Some works utilize the effect of changes in an electro magnetic field when an intruder is crossing through [45, 46]. One or two coaxial cables are buried in the ground and energy is pulsed along one leaky coaxial cable. The coupled energy is monitored from a parallel buried leaky coaxial cable. An object, person or animal that passes over the buried cable and through the electromagnetic field, that couples energy from the transmitting cable to the receiving cable, can be measured with Digital Signal Processor (DSP) techniques [47, 48, 49]. This type of sensing does not require a line of sight with the target. The range for this type of sensing is limited by the length of the cable, available power and quality of processing technology. This implies that this type of sensor is mostly used along a perimeter.

Accelerations are generated due to movements of an object. An accelerometer based mechanism is shown to be an accurate, robust and practical method for objectively monitoring the free movement of objects and persons [50]. The mechanism responds to both frequency and intensity of movement. However, accellerometer readings are sensitive of the node placement. Accellerometer motion sensors convert physical motion into an electrical signal that can be processed. Multiple reviewed works have utilized motion sensors with accelerometers [51, 52, 53, 54, 55, 56, 57, 58]. They are used to monitor movement in fences, structures or the ground. Motion sensors are very sensitive and can be used to classify type of intrusion. Motion sensors are relatively cheap and energy efficient. The range of motion sensors is determined by the physical structure they are attached to.

Seismic sensors measure seismic waves generated by the impact of vehicles or footsteps on the ground. Geophones are very sensitive sensors that are used to measure seismic waves [41, 59, 60]. The propagation velocity of seismic waves depends on the density and elasticity of the medium they travel through. The quality of a vibration signal heavily depends on the type of soil it travels through, thus the quality of seismic measurements is different for each environment [59]. Loose and inconsistent soil will yield poor detection capabilities [59]. Because of the physical properties of seismic waves and their high dependence on the environment, it is difficult to develop a uniform approach that can be used over large areas (with varying types of soil) [59].

Animal behaviours and reactions are sometimes used as part of the detection systems. A well known example is the 'canary in the coal mine'. Until late in the 20th century, a canary was taken into coal mines by miners to be utilized as an early-warning signal for toxic gases, primarily carbon monoxide. The birds are more sensitive than humans and would become sick, or die, before the miners would and thus act as a 'chemical indicator' [16, 2, 61, 62]. Animal sentinels are often used in situations when: (i) humans cannot always be on the alert, (ii) animals have better senses, or (iii) humans cannot safely go to places. Some reviewed works suggested to utilize animal sentinels for the detection of poachers [2, 61, 62]. In the natural environment, animals are used indirectly for surveillance [16]. Animals make sound calls and physical reactions when they sense danger. A barking dog or strident bird calls are sounds that are recognized by multiple species, including humans, and can be utilized as an alarm or early warning. The frenetic behavior of bees, beetles, birds, and rodents can indicate a forest fire or impending storm. While elephants can hear and feel infrasonic vibrations and know when a large animal, vehicle, earthquake, or storm might be approaching [63, 64]. Hence, animal behaviour can provide an early warning that can help to detect a disturbance in their environment.

In this chapter, we discuss the existing works utilizing wireless sensor networks and long-range wireless technologies for monitoring wild animals in Section 2.2. We present comparison overview of the works in Section 2.3 Finally, we discuss the concluding remarks in Section 2.4.

2.2 Wildlife monitoring techniques

In the past, several wireless sensor networks (WSNs) are utilized to provide wildlife monitoring [13, 14]. For the sake of clarity, in this subsection, we categorize the works into five groups: (i) sensor tagging, (ii) perimeter monitoring, (iii) area monitoring, (iv) long-range monitoring, and (v) hybrid techniques. Animal behaviours and reactions can be used to better protect them. One approach to capture animals' reactions to their environment is by tagging or attaching sensing devices directly to their body. Tagging is used to monitor the changes in the animals' body or movement behaviour. This sensor tagging could deployed to monitor either the perimeter or the are of habitat. Alternatively, the perimeter monitoring are usually deployed in the vicinity of a boundary and aligned with a barrier or linear premises [65]. When one thinks of securing a perimeter, a fence rapidly comes to mind. Developing a WMS on or near an existing fence is attractive mainly in terms of power constraints. Many game parks have an existing (solar) powered fence. Fences need to be electrified in order to keep large mammals from breaking through the fence [65]. This opens up the possibility to utilize technology that requires more power. Additionally, adding technology to existing infrastructure is non-obtrusive and pervasive. Area monitoring, on the other hand, can monitor animals over a large area and do not have to be constrained to a linear monitoring zone. They can monitor an animal entering and/or moving within a defined monitoring zone, ideally with tracking capability to monitor the direction of single or multiple intruders [65]. Such technologies usually utilizes volumetric sensor technologies that cover a large usually

omnidirectional area rather than a linear monitoring zone. The monitoring zone can have a radius ranging from tens of metres to a few kilometres. An intrusion alarm is triggered by entering the zone or moving within it.

2.2.1 Animal sensor tagging

Several efforts are proposed to use sensor tagging as part of an intrusion monitoring system [66, 4]. For instance, the ZebraNet [66] project was aimed at monitoring the movement and activity of zebras at the Mpala Research Center, Kenya. Such wildlife movement spanned over a large terrain size and a long temporal scale. Although ZebraNet can be considered as a typical project on ad hoc WSNs, it exhibited several challenging requirements. For example, the size and weight of the collars are large and they inhibit the movement of the zebras. On the other hand, with collars attached to the necks of zebras, a sparse network topology is created with lower chances of communication. Moreover, since the tracking devices, equipped with GPS sensors, were required to operate over long periods of time without human intervention, relying only on battery sources for power was not feasible. These factors led to the design of custom-made hardware for the collars. However, from the perspective of network communications, a more stringent requirement was that the base station, which itself was mobile, should receive almost all the tracking data gathered. The delay in obtaining all such data was not critical. In other words, the ZebraNet project exhibited simple Epidemic routing protocol characteristics, where eventual delivery of messages was acceptable. The collars attached to the zebras would normally transfer data in peer-to-peer fashion. Subsequently, the base station received data when they came within close proximity.

RatWatch [67] employed wireless sensor networks to observe the social interaction and motion behavior of rats. A sensor node was attached to a lab rat via a special leather jacket, which has a pocket fitted for this equipment. The wild rats lived in underground burrows. Thus, radio propagation was very limited. Therefore, sensor nodes could only communicate when the rats carrying these sensors somewhere in the burrow limiting the realization of RatWatch. As a result, sensor nodes were only sporadically connected and the topology was highly dynamic, making their deployment scenario significantly different from the typically envisioned networks. Data is gathered with a simple epidemic-like (flooding) to the sink node, which often leads to a low energy efficiency in the overall network.

In 2007, Yasar et. al. [2] proposed a Mobile Biological Sensor (MBS) based wildlife monitoring system, utilizing animal behaviour to assist in early monitoring of forest fires (Figure. 2.1). The main idea presented in this paper was to utilize animals as sensors by tagging them with body sensor devices to monitor their behavioural changes. The animals used in this monitoring system are native to the forest. The attached sensors (thermo and radiation sensors with GPS features included) measured the temperature and transmit the location of the animals.

MBS utilized wireless access points to relay data to the central system which further classifies actions of the animals. Continuous panic in the MBSs shows that a problem with the animal is occurring and should be investigated. A challenge with

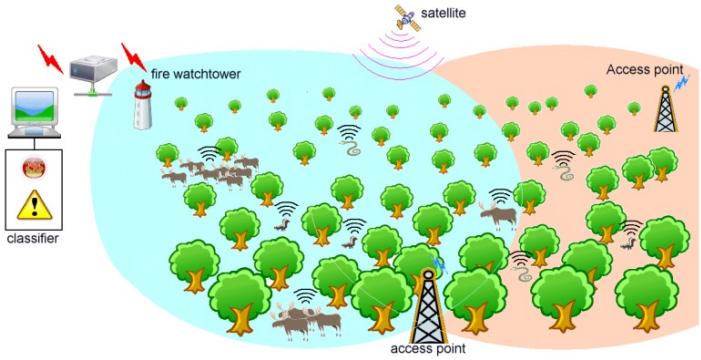

FIGURE 2.1: *Forest fire monitoring system's infrastructure [2]*

this concept emerges when a considerably large number of animals are to be monitored. A lot of animals need to be tagged, which requires the capture and sedation of the animals. Data is collected with a simple flooding protocol, which creates a large routing overhead, therefore, high latency, and high cost of deployment for tagging individual animals in the park. Possibly limiting its applicability to large scale wildlife monitoring applications.

2.2.2 Perimeter monitoring

Wittenburg et al. [52] attached a small number of ScatterWeb [68] sensor nodes to a fence with the goal of collaboratively monitoring and reporting security-relevant incidents, such as a person climbing over a fence. The sensor nodes were equipped with an accelerometer that was used to measure the movement of the fence. For routing the collected data, they implemented a simple spanning tree routing algorithm with the base station being the root of the tree. The sensors share information within an n-hop neighborhood and collaborate in order to distinguish a nuisance alarm from a real alarm. In their current implementation, there is no mechanism to ensure a reliable delivery of events within the neighborhood. Another problem with this work is that the failures of the individual nodes results in variation of the average node degree of the network, thus, adversely affecting neighborhood event monitoring.

Dziengel et al. [69] developed a WSN based monitoring system. In their research, they utilized the DSR routing protocol [70], where all network routes are already pre-configured. They utilize a battery supplied relay node (RN) in the WSN, which is responsible for transferring packets wirelessly during the last hop to the gateway node at the control center. If the RN fails or overloaded, the WSN has to find a new route with a possibly increased number of hops to the gateway. If no alternative route is available the WSN cannot communicate with the gateway anymore. Hence, the RN represents a natural bottleneck in this approach. The authors concluded that a relay node can achieve a high network life-time when the communication to a control center can be reduced by cooperating with other peer nodes.

Cambron et al. [51] proposed a fence equipped with motion sensors and a laser curtain to monitor poachers when crossing a fence bordering the Kruger National

Park (KNP). The laser can cover segments up to 500 m and the motion sensor covers wide areas near the fence. After a potential poacher was monitored authorities are alerted wirelessly so that they can intervene and stop the individual. If the crossing occured in area outside of cell phone coverage a radio frequency message is sent using the peer-to-peer ZegBee network.

Rothenpieler et al. [71] designed a wireless sensor network with infrared sensors that is able to monitoring an intrusion. The system is triggered by an alarm when an intruder being monitored crosses the perimeter. The data-link layer includes a CSMA based transmission scheme that is capable of emulating the IEEE 802.15.4 radio interface. The authors developed an algorithm to first monitor any unusual movement across the perimeter and then fine-tune the triggered signal locally in the network to eliminate false alarms and eventually sending the alarm to central authority. They present simulation results of networks containing 2000 nodes and validated the results with their first prototype network that contained 16 nodes.

Aseeri et al. [72] discussed a method to improve data security in small and energy efficient WSN that was used for border surveillance. They argue that information collected from Wireless Sensor Network (WSN)s is crucial in making border surveillance decisions. They simulated a distributed sensor network and analyzed possible attack scenarios such as sensor destruction or signal jamming. In this work the authors presented a neighbouring peer trust based communication model that can maintain a high level of security in a WSN.

He et. al. [42, 43] designed and implemented an energy-efficient surveillance WSN. Their system allows a group of cooperating magnetic sensor devices to track the positions of moving vehicles. They evaluated the performance of their system on a network of 70 MICA2 motes equipped with dual-axis magnetometers, distributed along a 85 m long perimeter, on both sides of a grassy path. From the experiments, they determined that these magnetometers can sense a small magnet at a distance of approximately 30 cm and a slow moving car at a distance of approximately 2.5-3 m.

The authors tackled the trade-off between energy efficiency and surveillance performance by adaptively adjusting the sensitivity of the system. The key parameter they use to do this is the Degree of Aggregation (DOA), defined as "the minimum number of reports about an event that a leader of a group waits to receive from its group members, before reporting the event's location to the base station". Increasing the DOA leads to less false alarms and messaging overhead but increases the reporting time from a local cluster to the gateway. Thus, an optimization problem is to find the optimal DOA to achieve an acceptable report latency whilst minimizing the messaging overhead and false alarms.

Kim et al. [41] prototyped a wireless sensor network based system for perimeter surveillance. They developed the system on ANTS-EOS (An evolvable Network of Tiny Sensors - Evolvable Operating System) [73] architecture which is adaptive to changing network conditions. They integrated sensors located on a fence and on the ground with a mobile robot, an Unmanned Aerial Vehicle (UAV), and a visual camera network to monitor the fence. All sensor-nodes were installed with acoustic, magnetic, and Passive Infrared (PIR) sensors to monitor intruders. Seismic sensors were installed on the ground nodes and piezoelectric sensors on the fence nodes.

When the energy of a sensor is above the real threshold for a longer period, the node will signal that an intruder has been monitored. The system seems to be very complex when it is scaled up due to the large amount of different sensors that have been used in this approach.

Sun et al. [60] introduced BorderSense, which utilizes sensor network technologies, including wireless multimedia sensor networks and wireless underground sensor networks. BorderSense is a system that coordinates multiple technologies such as unmanned aerial vehicles, ground sensors, underground sensors, and surveillance towers equipped with camera sensors to monitor intruders. The sensors are responsible for more complex tasks such as collecting the sensing reports from the ground/underground sensors, monitoring possible intrusion according to the sensing reports. Due to the number of sensors it needs to be deployed, the cost and coverage is less suitable for WMS.

Arora et al. [44] proposed a WSN with metallic object monitoring capabilities. The sensor nodes utilize magnetometers and micro-power impulse RADAR sensors. Metallic mobile intruders such as vehicles are monitored. They use pulse doppler sensors as their RADAR platform. These sensors can identify the intruder from up to 18 m distance. The sensor nodes cooperatively network among each other, to intelligently decide if the mobile event is metallic or non-metallic. The authors tested their performance in a confined perimeter within an area. To accomplish this task, the authors recommend that accurate periodic time synchronisation should be maintained among the individual WSN sensor devices. They propose to use a master node that would be responsible to send periodic synchronisation values. The authors implemented the so called 'influence field', which represents the sensor nodes that simultaneously hear the moving intruder or object and autonomous predict the pattern of movement.

He et al. [3] described their current implementation of networked eMoteNOW sensor nodes that utilize BumbleBee micro-power RADARs in [74]. These RADARs have an omnidirectional sensing range of 10 m. The implementation is being used in an ongoing human and wildlife protection WSN in the Panna Tiger Reserve in Madhya Pradesh, India (see Fig. 2.2).

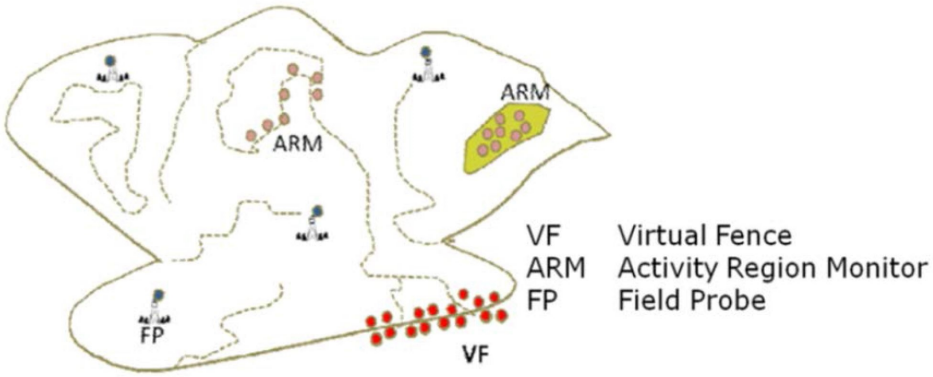

FIGURE 2.2: *Architecture Panna Wildlife Protection Project [3]*

Aseeri et. al. [72] prototyped a WSN based system for perimeter surveillance. They developed a system architecture which is adaptive to changing network conditions. The system appears to be very complex to scale up, due to the large amount of different sensors involved in generating data traffic that have been used in this approach. The work tackle the trade-off between energy efficiency and monitoring performance by adaptively adjusting the responsiveness of the system for different activities.

2.2.3 Area monitoring

In area monitoring, sensors can be buried a few centimeters below the surface to deploy a WSN around a fixed area on the ground. Because these types of systems are usually hidden, they are often used where a fence would be considered obtrusive. Wildlife such as warthogs dig a lot of holes, especially underneath fences [75]. This means that a buried system in a wildlife park has a higher probability of being damaged. Similar to the perimeter monitoring techniques, these WMS solutions are primarily based on IEEE 802.15.4 wireless protocol [27, 76].

Souza et al. [77] proposed a WSN based framework for wildlife tracking for the purpose of event monitoring in their territorial habitats. They divided the field area into clusters of networks by deploying fixed sensor nodes on the ground to predict the path followed by the target being tracked. Their system monitors animals then computes their current location and predicts the next possible position. The main data learning and processing is performed centrally. Due to low reliability in the sensor data collection and energy limitations, implementation of this solution by only using clustered wireless sensor networks have been a challenge to real-time applications such as WMS.

Zhang and Jiang et al. [78, 79] utilized an ultra wide band based WSN to monitor intruders in forested areas. Their work shows the potential to use off-the-shelf Ultra Wide Band (UWB) transceivers to monitor an intruder. They proposed to utilize a combination of principal component analysis (PCA) [80] coefficients and the channel characteristic parameters from the received waveform to monitor intruders. This resembles a passive RADAR on the receiving end. The authors used a Support Vector Machine (SVM) [81] based classifier to classify the type of intrusion. They claim that the proposed system distinguishes an armed from an unarmed intruder through analyzing the effects of metal on electromagnetic waves. Through extensive practical evaluation of their system, the authors claim their method to be efficient, accurate and robust in identifying the target in dense forests.

2.2.4 Long-range monitoring

In this subsection, we discuss the existing WMS works and wildlife conservation organizations utilizing long-range wireless technologies.

Antonin et al. [82] presented AMBLoRa to monitor and follow the terrestrial and underwater activities of animals. They were able to introduce a GPS tracker system

using LoRaWAN network. AMBLoRa is a complete IoT system that allows wildlife researchers to visualize the relative real-time data from GPS tracking collar using LoRa communication. According to their first test, they concluded that AMBLoRa has achieved the long-range communication, low power consumption, easy of deployment and relative real-time visualization. However, the energy consumption, and real-time data visualization is still in its initial stage and not clearly defined. They log the GPS position for a certain amount of time. But, there is a delay due to all the processes involved in data sending and displaying chain. Moreover, they only tested it with one collar while it is essential to further develop a large scale experiment with more GPS trackers. The physical size of AMBLoRa is still too large to collar it on the animals.

In [83], the development of LoRaNET, a LoRa based mobile wireless network for underwater animal monitoring, is discussed from the hardware and firmware perspective. The authors claim these two developments, applied to the SIMMA end-devices, provided an easy-to-use and low power solution, with an extended range of several kilometers, and a more cost-effective alternative with fewer infrastructure requirements. Furthermore, LoRaNET could serve as a less invasive method for monitoring natural protected areas and reservoirs. The integration of the LoRa communications as a single system, adds a the required flexibility to current animal monitoring systems and the possibility of studying geographically remote areas given LoRa radio's long-range communications coverage.

There are several organizations working on wildlife monitoring utilizing GPS tracking and LoRa. For example, in [84], animal conservation with LoRaWAN is discussed. This solution is demonstrated to monitor animals such as turtles, fishes, etc. They implemented the system primarily as part of LoRaWAN The Things Network (TTN) infrastructure [85]. Similarly, in [86], LoRaWAN network based *Smart-Park* has successfully been implemented with loRa sensors implanted inside the horn of rhino and as well as using geolocation for greater tracking accuracy. They are also using GPS in combination with LoRaWAN in other wildlife tracking applications where bigger batteries and/or solar cell are available as required. Currently, they are operating a number of large smart park networks in several national parks across Africa to help protect endangered wild animals.

All these LoRaWAN projects have the following similar components: (i) the location/GPS module and (ii) the LoRa radio transceiver module. LoRa radio is very suitable for a low power long-range radio coverage, however, if a real-time location information is required then LoRaWAN might not be suited unless it is combined with other wireless technologies. For very remote areas, LoRaWAN infrastructure could be extended with *Iridium satellite* modems to send data from anywhere in the world. Furthermore, Lacuna [87] is launching low earth orbiting (LEO) LoRaWAN gateway satellites, to provide coverage for blank-spots of moving devices as they pass through remote regions. Lucana works with LoRa sensors to transmit a signal directly to a passing LoRa gateway satellite, the signals use a LoRaWAN network protocol. The lucana satellites are low-cost cubesats (about the size of a shoe-box) and fly in a 500 km orbit, circling the earth fourteen times each day. Then the received messages are relayed automatically from the ground station to lucana cloud

platforms. These organization is still in its early stages of their deployment, but they promise a high internet connectivity provision in the long-run.

Alternatively, satellite telemetry has been used extensively in tracking of animals since the 1980s [88]. After an animal has been captured and a tracking device is attached as collar, thus, researchers can monitor movements of that individual animal for extended periods of time without having to recapture it. Satellite telemetry uses Platform Transmitter Terminals (PTTs) that are either attached externally [89] or surgically implanted [88]. The PTTs then communicates via radio-signals to orbiting satellites, which will localize the signal and give positional fixes (latitude and longitude) on the PTT, and thus, the animal [89]. The satellite telemetry, however, often requires an expensive monthly subscription, which is a possible setback for projects operating on a smaller budget. Furthermore, as the satellites do not pass over a particular location at a constant rate, it may not be possible to obtain sufficient location data to accurately determine movements of individual animals [89].

A lot of useful information about animal migration can be obtained from satellite telemetry. Miller et al. [90] used satellite telemetry to elucidate the chronology, migration routes, and the most important stopover sites of adult female northern pintails (anas acuta). Another study showcasing the value of satellite telemetry used animals with subcutaneous transmitter implants [91]. This study helped to determine temporal and spatial patterns of movement of loons during migration, and identified the staging areas, critical stopover sites, and wintering grounds. Kenow et al. [91] also noted that southward departure in the fall coincided with low-pressure weather systems.

Use of satellite telemetry in conjunction with Bio-telemetry provides insight into wild animals behaviour. However, bio-telemetry does not usually provide information on an animal's location. Combining GPS satellite and bio-telemetry systems can link spatial and temporal activities with behaviours, giving novel insight into animal movement behaviours [92].

Recio et al. [62] also demonstrated the application of Global Positioning System (GPS) tagging of wild animals to track the different behavioral changes in animals, mainly to asses the main environmental, technical and behavioural causes of error in lightweight GPS-collars suitable for medium to small terrestrial mammals. GPS tracking allows localization of animals in areas where there is low accessibility to other infrastructures. It does not prevent poaching incidents but is mainly meant to track animals' position.

A GPS telemetry implementation is further extended in Project RAPID [4]. The researchers have demonstrated the usefulness of GPS in rhino poaching prevention with GPS communication to track down poaching incidents and alert the park rangers. They also installed a camera system on the horn to capture the poaching event for criminal conviction purposes. GPS satellite collars and VHF radio techniques have been combined to improve the tracking and monitoring capability of GPS systems in [93] (Fig. 2.3). However, these solutions incur the low communication reliability and data update accuracy problems of the conventional GPS integration. The authors use the satellite to relay real-time information and monitored

FIGURE 2.3: *The camera component implanted in the front lobe of the rhino's horn [4]*

events to the central system for analysis. The high latency or response time associated with this communication system makes it difficult to prevent the poaching incident before it happens. The legal and ethical issues involved with drilling the rhino horn to implant the visual camera also hinders its practical implementation in real world scenarios (Fig. 2.3).

The main limitation of both the satellite/GPS telemetry is that they do not function if the line-of-sight (LOS) signal path is blocked (e.g., by dense forest canopies or natural topography) [88, 89]. Positional fixes of wild animals can thus only be obtained during a brief periods when the satellite is available, and the PTT or GPS device itself is in line-of-sight. In addition, the size and mass of transmitters can pose a challenge for small animals. As a rule, a transmitter's mass should not exceed 5% of the animal's body mass [89]. This is important, as carrying heavy transmitters interferes with the natural living behaviour of animals. Moreover, satellite based systems have been found to be suitable for WMS to track and monitor wild lives, however, the inherently high cost and intolerable communication latency makes these approaches less attractive for WMS.

2.2.5 Hybrid monitoring techniques

Paul et. al. [13] proposed a novel tracking method that could be used to implement real-time WMS. They designed an WMS module fitted with miniature devices to detect a poaching incident and locate the poaching event and rhino positions in real-time. A camera device is implanted in the front lobe of the rhino's horn. Multiple body sensors continuously monitor the physiological behaviour of the animal. When an on going active poaching event is sensed, the GPS device sends the location of the rhino.

Meanwhile, data about the poaching event is directly sent to the central system to alert the rangers to arrive at the poaching location in the hopes of saving the rhinos. Such systems will significantly increase the chances of successfully catching the poachers. In combination with other WMS techniques, this approach could lead to a more robust WMS solution to fight the poaching schemes. However, this kind of WMS is non-preventive, meaning it usually does not save the rhinos before being

poached to death. But it will help in the criminal prosecution of the poachers by keeping a video record. Moreover, locating the rhino's position might be dangerous, because of corruption this valuable information might fall in the hands of the poachers themselves.

Similarly, in a concept paper Banzi et al. [61] suggested to utilize wild animals behaviour to stop poaching. They proposed to protect elephants from poaching by attaching an appropriate sensor on their body with a visual camera, infra-red camera, and GPS. In their concept, access points received mobile node's locations continuously and sent it to a central computer using long-range radio system, where it was stored in a database. A classifier continuously indexed to a central database to determine any abnormalities in the behaviour of the mobile nodes. Using artificial intelligence tools, a classifier attempted to determine whether or not there were abnormalities in animal behaviour. A sudden panic of animals caused an abrupt change in the graph of a classifier in the central computer, this showed a potential incident and the system responded by first rising an alarm, and then displaying the current GPS location.

An alternative collar based solution is proposed by Intel, as a contribution to a conservation effort in the Madikwe Conservation Project [94]. A kevlar-based ankle collar was attached to the rhino's ankle during a pilot project with 5 black rhinos. The collar contains Intel's Galileo board that is used to track the rhino's location and can communicate through a long-range connection. A durable solar panel is attached to the collar to recharge the batteries. An RFID chip was placed inside the rhino's horn, when the chip is out of reach of the Galileo board an alarm is triggered and Anti-Poaching Team (APT)s are alerted via the long-range connection. They can then rush to the scene with helicopters, drones or other vehicles. This approach requires to tranquilize the rhino to attach, repair or remove the collar, and each time the Radio-Frequency Identification (RFID) grow out of the horn. This system is only helpful to try and catch the poachers. It does not save the rhino from being shot directly. It can be argued that the improved poaching detection causes more fear of being captured and will eventually stop more poachers from any poaching activity.

2.3 Discussion

A comparison overview of the wireless monitoring technologies is shown in Table 2.1. Throughout the surveyed works, it became apparent that currently there is no single wireless solution that is entirely suitable for wild animal monitoring. This is mainly because wildlife monitoring poses multiple requirements and challenges. For instance, none of the reviewed works provide high monitoring reliability and low response times that are needed. Thus, increasing the reliability and responsiveness of an WMS remains a general open issue.

In addition, using wireless technologies to cover large forested areas in rugged terrains against intruders proves to be a daunting challenge. There is a need for new approaches that take up the research challenges and provide better protection

TABLE 2.1: *Overview of wireless technologies for wildlife monitoring system*

WMS solutions	*Energy*	*Reliability*	*Latency*	*Coverage*	*Robustness*	*Scalability*	*Deployment*	Features	Adv.	Disadv.	Ref.
Animal sensor tagging	×	×	×	✓	✓	✓	×	• attach various sensors (cameras, motion, GPS, etc.) • monitor physiological activity	• large area coverage • timely rangers notification • intruder identification	• many sensors needed • deployment difficulties such as power usage and collaring • difficult to differentiate between animals • high chance of animal killed • exact rhino location data is prone to corruption	[2, 66, 4, 67]
Perimeter monitoring	✓	×	×	×	✓	✓	×	• fence motion sensors • sensor networks of (infrared, magnetic, accellerometer, gyroscope, etc.)	• electrified fences • commercial • classification and localization of intrusion • up-to 1000 m range • no power needed along perimeter	• linear detection zone • intruders can enter through main gate, e.g. disguised as tourist operators • many sensors needed • expensive • large overhead • pron to false alarm	[41, 42, 43, 44, 51, 52, 60, 68, 69, 70, 71, 72, 73, 72]
Area monitoring	✓	×	×	✓	✓	✓	×	• Fixed sensor node placement of (motion, RADAR, microphone, light intensity, magnetometers, UWB	• not limited to linear zone • improved animal tracking	• prone to damaged by wild animals • many sensors needed • limited range • deployment difficulties such as power usage and destruction of nodes	[27, 75, 76, 77, 78, 79, 80, 81]
Long-range monitoring	✓	×	×	✓	✓	✓	✓	• uses long-range radios • used to track terrestrial animals	• large area coverage • low energy • easily deployed • scales well	• only low data-rate applications • high latency	[62, 82, 83, 84, 85, 86, 87, 88, 89, 90, 91, 92, 93]
Hybrid monitoring	✓	✓	✓	✓	✓	✓	×	• combination of multiple wireless technologies	• real-time monitoring • relatively accurate animal location • large coverage area • low power	• monitoring endangered animals' position might be dangerous, prone to corruption. • open research issues	[13, 61, 94]

Legends: '✓'= Satisfy, '×'= Does not satisfy, '(n/a)'= Not applicable.

against intruders or poachers. For most sensor systems high spatial and temporal resolution is a very costly requirement because they scale up poorly or are too slow for the large conservation areas. Hence, the development of hybrid wireless systems, through the combination of opportunistic networks and low power long-range wireless technology, will be able to tackle the challenges outlined in WMS.

Moreover, the available energy source for each sensor nodes is limited and scarce in WMS, thus the node should be able to mange their energy source locally. It should not merely sense the environment, but make decisions locally and collaboratively with other sensors in the neighborhood. For example, the lifetime of a wireless sensor that runs on a battery can be extended by transmitting only data when it is perceived as important. Additionally, when data is transmitted over longer distances, energy of multiple nodes can be saved when sensors cooperate and prune received data prior to sending the aggregated data over a longer distance with a low power long-range radio.

Finally, in our research, satellite communication for WMS have been found to be invaluable technique, especially for providing a GPS location data. However, the main challenge in utilizing satellite for WMS is their high energy consumption. They can still provide a complementary benefit in combination with other techniques by providing the ground truth location of the area for monitoring the animals efficiently.

2.4 Conclusion

In this chapter, we investigated several wireless wildlife monitoring solutions. Several existing wireless technologies are explored and compared for WMS applications. Most the technologies are noted to have a relatively high latency and energy consumption. This will make them less suitable for wildlife monitoring, where energy resources are very limited. Furthermore, low power long-range and satellite technologies are also explored. Most of the discussed wildlife solutions utilizing single technique was found to be insufficient in monitoring wildlife. Based on this study, we suggest the utilization of hybrid wireless solution by collaboratively combining opportunistic sensor network with long-range low power technology for efficient WMS. It is our believe that the long-term solution for the animal poaching problem is to eradicate the drivers of demand. People in the demanding countries should be made aware of the poaching crisis. Until these kind of actions take effect there will be a continuous urgent need for effective WMS solutions that assure the survival of endangered animals such as rhinoceros and elephant species.

Chapter 3

Review of Existing Multi-hop and Opportunistic Network Protocols

---

In wireless sensor network based WMS, sensor nodes could be mobile, especially involving collared animals. Dealing with such animal mobility can pose some formidable challenges, particularly, wireless protocol design at the medium access control (MAC) and routing layer. These difficulties require mobility adaptation algorithms to estimate the quality of link that can be established between two nodes. Hence, this section discusses the current state-of-the-art work on wireless multi-hopping and opportunistic network protocols. Furthermore, we present the existing wireless communication protocols suitable for WMS application.

3.1 Adaptive multi-hop protocols

Adaptive MAC protocols suitable for WMS could be broadly categorized into the following schemes:

- Synchronous schedule-based network protocol
- Asynchronous contention-based network protocol

3.1.1 Synchronous schedule-based network protocol

In synchronous schedule-based approach, the medium access is synchronizing by allocating all of sensor nodes within a scheduled time-frame [95]. This approach offers collision-free transmission and communication because of established time-schedules. This will largely reduce energy consumption and boost the efficiency of the network throughput. However, time synchronization is also a necessary factor for time schedule among the nodes. Any error in the synchronization process could lead to network efficiency decline or sometimes even failure in network operation. Performance evaluation of synchronous schedule based protocols have proved that they are able to deal with slow dynamicity in network topology [95].

As traditional time-slot reservation algorithms are computationaly complex as well as non-adaptable, researchers have been exploring efficient schemes [95]. For instance, for sensor network applications, an efficient mobility-aware MAC protocol [MS-MAC] is discussed in [96]. At the start of the LISTEN phase, a SYNC packet is broadcasted during each predetermined cycle time-frame by the synchronization (for instance, 5 seconds for virtually every 1 min). A sensor node starts the schedule by listening for some amount of time. In case none of the SYNC packets is received during this time schedule, the node is going to sleep for a random time period and at the same time broadcast the information. Nevertheless, the node will adopt both schedules in case if a completely different schedule is received by the node after already selecting one.

To increase the node versatility, a Medium-Access-Controlled-Protocol (MMAC) is suggested, which proposes a collision-free and adaptive mobility agent [97]. MMAC is synchronized as schedule-based MAC protocol network [97]. MMAC adapts a flexible time-frame rather than the pre-set fixed time-frame thus enabling a mobility adaptable network protocol as well as making it well suited for wireless sensor network environment. In this scheme, time-frame is split up into epochs and each individual epoch is comprised of 'm' casings i.e 'm' is any integer that is greater than one. At the start of every time-frame, all the network nodes estimate their own mobility pattern or state at different time-frames and then the subsequent time-frame is determined by the $AR1$ mobility estimation algorithm [97].

Moreover, to deal with the network mobility, the authors introduced Mobi-Sense in [98]. MobiSense sets up a super-frame within a Synchronization slot, admission mini-slots, downlink and uplink data transmission slots, and discovery slots. All

of the cluster heads transmit SYNC packets at the start of every time-frame to notify sensor nodes with regards to the channel it uses for communication, the current cluster size, and the timing of its access window. Within the prevalent channel, the probe is delivered by every cluster head to deliver data regarding the channel. The channel is selected based on a few parameters as access to window timing, the cluster size and the communication. Data statistics of the network are collected by engaging with these time slots as the nodes meet or one cluster replicated data to another thus indirectly building a prioritized list of access points. As the discovery slot size is fixed, the nodes only listen for the predetermined period. Immediately after collecting network information, an access mini-slot is picked up by a mobile node which leads to the next step of join request message. For a low contention scenario, the collision probability is low, hence MobiSense accomplishes an instant network convergence as well as minimal latency. Moreover, 2-way data transmission and communications is achieved through downlink and uplink slots.

Jhumka et. al [99] present M-TDMA, an energy-efficient low duty-cycle MAC protocol that enables access to the physical layer for a hierarchical topology consisting of nodes communicating with master nodes, which in turn communicate with the monitoring station. This hierarchical-topology eliminates the demand for sensors to spend high energy by simply sending data to the monitoring station. Another main advantage of using TDMA is a collision-free transfer system as well as it has minimum idle-listening. The performance test results indicate that the protocol is highly energy efficient for small burst data communication.

3.1.2 Asynchronous contention-based network protocol

For asynchronous contention based MAC protocols, the random access of the physical medium is carried out by a Carrier Sense Multiple Access/Collision Avoidance (CSMA/CA) scheme or its derivatives. The collision avoidance is performed by setting a back-off counter to a random integer.

Authors in [100] presented B-MAC protocol which renders typical properties of a mobile network with tolerance to network changes. B-MAC has relatively high data reliability [101]. However, it also suffers from high energy consumption and computational overhead due to its frequent data transmission to lower the effect of data collision. Likewise, X-MAC [102] is a MAC protocol based on BMAC with asynchronous listen-intervals. For each packet, X-MAC transmits a short strobe of preambles, between which the receiver can signal reception-readiness with a so-called EarlyACK. X-MAC derives a formula for optimal wake-up/sleep intervals given data traffic at a certain fixed rate and outlines a mechanism to adapt the duty cycle to best accommodate the traffic load in the network. Since the basic mechanism of X-MAC still requires a certain fixed minimum interval between two active intervals and a generally high overhead per-packet, both its latency and energy consumption are high. As such its is applicability is limited to situations with low node movement.

A-MAC [103] is a receiver-initiated asynchronous MAC protocol that aims at handling variable traffic. Receiver nodes frequently wake up and send out probing beacons for polling possible incoming data without using preamble packets. A-MAC enhances throughput by reducing medium occupation interval. However, it suffers from packet collisions when there are multiple senders. A-MAC throughput is acceptable for applications with many bursts or heavy traffic.

Wang et al. [104] proposed an off-line data-driven MAC protocol which is initialized by fixed duty-cycle duration for different packet rates as required by specific scenarios. For every packet arrival rate, it sets a specific duty-cycle duration and transmission power level. These information is stored locally in a table, based on which every sensor node autonomously selects its duty-cycle at run-time. This procedure is not suitable for a network which experiences high trend of topology dynamics [104]. Likewise, Ayele et al. [101] suggested a theoretic control model to determine the optimal duty-cycle in a wireless sensor network.

pTunes [105] is a centralized protocol to adjust the MAC layer settings on-line in such a way that an appropriate trade-off between network lifetime and application requirements in terms of end-to-end reliability and latency can be found. It employs a flooding algorithm to disseminate information pertaining to the state of the network. The optimal MAC parameters are determined centrally out-side the network. The disadvantage of pTunes is that it has large communication overhead for monitoring MAC layer parameters centrally and flooding the adjusted settings back to the nodes. To reduce such overhead, Challen et al. [106] proposed a decentralized MAC protocol by arguing that local changes in the state of the network often affect local nodes only, therefore, it is sufficient to optimise MAC parameters locally. Unlike pTunes, Challen et al. [106] focuses on minimizing the energy consumption of the network and does not consider other constraints like latency or reliability. Each node maintains a vector of combined energy load and calculates the optimal trade-off between energy and network utility.

Li et al. [107] proposed a distributed algorithm to control the duty-cycle duration of nodes by employing convex-optimization. Nodes adjust their sleep time locally by exchanging their current duty-cycle interval and energy consumption with their neighbors. The algorithm is self-adaptive for different traffic loads. However, the work does not reveal the overhead cost of exchanging information. Authors of [101] and [108] proposed effective queueing models in a feedback control system to dynamically adjust the duty-cycle interval of a node. When the pre-defined queue size is reached, the MAC protocol sets a duty-cycle that leads to low energy consumption and delay. Although analytic and simulation results confirm usefulness of these types of models, they are often too complex for practical realization.

3.1.3 Discussion

In Table 3.1, we provide a comparison of mobility-aware network protocols. Asynchronous preamble-based MAC protocols such as [110, 102, 111] avoid the need for

TABLE 3.1: *Comparison of MAC protocols against of WMS requirements, (energy consumption, reliability, and latency)*

MAC protocol	Characteristics					
	Energy-efficiency	**Reliability**	**Latency**	**Access-mechanism**	**Adv.**	**Disadv.**
MS-MAC[96]	×	×	✓	*Sync.*	Adaptive frequency Sync.	Higher energy consumption.
MMAC [97]	×	(n/a)	✓	*Sync.*	Dynamic time-slot allocated.	High energy consumption.
MobiSense [109]	×	×	(n/a)	*Sync.*	Rapid network info. gathering. Allows multi-channel communication.	Requires high sensor resources. High collision, low reliability.
M-TDMA [99]	×	✓	×	*Sync.*	Guaranted collision-freedom.	Increased Energy consumption and high latency.
B-MAC [100]	×	✓	×	*Async.*	Contention based MAC.	High energy, memory and computational overhead.
X-MAC [102]	×	✓	×	*Async.*	Accommodates high data traffic.	High data overhead, latency and energy consumption.
A-MAC [103]	✓	×	×	*Async.*	Enhances energy.	High packet collision and high latency.
Sleep in the Dins [104]	✓	×	×	*Async.*	Adaptive Sync. frequency.	Not for dynamic network.
pTunes [105]	✓	×	×	*Async.*	Adaptive Sync. frequency.	High communication overhead.
IDEA [106]	✓	×	×	*Async.*	Low energy.	High latency and low reliability.
Li et al. [107]	✓	×	✓	*Async.*	Energy efficient and low latency.	High computational overhead.

Legends: '✓'= Satisfy, '×'= Does not satisfy, '(n/a)'= Not applicable.

periodic synchronization by enabling transmitting nodes to send a burst of preambles. In [112] and [96], nodes update their knowledge about their neighbors by exchanging short strobe of preambles for asynchronous duty-cycled MAC protocols, such as [110, 102, 111], perform well in terms of energy consumption, latency, and throughput [113] for applications of WSN in which nodes move slowly. For high mobility WSN applications, the synchronized MAC protocols will not suffice mainly because of the overhead associated with the re-synchronization process when communication links break [114, 110]. In asynchronous MAC protocols, there is no need to continuously share synchronization information. They rather proactively sample the channel to determine when an activity can be performed. As presented in [114, 110], the overall effective active period for asynchronous MAC protocols could be much shorter than of synchronous protocols. As such their energy consumption may be significantly lower.

3.2 Opportunistic network protocols

The primary objective of communication network system is to deliver data to its destinations. For significant networks, statistics need to be directed down a suitable path among various from a provided reference to a destination. One of the most important features to find data route path is least hop count. Typically, the opportunistic routing network protocols are classified in two as single copy replication and multi copy replication. Among these opportunistic routing network protocols, the single copy replication is rare in opportunistic networks. A typical example of this protocol is 'Direct Delivery (DD) Routing' which deals with the source node directly delivering data to the desired location or destination node [70]. 'First Contact (FC) routing' [70] also falls under these class, it mainly deals with relaying data to the first node it comes in contact and the procedure keeps repeating until the data is delivered to its intended location. The multi copy replication routing scheme includes two sub-categories i.e. limited and Unlimited. In the first one, before data is delivered to a node in close proximity, it is first duplicated for a fixed amount of times. There could be extreme situations where data is replicated to all the nodes within the network. This is true in case of Epidemic (flooding) [115].

In the remainder of this subsection, we briefly look at some of the well-known multi-copy opportunistic routing protocols. The review provides insights about their basic operation characteristics. Furthermore, we also look at the different extensions suggested and updates made to these routing protocols in the literature.

For networks with high partitions, Vahdat et al. [115] suggested Epidemic or Flooding routing network protocol especially keeping for Ad-Hoc networks. This network protocol was based on the spreading of epidemic diseases in real life. Based on this analogy, a node containing the data is considered to be infected. If this node interacts with another node having no information, it transfers its data to the later thus infecting it. Ultimately the data arrives to its destination as a result of infecting multiple nodes in the network. This topology focuses more on data delivery rather than data latency thus increasing the total resource utilization in the network such as be bandwidth or energy [115].

Theoretically, with the creation of n data, the complexity of storage and transmission, will follow a linear increasing trend (i.e it will increase with the number of data). It can be represented as $O(n)$ with variables such as overhead, transmission and storage complexity. To solve this issue, several recovery strategies are suggested including vaccines or immunity. The effects of these strategies were analyzed by various research worker [116, 117, 118, 119, 120]. This is similar to the biological analogy we have discussed earlier such as mostly a person either has developed immunity for a specific disease thus there would be no effect of the disease or there could be the use of vaccine. The aim of these kinds of strategies is usually to make sure of data delivery to different nodes without duplicating and storing. In the Immunity Scheme [116, 117], the process continues by deleting the data from its buffer after delivering it to the corresponding destinations. Furthermore, this scheme also has a prominent feature of keeping the ID of the shipped data to certain node thus reducing the chance of receiving the same data again.

Modified routing scheme for updating Epidemic routing network protocol was introduced by Zhang et al. [117] along with previous schemes discussed before. The idea of natural scaling by different models, e.g. Markov model derived ordinary differential equations have been used by the authors. To ensure data deliver, Li et al. [118] also worked on a two-dimensional continuous-time Markov chain. They analyzed the presence of social interaction on the routing performance outcome.

Opportunistic network protocols can be integrated with immunity scheme to update the Epidemic Routing Scheme as demonstrated by Mundur et al. [119]. Each node stores the data sender IDs with each delivery and develops its own immunity list similar to the summary vector (SV) list. Thus, both lists are interchanged by nodes during a collision. This prevents the node from receiving duplicate data which has been transferred to its corresponding destination.

Opportunistic protocols in which the data is randomly duplicated by a node is termed as (p, q)-Epidemic routing network protocol as introduced by Matsuda and Takine [120]. This topology works by duplicating data from a certain relay node to a corresponding forwarder node having with certain probability ratio. At the same time, source node also replicates data to the relay node again with a certain probability ratio.

Spyropoulos et. al. [121] introduced an Opportunistic network protocol called Spray and Wait (SnW). Its functionality is based on imposing a maximal upper limit on data replicated. There are several types of spraying scheme while processing data. In the 'source' spraying technique [121], the source node itself distributes L copies of a given data up to first L nodes that it comes in contact with which does not already have a copy of the data.

To efficiently end a particular data routing, the data is instantly redirected to the destination node even if it is encountered prior to the probabilistic destination. In any other case, if L nodes come in contact with other nodes, it may exclusively transfer the data towards the desired destination node. Another spraying technique is 'The Binary Spraying Technique' [121] that uses a slightly different principle. With this scheme, the source node is set to have L copies of provided data. It has been shown that the best technique among from the Spray and Wait routing mechanism

is the Binary Spraying Technique. It tends to provide more efficient results interms of a minimum delay when compared with other techniques.

SnW protocol is noticed to combined the Epidemic protocol's speed and Direct Delivery's simplicity [121]. Thus creating a trad-off between single copy and multi copy routing protocol. Sensor nodes' transmission range and network size do not affect the delay that results in minimum 'L' value. But the actual cause of delay is the quantity of nodes in the network facility. Consequently, in scenarios when significant network parameters are unknown, even then the value of 'L' can be estimated. Another highlight of SnW network protocol is the fastest sprayed data copies in correlation with the nodes' neighbourhood [121, 122].

The probability of encounter and data delivery could decline if node movement is limited [123]. Even-though SnW is a fast and resource-friendly protocol, mobility issues could put a restriction it performance. To solve this obstacle, the Spray and Focus (SnF) Algorithm is introduced based on timer transitivity principle [121, 122, 124]. Both SnF and SnW algorithm have similar spray phase [122]. Nevertheless, SnF has a 'wait phase' in contrary to SnW which forward decisions based on timer utility.

Among the probabilistic routing protocols using history of encounter and transitivity, the PRoPHET maintains a significant improvement. It was proposed by Lindgren et. al. [125], by introducing the node encounter probability value termed as delivery predictabilities or DP [125]. A probability table is maintained to record each encounter probability. Furthermore, the DP values are self-adaptable such as with unexpected delay in one node encounter, the DP values for other node changes accordingly. Thus resulting in a high DP value for nodes with frequent encounters.

ProPHET was improved several times and also it was used as a base for many subsequent protocols. Huang et al. [126] proposed PRoPHET+, an upgraded version of PRoPHET. It do not only deal with DP but also engages other important performance metrics such as buffer capacity, energy consumption, and popularity. Moreover, along with these metrics, some significant factors are taken into account appropriately to identify the deliverability of a node based which data is replicated. It is among the main factors based on which the data is replicated. PRoPHET protocol is also integrated with other protocol for ensuring data distribution using trust-based mechanisms as proposed by Li and Das [127]. It was observed to be energy efficient.

The PRoPHET is a significant protocol considering its features, however, Grasic et al. [128] found out that DP values may not lead to desired netwok peformance when dealing with real-world node movement. It was observed that protocol could sometimes show high DP values when in reality they were not at all desired. In reality, the devices had multiple reconnection among themselves due to fluctuating wireless signals, which were treated as 'new' encounters. Thus to solve this issue another modification was added in PRoPHET by Grasic et al [128], to stabilize the balance between unpredicted amplification of the DP [128].

Encounter based routing (EBR) network protocol has been proposed by Nelson et al. [129]. TheyHe observed that some nodes have a greater encounter chance as compared to other nodes within the same network. EBR network protocol features

a small overhead enhancing the data delivery rate. It also uses protocol a quota based replication strategy, which deals with the maximum data replications without depending on the total number of nodes within the network. EBR aims at decreasing the routing overhead by diminishing the data replicas. Exponentially weighted moving average method is used in this protocol for maintaining the average encounter rate with the nodes within the network. The performance evaluation of EBR carried out under diverse event scenarios indicates an upgraded data delivery reliability in comparison with the Epidemic and SnW protocols. Thus EBR can be considered as a sensor resource-friendly protocol.

In most trivial routing network protocols, retaining a comparable data delivery ratio is a challenge, hence, contact based routing (CBR) protocol [130] is presented which significantly decreases the average data storage time period at a particular node while keeping high data delivery. In CBR, for every encounter, the node pair exchanges information such as contact frequency with other nodes. Based on these frequency of contacts, each node identifies the relatively better candidate nodes, and forwards their data to the such nodes.

Contact history maintenance along with candidate node selection are the two main metrics of CBR protocol. With every node encounter, the data or contact count is stored and updated in a contact list table for future preferences. Consequently, the most suitable node for the encounter is identified for each data recorded in the buffer, and this data is redirected to the identified node. The underlying strength of each node is driven by the encounter frequency only in the case of CBR. Hence, when a node encounters multiple receiver nodes, it selects the one that has maximum encounter frequency, and replicates a data to that node.

Erramilli et al. [131] proposed Delegation Forwarding (*DF*), a simple algorithm that can be used to decrease the overhead of data delivery. This technique was proposed by Erramilli et al. [131]. DF forwards the provided data to its desired destination by assigning a quality metric to each node. It works by determining the probability ratio of a node. To determine central node parameters signifying the node quality, different metrics are discussed, such as rate of encounter, last time of contact with any node, destination-specific frequency of encounters, and destination specific last contact time. Rate of encounter does not depend on the data destination. Experimental results indicated that the data delivery overhead obtained using *DF* is remarkably less when compared to other routing protocols. Nevertheless, such an optimization technique seems to come with a significant trade-off. The data delivery latency is significantly increased as the node have to wait for an optimum node to duplicate its data. Even so, when the focus is overhead delivery rather than delay DF is appropriate solution.

3.2.1 Discussion

Table 3.2 presents a summary of the opportunistic protocols discussed so far. We used the concluding remarks of each opportunistic protocols as detailed in their respective work to compare them with respect to the network requirements of wildlife monitoring such as energy efficiency, reliability, and latency. Most of the protocols

TABLE 3.2: *Comparison summary of opportunistic protocols*

Opportunistic protocol	Characteristics						
	Energy-efficiency	**Reliability**	**Latency**	**Routing intelligence**	**Max replication**	**Routing storage** OH^e	**Routing** OH
Epidemic [115]	×	✓	×	(n/a)	Unlimited	0^a	0
PRoPHET [125]	×	✓	×	Delivery Predictability	Unlimited	$O(n)$	$O(n)$
PRoPHET+ [125]	×	✓	×	Delivery predictability, buffer capacity, popularity.	Unlimited	$O(n)$	$O(n)$
Spray and Wait (SnW) [121]	×	✓	×	(n/a)	Limited (L)	0	0
Spray and F (SnF) [122]	×	✓	×	Timer transitivity	Unlimited	$O(1)$	$O(1)$
Encounter Based Forwarding (EBR) [129]	✓	✓	×	Most encounters	limited	$O(n)$	$O(n)$
Contact Based Forwarding (CBR) [130]	✓	✓	×	Neighbor with most encounters	Unlimited	$O(1)$	$O(1)$
Delegation Forwarding (DF) [131]	✓	✓	×	Quality and threshold	Unlimited^c	$O(n)$	$O(n)$

Legends: '✓'= Satisfy, '×'= Does not satisfy, '(n/a)'= Not applicable.
^{a}: Ignoring storage and transmission of summary vectors;
^{b}: Metadata exchanged includes expected meeting times with every node and data replication information;
^{c}: Practically, however, it is very low;
^{d}: OH, overhead;
^{e}: $O(n)$ when destination-specific metrics are used. Here, n is the number of nodes in opportunistic network.

except for *Epidemic* and *SnW* use some form of intelligence to make replication decisions. This is true because both Epidemic and SnW blindly replicate the data in the network. However, SnW, as well as SnF and EBR, replicates only up to a fixed upper limit. As such, they have relatively higher reliability in terms of the number of data replicas delivered. Among these routing protocols, Bubble uses social metrics for data forwarding which increases it reliability considerably.

Overhead of the routing protocols in terms of buffer storage and transmission cost are also noted in Table 3.2. In particular, if the opportunistic network has n nodes, the storage overhead of PRoPHET becomes $O(n)$. This is due to the reason that a node running PRoPHET has to store the predictabilites of the other nodes, which asymptotically reaches to $O(n)$. Similarly, the transmission overhead of PRoPHET is also $O(n)$, since the delivery predictabilities vector need to be exchanged between two nodes. SnW and Epidemic, however, have zero overhead in both the cases assuming that they do not exchange summary vectors of the data. If such an exchange is involved, then the transmission cost runs into $O(m)$, where m is the number of data created in the opportunistic network. Overhead of DF is either $O(n)$ or constant depending upon whether or not destination-specific utility values are used by the protocol. The majority of opportunistic routing protocols are noted to have a relatively high latency and energy consumption, due to the dynamic network topology and multi-copy replication. This will make them less suitable for wildlife monitoring, especially, where energy resources are very scare or limited.

3.3 Overview of short-range technologies

In this subsection, we highlight the existing standards for short range wireless communication protocols.

3.3.1 Bluetooth low energy (BLE)

Recently, Bluetooth Low Energy (BLE), also know as "Bluetooth Smart", has surfaced as an appealing low-power communication technology in the IoT sphere. BLE is the light-weight and low power version of classical Bluetooth technology [5]. It operates in the 2.4GHz ISM band spectrum range utilizing a GFSK modulation. In theory BLE can reach up to 200m in an open flat environment at maximum transmission power setting. Compared to IEEE 802.15.4 solutions, BLE offers a relatively higher data rate (upto 1Mbps) and a low latency (typically 6ms) suitable for WMS requirements. The power efficiency of BLE makes it suitable for applications that run for longer periods on power sources, such as coin cell batteries or energy-harvesting devices, as in wildlife monitoring scenarios. Despite these appealing features to WMS IoT application, BLE is a new standard thus it is still open to research and development for WMS implementation.

3.3.2 IEEE 802.15.4

IEEE 802.15.4 is the most commonly used IoT standard for MAC [132]. It defines a frame format, headers including source and destination addresses, and how nodes can communicate with each other. The frame formats used in traditional networks are not suitable for low power multi-hop networking in IoT due to their high communication overhead. In 2008, IEEE802.15.4e was created to extend IEEE802.15.4 and support low power communication. It uses time synchronization and channel hopping to enable high reliability, low cost and meet IoT communications requirements.

3.3.3 Zigbee smart energy

ZigBee smart energy is designed for a large range of wireless applications including smart homes, remote controls and healthcare systems [133]. It supports a wide range of network topologies including star, peer-to-peer, or cluster-tree. A coordinator controls the network and is the central node in a star topology, the root in a tree or cluster topology and may be located anywhere in peer-to-peer. ZigBee standard defines two stack profiles: ZigBee and ZigBee Pro. These stack profiles support full mesh networking and work with different applications allowing implementations with low memory and processing power. ZigBee Pro offers more features including security using symmetric-key exchange, scalability using stochastic address assignment, and better performance using efficient many-to-one routing mechanisms.

3.3.4 Discussion

Generally, the most widely used standards are IEEE 802.15.4, Bluetooth and ZigBee. However, due to the associated deployment complexity with these protocols, it is difficult to utilize them in WMS application scenario.

3.4 Overview of long-range technologies

Currently, a new class of wireless technology named LPWAN is emerging that provides long-range communication with low energy consumption. This allows LPWANs to achieve wide connectivity coverage through simple star networks where the end-devices are directly connected to the gateway. Proving large coverage, LPWAN technologies are suitable for low data-rate applications. Communication technologies such as LoRa, Sigfox, NBIoT and Weightless are prime examples of LPWAN [134, 135]. They support a star topology where a number of end-devices communicate to a gateway. In this section, we present the overview of these wireless technologies from the monitoring application perspective.

3.4.1 LoRa/LoRaWAN

LoRa is one of the proposed long-range wireless technologies that currently received large attention for internet of things applications [134, 135]. The LoRa radio, developed by Semtech, allows for long-range, low-power and low bit rate communications. The operating frequencies of LoRa are 433/868/915MHz depending on which country it is deployed in. LoRa radio link is based on a proprietary chirp spread spectrum modulation scheme. Depending on the LoRa radio configuration, the data payload size can be from 2 to 255 bytes, and the bit-rate could be upto 5.4 kbps when configured at the highest bit-rate setting. The maximum output power allowed by ETSI in Europe is +14dBM. There are duty-cycle restrictions under ETSI but no max transmission or channel dwell time limitations. LoRa radio modulation can be used in different network topology, however, the LoRaWAN version 1.0 specification steered by LoRa Alliance [135], is configured as a star-of-star topology. It proposes open standard LoRaWAN as the MAC layer which supportS mobile end-devices with uplink and downlink data communication. The network architecture basically includes three components, i.e. end-devices, gateways, and a network server. LoRaWAN gateway are able to forward the control signals and data between a central network server and end-nodes. They are able to decode multiple signals at the same time.

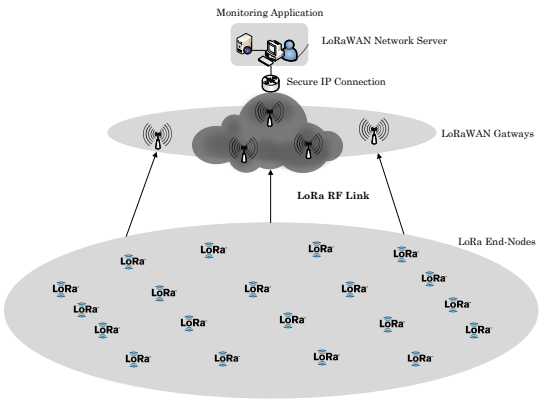

FIGURE 3.1: *Generic architecture of LoRaWAN star network topology*

Relative to the OSI reference model, LoRa represents the physical layer (layer 1), and LoRaWAN represents layer 2 and layer 3. They are able to decode multiple signals at the same time. The LoRaWAN specification [135] defines that the LoRa gateways are connected to the network server with an IP connection, whereas the end-devices communicate to the gateway through a single hop wireless communication. Communication between LoRa end-devices and gateway is bidirectional to support services such as software upgrade, over-the-air activation and multi-casting. The network server is used as the sole manager of the network. It can manage, among other things, the data rate (defined as DR0 till DR7) and throughput for each end-device separately through the adaptive data rate (ADR) scheme.

The LoRaWAN specification [135] describes three classes of end-devices (i.e. Class A, Class B and Class C). The difference between these classes relates to the timing of

the so-called receive-windows. Class A is the default LoRa end-device operation. It allows a bidirectional link with the gateway, whereby each end-device's upstream transmission is followed by two time-slots for a short downstream reception. Class B end-devices allow a bi-directional link with scheduled listening time-slots. Class C end-devices allow continuous listening time-slot but the listening slot will be closed during transmission.

3.4.2 Sigfox

Sigfox [134] is developed by a french company founded in 2009 and is the first LP-WAN technology on the market. It uses a BPSK modulation to transmit data using ultra-narrowband (UNB) technology. It is designed to transmit small payload size (12 bytes) at a slow bit-rate (100-600bps) utilizing Ultra Narrow Band (UWB) modulation scheme. Sigfox operates in the 200 kHz bandwidth of the publicly available 868 or 915 MHz bands [134]. Sigfox can reach upto 50 km in rural and 10 km in urban areas, which is higher than LoRa radio. By utilizing ultra-narrow band, Sigfox uses the carrier bandwidth efficiently and experiences very low noise levels, leading to ultra low power consumption, high receiver sensitivity, and low-cost antenna design at the expense of a maximum data rate of only 100 bps. Sigfox initially supported only uplink communication, but later evolved to bidirectional technology with a significant link asymmetry. As the gateway can receive messages simultaneously over all channels, the end device can randomly choose a frequency channel to transmit their messages. This simplifies the end-device design and reduces its cost.

3.4.3 NB-IoT

NB-IoT [136] is the Narrow Band wireless technology specified in Release 13 of the 3GPP in June 2016. NB-IoT can coexist with GSM (global system for mobile communications) and LTE (long-term evolution) under licensed frequency bands (e.g., 700 MHz, 800 MHz, and 900 MHz). NB-IoT occupies a frequency band width of 200 KHz, which corresponds to one resource block in GSM and LTE transmission [136]. NB-IoT can be supported with only a software upgrade in addition to the existing LTE infrastructure. The NB-IoT communication protocol is based on the LTE protocol. In fact, NB-IoT reduces LTE protocol functionalities to the minimum and enhances them as required for IoT applications. For example, the LTE backend system is used to broadcast information that is valid for all end devices within a cell. As the broadcasting back end system obtains resources and consumes battery power from each end device, it is kept to a minimum, in size as well as in its occurrence. It was optimized to small and infrequent data messages and avoids the features not required for the IoT purpose, e.g., measurements to monitor the channel quality, carrier aggregation, and dual connectivity.

NB-IoT technology can be regarded as a new air interface from the protocol stack point of view, while being built on the well-established LTE infrastructure. It allows connectivity of up to 100K end devices per cell with the potential for scaling up the capacity by adding more NB-IoT carriers. It also uses the single-carrier frequency

division multiple access (FDMA) in the uplink and orthogonal FDMA (OFDMA) in the downlink, and employs the quadrature phase-shift keying modulation (QPSK) [136]. The data rate is limited to 200 kbps for the downlink and to 20 kbps for the uplink. The maximum payload size for Nb-IoT is 1600 bytes.

3.4.4 Weightless

Weightless [134], developed by the Weightless Special Interest Group (SIG), is an alternative protocol for IoT applications. Similar to LoRa and Sigfox, Weightless is designed to provide low power and longer range star network while using a TDMA combined with frequency hopping modulation to increase its robustness against interference. It operates in the sub-1GHz ISM frequency band and the channel bandwidth is 200 Hz, 12.5 kHz or 5 MHz depending the configuration [134]. The packet size is flexible and has a maximum packet size limit of 20 bytes. The communication range in urban areas could reach upto 5 km. Currently, the technology is under development by Weightless Special Interest Group (SIG).

3.4.5 Discussion

In this section, existing long-range technologies are presented in terms of WMS requirements and their technical differences. Table 3.3 presents a summary comparison of the technologies. Sigfox, Weightless and LoRa employ unlicensed spectra and asynchronous communication protocols. They can bounce interference, multipath, and fading. However, they cannot offer the high data rate and low latency quality of service provided by NB-IoT. NB-IoT employs a licensed spectrum and an LTE-based synchronous protocol, which are optimal for high QoS at the expense of high deployment and device cost [136]. Owing to these trade-off, NB-IoT is suitable for applications that require guaranteed real-time services, whereas applications that do not have this constraint should opt for LoRa, Weightless or Sigfox.

In Sigfox, LoRa, Weightless and NB-IoT, end devices are in sleep mode most of the time, which reduce the amount of consumed energy, i.e., long end-devices lifetime. However, the NB-IoT end device consumes additional energy because of synchronous communication and QoS handling, and its OFDM/FDMA access modes require more peak current [136]. This additional energy consumption reduces the NB-IoT end-device lifetime as compared to Sigfox and LoRa. Therefore, for applications that are insensitive to the latency and do not have large amount of data to send, Sigfox and class-A LoRa are the best options [135]. For applications that require low latency, NB-IoT and class-C LoRa are the better choices.

Support for large number of devices is one of the key features for aforementioned LPWAN technologies. These technologies work well with the increasing number and density of connected end-devices. Several techniques are considered in LPWAN to cope with this scalability feature such as the efficient exploitation of channel diversity. However, NB-IoT offers further advantage of very high scalability than Sigfox and LoRa. NB-IoT allows connectivity of up to 100K end-devices per

TABLE 3.3: *Comparison long-range technologies for WMS*

WMS solutions	*Energy*	*Reliability*	*Latency*	*Coverage*	*Robustness*	*Scalability*	*Deployment*	**Adv.**	**Disadv.**
Sigfox [134]	✓	✓	×	✓	✓	✓	✓	• Unlicensed ISM band • large coverage 10km (urban), • 40km (rural)	• Low bandwidth • limited or half-duplex • no adaptive data rate
LoRaWAN [135]	✓	✓	×	✓	✓	✓	✓	• Unlicensed ISM band • large coverage 5km (urban), • 20km (rural), • with adaptive data rate	• Low bandwidth • limited or half-duplex
NB-IoT [136]	×	✓	✓	✓	✓	✓	×	• licensed LTE bands • bidirectional/full-duplex • large coverage 1km (urban), • 10km (rural) • high bandwidth	• high energy consumption • no adaptive data rate
Weightless [137]	✓	✓	×	✓	✓	✓	✓	• unlicensed ISM band • bidirectional/half-duplex • large coverage 10km (urban), • 40km (rural)	• low bandwidth • no adaptive data rate

Legends: '✓'= Satisfy, '×'= Does not satisfy, '(n/a)'= Not applicable.

cell compared to 50K per cell for Sigfox, Weightless and LoRa [138]. The major utilization advantage of Sigfox is that it can cover a range of $\geq 40km$. By contrast, LoRa has a lower range (i.e., range $20km$). NB-IoT has the lowest range and coverage capabilities (i.e., range $\leq 10km$). It focuses primarily on the class of devices that are installed at places far from the typical reach of cellular networks (e.g., indoors, deep indoors).

Generally, the star topology based wireless technologies, such as LoRa, Sigfox, and Weightless are a good fit for applications that send small packet sizes less frequently over longer range. Use cases such as basic status monitoring and simple data collection are all examples of IoT operations that could be deployed by LPWANs. However, applications requiring a degree of local pre-processing of data and high throughput, as in wildlife monitoring system (WMS) scenarios, are not the focus of LPWAN technologies. In addition, the deployment of NB-IoT for WMS is limited to LTE base stations availability. Thus, it is not suitable for wildlife habitat regions that do not benefit from LTE coverage such as WMS applications.

3.5 Conclusion

In this chapter, we investigated several existing opportunistic MAC and opportunistic protocols are explored for WMS applications. Moreover, an overview of wireless communication technologies are provided in this chapter. For high mobility scenarios, synchronized protocols do not suffice for MWS, mainly because of the overhead associated with the re-synchronization process. In asynchronous protocols, however, there is no need to continuously share synchronization information, it rather proactively samples the channel to determine when an activity can be performed. The overall effective active period for asynchronous MAC protocols could be much shorter than that of synchronous protocols. Thus the energy consumption of asynchronous communication protocols is significantly lower synchronous protocols. In addition, opportunistic communication protocols are noted to have a relatively high latency and energy consumption, due to the frequent network topology changes and the inherent multi-copy data replication. This will make them less suitable for wildlife monitoring, where energy resources are very limited.

Generally, due to the animal movement dynamicity in WMS application, the way mobility should be captured and handled requires a careful consideration. Most of the discussed wireless sensor network protocols (encompassing MAC, and opportunistic protocols), implicitly assume that the number of static nodes is significantly larger than the number of mobile animals. Experiment and simulation results indicate that being aware of animal mobility is essential to reducing unnecessary oscillation in link establishment caused by the movement of animals [113]. However, the results also indicate the existence of a strong trade-off between movement estimation accuracy, estimation time, and signal processing cost (both in terms of energy consumption and computing resources). Therefore, opportunistic protocols should be integrated with a mobility estimation techniques that optimize the required trade-off. Moreover, estimation techniques that are based only on RSSI values are found to perform poorly, leading to frequent oscillations even when nodes

are not mobile. Unfortunately, most of the surveyed approaches rely on this technique. The limited size of a sensor node and its limited resources put significant constraints on the type of data sources that can be used for mobility estimation. For example, knowledge of the pattern of animal mobility can significantly reduce both false positives and false negatives. We realise that most of the proposed opportunistic protocols do not fully take advantage of this knowledge.

Chapter 4

Leveraging IoT Networks for WMS

IN THIS *chapter, we introduce single-hop, multi-hop, and opportunistic multi-hop communication networks with hybrid tree topologies that are suitable for wireless wildlife monitoring system (WMS). They all leverage bluetooth low energy (BLE) in combination with low power wide area networks to facilitate ultra-low power end-devices to be deployed for sustainable wildlife monitoring applications. We present an analytical model to investigate and compare the performance of the these networks interms of energy consumption under a wildlife monitoring scenario. Moreover, we discuss the feasibility test performed for long-range radio to WMS. The results show that single-hop communication with hybrid tree network topology leads to a higher energy efficiency when compared to the networks utilizing multi-hop, opportunistic multi-hopping, or star topology.*

Part of this chapter has appeared in:
[31] Eyuel D. Ayele, Kallol Das, Nirvana Meratnia, and Paul Havinga, "Leveraging BLE and LoRa in IoT network for wildlife monitoring system (WMS)," 2018 IEEE World Forum on Internet of Things (WF-IoT). 2018 Feb., Singapore
[139] Eyuel D. Ayele, Hakkenberg, C. , Meijers, J. P., Zhang, K. , Meratnia, N. , and Havinga, P. J. M. (2017). Performance analysis of LoRa radio for an indoor IoT applications. In Internet of Things for the Global Community, IoTGC 2017 - Proceedings IEEE.

4.1 Introduction

As discussed in Chapter 2, with the outlined WMS requirements and features of wild animals, numerous wireless technologies are utilized for wildlife monitoring purpose. Radar, GPS and satellite based systems have all been deployed to track and monitor wild animals [140]. However, the inherently high cost and intolerable communication latency made these approaches less attractive to WMS design. Some efforts have been made to develop wireless sensor network based WMS, where short-range wireless technologies are utilized by forming multi-hop mesh networks (Chapter 2). Most of these systems are developed on top of IEEE 802.15.4 standard [141], which often suffers from high communicaiton overhead in-terms of energy, reliability, and latency due to the complex implementation and scales poorly [27, 76].

More recently, the energy efficient version of Bluetooth known as *Bluetooth Low Energy (BLE)* or *Bluetooth Smart*, has surfaced as an appealing alternative to commonly used IEEE802.15.4 based solutions due to its higher data rate (upto 1 Mbps), lower latency (typically 6 ms), higher energy efficiency and wider coverage [5]. While making some progress in energy efficiency aspect, short-range wireless technologies are still not suitable for wide and sparse monitoring applications as in WMS. Although this aspect can be addressed by using long-rage wireless technologies (e.g. cellular), they are often considered to be power hungry. In addition, remote areas where wild animals dwell are often out of cellular coverage.

Fortunately, low power wide area network (LPWAN) technologies provides larger coverage at lower energy consumption supporting many requirements of remote wildlife monitoring applications [135, 134]. LPWANs in general are fundamentally designed to ensure very long battery lifetime and provide seamless interoperability among end-devices without the need for complex local installations. However, as discussed in the previous chapter, supporting IoT applications requiring high data rate and low latency are not particularly the strength of LPWANs mainly due to the generic low bit-rate, stricter duty-cycle restrictions and the larger packet header associated with it.

In addition, LPWANs are not as efficient as short range technologies when used for short distance communication, which is often required in wildlife monitoring scenarios (e.g., to detect group behavior of animals). Thus to realize the WMS design requirements, a mechanism to control the trade-off between energy consumption and data rate is necessary, which is not practically achievable by using a single category of wireless technology alone. Although a few works have addressed this issue by proposing an architecture for WMS [19], to the best of our knowledge, none of these works utilize LPWAN technologies in their approach.

Therefore, in this chapter, we present a hybrid tree based IoT network architecture for WMS that exploits short-range and LPWAN wireless technologies. Through the usage of hybrid tree network, the proposed network architecture manages the trade-off between energy and throughput, eventually, making the system more energy efficient. Moreover, WMS also optimizes the system bandwidth requirement through local data pre-processing and concatenation that merges multiple BLE packets under a single LoRa header. The results and analysis discussed in this chapter are

modeled by considering LoRa as an LPWAN technology and BLE as a short-range wireless technology. However, the design approach can also be applied to other LPWAN and short range wireless technologies. In addition, in this section, we also present investigation of performance of LoRa radio for IoT networks.

To this end, the contributions of this section includes:

The main contributions of this chapter are listed below:

- hybrid tree based IoT network architecture for wireless wildlife monitoring.
- theoretical analysis of network energy consumption of the hybrid tree networks.
- analysing the performance of LoRa radio and comparing it with the expected specifications defined by the LoRa Alliance [20];

The rest of this chapter is organized as follows: Section 4.2.1 presents the proposed network energy architecture and details the constraints for a WMS design. Section 4.2.2 discusses the use case scenario and evaluation set-up. Section 4.2.3 discusses the results. The experimental set-up and discussion of LoRa radio is presented in Section 4.3. Finally, Section 4.4 outlines the concluding remarks and future research challenges.

4.2 Utilizing BLE and LoRa in an IoT Network for WMS

4.2.1 Network wide energy consumption

In this section, we investigate the utilization of BLE and LoRa radios in single-hop, multi-hop, and opportunistic communication with hybrid tree topologies. We assess their suitability to WMS based on the network wide energy consumption comparison of the network topologies with the conventional star network topology. Furthermore, we present the design constraints as well as the analytical relationship between wireless channel path-loss model and communication range between nodes.

Network topologies

Single-hop, multi-hop, and opportunistic multi-hop, and star network topologies are shown in Figure 4.1. In all cases, the network consists of a group of AB, AS, and LG nodes with builtin BLE and/or LoRa radio. Within a herd of animals, the AB nodes use short-range BLE radio to communicate with each other or with AS nodes and AS nodes use the long-range LoRa radio to link to LG node. A single-hop hybrid tree topology is a network where the AB nodes send data to nearby AS nodes to be aggregated and forwarded to LG node. A multi-hop hybrid tree topology is a network where nodes have inter-cluster and intra-cluster communication between ($AS- > AB$) node pairs. AB nodes decide to which neighbour nodes to forward data to reach the closest AS node. Where as in opportunistic multi-hopping, data is

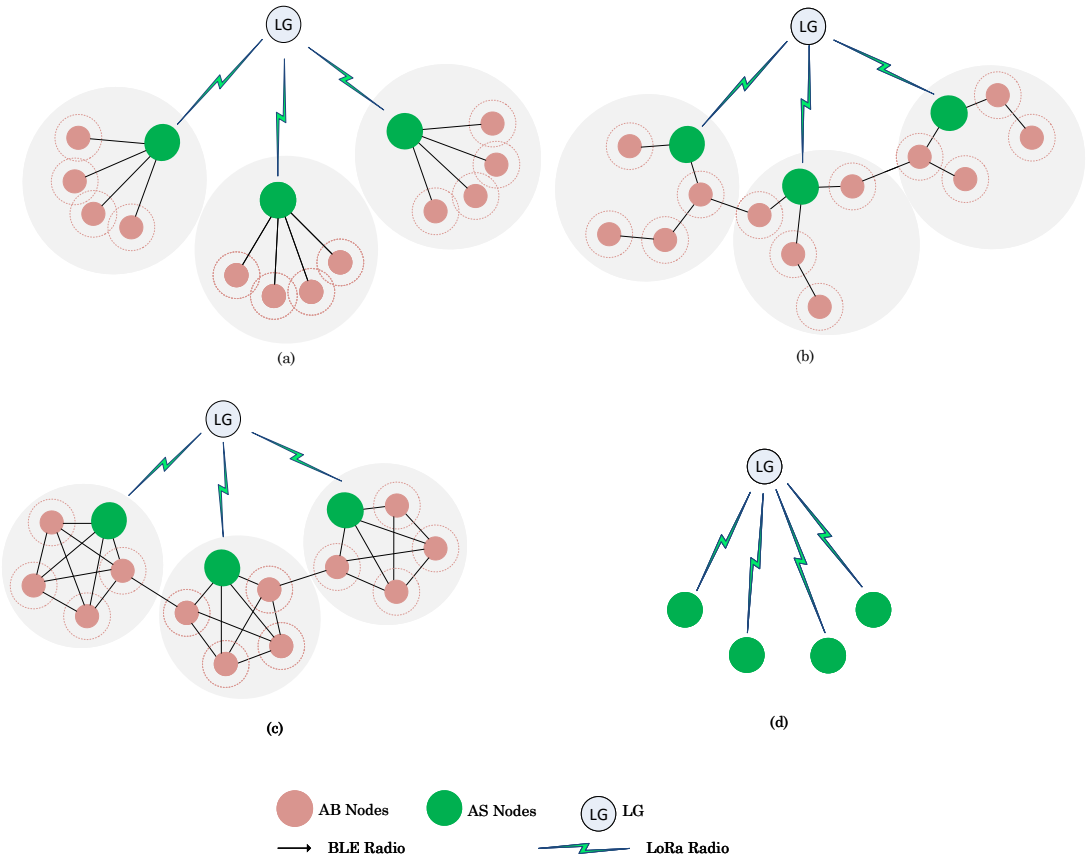

FIGURE 4.1: *A typical network topology approach for a herd/group of animals monitoring scenario: (a) single-hop hybrid tree topology, (b) multi-hop hybrid tree topology, (c) opportunistic multi-hop hybrid tree topology, (d) conventional star topology.*

relayed within the network based on contacts between pair of $AS->AB$ nodes, so that the data reach the intended AS nodes. Thus, compared to the single-hop and multi-hop topologies, in case of opportunistic multi-hopping there would be multiple redundant many-to-many $(m-m)$ communication links. In star based network topology, the end-nodes directly send data to LG nodes utilizing LoRa radio link.

Energy consumption model

To compare the energy performance of the network topologies illustrated in Figure 4.1, the topologies are modeled as a graph Λ defined as $\Lambda(n, L, AS_m)$, where n is the total number of nodes in the network including AB and AS nodes, AS_m is the number of AS nodes in the network, and L is the total number of established links in the network.

In our energy modeling we are aware of the implementation complexity associated with networking, however, for the sake of simplicity we made few network topology assumptions as follows:

- The gateway node (LG) is assumed to have continuous power source, thus, the received power consumed by LG is ignored. However, the link between AS node and LG ($AS- > LG$) is taken into account while performing the energy cost calculation.
- Both AS and AB nodes are assumed to transmit or receive packets.
- AS nodes are able to concatenate incoming data from AB nodes into a single LoRa packet.
- $AS--AB$ links have same link properties such as packet transmission and reception capacity, and energy measures.
- AB nodes will send the same payload size (PL).
- For both LoRa and BLE radio link, there is a short time interval for detecting the channel for any activity before transmitting data called time-of-channel activity detection (ToC). The typical ToC is $ToC = (2^{SF} + 32)/BW$ seconds and $ToC = 1.28ms$ respectively for LoRa and BLE link [135, 6].
- The total time-of-reception (ToR) for the BLE links would be $((ToR) = ToA_{BLE} + ToC)$.

Let $L(t, r)$ be the link between transmitter t and assuming the wireless link is reliable with no loss of transmitted packets, and the sleep mode power consumption is negligible (which is typically less than 0.1% of transmission mode) [23]. Thus, the generic per-packet energy (E) consumed to transmit a packet of length (PL) bytes over a link L is the sum of (i) the energy the transmitter (t) spends to transmit the packet and (ii) the energy the receiver spends on decoding and processing the received packet. This is expressed by Equation 4.1:

$$E = (\overbrace{ToA \times P_{Tx}}^{\text{transmit energy}} + \overbrace{ToA \times P_{Rx}}^{\text{receive energy}}) \tag{4.1}$$

, where: ToA is the time-on-air for the given packet length, P_{Tx} is the power required to transmit a packet by sender t, and P_{Rx} is the power the receiver spends to successfully decode and receive the given packet by the receiver (r) [142]. P_{Tx} level and the channel path-loss model impacts the received signal level and transmission distance. P_{Rx} is not related to the receiver signal power level, instead it relates to the hardware circuitry type chosen.

Therefore, the per-packet energy consumption (E) directly depends on the ToA and the P_{Tx} level used by transmitter (t) (Equation 4.1). ToA for LoRa and BLE is expressed in Equation 4.2.

$$ToA(PL) = \begin{cases} (T_s) \times \left((T_{pre}) + max\left\{\lceil\Gamma\rceil \times (CR+4), 0\right\}\right) & \textit{for LoRa} \\ 8 \times \frac{(n_{preamble} + AddressH + PL_{BLE} + CRC)}{DR} & \textit{for BLE} \end{cases} \tag{4.2}$$

where: $T_s = (2^{SF}/BW)$ is symbol period, $T_{pre} = (n_{preamble} + 12.25)$ is the preamble duration, $\Gamma = \left\lceil\frac{8PL_{LoRa} - 4SF + 28 + 16CRC - 20H}{4 \times (SF - 2DE)}\right\rceil$, BW is bandwidth, SF is spreading

factor, CR coding rate, $AddressH$ address header bytes for BLE, DE transmission robustness to frequency variation, DR data rate, PL payload size [135].

In case of LoRa: the physical layer parameters such as SF, BW, and CR, can influence the effective ToA, its resistance to radio interference, and ease of received data decoding. Theoretically, a high SF results in an easily decodable packet and lower minimum receiver sensitivity, but a longer ToA duration. A higher CR enables to transmit more redundant data bits, consequently, increasing LoRa radios resilience to frequent packet errors.

Thus given the ToA and radio parameters, we present the network wide energy consumption model for (i) single-hop, (ii) multi-hop, and (iii) opportunistic multi-hop, and (iv) star networks as follows:

- **Single-hop hybrid tree topology:** In case of single-hop network, shown in Figure 4.1.a, the $(AB \rightarrow AS)$ links are are to be unidirectional links and a conventional data sender with a uniform periodic transmission interval is used. Thus, applying graph theory principle on the single-hop topology, within in a herd/cluster that is using $((AB- > AS))$ BLE links, the total number of packets exchanged for one period would be $TX_{pckt} = (n-1)$ and $RX_{pckt} = (n-1)$ for the transmitted and received packets respectively [143]. Utilizing Equation 4.1 for each packet exchanged, then the overall energy for the single-hop hybrid tree topology while considering data concatenation at the AS node and the $(AS- > LG)$ links energy cost is given by Equation 4.3:

$$E_{Single-hop} = \lceil t/IPI \rceil \times AS_m \times \left((n-1) \times \left[\overbrace{ToA_{BLE} \times P_{TxBLE}}^{\text{BLE links tx energy}} + \overbrace{ToR \times P_{RxBLE}}^{\text{BLE links rx energy}} \right] + \overbrace{ToA_{LoRa} \times P_{TxLoRa}}^{\text{(AS->LG) link tx energy}} \right) \tag{4.3}$$

  , where $(\lceil t/IPI \rceil)$ is the periodic data transmission time epoch and t is total simulation duration.

- **Multi-hop hybrid tree topology:** The multi-hop network, shown in Figure 4.1.b, is modeled as a minimum spanning tree (MST) [143], i.e. the multi-hop path connects all nodes (n) of the graph $\Lambda(n, L, AS_m)$ and is a sub-graph of Λ (every edge in the tree belongs to Λ). In this topology, the shorter-range links $(AB \leftrightarrow AS)$ is assumed to be bidirectional, i.e. they can have the role of receiving and transmitting. Moreover, to avoid the loss of data due to packet collision, AB nodes are assumed to be tightly synchronized with AS node.

  Thus, in case of multi-hop network, there are three main parts of network energy consumption: (i) initial (node joining) (k), (ii) periodic re-synchronization (k_{resync}), and (iii) energy consumed for each packet transmitter and received. In this topology, the classical approach of sender-receiver synchronization, as presented in [144], is used for node synchronization. Applying MST graph theory concepts on the multi-hop topology, that is using $((AB- > AS))$ BLE links, therefore, the total number of packets exchanged to maintain network synchronization and joining for one synchronization period would be ($TX_{pckt} = 2 \times (n-1)$ and $RX_{pckt} = AS_m \times (n-1)$ for transmitted and received respectively [143, 144].

Therefore, the network energy overhead for the initial phase (k) is expressed as:

$$k = (2(n-1) \times ToA_{BLE} \times P_{TxBLE} + AS_m \times (n-1) \times (ToR) \times (P_{RxBLE}) \tag{4.4}$$

The network overhead with periodic re-synchronization (k_{resync}) of the link $(AB->AS)$ is given by:

$$k_{resync}(t) = \begin{cases} 0, & \text{if } 0 \leq t < x \\ \lceil t/x \rceil \times (n-1)\Big(2 \times (ToA_{BLE}) \times (P_{TxBLE}) + AS_m \times (ToR) \times (P_{RxBLE})\Big), & \text{otherwise} \end{cases} \tag{4.5}$$

, where if $0 \leq t < x$ is time before the start of the first re-synchronization, x is the re-synchronization period ($x = (\delta - ppm)/4.75 \times 10^{-6}$) [144], ppm is the clock accuracy and depends on the radio hardware used, $\delta = 10ms$ is the accuracy bound between a pair of neighboring nodes in the network [144].

Here $k_{resync}(t) = 0$ because the first synchronization overhead already included in k as per Equation. 4.4. Hence, the energy cost for the multi-hop hybrid tree topology including aggregation at the AS node and the total $(AS->LG)$ links energy cost for periodic communication of ($\lceil t/IPI \rceil$), is given by Equation 4.6.

$$E_{Multi-hop} = \lceil t/IPI \rceil \times AS_m \times \Big((n-1) \times \Big[\overbrace{ToA_{BLE} \times P_{TxBLE}}^{\text{BLE links tx energy}} + \overbrace{ToR \times P_{RxBLE}}^{\text{BLE links rx energy}}\Big] + \overbrace{ToA_{LoRa} \times P_{TxLoRa}}^{\text{(AS->LG) link tx energy}}\Big) + k + k_{resync}(t) \tag{4.6}$$

- **Opportunistic multi-hop hybrid topology:** The shorter links ($AB \leftrightarrow AS$) are bidirectional. AS to AB communications are asynchronous. Both AS and AB nodes are assumed to transmit or receive packets. In opportunistic multi-hopping is that there is no synchronization, no node joining, and initial stage energy overhead. However, since there is no unique data path specified in case of opportunistic multi-hop topology, all nodes involved replicate multiple copy of the data by establishing network topology which is modeled as complete graph network [143]. Assuming transceiver nodes are within communication range of BLE radio, thus the total number of packets exchanged for one period using BLE links would be similar to the number of links and AS node's degrees in the complete graph, i.e. $TX_{pckt} = \frac{(n(n-1))}{2}$ and $RX_{pckt} = AS_m \times (n-1)$ for transmitted and received respectively [143]. Hence, the overall energy cost for the opportunistic hybrid topology including data concatenation at the AS node and the total $(AS->LG)$ links energy cost for periodic communication of ($\lceil t/IPI \rceil$), is given by Equation 4.7:

$$E_{Opp} = \lceil t/IPI \rceil \times AS_m \times \Big[\overbrace{(\frac{(n(n-1))}{2}) \times ToA_{BLE} \times P_{TxBLE}}^{\text{BLE links tx energy}} + \overbrace{(n-1) \times ToR \times P_{RxBLE}}^{\text{BLE links rx energy}} + \overbrace{ToA_{LoRa} \times P_{TxLoRa}}^{\text{(AS->LG) link tx energy}}\Big] \tag{4.7}$$

- **Star topology:** The longer-range LoRa links ($AS \leftrightarrow LG$) are unidirectional. AS and LG are asynchronous. For conventional star topology (i.e. LoRa only link) the energy consumption overhead is given in Equation 4.8:

$$E_{Star} = \lceil t/IPI \rceil \times n \times (ToA_{LoRa})(P_{TxLoRa}) \tag{4.8}$$

Critical range and path-loss constraints

Generally, when a radio signal is transmitted through a wireless channel several factors will influence its radio propagation range (d) subsequently the received radio signal at the receiver (P_{Rx}). The critical range (d_c) is the maximum range beyond which there is no wireless connectivity between a pair of nodes, it depends on the radio and wireless channel parameters such as: (i) transmit power level (P_{Tx}) set, (ii) minimum receiver sensitivity ($P_{r_{min}}$) and (iii) outage probability under path-loss (K) and log-normal shadowing ($\sigma_{\psi_{dB}}$). Its is expressed by Equation 4.9 for BLE and LoRa radios:

$$d_c = \begin{cases} 10^{\frac{P_{Tx} - P_{Rx_{min}} + \sigma_{\psi_{dB}} \times C_{inv} - K}{D}} & \textit{for LoRa} \\ 10^{\frac{P_{Tx} - P_{r_{min}} + \sigma_{\psi_{dB}} \times C_{inv} - K}{10 \times \gamma}} & \textit{for BLE} \end{cases} \tag{4.9}$$

$$P_{Tx} = \begin{cases} P_{Rx} + K - \sigma_{\psi_{dB}} \times C_{inv} + D \times Log(d) & \textit{for LoRa} \\ P_{Rx} + K - \sigma_{\psi_{dB}} \times C_{inv} + 10 \times \gamma \times Log(d) & \textit{for BLE} \end{cases} \tag{4.10}$$

The path-loss (K) is determined by utilizing an empirical models such as Hata Cost-231 [145] and simplified path-loss model [145]. Hata Cost-231 is used for LoRa radio, since it is suitable for path loss estimation with large and open rural radio coverage (i.e., 0 to 20 km) at lower frequency (i.e., f_{LoRa}=868MHz) [145]. However, BLE is often utilized for shorter-range communication and its frequency is relatively higher (f_{BLE}=2.4GHz), therefore, the simplified path-loss model is adopted as suggested in [145]. Thus the path-loss (K) is given by Equation 4.11:

$$K = \begin{cases} 46.3 + 33.9 \times log10(f_{LoRa}) - 13.82 \times log10(h_t) - ahMS + C_m & \textit{for LoRa} \\ 20 \times (log10((4 \times \pi \times d_0)/(c/f_{BLE}))) \approx 40.04 & \textit{for BLE} \end{cases} \tag{4.11}$$

, where: $c = 2.99 \times 10^8$m/s, $ahMS = (1.1 \times log10(f_{LoRa}) - 0.7) \times h_r - (1.56 \times log10(f_{LoRa}) - 0.8)$; and $C_m = 0$ for flat rural environment; $D = 44.9 - 6.55 \times log10(h_t)$.

Consequently, based on the radio range (d) computed from the transmission power and the path-loss information, it is possible to enable an optimal hybrid tree WMS that is able to operate at a specific radio interface for each d range, as shown in Algorithm 6.3. Hence, the energy consumption for the optimal hybrid tree leveraging all network topology is expressed by Equation 4.12:

$$E_{Optimal} = \begin{cases} E_{Single-hop} \vee E_{Multi-hop} \vee E_{Opp}, & \textit{for } 0 < d < d_{cBLE} \\ E_{Star}, & \textit{for } d > d_{cBLE} \end{cases} \tag{4.12}$$

Algorithm 4.1 Optimal hybrid tree radio scheme

Input: P_{Tx}, $P_{Rx}min$, path-loss (K) and log-normal shadowing ($\sigma_{\psi_{dB}}$), area coverage ($Cov(C)$).

Output: radio range d, critical range $d_{c(BLE)}$, $d_{c(LoRa)}$.

1: **procedure** HYBRID RADIO
2: **top**:
3: $Log(d_c) \propto (P_{Tx} - P_{r_{min}} - K + \sigma_{\psi_{dB}} \times C_{inv})$
4: *Determine the critical ranges* $d_{c_{(BLE)}}$, $d_{c_{(LoRa)}}$
5: $d_{c_{(BLE)}} \leftarrow Eq.\ 4.9$
6: $d_{c(LoRa)} \leftarrow Eq.\ 4.9$
7: **if** $0 < d < d_{c(BLE)}$ **then**
end
$\leftarrow$ *BLE Radio*
8:
9: **if** $d_{c_{(BLE)}} < d < d_{c_{(LoRa)}}$ **then**
end
$\leftarrow$ *LoRa Radio*
10:
11: **goto top**
12: **end procedure**

4.2.2 Evaluation

In this subsection, the evaluation setup for network energy consumption comparison of star, single-hop, multi-hop, and opportunistic communication with hybrid tree topologies is discussed.

TABLE 4.1: *Time-on-air (ToA) parameters for LoRa and BLE. (n/a) = not applicable.*

Notations	BLE	LoRa	Details
BW	700 kHz	125 kHz	Bandwidth
SF	n/a	7 to 12	LoRa spreading factor
CR	n/a	CR=1 (4/5), CR=4 (4/8)	coding rate
$n_{preamble}$	1 Byte	8 symbols	number of preambles
AddressH	6 Bytes	n/a	address header bytes
DE	n/a	0	Tx Robustness to freq. var.
H	n/a	0	H = 1 without header mode, H = 0 with header mode
CRC	2	1	for LoRa CRC = 1 for on, CRC=0 for off
DR	250 kbps	50 kbps	data rate

In wildlife monitoring applications, the herd/group size (n) are proportional to the number of animals in a herd [14, 146]. Depending on the animal species, empirical and modelled data have shown that the optimal average group size in a herd is in the range of $1 \leq n \leq 400$, for instance, impala and zebra has a mean herd size n of $n \leq 70$ [147]. Hence, in this evaluation we set the group size to be 70 as in [147]. Moreover, at anytime, the radio transmission is assumed to cover a maximum disk area of radius d_c. The performance evaluation is simulated in Matlab. Within a cluster the distance between animals is denoted by the critical range d_c. The carrier frequency is set to BLE (2.4 GHz) and LoRa (868 MHz). For all simulation set-ups, we assume that nodes are homogeneous in their initial amount of energy [14, 135]. To avoid the effect of AS node location on the over-all performance, in each case the AS is assumed to be placed at the center of the area coverage at equidistant range (d) from AB nodes in case of single-hop hybrid tree topology.

In case of multi-hop hybrid tree topology and opportunistic multi-hop hybrid tree topology, all node pairs' links are assumed to be equidistant range (d) to control the effect of range variation on the energy consumption. Moreover, a stationary mobility scenario is used to model the network performance in a controlled manner. To observe the impact of spreading factor, the LoRa radio link (AS to LG) is set to the extreme values, i.e. highest (BW125SF7) and lowest (BW125SF12) setting. The respective parameters for ToA for LoRa and BLE radios are described in Table 4.1 and Table 6.1 summarizes the simulation parameters used.

TABLE 4.2: *Path-loss and critical range simulation parameters*

Notations	Values	Details
f_{LoRa}	868 MHz	LoRa Carrier freq.
f_{BLE}	2.4 GHz	BLE Carrier freq.
$\sigma_{\psi_{dB}}$	3.65 dB	log-normal shadowing
γ	2.7	path-loss exponent
h_t	20m	LG antenna height [m]
$Cov(C)$	97%	coverage area probability
P_{Tx}	max (20dBm), min (2dBm)	transmit power
P_{RxBLE}	41.58 mW	BLE receiver power
P_{RxLoRa}	35.64 mW	LoRa receiver power
d_c		critical range
d_0	$1m$	BLE near-field range
n	70	number of nodes
PL_{BLE}	31 Bytes	packet for BLE
PL_{BLE}	51 Bytes	packet for LoRa
x	36 minutes	resync. period
m	1000	number of resync period
V	1.225v	voltage
Q_p	$1150mAh$	battery capacity ($1mAh = 3.6J$)
t	$m \times x = 36000min$	simulation duration

4.2.3 Results and discussion

Critical range

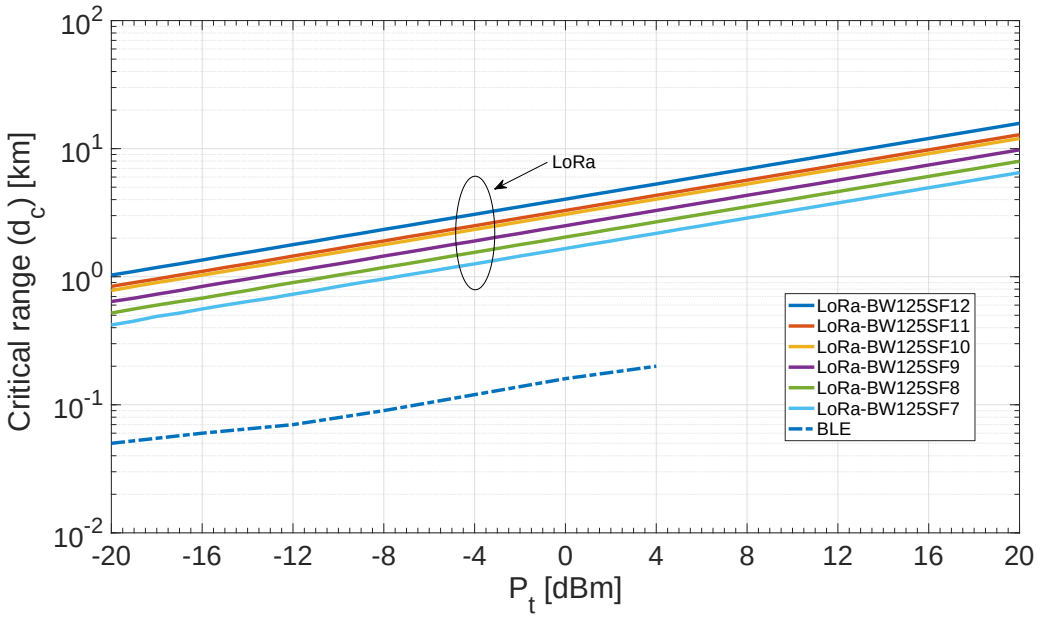

FIGURE 4.2: *Critical range (d_c)*

The critical range that could be achieved by BLE and LoRa radios against the required transmit power setting for a rural flat environment is shown in Figure 4.2. This figure is plotted by utilizing Equation 4.9 and extrapolating the P_{Tx} values from the specified P_{Tx} levels in the data sheets: for LoRa $-1 \leq P_{Tx} \leq -20$dBm in steps of 1dBm, and for BLE $20 \leq P_{Tx} \leq 4$dBm in steps of 4dBm. Hence, Figure 4.2 shows that at high transmission power results in a larger reception range. In an open rural enviroment, the range of BLE could reach up-to 200 m at maximum P_{Tx} = 4 dBm. The critical range d_c for LoRa at BW125SF12 setting is found to be 15.7 km, this range is achieved at the highest SF and P_{Tx} configuration (Figure 4.2). LoRa BW determines the noise floor and thereby the radio sensitivity level. An increase in LoRa radio operating channel BW decreases the receiver sensitivity, and higher SF lowers the receiver sensitivity [135]. Figure 4.2 shows that for every increase in SF, the transmission range increases accordingly. Higher SF indicates longer range with better reception, but longer packet ToA duration.

The received power strength against range is illustrated in Figure 4.3. It is plotted by using Equation 4.10 and extrapolating the P_{Tx} values from the specified P_{Tx} levels in the data sheets. For LoRa radio the minimum receiver sensitivity ($P_{r_{min}}$) is -136 dBm at band-width (BW=125 kHz) and spreading factor (SF=12); and maximum sensitivity is -123 dBm at BW=125 kHz and SF=7 [135]. The receiver sensitivity for BLE is -116 dBm as per the BLE datasheet [6]. For a given transmission power P_{Tx}, the P_{Rx} decreases linearly at $65dBm/km$ and $35dBm/km$ with respect to $log_{10}(d)$ for BLE and LoRa respectively. P_{Rx} of BLE radio decays faster than LoRa radio as the radio range increase.

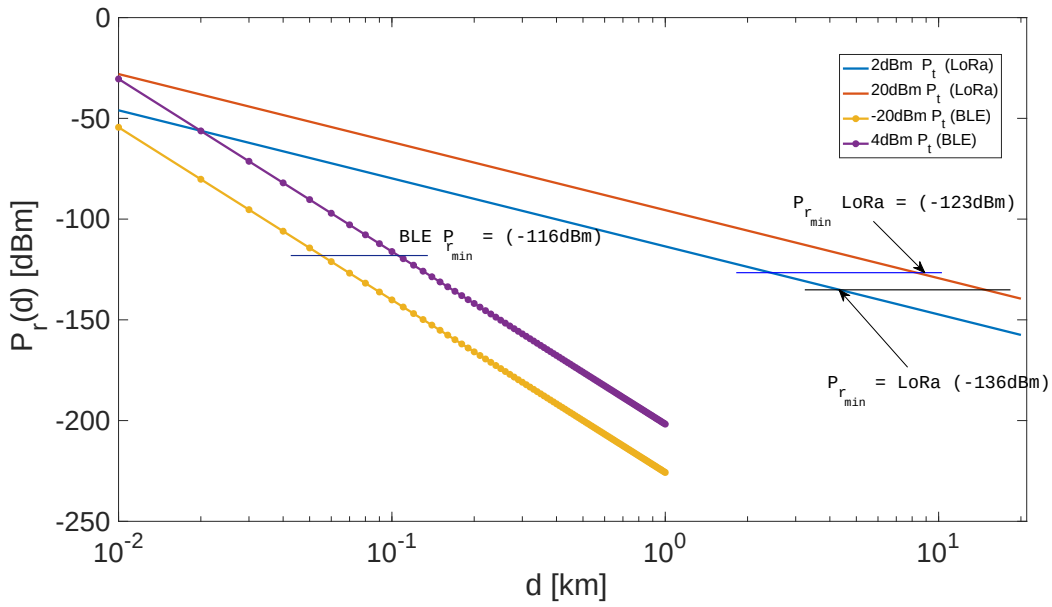

FIGURE 4.3: *Received power ($P_{Rx}(d)$), values are based on Hata Cost-231 (for LoRa) and simplified (for BLE) path loss models with log-normal shadowing.*

Network energy consumption

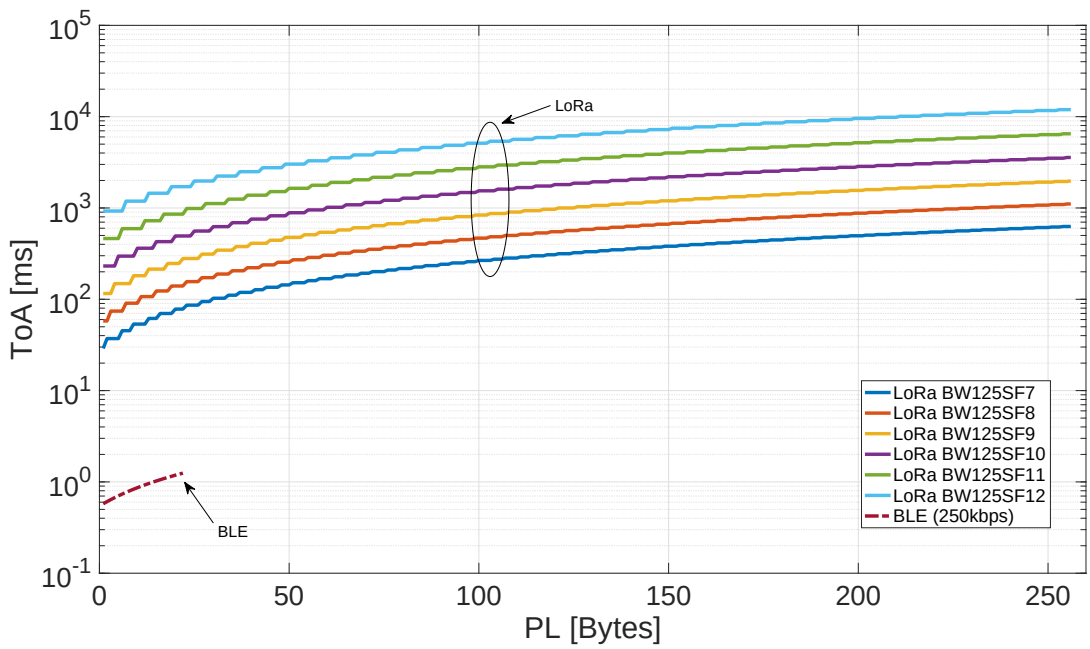

FIGURE 4.4: *Time-On-Air (ToA) for LoRa and BLE*

Figure 4.4 shows the *ToA* comparison of LoRa and BLE radios with respect to max payload size (*PL*). In theory, LoRa devices can transmit or receive at maximum size of 256 bytes in LoRa mode at any *SF* settings [135]. Higher *SF* provides a more robust transmission to environmental interference at a cost of slower data rate. However, at high *SF* (i.e. *SF*=12), the ToA for a payload of 256 bytes will be impractically

long (i.e. 7708ms) (Figure 4.4). It is often suggested, if a long PL is desired to be transmitted at a lower data rate, the data should be fragmented into smaller payloads. Thus, the exclusive ToA for LoRa (at SF = 7, CR = 1, DR = 5 kbps) and BLE (at DR = 250 kbps) is 46 ms and 0.544 ms, respectively.

Packets to the same destination is concatenated to one LoRa packet at the AS node before being relayed to LG. Here, $||$ denotes the concatenation operator. The maximum size of a concatenated packet may reach to the maximum LoRa packet size (i.e. 256 bytes) [135]. Moreover, due to the 1% transmission duty-cycle restriction in case of LoRaWAN, end-devices are not allowed to access the channel for at least $T_{offsubBand} = 99 \times ToA$ seconds, which will contribute to the high network latency for star based LoRa networks. Hence, instead of direct LoRa connectivity as in star topology, utilizing data concatenation at the AS node for single-hop, multi-hop, or opportunistic networks will drastically reduce the overall energy overhead, as will be demonstrated as follows.

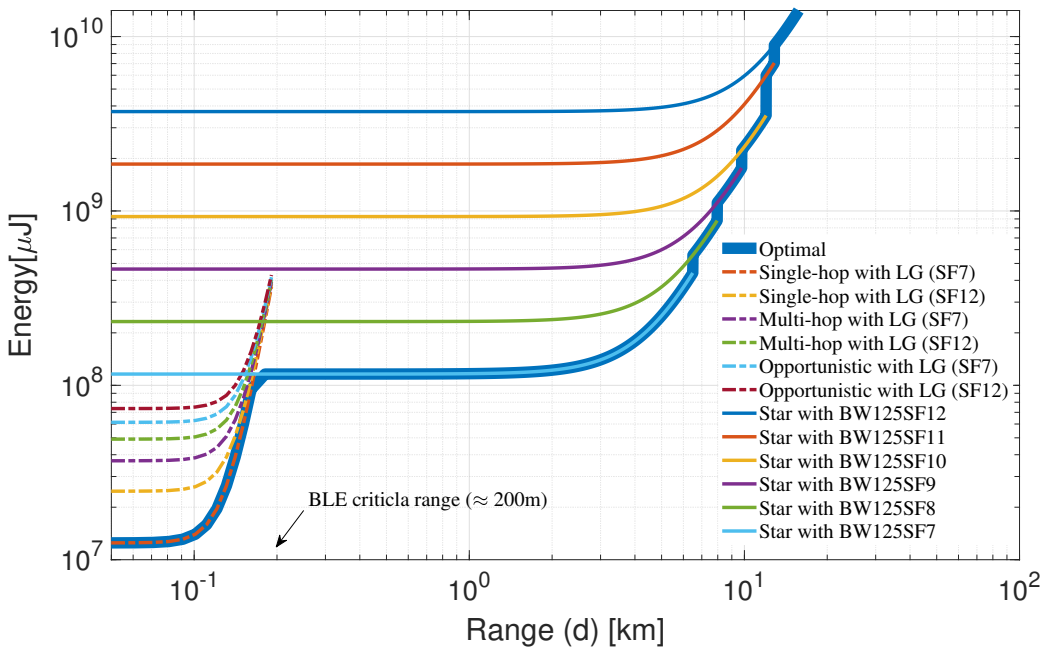

FIGURE 4.5: *Impact of range (d) on total network energy consumption considering path-loss and shadowing for rural (flat) environment*

A more interesting result for the network energy consumption overhead is presented in Figure 4.5, while considering path-loss and shadowing for rural (flat) environment into account. This figure is plotted utilizing Equation 4.3, 4.6, 4.7, and 4.8 for single-hop, multi-hop, and opportunistic, and star hybrid tree networks respectively, by rearranging Equation 4.10 for P_{Tx} to relate it to received signal strength P_{Tx}. Overall, the hybrid tree topologies for WMS decreases the energy consumption of star based network topology by up-to two fold by utilizing hybrid radios. Hence, as long as the communication range is within the proximity range between animals while in herds or groups (i.e. $d \leq 150m$) [13, 14], it is optimal to utilize the hybrid tree network with BLE and LoRa radios. This shortens the ToA tp be able

to send a burst of packets in a very short time, consequently, reducing energy usage considerably (Figure 4.5). The energy consumption for single-hop, multi-hop, and opportunistic networks exists until the critical range for BLE is reached, i.e. $d \leq d_{cBLE} \approx 200m$ (Figure 4.5).

In general, the energy consumption is directly to the ToA and radio range (which in-turn is related to transmission power and received signal power) [145]. As the range increases, there is a trend of increased energy consumption due to the higher transmission power need to reach the respective range. This relationship is specially more prevalent after 100 m for BLE and after 6 km for star network (Figure 4.5). Star network topology only performs better in-terms of energy compared to all other hybrid tree BLE networks after $\approx 150m$ at a cost of lower data-rates.

However, for ranges ($d150m$) the single-hop, multi-hop, and opportunistic hybrid tree networks perform better than star network. This is mainly because the hybrid tree topology types take advantage of the shorter ranges to make the overall system more efficient in-terms of energy and bit-rate trade-off by utilizing the relatively high bit-rate BLE (250 kbps) radio instead of low bit-rate LoRa (5 kbps) at shorter ranges. As shown in Figure 4.5, for the scenario where the communication range between pair of nodes becomes greater than 150m, then it becomes more optimal to use the conventional LoRa star network instead of BLE based hybrid tree networks. This type of network scenario is rare since animals often display a con-specific behaviour, where they live in groups close to each. As shown in 4.4 and Figure 4.5, senders located closer to the receivers can transmit using high date-rate (i.e. with shorter ToA and less energy), thus for shorter ranges utilizing BLE is more efficient than LoRa. The maximum range for BLE radio is 200m, however, LoRa allows adjustment of the SF for transmitting over a greater range at the expense of lower bit-rate.

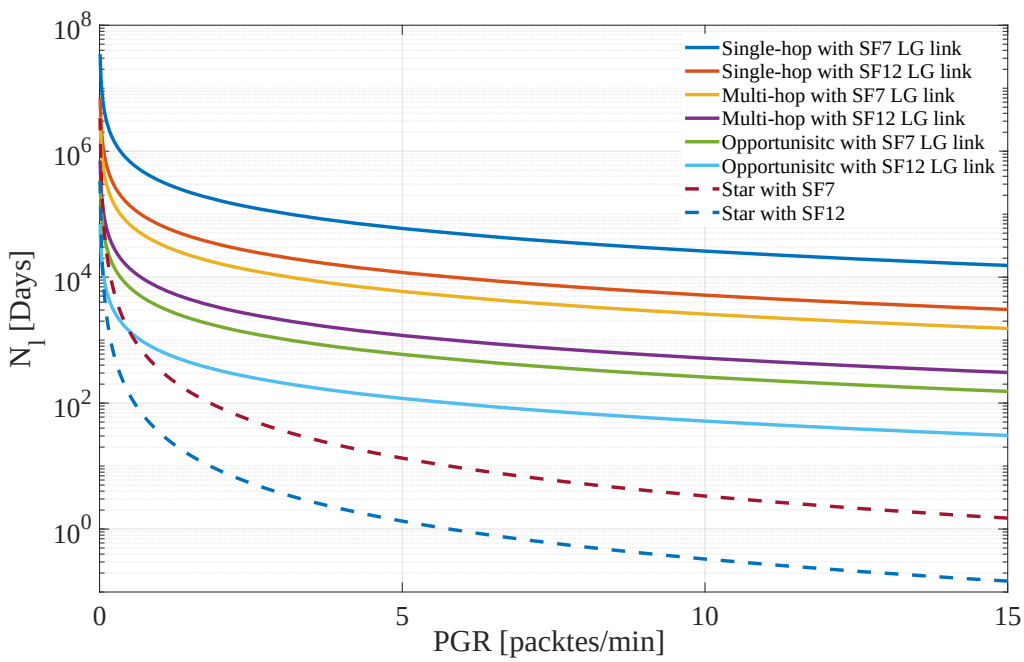

FIGURE 4.6: *Impact of PGR on the network life-time*

To make a fair evaluation of the impact of packet generation rate on the network life time, the radio range (d) is controlled by setting the transmission power (P_{Tx}) of BLE and LoRa radios to a value equal to the maximum transmission power of BLE radios, i.e. 4 dBm. This is because even at maximum power settings BLE reaches upto 200 m, which is in the range of LoRa radio at BW125SF7 and BW125SF12 settings. Given a battery capacity $Q_p[mAh]$, and supply voltage (v), the network life-time N_l of node n is defined as:

$$N_l = \frac{n \times Q_p \times V}{E \times PGR} \tag{4.13}$$

, where PGR is the packet generation rate.

As shown in Figure 4.6, for both hybrid tree and star topology, the network life-time depicts a decreasing trend as network packet generation rate (PGR) increases. However, for higher PGR, star networks has relatively shorter life-time compared to the all other hybrid tree modes, confirming that conventional star networks are not suitable during high rate of packet exchange, as it often happens in wildlife monitoring applications. This difference is mainly attributed to the higher data-rate of BLE radio (250 kbps) compared to LoRa (5 kbps), that leads to shorter ToA duration for BLE, hence, decreasing the overall network energy consumption substantially. Overall, for higher PGR the hybrid tree network almost doubles the network life-time compared to star based networks (Figure 4.6). This indicates how the hybrid tree topology is more optimal than the conventional star topology for animal monitoring applications requiring high data rates.

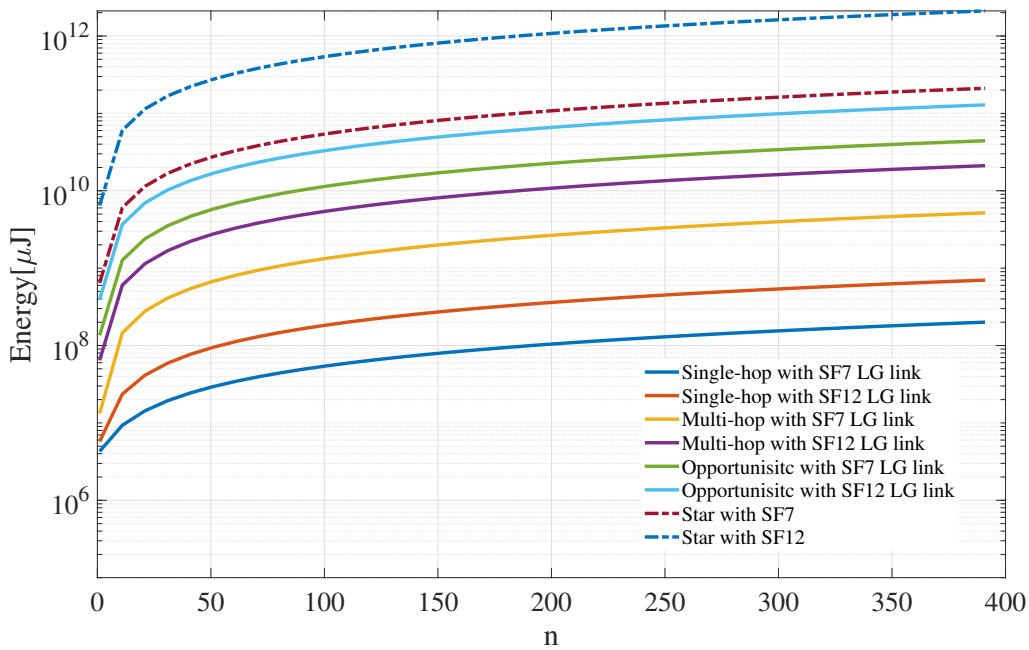

FIGURE 4.7: *Impact of number of nodes on energy consumption for rural (flat) environment.*

As shown in Figure 4.7, the energy consumption increases as the node number (n) increases, and as expected the hybrid tree network saves more energy than star network. It is clear from Figure 4.7, in general higher node density in the network will contribute to having a higher network energy consumption.

Discussion

The feasibility of star and hybrid tree wireless network topologies are investigated in this chapter. For applications requiring high network life-time at high packet traffic intensities, hybrid tree topology is more suitable. Moreover, BLE easily integrates with existing IoT technologies such as LPWAN. LPWAN solutions (e.g. LoRa) are suitable for providing a larger coverage range (up-to 15km) at lower data rate, lower packet traffic intensities and low energy consumption which is ideal for relaying concatenated data from BLE mesh network. Hence, in sparsely sensor node distribution, as in a herd of con-specific animal population, leveraging BLE with LoRa, would provide the desired WMS deployment.

The energy evaluation for similar cases as the previous test setups are used, except, transmitting nodes are set to send periodic packets every $IPI = 10$ minutes and the energy consumption overhead for this case is shown in Figure 4.8 with aggregation at AS node and considering the start-up and periodic network overhead and ToR without considering the path-loss and log-normal shadowing. Table 4.3 summarizes the performance comparison of hybrid tree and conventional start topology for different network configuration scenario including the communication and data aggregation overhead. In almost all the scenarios, the hybrid tree network topology is suitable for wildlife monitoring than the star topology.

4.3 Performance analysis of LoRaWAN

In this section, we provide an in-depth performance evaluation of LoRa radio for an IoT applications. Furthermore, from the analysis and evaluation results, we propose a suitable radio configuration to suitable for IoT applications.

4.3.1 Evaluation setup

Figure 4.9 shows the LoRaWAN network deployment at one of the buildings of the *University of Twente* campus, where our experiments took place. The indoor experiments were performed with end-devices and a gateway node placed on one floor of our office building as shown in Figure 4.9, the floor is roughly 103 m by 20 m. To test LoRa for performance for a different communication scenarios, the transmitting end-devices were placed at four locations (denoted by L1 - L4); while the receiving gateway was placed at the corner of the building. Experiments were performed during normal office working hours to include the influence of people movements and environmental dynamics on LoRa network performance.

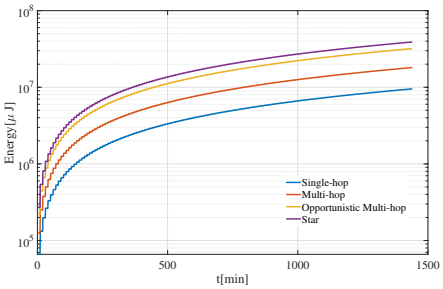

(A) *For hybrid tree: short range (DR=Fast, TXP=Low), long range (DR=Slow, TXP=High).*
For Star: long range (DR=Slow, TXP=High)

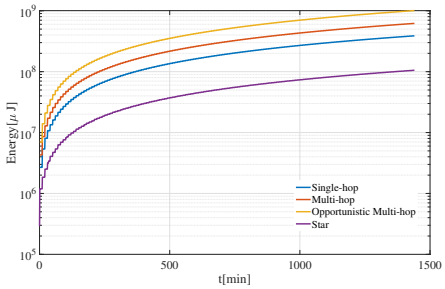

(B) *For hybrid tree: short range (DR=Fast,TXP=Low), long range (DR=Fast, TXP=High).*
For Star: long range (DR=Fast, TXP=High)

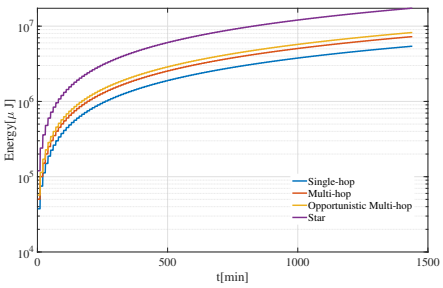

(C) *For hybrid tree: short range (DR=Fast,TXP=Low), long range (DR=Fast,TXP=Low).*
For Star: long range (DR=Fast,TXP=Low)

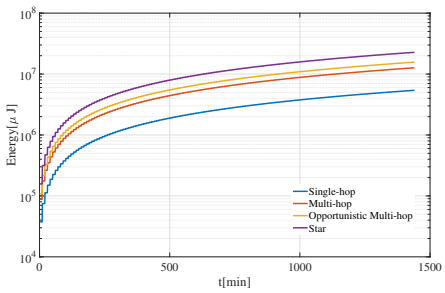

(D) *For hybrid tree: short range (DR=Fast,TXP=Low), long range (DR=Fast,TXP=Low).*
For Star: long range (DR=Slow,TXP=Low)

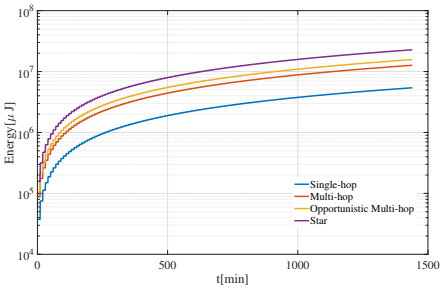

(E) *For hybrid tree: short range (DR=Fast,TXP=Low), long range (DR=Slow,TXP=Low).*
For Star: long range (DR=Slow,TXP=Low)

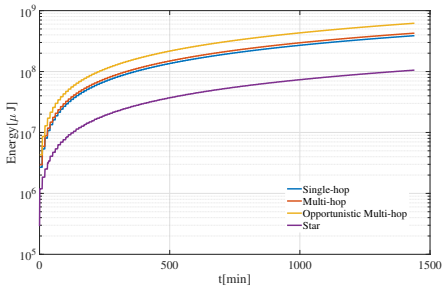

(F) *For hybrid tree: short range (DR=Slow,TXP=Low), long range (DR=Slow,TXP=Low).*
For Star: long range (DR=Slow,TXP=Low)

FIGURE 4.8: *Utilizing LoRa for all links with aggregation, and periodic re-synchronization with path-loss and shadowing*

Changing the spreading factor (SF) results in a change in $T_{OffSubBand}$ and time on air ToA, which will subsequently result in a change in the link budget, i.e. battery lifetime versus range trade-off. For example from Equation 4.2, it will take at least 2465.79 ms for $SF = 12$ and 102.66 ms for $SF = 7$ to finish sending a 51 Byte long data-frame. This is in accordance with the 1% duty-cycle regulation, calculated

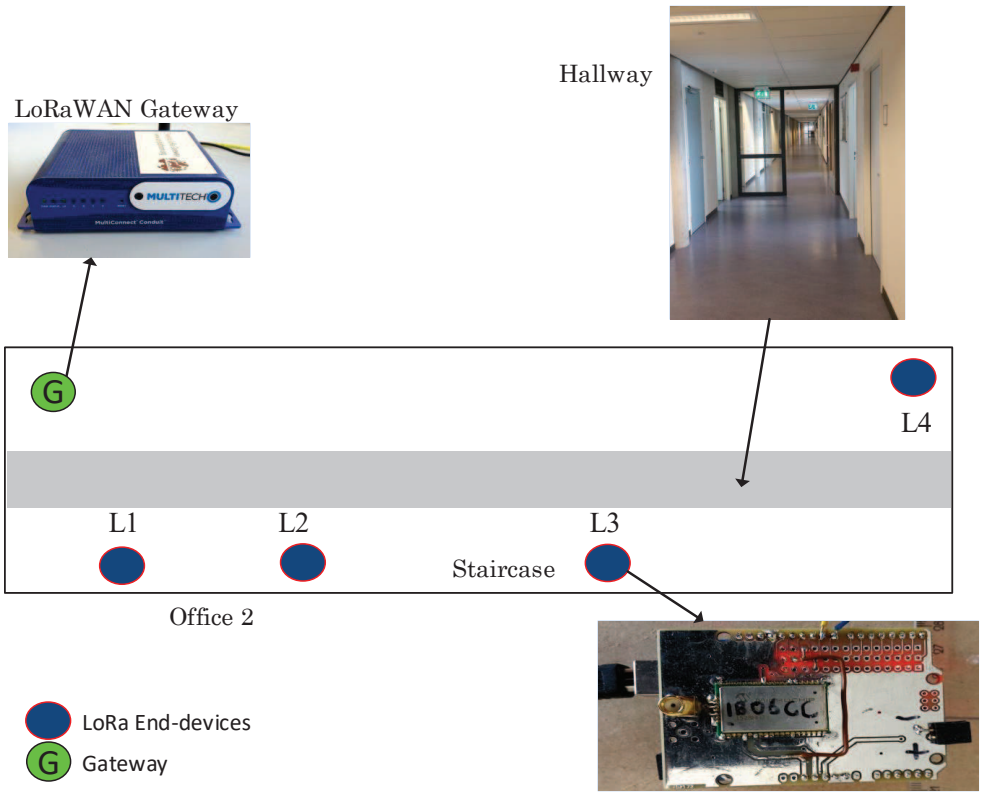

FIGURE 4.9: *LoRa End-nodes deployment across building hallway floor at locations L1 to L4. The four locations are chosen in an increasing order of transmission range from the gate way, which is located at the left corner of the building.*

with respect to the payload size for every spreading factor settings. In addition, all the measurements are performed using unconfirmed mode (unacknowledged) data frame types to prevent the acknowledgement from clogging the channel for upstream packets.

To evaluate performance of the LoRa radio, we built a LoRa radio enabled end-device using *RN2483* and Arduino Uno modules and mounted the LoRa radio module on top of a custom made Arduino shield equipped with an antenna [135] (Figure 4.9).

The the LoRa gateway is a *MultiConnect Conduit* gateway, as shown in Figure 4.9 [148]. Since the gateway is designed to listen for incoming messages on the 868 MHz band, all end-devices support the three default LoRa channels (0, 1 and 2, i.e. 868.1, 868.3, 868.5 MHz) that must be implemented in every EU868MHz end-device to comply with the LoRaWAN specifications. We set up a local *Node.js* web application set as the server-side of LoRa network server. It runs a *Mariadb* database to collect and store LoRa packets. The database will provide various information about the received packets such as RSSI values and sequence number.

4.3.2 Results and discussion

Impact of DR on ToA and transmission delay

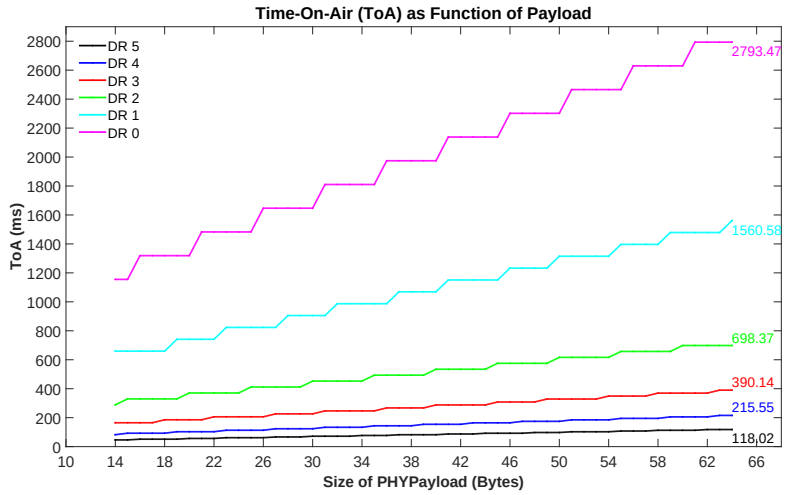

(A) *ToA as a function of payload for different DRs*

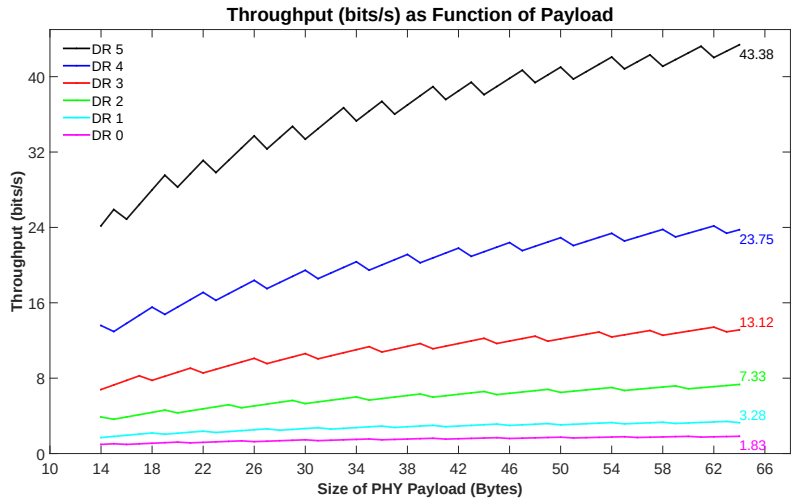

(B) *Maximum throughput per payload based on the 1% duty cycle restriction*

FIGURE 4.10: *Effect of Data Rate (DR) on Time on Air (ToA) and Throughput*

Based on Equation 4.2 expressing transmission time of a LoRa packet, ToA for varied payloads can be calculated. This will give an indication about the average time delay between each packet based on the duty-cycle restrictions specified in [149]. It also indicates the maximum achievable throughput for different transmission configurations. For this calculation, we assume that the transmitting end-devices send packets as often as possible. The graphs shown in Figure 4.10a and Figure 4.10b show the ToA and corresponding throughput as a function of payload for five different DRs. These graphs are obtained by setting the coding rate to 4/5, the channel bandwidth to 125 kHz. The payload size is varied between 14 and 64 bytes.

Small (one-byte payload) packets can approximately be transmitted 2.5 times more frequently than packets with 64-byte payload. The trade-off between transmission rate and payload size means that devices requiring frequent data updates should keep their messages as short as possible. This is to decrease the time delay before a new transmission is allowed. As long as they are still able to reach the gateway, end-devices should use the fastest (lowest numerical) possible DR when Time on Air reduction is required, since each increment in DR almost doubles the ToA (as shown in Figure 4.10a).

In general, the size of payload a device can send in LoRaWAN specifications is very limited. The maximum payload of 235 bytes on DR4 and DR5 allows transmitting a reasonable amount of data. However, the maximum throughput of 50.96 bits/s (on DR5, with a payload size of 235 bytes) makes fast transmission of large amount of data impossible (Figure 4.10b).

Figure 4.11 depicts the average time delay between the series of packets for each DR (in red) and the theoretical time delay between packets (in blue). On each spreading factor, 200 packets with a fixed payload length of 64 bytes and coding rate of 4/5 were transmitted from an end-device to a nearby gateway. The total time difference between the first and the last packet divided by the total number of transmitted packets in that time gives the average minimum time delay between each packet for each spreading factor. The measured average times between packets lies very closely to the calculated theoretical values calculated by Equation 4.2 and shown in Figure 4.11.

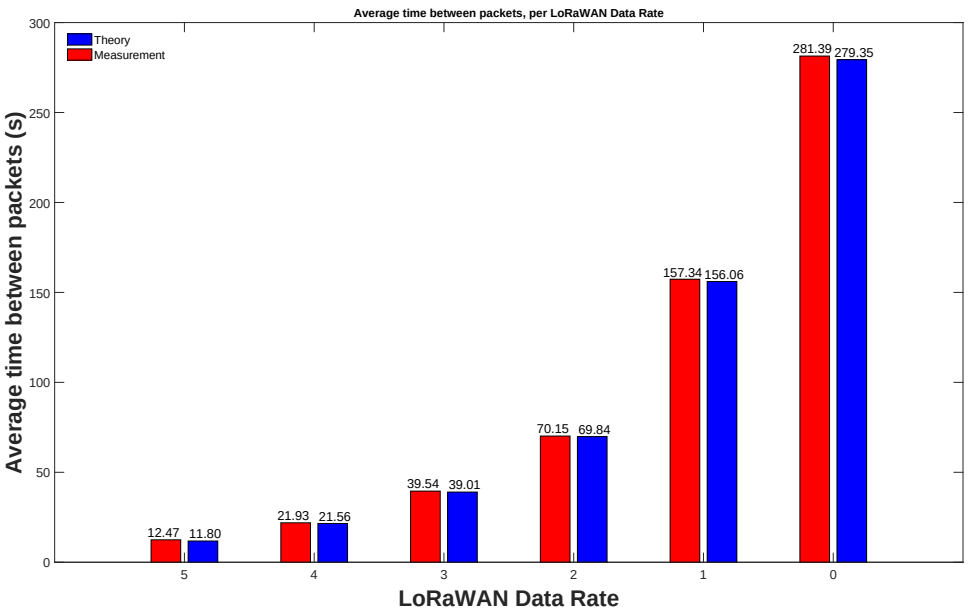

FIGURE 4.11: *Time delay between transmitted packets for data rates DR0-DR5, i.e. the delay from $T_{offsubBand}$ for every transmitted packet.*

LoRa end-devices current consumption profile

To obtain the current profile of LoRa end-devices, when they are powered with a 3.7 V Li-ion polymer battery. We program the end-device to join the LoRa network with Over-The-Air Activation (OTAA) procedure and once accepted into the network, it will transmit an unconfirmed packet on each possible transmission power and will switch to a deep sleep mode for 10 seconds afterwards.

Figure 4.12 shows the transmission current drawn by the Arduino and RN2483 module when it is not transmitting in the last column. The join procedure consists of a transmission at the maximum output power of 14 dBm. Lastly, the current draw during a receive-window is not influenced by the transmission power. On average, the total current draw equals 45.5 mA during receive-windows, and 11.4 mA when leaving out the current consumption Arduino. The measured values are slightly higher, most likely due to the higher supply voltage (3.3V instead of 3.0 V) to the RN2483 module. Knowledge of the energy consumption can help determining battery life based on transmission schemes of end-devices and the available battery power. Optimization based on these results can mostly be achieved by using a less energy consuming device to mount the LoRa module on, i.e. to replace the Arduino with a less energy consuming (dedicated) host device, and by putting the LoRa module in deep sleep mode in idle cases.

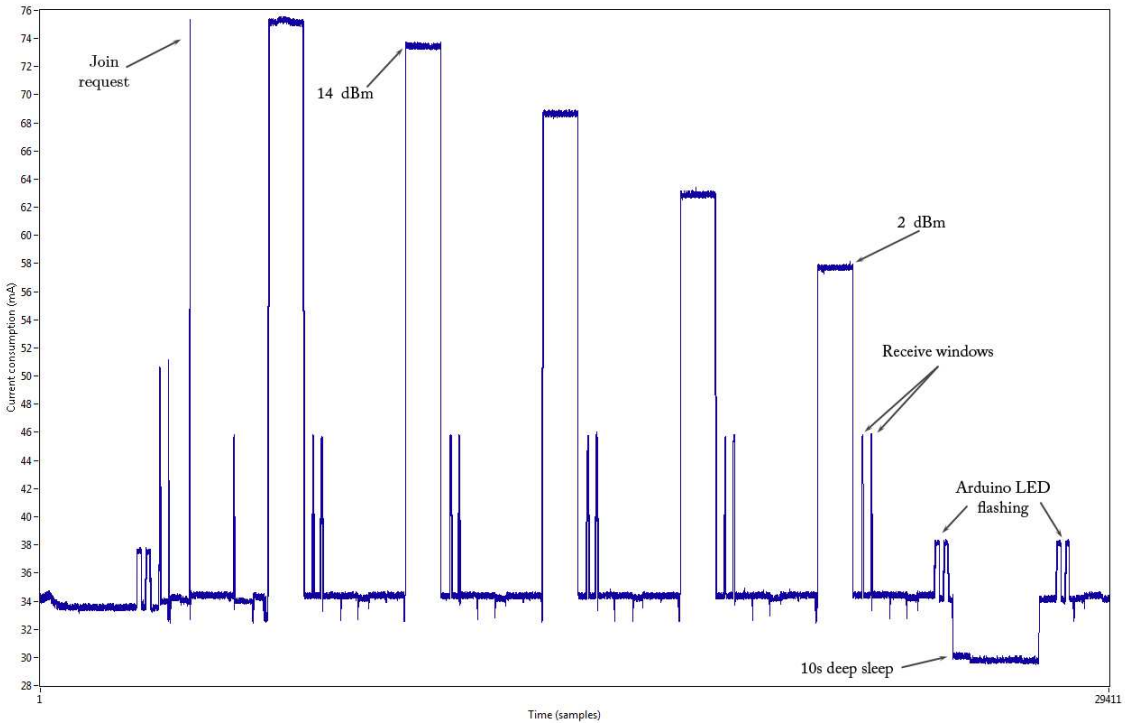

FIGURE 4.12: *Current usage of LoRa end-device when joining a network and transmitting 5 packets*

Impact of received signal strength

To test the overall capability of LoRa radio receiver to demodulate data from a received signal, we analyze the received packets in terms of their RSSI values. These values are compared to the Semtech SX1276 LoRa receiver theoretical sensitivity, which is specified for various BWs and SFs [150] settings (Table 4.4). In our experiment the end-device transmits 50 data packets, each with 50 bytes of payload, for each test location at all SF. All packets are sent with unconfirmed mode with no re-transmissions, as summarised in Table 4.4.

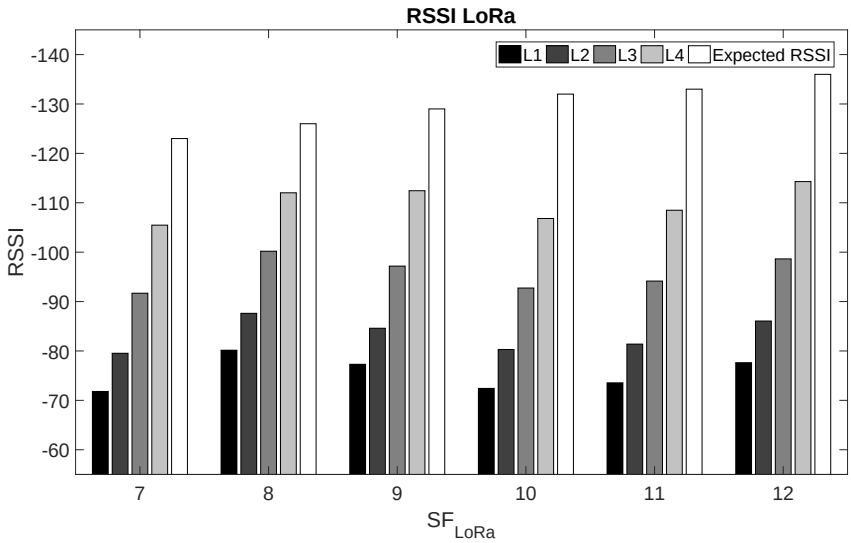

FIGURE 4.13: *Minimum RSSI (in dBm) for SF=7 to 12 at locations (L1, L2, L3 and L4)*

Figure 4.13 shows the minimum RSSI measured at locations L1, L2, L3, and L4. As the number of obstructions (non-line-of-sight) and distance to the gateway increases, the RSSI values decreases. This trend is observed for all SF values. The minimum RSSI for received packets decrease as the SF value increase as discussed in [134]. In our results this is only true for SF7, SF10, SF11, and SF12. In case of SF8 and SF9, SF9 performs better than expected, and SF8 performs *even much* better. In other words, SF7 and SF8 are performing as expected, while SF9 up to SF12 perform worse than expected.

It is not possible to prove this by only looking at the RSSI. Therefore we also measure the packet error rate and analyze it in the next section. A possible alternative reason for the unexpected high minimum RSSI values for higher SFs is the way the RSSI is calculated. For higher SFs, a packet has a longer ToA (Equation 4.2), giving a longer time over which the signal strength can be integrated. This depends on the method implemented inside the proprietary ("black box") LoRa radio module.

For locations closer to the gateway, the link fluctuation is high at high SFs, with maximum standard deviation of $\sigma = 4.18dBm$. The wireless link is observed to be more stable at the farthest location at high SFs (SF11, SF12), with maximum deviation of $\sigma = 3.6dBm$ only.

Impact of packet error rate

Figure 4.14 illustrates the packet error rate (PER) versus LoRa end-node locations (L1-L4) for spreading factors SF7 to SF12. The transmitted LoRa packet is set to unconfirmed with no retransmission. End-devices transmit 50 data packets each with 50 bytes of payload for every test location. One can see that in general the packet loss has an increasing trend when the transmitter end-device is farther from the gateway location. We expect that a higher SF should result in a lower PER [150]. This is, however, not observed at any one of the four locations.

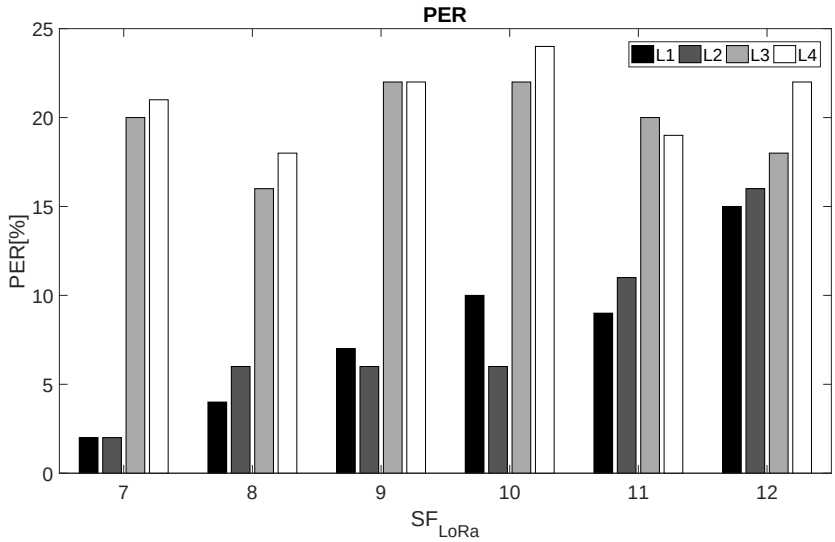

FIGURE 4.14: *Packet Error Rate (PER) for SF=7 to 12 at Locations (L1, L2, L3 and L4).*

Since the LoRa gateway is placed in an indoor environment, it is more susceptible to indoor signal shadowing and multi-path fading. Using high spreading factors, such as SF=12, increases the $Time - on - Air$ as expressed by Equation 4.2, resulting in a 50 byte payload LoRaWAN packet to have a $ToA = 2794$s. In an indoor environment with people moving around signal paths can change very fast.

The reason for higher SFs to perform worse than lower SFs is partly related to the longer ToA of higher SFs. When a packet is received by the gateway, the preamble of the packet is used by the receiver to lock onto the transmitter. This "*locking on to*" means both synchronizing in time and adjusting the gain of the receiver's preamplifier. Preamplifiers can have a relatively small dynamic range compared to the variations in the signal path at an indoor location. Our theory is that a packet with a long ToA will be received at a specific preamplifier setting, but shortly after this the signal strength will change rapidly because of multiple signal paths as well as quick fading due to movement of people in the building. As soon as the received signal strength falls outside the dynamic range of the receiver's preamplifier, the rest of, or part of the packet is not received. For longer packets, the fraction of the packet that is not received becomes more significant, causing the forward error correction to fail. For lower SFs, the ToA is much shorter. This lowers down the chance of falling outside the dynamic range of the receiver. This will lower down the fraction

of the packet that is not received and will consequently increase the probability of the forward error correction to succeed.

If our assumption about the preamplifier in the *"black box"* proprietary LoRa receiver is correct, then the results illustrated in Figure 4.14 can be described as follows: closer to the gateway, packets with shorter *ToA*s are more likely to be received. For locations further from the gateway, lower spreading factors are more likely to fail. Location L1 is close to the gateway and the effect of packet ToA can be clearly seen. The further we go from the gateway, the effect of SF is more visible as PER is rapidly increased for lower SFs and slightly increased for higher SFs.

Impact of coding rate and transmission power

To evaluate the impact of coding rate and transmission power on LoRa performance by fixing the data rate, hence, all packets are sent at a fixed SF. In the first test, we transmit 15 packets on each coding rate, transmission power and three data rates, i.e., DR 5, DR 3 and DR 1 at each transmission round. After every 15 packets, the coding rate is increased until the maximum is reached. Then the coding rate is set back to the minimum and the transmission power is decreased by one. The end-devices were programmed to start at DR5, coding rate 4/5, and transmission power of 14 dBm.

After each 15 packets, the coding rate was increased until the maximum of 4/8 was reached. Then the transmission power was lowered one step and the same process was repeated. The packet loss from the end-device at location L3 transmitting on DR5 (i.e. SF=7) is shown in Figure 4.15. It can be seen that generally transmitting packets with a higher transmission power decreases the packet loss.

We repeat the same experiment with DR3 and DR1. Figures 4.16 and 4.17 show the results. One can see that When the data rate is decreased (resulting in an increase of the spreading factor), the packet loss decreases as well. This behaviour is expected from the spread spectrum concept as signals with higher spreading factors are more likely to reach a gateway. There are, however, also some notable differences in packet loss between the end-device at different CRs.

Some end-devices show a slightly higher packet loss at higher coding rates or transmission powers, which contradicts the expected lower packet loss at higher coding rate and transmission powers. The numerical differences between the lost packets on different transmission settings are, however, small and might have been caused by environmental changes of office environment due to factors such as people moving around and doors being opened and closed.

4.3.3 Summary

In this section, we studied LoRa wireless technology, a new LPWAN protocol for IoT applications, and conducted its network performance analysis. A general overview of LoRa modulation and network architecture is introduced. The associated LoRa

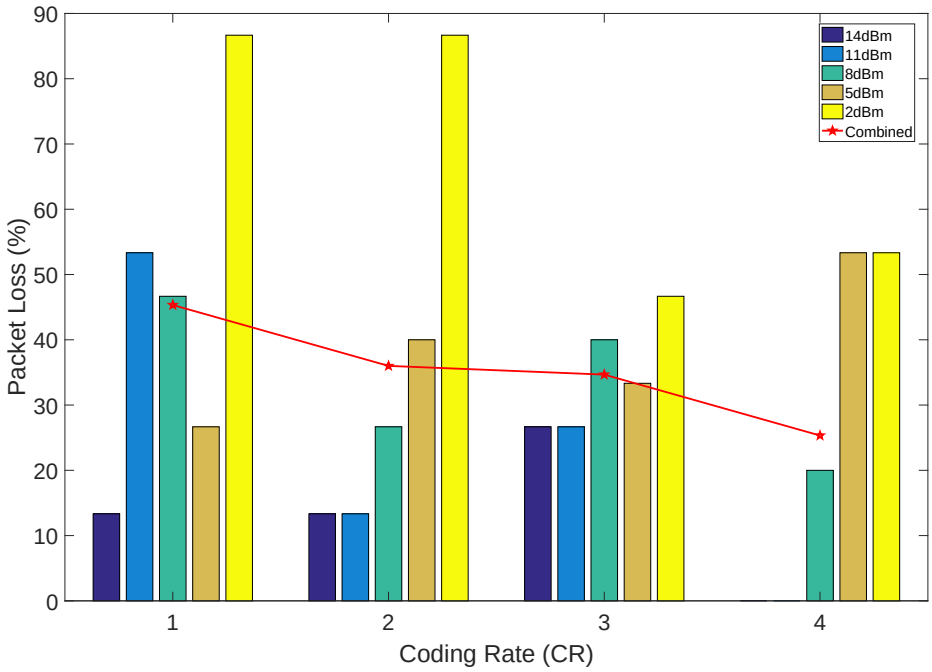

FIGURE 4.15: *The packet loss from the end-device at location L3, transmitting on DR=5*

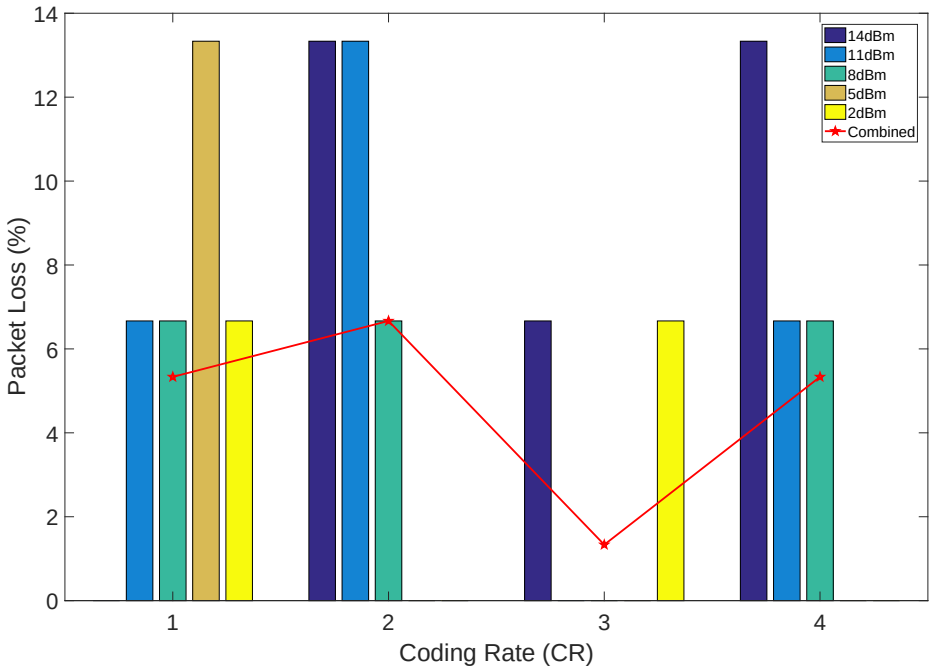

FIGURE 4.16: *The packet loss from the end-device at location L3, transmitting on DR=; for varying transmission power and coding rate.*

physical layer parameters such as spreading factor, bit rate and coding rate are

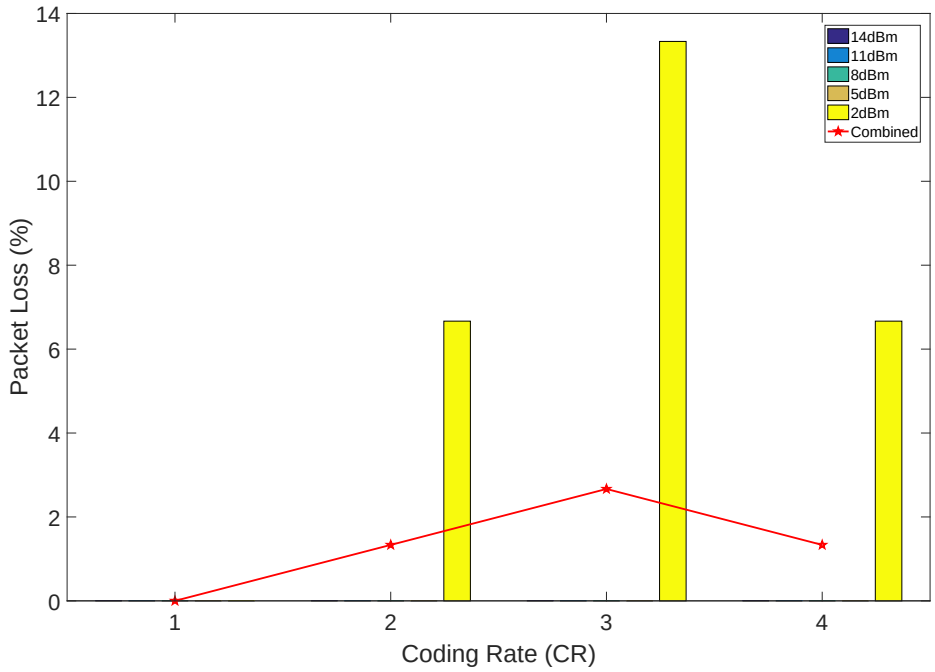

FIGURE 4.17: *The packet loss from the end-device at location L3, transmitting on DR=1*

discussed. We built and prototyped LoRa radio enabled network, to test the network performance. From our investigation of LoRa radio RSSI values, we observed that due to the broadband chirp pulses and higher sensitivity of the LoRa modulation, LoRa offers immunity against multi-path and signal fading especially at high spreading factor. At closer distances to the gateway, the RSSI is high for low spreading factor scheme. In addition, when the spreading factor is increased the packet loss decreases at the expense of decreased effective bit rate, which is not suitable for high throughput IoT applications. And at farthest locations from the gateway interferences are significantly high, therefore, end-devices should communicate at high spreading factors.

4.4 Conclusion

In this chapter, we presented a hybrid tree IoT network for wildlife monitoring that achieves wider control on the trade-off between energy consumption and range. This is achieved by the operating radio of WMS based on proximity measures and applying data concatenation scheme at the cluster-head. The evaluation results indicate that the hybrid network outperforms the traditional systems that use a single type of transceiver radio alone (i.e. LoRa or BLE). On average, our approach reduced the energy consumption of star topology (LoRaWAN) by up-to two fold. In addition the hybrid network improved the network life time by up-to 99% for various packet traffic rates in the network. Therefore, for con-specifically sparse animal population, our hybrid approach is more optimal to deploy than utilizing only LoRa network.

We are aware of the practical limitations associated with the proposed model, such as the path-loss based range calculation and the various modeled wireless parameters are not directly available for the physical radio hardware. However, we investigated the various techniques to address this issues, for instance, to develop a simple received signal based proximity analysis.

TABLE 4.3: *LoRa for long-range and BLE for short-range/inter-cluster: hybrid tree and star network topology overall energy consumption performance comparison. Legends: BLEDR= BLE data rate, i.e. 250kbps, DR= LoRa data rate, high=SF7BW125, low=SF12BW125, TXP= LoRa transmission power, and BLETXP = BLE.*

	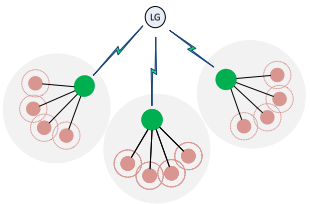				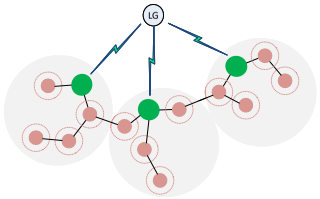				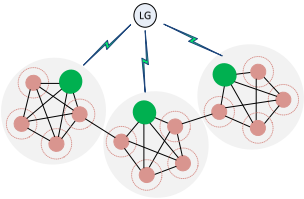				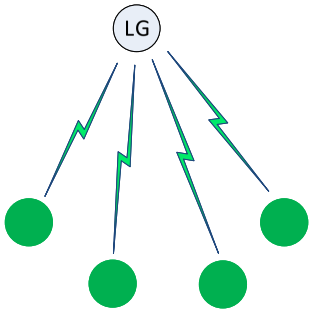		
	Single-hop				Multi-hop				Opportunistic				Star		Resolution
	AB->AS link		AS->LG link		AB->AS link		AS->LG		AB->AS link		AS->LG		AS->LG link		
	DR	TXP	DR	TXP	DR	TXP	DR	TXP	DR	TXP	DR	TXP	DR	TXP	tree
With Aggr. and no network OH	BLEDR	BLETXP	Fast	High	BLEDR	BLETXP	Fast	High	BLEDR	BLETXP	Fast	High	Fast	High	Single-hop hybrid tree
	BLEDR	BLETXP	Slow	High	BLEDR	BLETXP	Slow	High	BLEDR	BLETXP	Slow	High	Slow	High	Single-hop hybrid tree
	BLEDR	BLETXP	Fast	Low	BLEDR	BLETXP	Fast	Low	BLEDR	BLETXP	Fast	Low	Fast	Low	Single-hop hybrid tree
	BLEDR	BLETXP	Slow	Low	BLEDR	BLETXP	Slow	Low	BLEDR	BLETXP	Slow	Low	Slow	Low	Single-hop hybrid tree
	BLEDR	BLETXP	Slow	Low	BLEDR	BLETXP	Slow	Low	BLEDR	BLETXP	Slow	Low	Slow	Low	Single-hop hybrid tree
	BLEDR	BLETXP	Fast	Low	BLEDR	BLETXP	Fast	Low	BLEDR	BLETXP	Fast	Low	Fast	Low	Single-hop hybrid tree
With Aggr. and network OH	BLEDR	BLETXP	Fast	High	BLEDR	BLETXP	Fast	High	BLEDR	BLETXP	Fast	High	Fast	High	Single-hop hybrid tree
	BLEDR	BLETXP	Slow	High	BLEDR	BLETXP	Slow	High	BLEDR	BLETXP	Slow	High	Slow	High	Single-hop hybrid tree
	BLEDR	BLETXP	Fast	Low	BLEDR	BLETXP	Fast	Low	BLEDR	BLETXP	Fast	Low	Fast	Low	Single-hop star
	BLEDR	BLETXP	Slow	Low	BLEDR	BLETXP	Slow	Low	BLEDR	BLETXP	Slow	Low	Slow	Low	Single-hop hybrid tree
	BLEDR	BLETXP	Slow	Low	BLEDR	BLETXP	Slow	Low	BLEDR	BLETXP	Slow	Low	Slow	Low	Single-hop star
	BLEDR	BLETXP	Fast	Low	BLEDR	BLETXP	Fast	Low	BLEDR	BLETXP	Fast	Low	Fast	Low	Single-hop hybrid tree

LoRa settings		
Parameter	**Value**	**Details**
Center Freq.	EU 868MHz	Class A (Either of the Default three channels in case of 868MHz band)
Band Width (BW)	125Hz	Default for LoRaWAN configuration
Spreading Factor (SF)	SF7-SF12	SF7-SF12 are to be set (as per [**alliance2016lora**])
Tx-Power	14dBm	The maximum default tx power for 868 MHz
Tx Payload Size (byte)	50	(used with all Spreading Factors (SF)
Data Frame Mode	Unconfirmed	Unacknowledged data frame
Radio Antenna Properties		
End-Mote	Frequency range: 868MHz, Gain: 2.1dBi	RN2483 MICROCHIP LoRa Module, VSWR: $<$ 1.5
Gateway	Female SMA, 2dBi	Detachable Omni-directional antennas MUTITECH-Gateway

TABLE 4.4: *LoRa Radio parameter settings used in the performance test.*

Chapter 5

Single-hop Communication With Hybrid Tree Network

IN THIS *chapter, we introduce a single-hop communication with hybrid tree network for wildlife monitoring. Unlike conventional networks which are based on multi-copy data replication techniques, our approach utilizes an optimized single-copy beacon data transmission to achieve high energy efficiency. Furthermore, the collected data is concatenated and relayed to the central system by leveraging a low power and long range radio to provide high connectivity coverage. We evaluated the proposed approach in an actual animal movement scenario. The results indicate that the proposed solution outperforms the traditional opportunistic network protocols in-terms of energy consumption, packet delivery ratio, and latency.*

Part of this chapter has appeared in:
[22] *E. D. Ayele and N. Meratnia and P. J. M. Havinga, Asynchronous Dual Radio Opportunistic Beacon Network Protocol for Wildlife Monitoring System, 2019 10th IFIP International Conference on New Technologies, Mobility and Security, Gran Canaria, Spain, June, 2019, pp. 1-7.*

5.1 Introduction

Based on the movement behavior of wild animals and the requirements outlined in Chapter 1, conventional opportunistic networks, e.g Epidemic or PRoPHET [151, 123], are found to be not suitable for WMS application. This is mainly due to their multi-copy replication approach that leads to high sensor node resource consumption such as energy and data storage space. In addition, the movement behavior of wild animals often show a sparse and con-species (clustered) movement behavior. This behavior results in frequent change in the network topology, which gives rise to challenges in peer-to-peer network connectivity and energy management issues [21]. Even-though mobility is considered as the fundamental facilitator for information dissemination in opportunistic networks, recent works have revealed that current opportunistic protocols perform worse than expected for sparsely mobile networks with non-deterministic movement [151, 123]. For instance, Epidemic [151] and PRoPHET [152], offer a high data delivery ratio at the expense of high network overhead and latency [123]. Spray and Wait (SnW) [151] on the other hand results in low latency but has high network overhead [123].

There are several projects that use opportunistic networks for wildlife monitoring, for instance, ZebraNet [27] and Rat Watch [153]. These projects, however, implement opportunistic networks by leveraging an Epidemic like flooding, which is prone to low delivery ratio and high latency [151]. Moreover, they lack the low power data concatenation backbone network to relay data to a central system. Instead, they often utilize offline data gathering or cellular and satellite based systems [154]. However, the inherently high energy cost and intolerable communication latency makes these approaches less attractive.

In this chapter, we present a single-hop hybrid tree network based on an asynchronous dual radio opportunistic beacon network for wildlife monitoring. Our proposed opportunistic beacon network leverages a high data rate BLE radio in a low power long range LoRaWAN network [21]. Utilizing LoRaWAN for long range data relaying introduces a *1% duty-cycle* communication restriction, which impacts the real-time latency requirement. We, therefore, address this challenge by utilizing dual interface, to provide a wider control over the trade-offs in energy versus latency, and by not sending all the received raw data to the LoRaWAN server. Instead, data pre-processing within animal herds or groups is applied before relaying the data to the central server. This is mainly because data processing is computationally cheaper than data transmission. This approach will ultimately reduce the implementation complexity of the WMS solution [21]. Unlike existing opportunistic protocols that use a multi-copy data replication scheme, our protocol utilizes a single copy replication scheme with data concatenation and pruning at the receiving nodes. This will have a higher impact on the network performance, in-terms of energy consumption, latency, and reliability, as demonstrated in the evaluation section. In this chapter, we make the following contributions:

- an asynchronous dual interface opportunistic network protocol for animal monitoring

- evaluation and comparison of the protocol with the existing opportunistic protocols

The rest of this chapter is organized as follows: Section 5.2 presents the proposed network protocol and design approaches for the wildlife monitoring system. Section 5.2.6 discuses the use case scenario and presents the large scale evaluation results. Finally, a concluding remark and challenges are described in Section 5.3.

5.2 Protocol design

In order to carry out fine-grained monitoring applications, our proposed network protocol introduces a versatile and lightweight connectivity scheme, called opportunistic beacons, that expedites rapid and energy-efficient information sharing between mobile sensor devices without requiring connection establishment and complex configurations.

5.2.1 Opportunistic beacon communication scheme

As discussed in Section 1.2, the proposed network protocol have three network device types: (i) Animal Scanner (AS), (ii) Animal Broadcaster (AB), and (iii) LoRaWAN Gateway (LG). The AB-to-AS communication utilizes an opportunistic beaconing technique that includes three main schemes:

- periodic beacon advertising by AB nodes,
- periodic beacon scanning by AS nodes, and
- beacon data pruning and aggregation by AS node.

The overview of the proposed beacon protocol scheme is illustrated in Figure 5.1. In what follows we elaborate on each of these three schemes.

Periodic beacon advertising

Beacon discovery is initiated by *AB* nodes by periodically sending beacon data to AS nodes and *AS* nodes scanning for nearby beacons by listening for AB's data in advertising channel. AB nodes use periodic asynchronous BLE mode to broadcast data to AS nodes within range. This sequence of events is called an advertising event. Advertising activities occurs at regular intervals called broadcast interval. AB-AS beacon communication is a *many-to-many (m-to-m)* BLE communication, where AB nodes can send to multiple AS nodes as long as they are within the critical range of BLE radio [5].

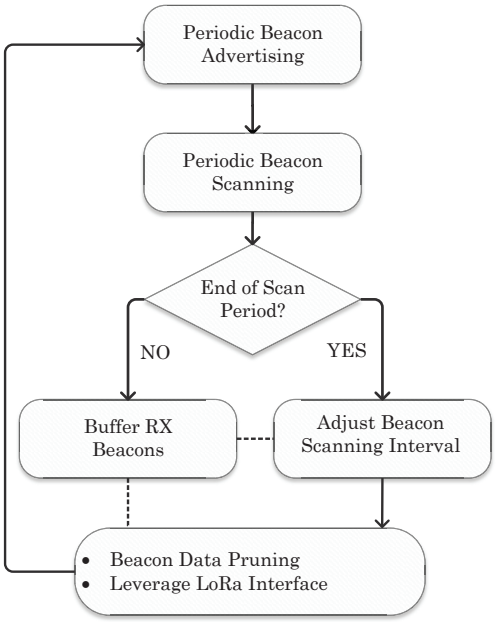

FIGURE 5.1: *AB-to-AS opportunistic beacon communication scheme.*

Periodic beacon scanning

As AS node commences its scanning operation, it listens and buffers the number of beacons it has received during its current and previous scanning window. Scanning activities occur at regular intervals. At the end of every scan window, AS node adapts the duration of the scanning interval according to the number of beacons received in the current and previous scanning. AS node changes to LoRa interface to relay beacons to LG node. This enables the AS node to considerably decrease the energy consumption.

Beacon data pruning and leveraging LoRa radio

AS nodes use short range BLE to receive beacons from AB, and long range LoRa radio to send aggregated data to LoRaWAN Gateway (LG), while obeying the 1% duty-cycle of limitation of LoRa radio. This restriction together with node mobility could contribute to a high network latency. To solve this challenge, our proposed approach utilizes data merging and pruning at AS node to reduce latency. Thus, AS nodes encode several AB BLE beacons into a single LoRa packet to be relayed to the LG node. After finishing sending LoRa packets, AS node switches back to listening the incoming BLE beacon data from AB nodes.

5.2.2 Operation of AB and AS nodes

As shown in Figure 5.2a, AB nodes start beacon advertising with a single copy beacon data by periodically (with T_{BC}^{+}) interrupting BLE radio from low power *BLE:*

Sleep Mode to *BLE: TX Beacon Mode*. In case of opportunistic BLE beacons operation, AB and AS nodes are not *synchronized*; so these activities should *overlap* for beacon discovery to initiate.

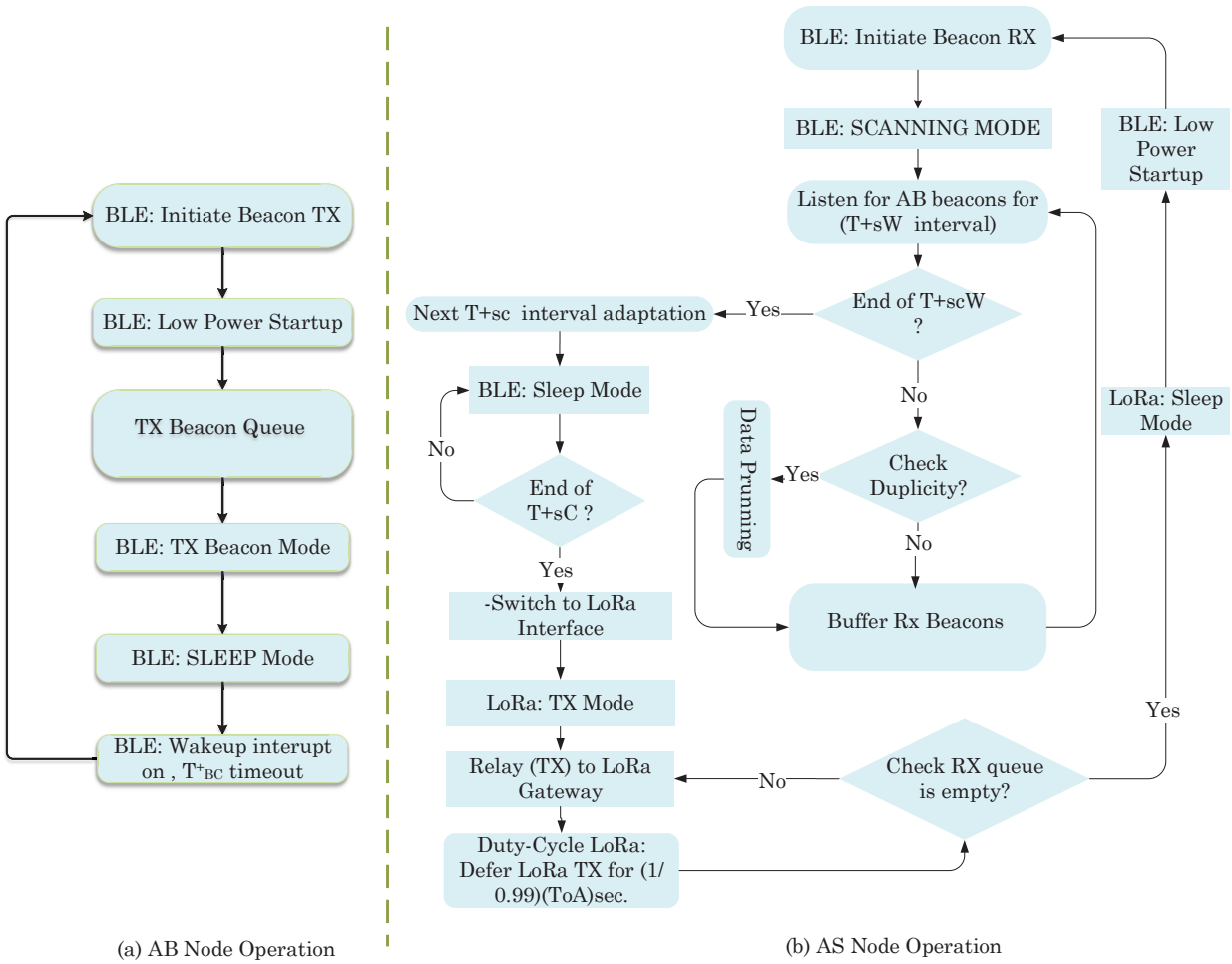

FIGURE 5.2: *AB and AS node operation flowchart.*

Similarly, as illustrated in Figure 5.2b, AS nodes also commence periodic scanning operation by changing their BLE radio from *BLE: Low Power Mode* to *BLE: RX Scanning Mode*. An AS node starts the beacon scanning with predefined default $T^{+}_{sw} \geq T^{+}_{s,min}$ values, to allow the asynchronous AB beacon data to overlap with the listening window of AS node. To cope with the variable number of incoming AB beacons, AS node adjusts the scanning time interval based on the number of beacons received from AB nodes. An AS node listens and keeps track of the number of beacons it has received during its current and previous scan period (T^{+}_{sw}) with ($prevBeaconNum$ and $curBeaconNum$) variables. Each AS node compares its ($prevBeaconNum$) with $curBeaconNum$ to decide the duration of the next scanning interval (T^{+}_{sw}). This approach will contribute to lower energy consumption for AS nodes by adaptively controlling the scanning interval (T^{+}_{sw}). Algorithm 5.2 summarizes this procedure.

The $T^{+}_{s,min}$ is equal to the recommended minimum broadcast interval ($T^{+}_{BC} = 100$ms) in BLE protocol specification for beacon functionality [6]. When ($curBeaconNum \geq$

Algorithm 5.2 AS node operation: T^{+}_{sw} time adaptation to received beacons

Input: $T^{+}_{s,min}$, $curBeaconNum$, $prevBeaconNum$
Output: T^{+}_{sw}

```
procedure AS Beacon Scan
top:
    T+_sw ← T+_s,min repeat every T+_sw if curBeaconNum ≥ prevBeaconNum then
        end
        T+_sw ← T+_s,min + 0.625 × curBeaconNum
        if curBeaconNum ≤ prevBeaconNum then
        end
        T+_sw ← T+_s,min
        continue
curBeaconNum ← 0
prevBeaconNum ← 0
goto top
end procedure
```

prevBeaconNum), then AS node updates its next service to start with longer scanning window of ($T^{+}_{sW} = T^{+}_{s,min} + 0.625 \times curBeaconNum$), where, $[2.5 \leq T^{+}_{sW} \leq 10240]$ms and $T^{+}_{sW} \leq T^{+}_{sc}$ as per BLE specification [6]. The longer the T^{+}_{sW} interval, the more beacon it can listen to in one period. In case of ($curBeaconNum \leq prevBeaconNum$), T^{+}_{sw} is by default $T^{+}_{sw} = T^{+}_{s,min}$ to start over the periodicity. In this way, AS node adapts its scanning time according to the dynamic number of beacons it receives.

Figure 5.3 shows the operation of AS nodes with the beacon timing required to establish a reliable opportunistic beacon network, where: T^{+}_{BC} - is advertising interval, T^{+}_{sc} - is scanning interval, and T^{+}_{sW} - is scanning window, where $T^{+}_{sW} \geq T^{+}_{BC}$ for the AS node to pickup the AB BLE beacons in the area. As guideline, choosing the right AB beacon timing parameters, (T^{+}_{BC}, T^{+}_{sc}, and T^{+}_{sW}), should be based on application requirements. Both fast or slow beacon modes have advantages and disadvantages. For instance, longer T^{+}_{BC} duration leads to slower beaconing and have a lower power consumption. Consequently, AB beacons will have a lower probability of shorter discovery time at AS nodes. While shorter T^{+}_{BC} duration for fast beaconing results in a higher power consumption, it also has with higher probability of short discovery time by AS nodes.

In a time-constrained application such as WMS, when the AS needs to receive data in real-time, T^{+}_{sW} should be $T^{+}_{sW} \gg T^{+}_{BC} + \beta$ to guarantee discovery. Moreover, to prevent advertising events from multiple beacons colliding, a small random time ($\beta = [0 - 10]ms$) is added between advertising events. Adhering to this beacon timing guide line will reduce beacon data collision and increase the packet delivery ratio. Table 5.1 summarizes the BLE beacon communication timings involved.

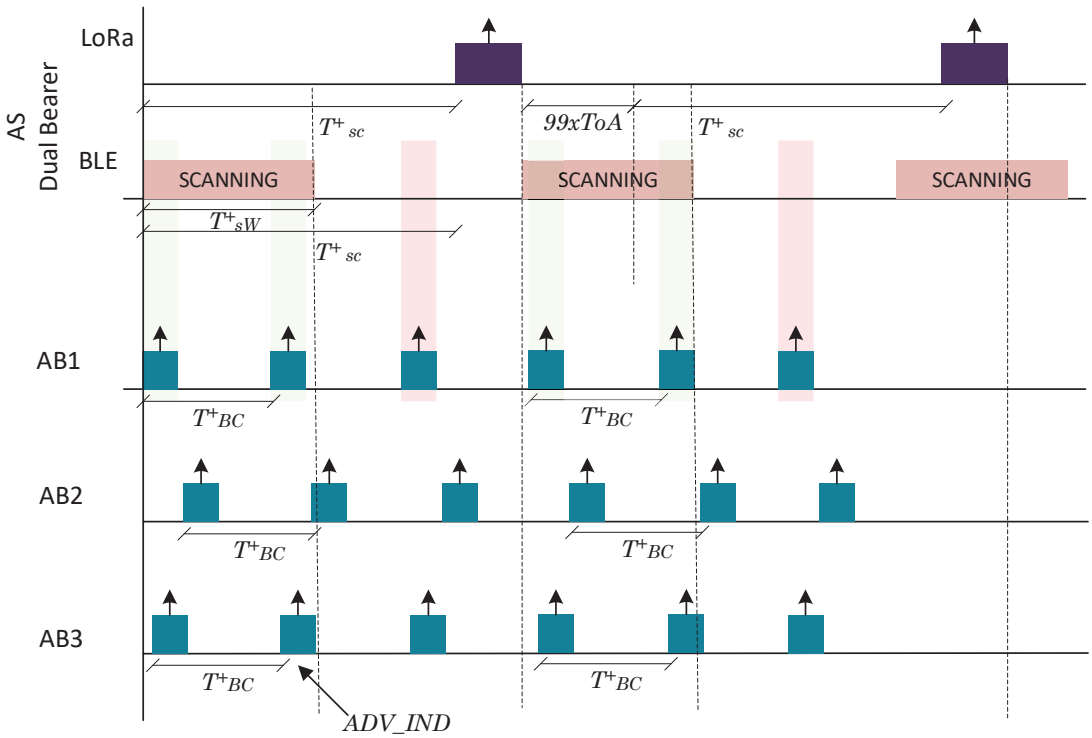

FIGURE 5.3: *Data transmission timing for AS node with dual interface (BLE and LoRa). BLE AB-to-AS communication timings:* T^+_{BC} *- advertiser interval,* T^+_{sc} *- scanner interval, and* T^+_{sW} *- scanner window, where* $T^+_{sW} \geq T^+_{BC}$.

TABLE 5.1: *BLE beacon recommended advertising timings based on the BLE specification [6]*

Notation	Meaning	Recommendation
T^+_{BC}	Adv. Interval	Int. multiple 0.625ms in $[20 \sim 10240]$ms
β	Upper delay bound	$[0 - 10]ms$
T^+_{sc}	Scan Interval	Integer multiple of 0.625 ms in $[2.5 \sim 10240]$ms
T^+_{sw}	Scan Window	Integer multiple of 0.625 ms in $[2.5 \sim 10240]$ms, $T^+_{sW} \leq T^+_{sc}$

At the end of every scanning window (T^+_{sw}), AS node periodically relays processed AB beacon data to LoRaWAN network by utilizing its LoRa radio interface. While leveraging LoRa, the AS node is restricted by the 1% LoRa transmission duty-cycle regulation [155]. This limitation together with network topology change contributes to increased network latency. For example, for LoRa payload of $PL = 51$ bytes using LoRaWAN (SF = 7, CR = 1, DR = 5kbps), the time on air will be $ToA = 71.936$ms

and AS node has to wait for sending for $T_{off} \approx 7.1936$s, which is practically long for real-time (fine-grained) monitoring of mobile network environment with frequently changing RSSI values [155].

To alleviate this issue, the network protocol utilizes data merging and pruning at AS node to reduce latency. Therefore, AS nodes merge received AB BLE beacons to LoRa packet to be relayed to the LG node (see Figure 5.2b). At the end of every scanning interval, AS node turns off LoRa interface and again switches back to BLE interface to continue receiving the BLE beacons while complying to 1% duty-cycle regulation.

5.2.3 Optimal beacon transmission intervals

The AB node's beacon advertising interval (T^{+}_{BC}) value for AB nodes has an impact on application requirements of a given opportunistic beacon network protocol. Achieving high *average delivery ratio (D_e), low average latency (ℓ), and high average network life-time (N_l)* are the main requirements often considered [155]. Hence, in this section, we formulate these requirements as an optimization challenge and discuss their practicality.

Let $S_r \subset N$ denote a set of AB beacon generating nodes in a network with N number of AB nodes, and L denote the set of wireless (AB to AS) links. The link $L_i \subset L$ originating from node $i \in S_r$ is the link that connects AB node i to a AS node. Hence, the beacon network requirement optimization could be expressed as:

$$\begin{aligned}
\underset{\ell \in L_i}{\text{Maximize}} \quad & D_e = \frac{1}{|S_r|} \sum_{i \in S_r} D_{eL_i} = \frac{1}{|S_r|} \sum_{i \in S_r} P_i \\
\text{Subject to} \quad & D_e \geq D_{emin},\ i = 1, \ldots, N. \\
& \ell = \frac{1}{|S_r|} \sum_{i \in S_r} \ell_{L_i + L_{LoRa}} \leq \ell_{max} \\
& N_l = \frac{1}{|S_r|} \sum_{i \in S_r} N_{l_i} \geq N_{lmin}
\end{aligned} \tag{5.1}$$

Per AB-AS link, the delivery ratio D_{eL_i} of link L_i is the expected beacons successfully delivered from AB node $i \in S_r$ to AS node along the L_i link. The *average delivery ratio (D_e)* is defined as the average of all links L_i (See Eq. 5.1). D_e is further simplified as the probability P_i that AB node i will successfully deliver to AS.

Similarly, we define the per-hop latency ℓ_{L_i} of link L_i as the time required for AB node i to deliver a beacon to AS nodes. In addition, a significant latency overhead is introduced due to the 1% LoRaWAN duty-cycle regulation (L_{LoRa}), when at the end of every T^{+}_{sC}, AS nodes utilize LoRa interface to relay data to the LG node. L_{LoRa} is directly related to the Time-on-Air (ToA) of the defined LoRa packet payload (PL). Thus, as shown in Eq. 5.1, the total average end-to-end network *latency (ℓ)* is expressed as a total average of ℓ_{L_i} and $L_{LoRa} = T^{+}_{sC} + 99 \times ToA$. Furthermore, the

Network life-time (N_l) is also defined as the average time before individual nodes (N_{l_i}) stops operating (see Equation. 5.1).

Therefore, to satisfy the given beacon network requirements, an upper bound could be introduced on the acceptable level of maximum latency, $\ell \leq \ell_{max}$, for a timely data delivery. Likewise, an applicable minimum average delivery ratio, $D_e \geq D_{emin}$, and minimum per node-life-time $N_{l_i} \geq N_{lmin}$ could be defined.

Since the performance of AB beacon advertising primarily depends on (T^+_{BC}), thus, AB nodes should be configured with an optimal T^+_{BC} beacon interval to satisfy the network requirements. To solve Equation 5.1, we define a simple mathematical model to describe the AS device discovery latency and to characterize the collision probability and/or reliability according to the ideal implementation of BLE specification [6]. Note that the beacon collision probability depends on three main factors: (i) collisions between AB beacon packets, (ii) AB beacon timing parameter configurations, and (iii) channel and interference conditions.

Thus, we model the probability of how likely it is that an AB device sends an AB beacon packet AS without a collision, given that T^+_{BC} is beacon interval and Γ is the duration of AB beacon data. The number of BLE devices involved in the analysis is $N+1$, i.e. a device is configured as a scanner (AS), whereas the other N devices are configured as advertisers (ABs). Hence, AB beacon data will overlap and create collision if it starts anywhere in Γ duration, inclusive before AB starts up until when it finishes advertising $[0, \Gamma]$, then it will be an overlap window of 2Γ or $[0, 2\Gamma]$ length, within which there is a chance of collision.

$$P_i(\forall\ (N-1)) = (1 - 2\Gamma/3T^+_{BC})^{(N-1)} \tag{5.2}$$

For N number of AB nodes in the network and assuming the best case scenario, (i.e. the transmitted AB beacons are all successfully received by the AS node), the probability that i^{th} node's beacon misses (no collision) all other (N-1) AB's beacons in the same channel is $P_i(\forall\ AB) = P(nocollision)^{(N-1)}$. This is expressed in Equation 5.2.

Thus, the average network reliability (R) for the beacon network, would be, $D_e = \frac{1}{N}\big(\sum_{i \in N-1} P_i(\forall\ AB)\big)$. This generalization holds true even when multiple AS nodes exist in the same radio coverage area, since BLE beacon is based on broadcast communication mode where multiple AS and AB nodes share the same channel.

Similarly, the expected per-link i^{th} beacon discovery latency at AS node is given by:

$$\ell_{L_i} = [T^+_{BC} + \beta_{Bd_{max}} + P_i(\forall\ (N-1)) \times (\Gamma)] \times 10^3 [ms] \tag{5.3}$$

Thus, the average network latency (ℓ) for the beacon network, would be $\ell = \frac{1}{N}\big(\sum_{i \in N-1} \ell_{L_i + L_{LoRa}}\big)$.

In addition, given a battery capacity $Q_p[mAh]$, E is the average energy consumption, and supply voltage (v), the individual i^{th} AB node's life-time (N_{l_i}) is expressed as:

$$N_{l_i} = \left(\frac{Q_p \times V}{E_i \times T^+_{BC}}\right) \tag{5.4}$$

Likewise, the average network node-life time would be $N_l = (\frac{1}{N})(\sum_{i=1}^{N} N_{l_i})$, where $E = \Gamma_i \times P_{t_i}$, P_{t_i} is the transmission power, N is the number of end-nodes.

Hence, finding the optimal T_{BC}^{+}, is straight forward given the required expected beacon data reliability (D_e), latency (ℓ), and network node-life time (N_l), by averaging Eq. 5.2, Eq. 5.3, and Eq. 5.4 for N AB nodes, respectively. This approach is demonstrated in the evaluation section.

5.2.4 Evaluation

In order to evaluate the proposed protocol for large scale scenario, a realistic simulation environment is setup.

FIGURE 5.4: *Simulation setup with dual interface NS3 simulation environment, color labels: BLUE=AB, GREEN=AS, RED=LG nodes*

Simulation set-up

We evaluate the performance of the protocol in the NS3 simulation environment [156]. For more detailed explanation of the NS3 module for BLE and its validation, the reader is referred to Appendix A. Figure 5.4 shows the simulation setup for typical NS3 deployments with AB and AS nodes moving in a defined trajectory in a grid area of 1000mx1000m, with LG node to receive data from the AS nodes. We setup the simulation with a range of parameters as summarized in Table 5.2.

TABLE 5.2: *Simulation parameters. (n/a) - not applicable.*

Notations	BLE	LoRa
Mobility model (M_1)	M_o^1: ZebraNet	stationary
Freq.	2.4 GHz	868 MHz
Duty-cycle	n/a	1%
Coding rate	n/a	4/5
BW	2 Mhz	125 kHz
SF	n/a	7
DR	1 M bps	5.1 kbps
P_t	4 dBm	4 dBm
AB node density (N)	N^0: 15, N^1: 50, N^2: 100, N^3: 150, N^4: 200, N^5: 250, N^6: 300, N^7: 350, N^8: 400	n/a
AS node density (AS_N)	AS_N^0:1, AS_N^1: 3	n/a
LG node density (LG_N)	n/a	LG_N^0:1
Simulation area (S_A)	1000mx1000 m	1000mx1000 m
PL (bytes)	31 (max for ADV)	51
T_{BC}^+	[100∼600] ms in 100 ms steps	n/a
T_{sc}^+	700 ms, 800 ms, 1000 ms	n/a
T_{sW}^+	600 ms, 700 ms	n/a
Simulation duration (hr)	15	n/a

AB nodes generate beacons with 31 bytes (i.e. max BLE payload). We configured N number of AB and N_{AS} of AS devices in NS3 simulator. To investigate the effect of T_{BC}^+, T_{sc}^+, and T_{sW}^+ on the network performance metrics, we run several simulations, where AB nodes transmit beacon at varying T_{BC}^+ and AS nodes perform scanning with particular T_{sc}^+, and T_{sW}^+ settings.

For each T_{BC}^+, we use the values in steps of 100ms in range [100∼600] ms. To make sure that AS and AB timing overlap, we follow the BLE timing guide line, i.e. for T_{sc}^+ values of setting 700ms, 800ms, 1000ms and T_{sW}^+ values of setting $T_{sW}^+ \gg T_{BC}^+ + 10$, 600ms, 700ms. While, this setting is not optimal for power, it is useful to test the beacon packet collision and delivery.

We recorded the packet generation time at AB nodes, as well as the time when they are received at the LoRaWAN gateway. The simulation measurement is performed for a total of 15hr simulation time. In our simulations, animals are assumed to be

mobile, hence, the (M_1) mobility model for group (herd) of animal from the ZebraNet project is utilized [27]. For Epidemic and ProPHET protocols the replication data is set to TTL=10s. All parameters are set according to values in Table 5.2.

5.2.5 Benchmark protocols

The proposed network protocol is investigated under the following commonly used benchmark opportunistic protocols to characterize their application for WMS applications [157, 158]: (i) Epidemic, it is modeled after the spreading of epidemic diseases, i.e. a source node spreads data through the entire network until it reaches she destination nodes. (ii) ProPHET, it estimates delivery predictability for each known destination at each node before forwarding a data.

5.2.6 Results and discussions

In this section, we evaluate the network in comparison to existing opportunistic protocols in NS3.

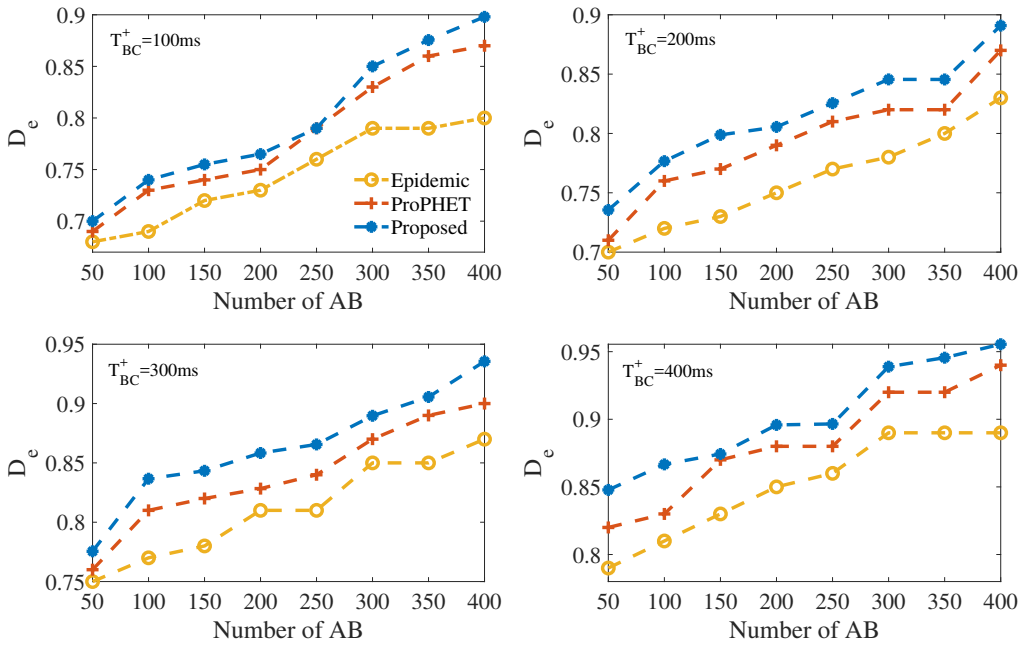

FIGURE 5.5: *Comparison of average reliability (D_e) for proposed, Epidemic, and ProPHET opportunistic protocols in Zebar mobility scenario: with $T^+_{sc} = 700ms$, and $T^+_{sW} = 600ms$ for variable number of AB nodes.*

Figure 5.5 shows that our approach performs better than Epidemic and ProPHET network in terms of average data delivery ratio (D_e). The main reason for this is that Epidemic and ProPHET have a multiple copy data delivery approach compared to our single copy approach. This will create a high collision at the receiver nodes. Hence, they have lower probability of data delivery than our proposed protocol.

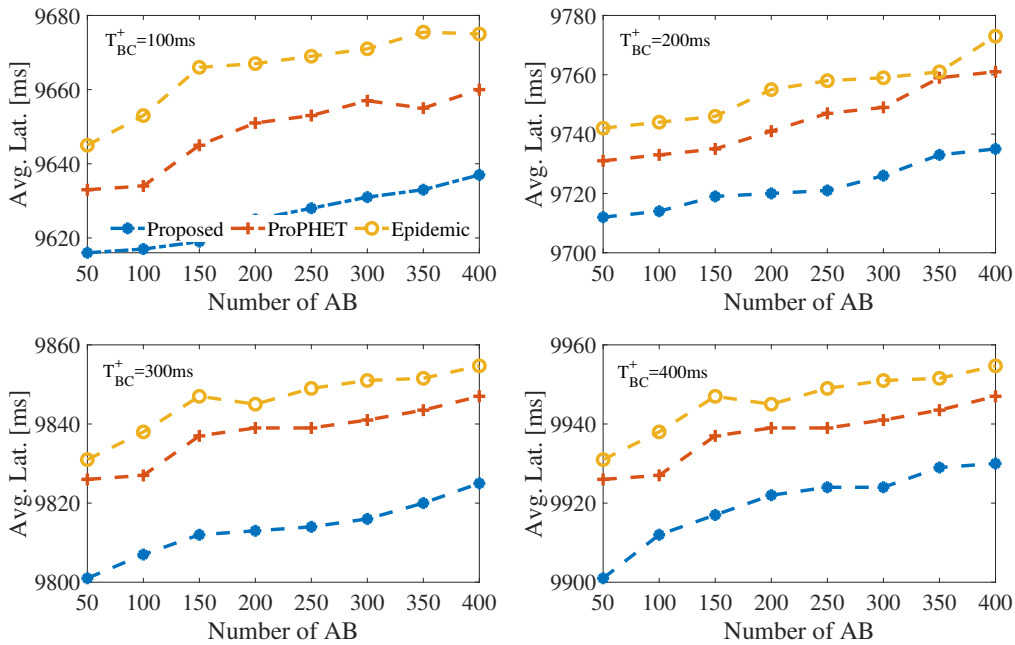

FIGURE 5.6: *Comparison of average latency (ℓ) for proposed, Epidemic, and ProPHET opportunistic protocol in Zebar mobility scenario: $T^{+}_{sc} = 700ms$, and $T^{+}_{sW} = 600ms$ for variable number of AB nodes.*

Moreover, Epidemic and ProPHET often demand higher network resources such as buffer and battery, which are very scarce in the wildlife monitoring applications, this result in higher latency and high energy consumption (Fig. 5.6). As shown in Figure 5.7 and Figure 5.8, the network life-time is very short for Epidemic, due to the same reason that it increases the communication overhead than the our simplified protocol [123].

Figure 5.7 and Figure 5.8 shows the average network energy and life-time assuming all AB nodes in the beacon network are configured with same T^{+}_{BC} settings. The network life-time is independent of the number of AB nodes in the network, however, it highly depends on the value of advertising interval set (T^{+}_{BC}). For example, longer T^{+}_{BC} interval has slower advertising rate with a lower power consumption. Consequently, has a lower delivery ratio for short discovery time by AS nodes. One of important issue to realize is the trade-off between power consumption and latency. Generally, the less frequent advertisements, the longer the beacon network runs (Figure 5.8). For example, if the total number of AB nodes in the network is N=200, therefore, in order to ensure a network life-time of $N_l \geq 1$ years, average delivery ratio $D_e \geq 80\%$ and average discovery latency of $\ell \leq 9800ms$, thus, the common optimal T^{+}_{BC} for our proposed protocol would be in the range of $T^{+}_{BC} =\approx [200, 300]ms$ (as per Figure 5.5, 5.6 and 5.8). Hence, the optimal value of T^{+}_{BC} should be chosen depending on N and the required beacon network performance measures, to optimally reduce collision in beacon network.

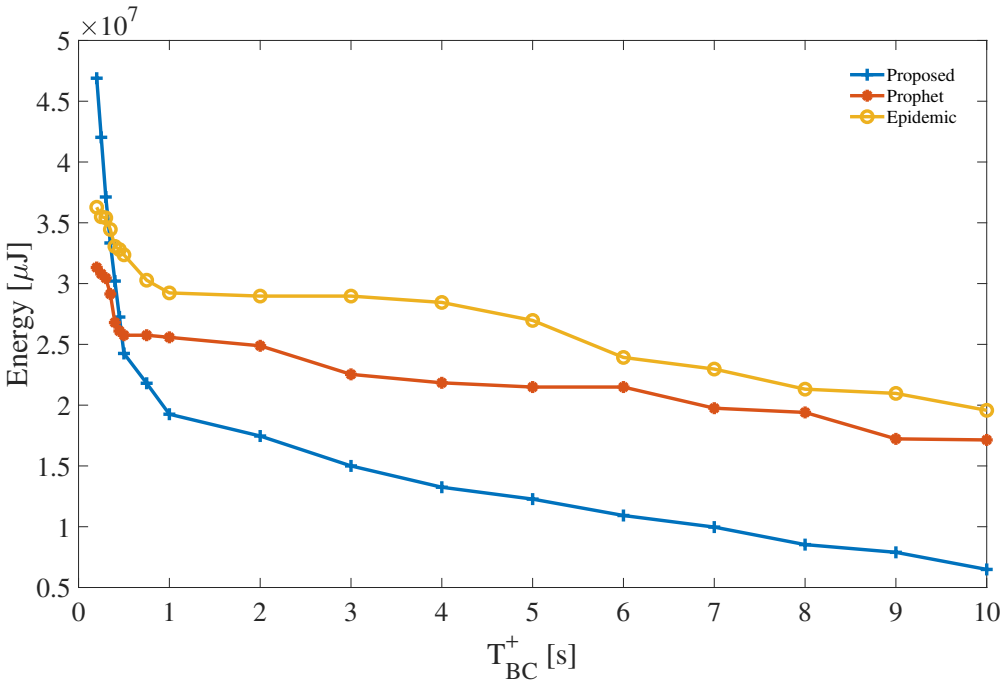

FIGURE 5.7: *Comparison of energy consumption for proposed, Epidemic, and ProPHET opportunistic protocols.*

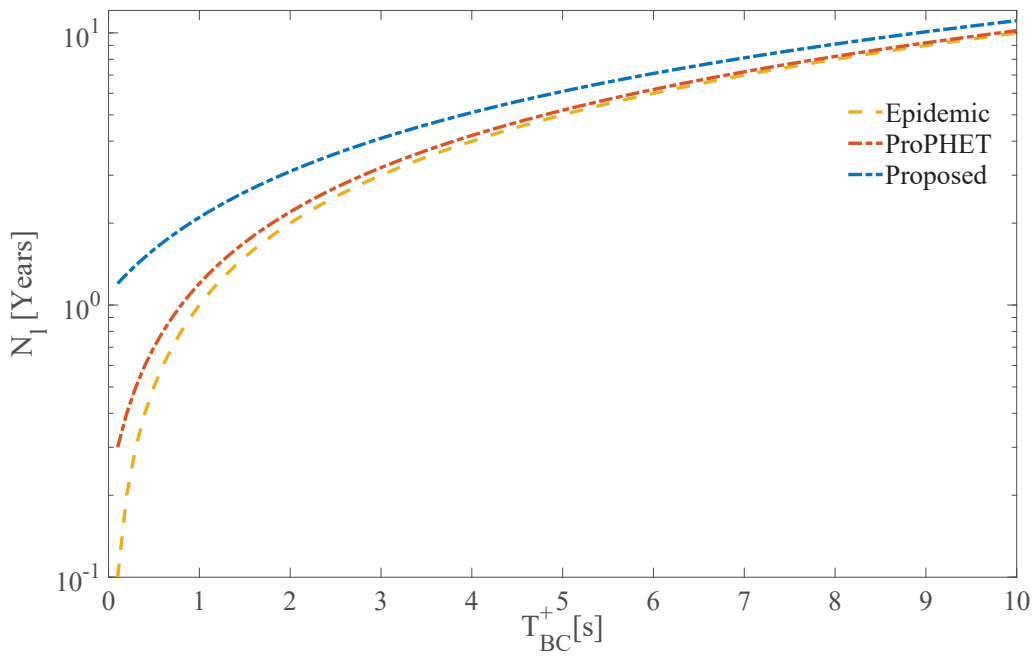

FIGURE 5.8: *Comparison of network life-time (N_l) for proposed, Epidemic, and ProPHET opportunistic protocols.*

5.3 Conclusion

In this chapter, we presented a single-hop hybrid tree based asynchronous opportunistic beacon network with dual interface for animal monitoring. The key advantage of this architecture is that nodes achieve wider control on the trade-off between

total energy consumption and latency. The evaluation results show that the proposed network protocol outperforms the traditional opportunistic networks. On average, our protocol improved the data delivery radio and latency in-cured by up-to 60% and 75% respectively. In addition, the architecture improved the network life time by up-to 50% especially for the higher packet traffic rates in the network. Hence, the proposed protocol is more optimal to deploy than utilizing only conventional opportunistic network.

Chapter 6

Mobility Aware Communication Protocols

WIRELESS sensor networks are the basis for wildlife monitoring systems because of their flexibility and energy-efficiency. However, their utilization often involves an inherently frequent data advertising mechanism that can result in a significantly higher energy consumption for monitoring mobile animals. The main focus of the network protocols presented in this chapter is the adoptation of herd movement patterns to make the communication more energy-efficient and reliable.

Part of this chapter has appeared in:
[23] *E. D. Ayele and N. Meratnia and P. J. M. Havinga, HAMA: a herd-movement adaptive MAC protocol for wireless sensor networks, in proceedings of the 8th IFIP International Conference on New Technologies, Mobility and Security (NTMS), pages 1–7, Nov 2016, Larnaca, Cyprus.*
[Accepted] *Fatjon Seraj, E. D. Ayele and N. Meratnia, Unsupervised learning of wildlife behaviour for activity-driven opportunistic beacon networks, in proceedings of the 13th International Conference on Sensing Technology (ICST), 2 December, 2019, Sydney, Australia.*

6.1 Introduction

WMS could utilize wireless beacon data to collect information about the animal activities. Generally, wireless data communication consumes higher energy than processing it, (e.g. sensor data sampling, memory management, etc) [113]. Hence, due to the limited energy supply and associated difficulty to recharge the battery, WMS often faces an energy management issue to extend sensor node life-time [123]. Ideally, to manage the energy, we need to implement a movement detection mechanism to accurately help decide when to transmit data, instead of unnecessarily transmitting continuously. Recent studies have suggested that node mobility plays an important role in network topology dynamics because of its impact on the communication link quality [159, 113]. Even though existing approaches provide a short term solution for low node mobility, they usually neglect the impact of high node mobility [100, 102]. Consequently, such high mobility will often introduce undesirable energy consumption and end-to-end latency [113].

As far as wireless communication protocols are concerned, the first approach to cope with topology dynamics is to translate these topology changes into a change in incoming or outgoing data traffic density at each node [101]. Thus, a higher number of received or transmitted packets means higher energy consumption and communication overhead. Despite the need to quantify node movement characteristics interms of the packet reception and transmission rates for designing a mobility-driven multi-hop communication protocol, not much attempt has been made in this aspect so far. Existing efforts to mitigate the effect of node mobility often ignore the use of local packet statistics to predict state of node's movement. They enable nodes to perceive a change in their surrounding only at the beginning of each active period. Consequently, there is a delay in packet transmission whenever topology changes. This delay is even higher in multi-hop networks.

The second alternative solution to improve the energy efficiency of WMS is to utilize the actual accelerometer sensor data to accurately detect the mobility states of animals to directly adapt the mobile node's duty-cycle. An accelerometer based movement sensing is known to be an accurate, robust and practical method for objectively monitoring the mobility of animals [12]. For wild animals, the high mobility state occurs less frequently and most of the time they are stationary (passive) state [160]. Thus, to save energy, sensor nodes can turn off or decrease their radio's duty-cycle and set their processor on a low-power mode whenever animals are in passive states. Utilizing this technique helps to reduce the energy consumption considerably.

In this chapter, we present a herd adaptive mobility-aware communication protocol with the objective to offer low power consumption and high packet delivery ratio in mobile WSNs.

The structure of this chapter is as follows: Section 6.2 presents the detailed HAMA protocol design and its performance evaluation and implementation. HAMA is an adaptive duty-cycling protocol to adjust data preamble polling times according to packet traffic statistics. It utilizes $G/G/1/K$ queuing model with feed-back control to estimate the run-time duty-cycle. This makes HAMA protocol more suitable

for supporting continuously changing network topology as in wildlife monitoring applications. Section 6.3 presents a unsupervised monitoring scheme called self organizing maps (SOM) to detect the animal mobility states and utilize it for data advertising control scheme, while concluding remarks are discussed in Section 6.4.

6.2 HAMA protocol design

In this section, we describe the HAMA protocol in detail.

6.2.1 Schemes of HAMA protocol

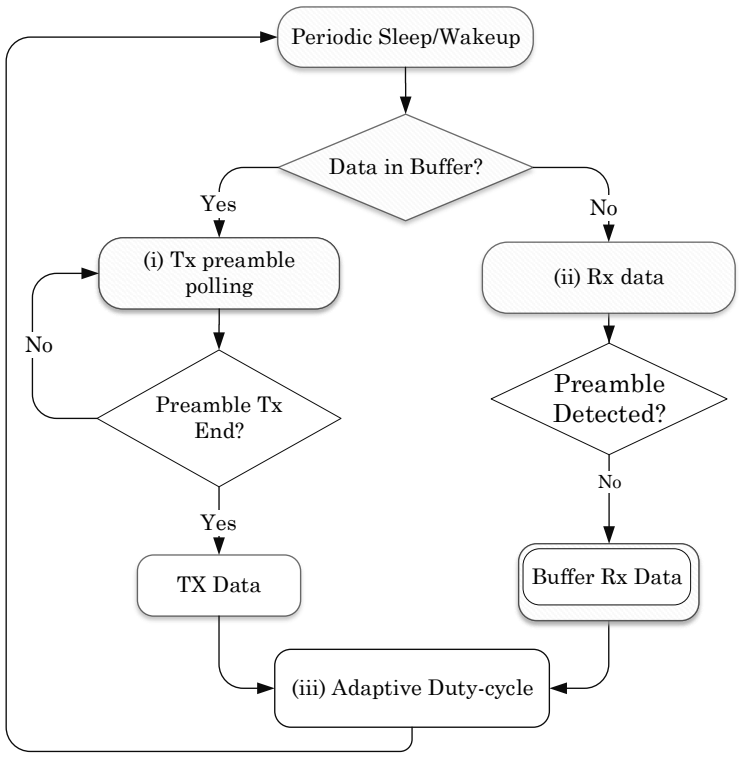

FIGURE 6.1: *HAMA scheme*

Figure 6.1 illustrates the overall HAMA with adaptive duty-cycling scheme based on received packet statistics. HAMA inherits several features from B-MAC [110], such as initialization of its access scheme by the sender and preamble listening. It additionally introduces features such as adaptation to polling and duty-cycle duration. HAMA has three modes of operation, i.e., (i) Tx preamble polling, (ii) Rx data, and (iii) adaptive duty-cycling. The main difference between HAMA and B-MAC is related to the third mode, as transmission and receiving modes are similar to B-MAC. In what follows, we explain each of these three modes of operation.

(i) Tx preamble polling: data transmissions is initiated by sender nodes periodically polling the channel for preamble before sending data. Sender nodes use asynchronous transmission to send data to a receiver within range. This sequence of events is called advertising events that could occur at regular intervals called advertising intervals.

(ii) Rx data: a receiver node picks up the polling preamble signal from the sender node, while keeping its radio on until it receives the data from the sender. It then buffers the data it has received. Receiving activity occurs at regular intervals.

(iii) Adaptive duty-cycling: In HAMA, receiver nodes adaptively change the sensor sleep-time based on the data packet statistics. HAMA collects information about the packet reception or transmission at the MAC layer.

6.2.2 Operation of HAMA protocol

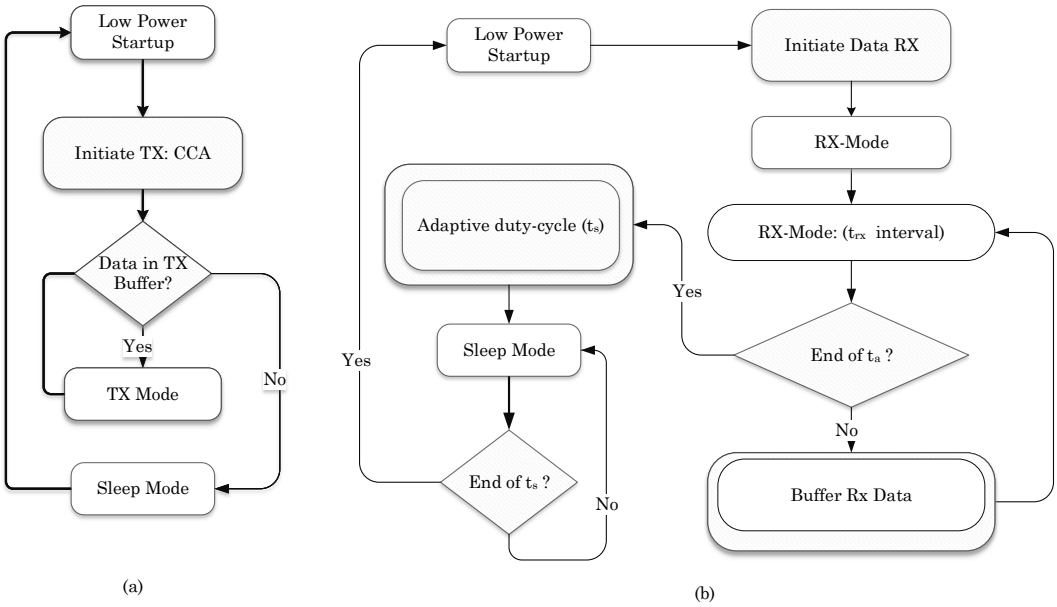

FIGURE 6.2: *HAMA operation flow-chart*

Figure 6.2 show the sender initiated HAMA protocol operation flowcharts, in which packet transmission is initiated by performing a series of clear channel assessments (CCAs). If the node wants to continue its transmission, it has to repeat the CCA process. It first sends a polling preamble and then transmits the packet with the header information identifying the respective receivers. Utilizing a preamble sampling technique will allow implementation of adaptive low power listening.

As shown in Figure 6.3, receiving nodes periodically sample the CCA after waking up from sleep at the end of every sleep-time t_s. If transmitter's preamble is detected,

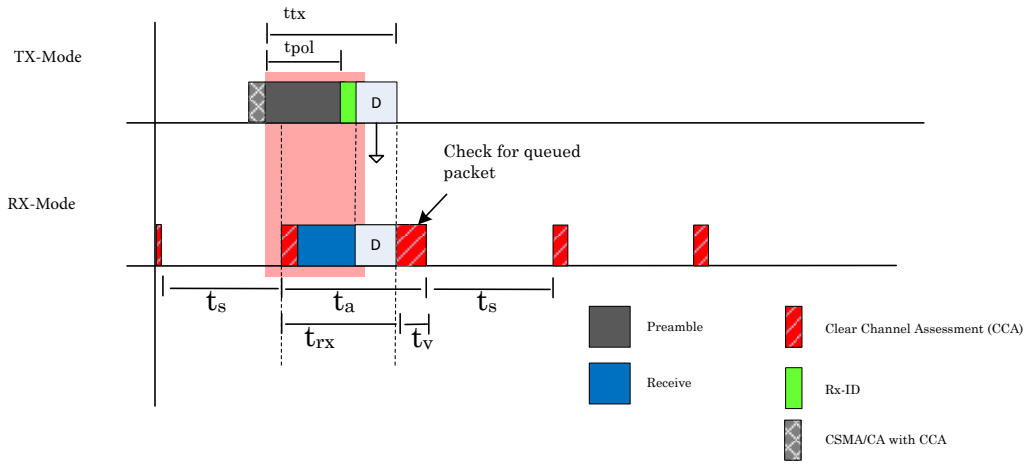

FIGURE 6.3: *HAMA protocol, t_s is the sleep duration, t_v the variable time spent after reception of the first data (D). t_{pol} is the length of the transmitter's polling preamble, t_{tx} is the time interval needed to complete transmitting a packet, t_a is the active state duration.*

the receiver(s) will keep their radio on until the transmitter finishes sending the preamble, even if the receiver(s) has already sensed the preamble signal. After this, receiver nodes determine whether they were the intended receiver by decoding the address header. If a receiver realizes that it is not the targeted receiver, it goes back to sleep immediately. By doing so, it frees the carrier channel and prevents any possible collision due to contention of the channel.

When there is an ongoing active packet exchange, the target receiver node stays awake for a period of t_a to finish receiving the packet after which it sends back an acknowledgement. The total time a node spends to receive a packet is expressed by $t_a = t_{rx} + t_v$, t_{rx}, where t_v shortens or extends the active period depending on availability of packets queued for next transmission or reception. Practically, t_v value is directly dictated by incoming packets and/or nodes own packet generation rates. While t_{pol} is the length of the transmitter's polling preamble, t_{tx} is the time interval needed to complete transmitting a packet. Actively controlling and setting the boundary condition for the HAMA timing is crucial. Therefore, for reliable communication to happen the duration of the receiver's sleep interval (t_s) should be made less than the transmitter's polling duration, $t_{pol} > t_s$. This will make sure that the receiving node will wake up on time and sample the channel for any existing preamble signal from the transmitter.

We aim to analytically determine the optimal sleep-time duration (t_s) by analysing the packet activity pattern in the queue model. To do so, the MAC layer is modeled as G/G/1/K queue system with idle-times. The model is used to drive stochastic estimation for sensor nodes sleep-time (t_s).

Figure 6.4 illustrates an example packet activity in the HAMA. After serving n data

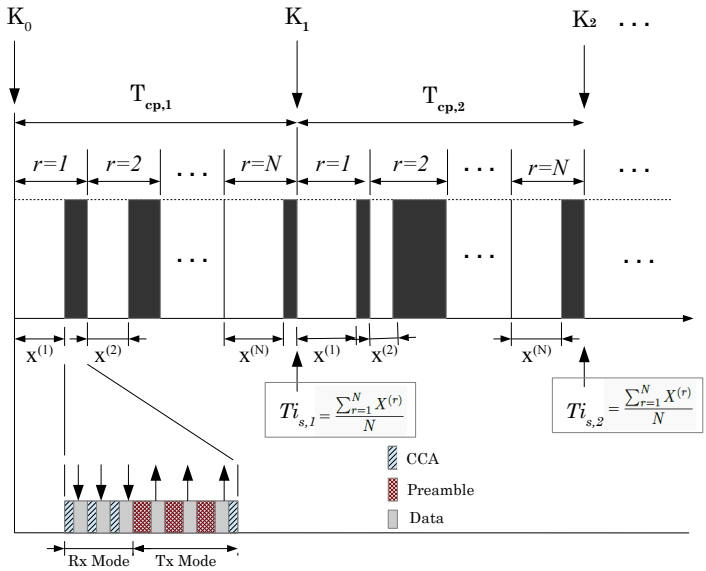

FIGURE 6.4: *Packet reception and transmission trend. Each control period $T_{cp,i}$, $(i = 1, 2, ...)$, has N-regeneration cycles, $(r = 1, 2, ...N)$ and estimated sleep-time $Ti_{s,i}$. $X^{(r)}$ is the idle-time for the rth regeneration cycle. K_i is the mean buffer size computed at the end of each control period $T_{cp,i}$.*

packets, the sensor node will be in idle state. This idle-time $X^{(r)}$ for the (r^{th}) regenerative cycle within the control period (T_{cp}), (see Figure. 6.4), is expressed by:

$$X^{(r)} = -min(0, W_n^{(r)} + S_n^{(r)} - \lambda_n^{-1^{(r)}}) \tag{6.1}$$

which then will be used to determine the node's sleep-time (t_s) by the HAMA algorithm. Algorithm 6.3 summarizes the basic steps towards computing sleep time and consequently the duty-cycle. There are N regeneration cycles in a single control period (T_{cp}). A control period also serves as an observation window for collecting the statistics for predicting the next sleep duration of a node.

In Rx-Mode, the sensor node samples the channel after receiving a packet. In Tx-Mode the sensor node sends preambles including the receiver's node ID. Let the number of packets transmitted, during the first regeneration cycle ($r = 1$) formed by the busy cycle of $G/G/1/K$ queue, be n-packets before the next sleep-time commences. For the busy cycle of $G/G/1/K$ queue, packets arrive at time epochs λ_n^{-1}, $(n = 0, 1, 2, ...)$, and λ_n^{-1} are random variables. Let the packet transmission time of the nth packet be S_n, and $S_n = (\mu^{-1}{}_n)$, $(n = 1, 2, ...)$ be random variables. Their mean values are denoted by, $E(\lambda_n^{-1}) = \frac{1}{\lambda}$ and $E(S_n) = \frac{1}{\mu}$, respectively. W_n $(n = 1, 2, ...)$ is the waiting time of the nth packet. After N regeneration cycles being completed, Algorithm 6.3 computes the actual estimated sleep-time ($Ti_{s,i}$) for the ith control period $T_{cp,i}$, $(i = 1, 2, ...)$, which is calculated using the expected mean value of the

Algorithm 6.3 Optimal duty-cycle estimation

Input: $N, K, \lambda_n^{-1}, S_i, W_n$
Output: $\mu^{-1}, \lambda^{-1}, X^r, K_{i+1}, T_{cp,i}$

1: **procedure** SLEEP TIME COMPUTATION
2: $i \leftarrow 1$ *//Initializing the Regenerative Cycle*
3: $r \leftarrow 1$ **if** $r < N$ **then**
end
//The rth Regenerative Cycle is over
4: $\lambda_n^{-1} \leftarrow \lambda_n^{-1}$
5: $S_n \leftarrow S_n$
6: $X^{(r)} \leftarrow -min(0, W_n^{(r)} + S_n^{(r)} - \lambda_n^{-1^{(r)}})$
7: r++
8:
if $r = N$ **then**
end
//The ith Control period is over
9: $\beta \leftarrow \mu - \lambda$
10: $Ti_{s,i} \leftarrow \frac{\sum_{r=1}^{N} X^{(r)}}{N}$
11: $K_i \leftarrow max(0, (\lambda - \mu)(T_{cp,i} - NTi_{s,i}))$
12: $\varepsilon \leftarrow \varepsilon$ *//Selecting the values for*
13: $\xi \leftarrow \xi$ *//the controller from the stable range*
14: $t_{s,i+1} \leftarrow Ti_{s,i} + \varepsilon(K_{i-1} - K_i) - \xi(K_i - K_{i-1})$
15: $r \leftarrow 1$
16: $i \leftarrow i + 1$ *//Start monitoring for the next* $T_{cp,i}$
17:
18: **end procedure**

individual idle-times ($X^{(r)}$):

$$Ti_{s,i} = E[X^{(r)}] = \frac{\sum_{r=1}^{N} X^{(r)}}{N} \tag{6.2}$$

, where $X^{(r)} = -min(0, W_n^{(r)} + S_n^{(r)} - \lambda_n^{-1^{(r)}})$ [161]. The optimal sleep time can be calculated using:

$$t_{s,i} = Ti_{s,i} + \varepsilon(K - K_i) - \xi(K_i - K_{i-1}) \tag{6.3}$$

, where K is the max threshold queue size empirically determined (to be described in Section 6.2.3). $Ti_{s,i}$ is the current estimated sleep, and $t_{s,i}$ is the next estimated sleep-time duration for the ith control period $T_{cp,i}$. ε and ξ are queue stability parameters. From queuing theory, to make the queue system controller stable, (ε,ξ) should satisfy the following criteria [108]:

$$0 < (\varepsilon + \xi) < \Omega \tag{6.4}$$

$$0 < \xi < \frac{1}{(N\beta - \beta + 1)} \tag{6.5}$$

$$\Omega = \frac{2(1+\beta)}{\beta(N\beta - \beta + 1)} \tag{6.6}$$

, where $\beta = (\lambda - \mu)$, and $\Gamma = (\xi + \varepsilon)\beta$, ε and ξ are the control parameters. Since λ, N, and μ are known, β and Ω, and consequently ε and ξ can be computed on run-time from Equation 6.4 and 6.5. The proposed controller will adjust the sleep time by first computing values for Ω and then choosing appropriate stable values for ε and ξ in real-time. By doing so $(\varepsilon + \xi)$ will be in a stable range as expressed by Equation 6.4.

6.2.3 Evaluation

Simulation set-up

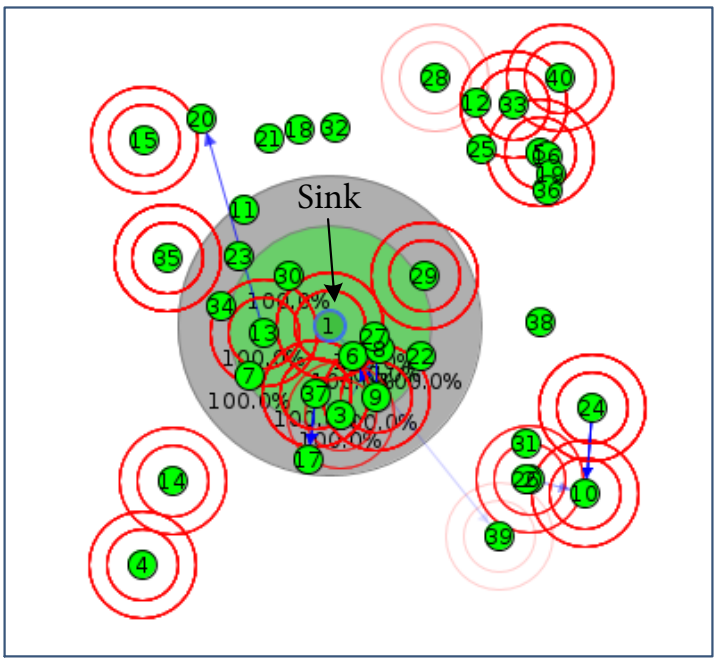

FIGURE 6.5: *Simulation set-up. The blue arrows illustrate data packet exchange, the red circles identify the transmission by sender nodes. In this case node-1 is the AS sink node, however, the network could be set-up to have more than one AS nodes.*

We evaluated performance of HAMA using the contiki cooja simulation environment. The transmission range of each node was set to 200 m and the carrier frequency was set at 2.4 GHz. The default transmission power was set at maximum available radio output power level in cooja [162], which is 31 (0dBm or 1mW). The unit disk graph medium (UDGM) distance loss was used to run the simulation [162]. As shown in Figure 6.5, we simulate 50 nodes moving in a defined trajectory in a grid area of 1000mx1000m.

To reflect real mobility scenarios as much as possible, we first consider the ZebraNet model [27]. In this mobility scenario, animals also show a conspecifics living behaviour, thus there exits 'herding' or clustering behaviour to some degree. We generated a second mobility model called RWP using BonnMotion tool [**aschenbruck2010bonnmotio** in which mobile nodes move with random way point [163] mobility trajectory and are set to move at random speed range of [10,30 Km/h] with max-pause = 5s. The summarized simulation parameters are shown in Table 6.1.

TABLE 6.1: *Simulation parameters*

Simulation area	1000x1000m^2
Simulation duration	15hrs
MAC protocols	HAMA, X-MAC and A-MAC
Frequency	2.4 GHz
Transmission power	31 (0 dBm)
Transmission range	200 m
Number of nodes	50
Mobility model	RWP and ZebraNet
Max buffer size (K)	10
Regenerative cycle (N)	10
IPI	2000 ms

The network was operating in a tree network topology to simulate a more realistic data collection scenario. In this topology, a number of sender nodes generate packets to be relayed by intermediate nodes towards the sink. To form a tree topology, we deployed the collection tree protocol (CTP) [164] to collect data packets towards the sink(s). In this case the root node will be the sink and the other nodes will automatically configure themselves as relay nodes. The nodes randomly generated data packets with 20 bytes payload at inter-packet interval IPI(ms) or ($\lambda^{-1} = 2000ms$). We recorded the packet generation time as well as the time when they are received at the sink(s).

The value for regeneration cycles N and max buffer size K (to be used for Equation 6.3 and 6.4) are determined empirically. Figure 6.6 shows the maximum observed queue buffer length for different regeneration cycles ($N = 1, 2, 3, ...30$) run at IPI ($\lambda^{-1} = 200ms$). A relatively faster IPI is selected to reflect the worst case scenario, in which nodes will be generating packets in case of burst communication. As shown in Figure 6.6, the maximum buffer size is 9 packets in case of X-MAC and A-MAC and only 6 packets in case of HAMA (for significantly high traffic). The next issue is to set the appropriate N range of values that will provide a stable queue buffer size. For $N > 18$ we can observe in Figure 6.6 that there is an increase in the accumulation of queue buffer.

While this will help reduce the computational overhead, it will dramatically increase the response time, because it will take more time to process or forward packets in the buffer. The opposite is true for the case of $N < 8$. Hence, the empirically suitable range of values for N has to be chosen from $8 < N < 18$ region to optimally balance between the system response time and computational overhead. To evaluate response time and computational overhead, without lose of practicality, for the

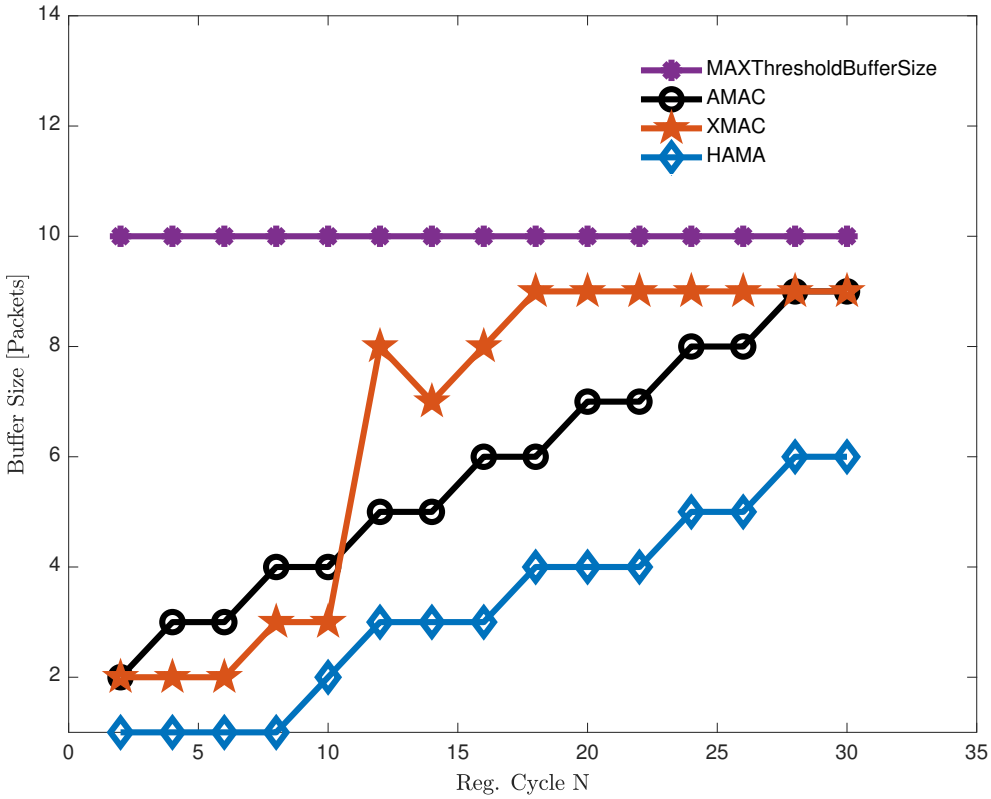

FIGURE 6.6: *Modeled queue buffer size with respect to various generation cycle values. Each point is the max buffer size value observed for various regenerative cycle (N) at* $\lambda^{-1} = 200ms$.

following simulation, we set $N = 10$ and $K = 10$ (see Figure 6.6). We evaluated the performance of HAMA considering these two mobility scenarios as well as the case when all nodes are at a fixed position or are stationary.

Benchmark protocols

We compared the performance of HAMA with the state-of-the-art adaptive duty-cycle MAC protocols such as X-MAC [165] and A-MAC [103] protocols. A-MAC renders properties of adaptive networks such as simple implementation on hardware, predictable performance parameters, and tolerance to network topology changes. X-MAC [102] is a network protocol that transmits a series of short preamble packets to the intended receivers. In the simulation run, each node forwards packets towards the sink (s) node via the relay (s) nodes after wining the medium through contention, as per the implementation specifics of the HAMA protocol. In the following sections, we discuss the evaluation results.

6.2.4 Results and discussion

Reliability is measured by counting number of transmitted packets and number of successfully received packets by the sink. The number of packets sent by each node was recorded and compared with the packets received at the sink. The received packets was higher when the number of AS sinks increases. As shown in Figure 6.7, compared with mobile networks, reliability is higher for the network with stationary (fixed) nodes. In case of mobile network, it can be seen that as expected when the node movement speed increases, the reliability decreases. This effect can be seen in Figure 6.7a and Figure 6.7b.

However, for both mobility scenarios, HAMA performs better compared to X-MAC and A-MAC. This is particularly true in case of mobile nodes with random way point (RWP). There is not much difference in reliability among the MAC protocols in the case of fixed (stationary) topology scenario. This is particularly true for the X-MAC and A-MAC protocol.

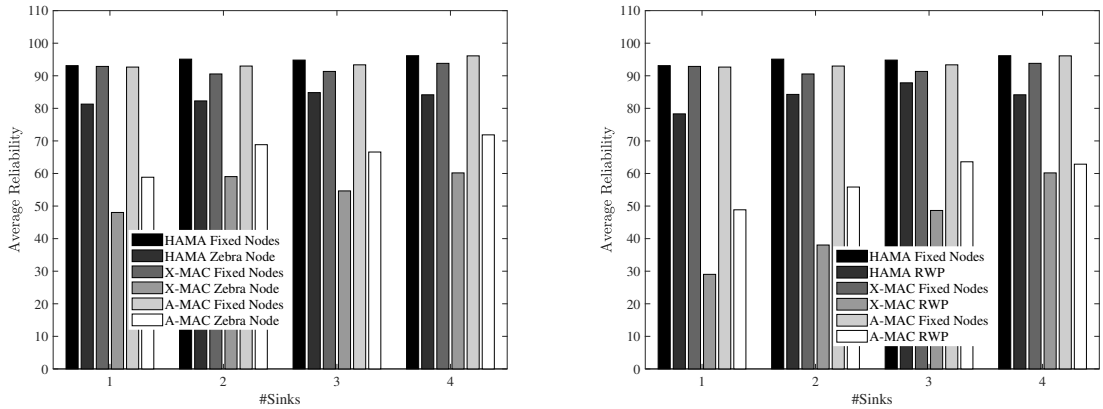

(A) *ZebraNet mobility* (B) *Random way point mobility*

FIGURE 6.7: *Average reliability percentage: (A) ZebraNet, where animals depict a herding or clustering scenario, and (B) RWP mobility scenarios, both compared to stationary (fixed) network topology.*

It can be seen in Figure. 6.7a and Figure. 6.7b that the reliability of HAMA protocol with adaptive duty-cycle controlling algorithm is consistently high. Overall, packet reliability of HAMA is at least 12.3% (for mobile nodes with ZebraNet mobibity) and at most 16.3% (for mobile nodes with Random Way point) higher than of X-MAC and A-MAC. Furthermore, one can see that increasing number of cluster heads or sinks leads to a decreased difference between the reliability performance of all protocols. This is because an increase in the sink density counters the effect of mobility and consequently increases the reliability.

Average end-to-end latency is calculated for all received packets based on the average time difference between when a packet was transmitted and when it was received at the sink node. It is apparent from Figure 6.8 that in general higher number of sinks in the network will normally contribute to having a lower latency. The maximum latency observed is 2200ms and 2750ms for X-MAC in case of Zebras mobility

and BonnMobility Random Way point mobility having one sink node. As expected, the average latency is higher when node's speed increases (as it can be seen from results of Figure 6.8.b). Overall, the average latency is decreased by at-least 11.65 - 14.63% when HAMA is used.

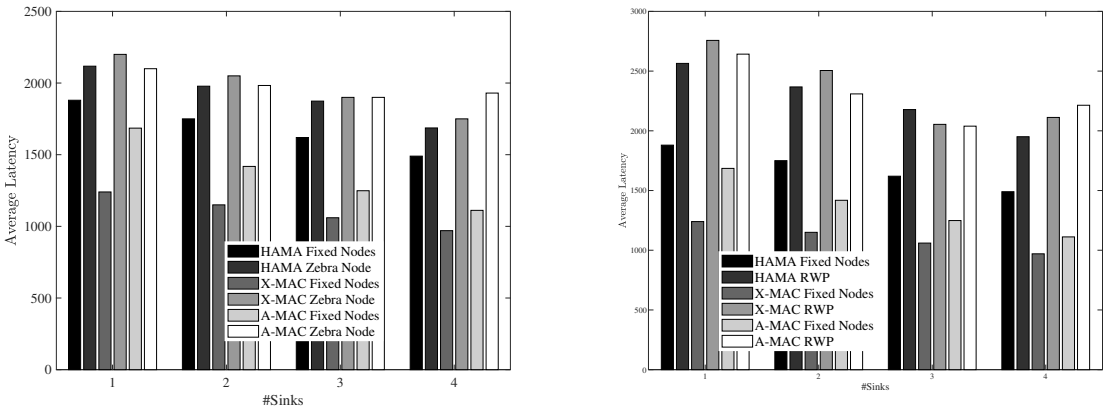

(A) *ZebraNet mobility* (B) *Random way point*

FIGURE 6.8: *Comparison of average end-to-end latency: (A): Zebras mobility scenario. (B): RWP mobility scenarios*

We record the average energy consumption of the individual sensor nodes to analyse how the network perform with respect to various packet generation rates. Figure 6.9 shows the average energy consumption of the entire network at various IPIs ($200 \leq \lambda^{-1} \leq 4000$ ms). All MAC protocols consume a comparable amount of energy at smaller IPI (higher packet rate), which is plausible since nodes are active most of the time in high traffic scenario.

For both ZebraNet and RWP mobility scenarios, the energy consumption of the HAMA protocol increases as network packet arrival rate increases. For both X-MAC and A-MAC, energy consumption remains relatively the same as data packet arrival rate increases. However, A-MAC consumes comparably lower energy than X-MAC. HAMA has a relatively high energy consumption compared to X-MAC or A-MAC for IPI ranges of $200 \leq \lambda^{-1} \leq 500$ ms. This is due to implementation of its adaptive mechanism. As packet transmission and reception rates increase, duration of each epoch becomes smaller. Consequently, the control period becomes shorter and the HAMA frequently sets smaller sleep-time to cope with increasing packet rate.

However, as the packet reception rate decreases, HAMA sets longer sleep-times, which will significantly reduce the energy consumption. Generally, HAMA reduces the average power consumption of the conventional MAC protocols X-MAC and A-MAC. Overall, compared with fixed networks and X-MAC and A-MAC, energy consumption of HAMA increases by 22.28% for high packet traffic ($\lambda^{-1} \leq 1500$ ms) and decreases by at least 52.28% for low packet traffic ($\lambda^{-1} \geq 1500$ ms). This implies energy efficiency of HAMA for high mobility WSN applications.

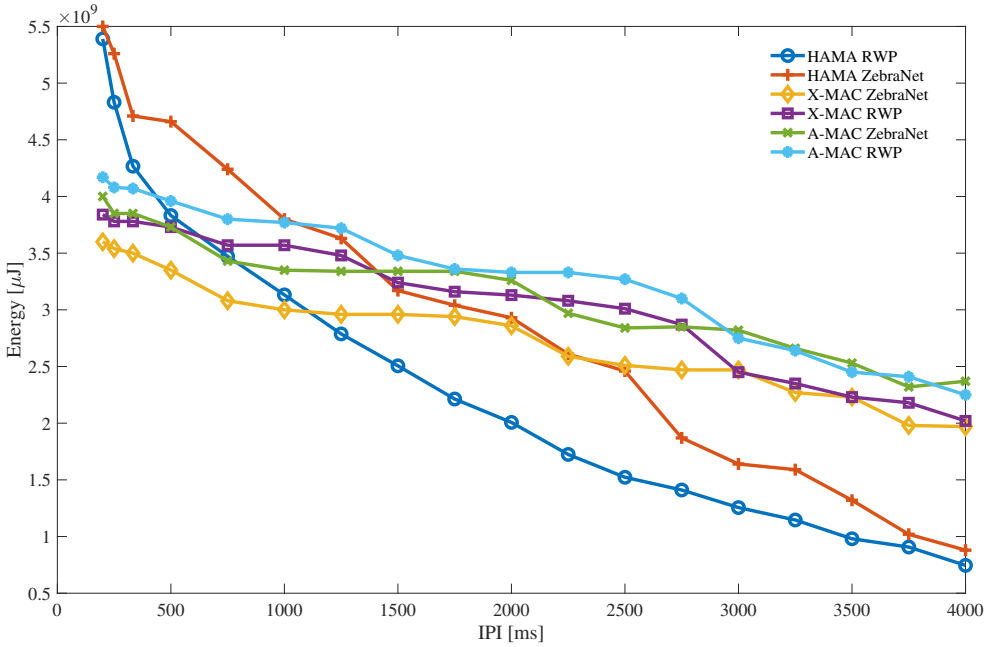

FIGURE 6.9: *Network wide average energy consumption of with respect to different inter-packet intervals (IPI). Measured for ZebraNet and RWP mobility scenarios.*

6.3 Mobility state driven beacon advertising control design

This sub-section discusses a mobility state driven BLE advertising protocol that is inherently low in energy consumption [123]. First, we introduce the overview of unsupervised learning algorithms and their suitability to animal mobility state detection. In addition, we also introduce animal mobility state-driven beacon advertising technique.

6.3.1 Overview of SOM and K-Mean algorithms

The SOM algorithm is based on unsupervised, competitive learning technique [166, 167]. The proposed SOM algorithm is suitable for clustering problems, i.e. grouping different elements according to the similarity in pattern and feature set. SOM creates a bi-dimensional map of neurons, a neuron lattice, in which the input features are grouped through a neighborhood function that calculates the degree of similarity between them. Features representing similar information will be closer on the neuron map. Figure 6.10 shows a typical visualization of a SOM neuron network lattice. The features are recursively shown to each of the neurons. The neighbourhood is characterized by the distance between neurons.

The behavior of a SOM algorithm utilized is summarized in the following steps: we calculate the input features D^i every given time Δt^i, $D^i = \{x_1, x_2, ..., x_m\}$, where

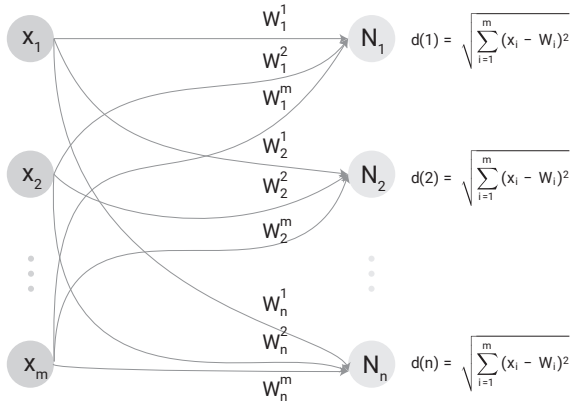

FIGURE 6.10: *Self Organizing Maps*

m is the number of features. We set the initial weight vectors W for each neuron N randomly close to zero. Each time the feature vector D^i is shown to the neuron N, the distance d_i is calculated as Euclidean distance, between the feature vector and weights of the neuron. Once, all distances are calculated, the neuron with the shortest distance will be selected as Best Matching Unit ($BMU = \text{argmin}(d)$). The wining neuron will adjust the weights using the neighbourhood function $\Theta\left(u, n, s\right)$ and the update rule $\alpha\left(s\right)$, where s is the present iteration or epoch.

$$W_n\left(s+1\right) = W_n\left(s\right) + \Theta\left(u, n, t\right)\alpha\left(s\right)\left(D^i\left(m\right) - W_n\left(s\right)\right) \tag{6.7}$$

On the other hand, K-Means clustering [168] is a clustering algorithm that assigns n observations $(x_1, x_2, \ldots, x_n)$, where each observation is a d-dimensional real vector, to exactly one of k clusters $k(\leq n)$ sets $S = S_1, S_2, \ldots, S_k$ by minimizing the distance of point to the centroid S_k as in Equation. 6.8.

$$\underset{\mathbf{S}}{\arg\min} \sum_{i=1}^{k} \sum_{\mathbf{x} \in S_i} \|\mathbf{x} - \boldsymbol{\mu}_i\|^2 = \underset{\mathbf{S}}{\arg\min} \sum_{i=1}^{k} |S_i| \operatorname{Var} S_i \tag{6.8}$$

In a nutshell K-Means works as follows: k initial cluster centers are chosen randomly from the observation as cluster center initialization. Then the point-to-cluster-centroid distances is computed for all observations with each centroid. Assign each observation to the cluster with the closest centroid. Recalculate the new centroid location by the average of the observations in each cluster. Repeat until centroids do not change anymore.

6.3.2 Scheme of beacon advertising control

The network architecture of a typical BLE beacon based WMS is shown in Figure 6.11. There are two network devices: (i) AS - Animal scanner, and (ii) AB - Animal Broadcaster. AS is a BLE scanner node, which listens for BLE beacons in the surrounding area, where as AB is a BLE beacon broadcasting node, which uses the short-range BLE radio to advertise their beacon data to AS node.

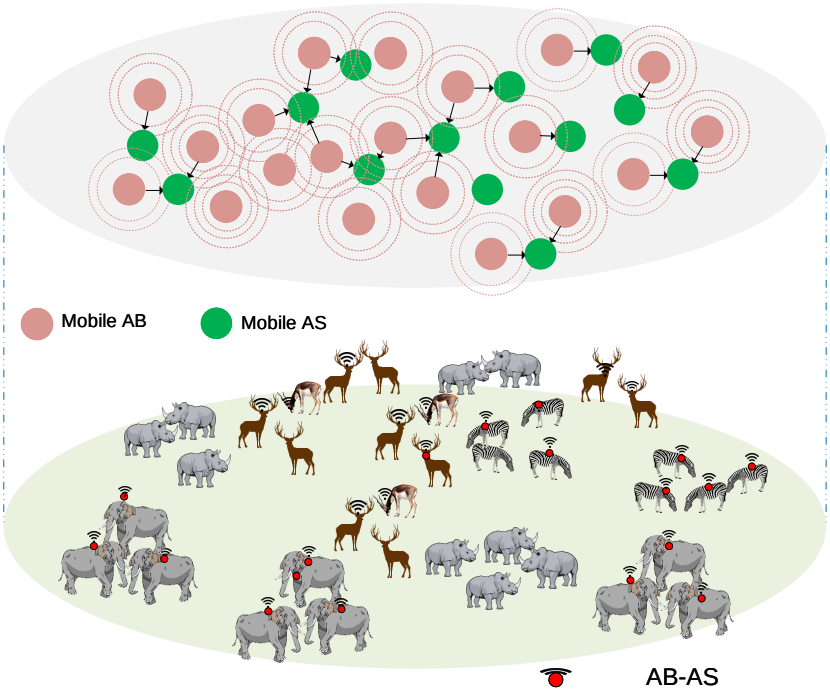

FIGURE 6.11: *A BLE based beacon network architecture. AS-AB network mode. device roles: (i) AS - Animal Scanner, (ii) AB - Animal Broadcaster*

In general, animal mobility could be broadly classified into: (i) passive state with no movement, (ii) active state with relatively low mobility (e.g. grazing, graze-walking); and (iii) panic state for high mobility (e.g. running away from predators or illegal poachers) [155, 160, 169]. Thus, as far as wireless communication is concerned, instead of using conventional periodic beacon transmission as in [170], AB nodes in our approach advertises beacons in two mode: (i) stationary mode (SM), used in passive and active animal mobility states and (ii) beacon-on-motion (BOM) mode used for the panic animal mobility state. Each AB nodes selects their beacon advertising modes (i.e. SM or BOM modes) based on the sampled mobility states (i.e. passive, active, or panic states) by applying local sensor data classification and processing algorithm on accelerometer data.

As shown in Figure 6.12.a, in conventional BLE beaconing each AB node periodically wakes-up every fixed (i.e. T^{+}_{BC}) interval for a very short duration (ToA) to send data. In our approach, as shown in Figure 6.12.b, we utilize an unsupervised animal mobility detection and classification algorithm to optimize the BLE beacon advertising time for each AB node. Figure 6.13 depicts how AB nodes control their advertising interval by adapting the ($T^{+}_{sl,BOM}$ or $T^{+}_{sl,SM}$) intervals depending on its detected mobility states. $T^{+}_{sl,SM} = T^{+}_{BC}$ and $T^{+}_{sl,BOM} = WL/2$ are the advertising intervals configured for SM and BOM beacon advertising modes respectively. These intervals depend on the optimal data processing window length (WL) that will be determined by the classification algorithm in the run-time as detailed in the following subsection.

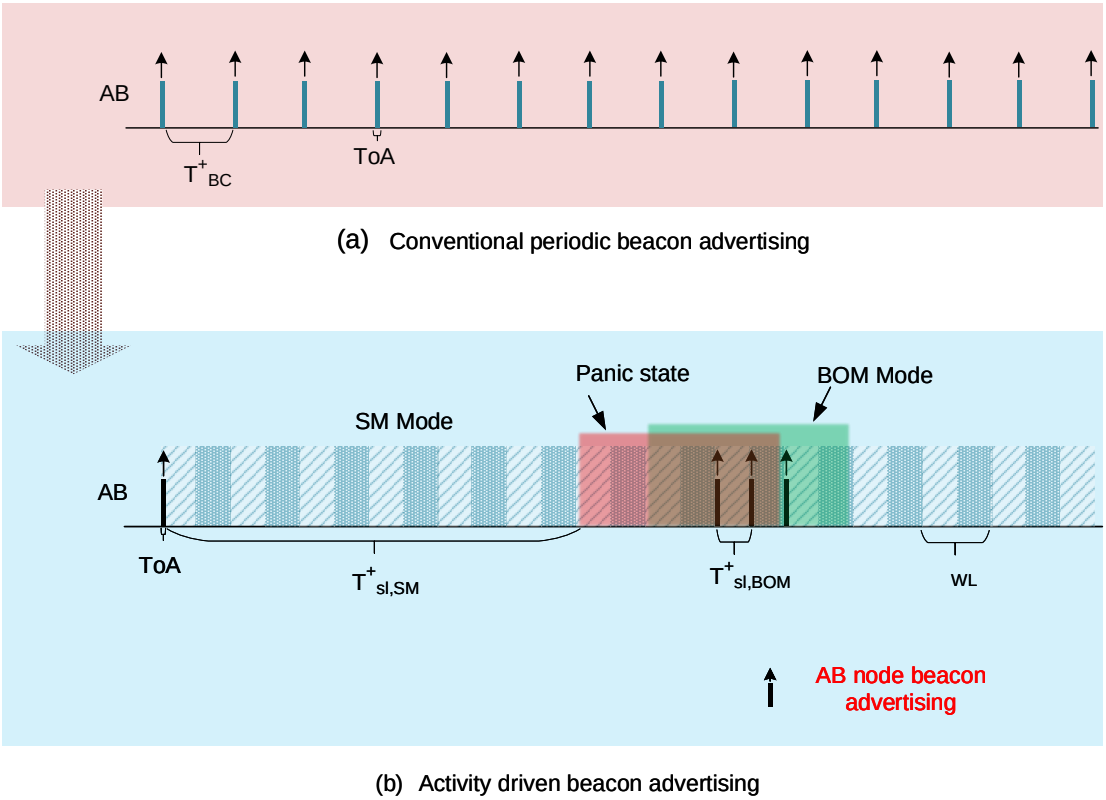

FIGURE 6.12: *Mobility driven BLE beacon advertising scheme (AB* $\xrightarrow{beacon}$ *AS). SM - stationary mode, BOM - beacon-on-motion mode*

6.3.3 Operation of beacon advertising control algorithm

Detecting animal mobility states (i.e. passive, active, and panic) using sensor data requires implementation of an algorithm that is able to identify the mobility states. Generally, there are two main algorithm groups, supervised and unsupervised learning algorithms [166, 167]. In addition, a conventional threshold algorithm could also be used, however, the major drawback to threshold-based approaches is that they often lack the sensitivity and specificity needed for accurate data classification [171]. Sensitivity is defined as the true positive rate (TPR) for a function or a test that must detect the presence or absence of some intrinsic animal movement [171]. Moreover, supervised learning algorithms learn by example, thus requiring huge amount of labeled data representing the case being learned. However, in this work, we utilize a simple and efficient unsupervised learning algorithm called self organizing maps (SOM) to classify the mobility states in real-time. We selected this unsupervised learning algorithm for our approach because it has the capability to group the sample data into clusters with similar level of features to the supervised learning algorithm without requiring large amount of data and computational complexity [166, 167].

As shown in Table 6.2, to align with the three mobility states defined in this work, we re-classify the number of raw labeled activities as reported in [12] from *16 classes:*

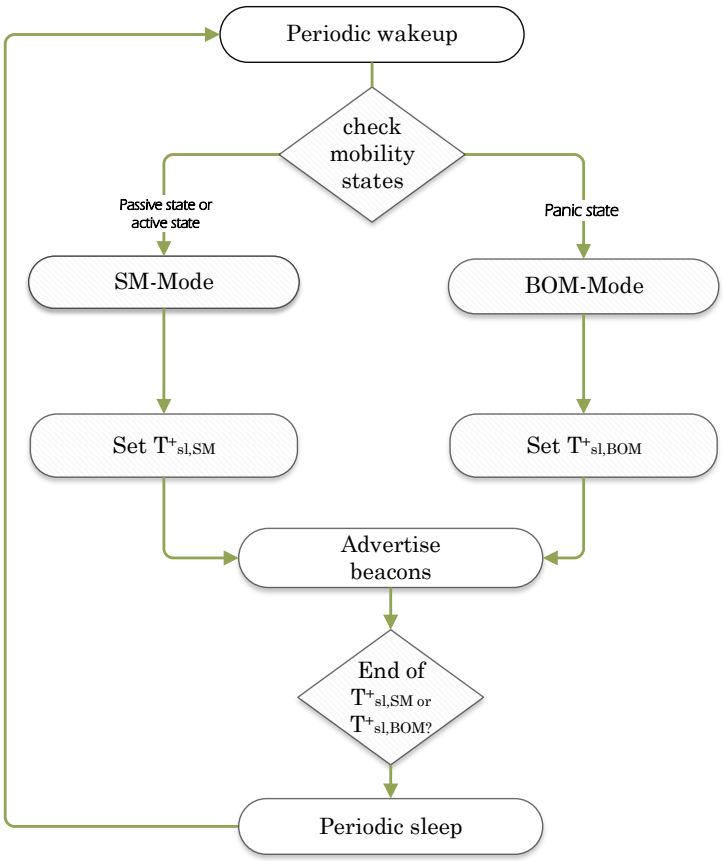

FIGURE 6.13: *Scheme of beacon advertising flow chart*

i.e. { shaking, standing, lying, grazing, eating, breast-feeding, scratch-biting, rubbing, standing-up, walking, fighting, food-fight, climbing-up, climbing-down, trotting, running } , to *3 classes* i.e. (i) passive: { shaking, standing, lying, grazing, eating, breast-feeding, scratch-biting, rubbing, standing-up }, (ii) active: {walking, fighting, food-fight, climbing-up, climbing-down }, (iii) panic: {trotting, running }. Table 6.2 also shows the distribution of the three mobility states, i.e. passive (68.55%), active (29.07%), and panic (2.37%). Meaning that for approximately 97.63% and 2.37% of the time the animals are in passive/active and panic mobility states respectively. Consequently, this leads to configure the respective beacon advertising modes as $\approx$ 97.63% and $\approx$ 2.37% of the total time as SM and BOM modes respectively. Hence, the panic mobility state tends to occur very intermittently for a short duration of time. Thus, we assume that each mobility states will last for at least n second, hence, we use an optimal window length ($WL = \Delta t$ seconds).

6.3.4 Evaluation

In this section, the evaluation of the proposed unsupervised algorithm is discussed for different parameters that can affect both the efficiency and accuracy of the results in a practical deployment. The impact of the proposed algorithm on energy

TABLE 6.2: *Re-classifying of the mobility states from* 16 *to* 3 *classes (i.e. (i) passive, (ii) active, (iii) panic)*

	(i) passive	(ii) active	(iii) panic
1	shaking	walking	trotting
2	standing	fighting	running
3	lying	food_fight	
4	grazing	climbing_up	
5	eating	climbing_down	
6	breast_feeding		
7	scratch_biting		
8	rubbing		
9	standing_up		
10	null		
Total dwell time (%)	68.55	29.07	2.37

consumption is investigated and compared to k-mean clustering scheme. The simulation and modeling is implemented in Matlab.

Parameter setup

TABLE 6.3: *Symbol notations*

Notations	*Details*
ToA	Time-on-air of BLE beacon data
$T^{+}_{sl,BOM}$	Advertising interval for the BOM states (i.e. $WL/2$ from Sec. 6.3)
$T^{+}_{sl,SM}$	Advertising interval for the SM states ($\approx$ 10minute)
T^{+}_{BC}	Advertising interval for the conventional states ($\approx$ 10seconds)
WL	Optimal window length of detecting activity, (2sec,4sec,6sec)
ρ	Proportion AB node is in BOM ($\rho = 0.0237$ for SOM, $\rho = 0.057$ for K-Mean)
I_{tx}	Transmit current consumption
Ti	Training instances
LS	Lattice size
SR	Sampling rate

Table 6.3 lists the parameter notations used in this paper.

We used actual sensor labeled data collected with inertial collar sensors [12]. The data are generated by 5 goats equipped with collar, on which 6 sensor nodes are placed around the collar in different positions. The data are labeled for *16 types* of activities performed by the goats. The sensor sampling rate (SR) for the data set

was at sampling rate ($SR = 100Hz$) [12]. This is a typical set-up for most empirical studies, however, in real-life implementation the feature extraction and classification calculations performed at the node using this sampling rate ($SR = 100Hz$) will result in high energy consumption. Therefore, in our approach the measurements are first down-sampled to a sampling rate ($SR = \{10Hz, 5Hz, 2Hz, 1Hz, 0.5Hz\}$. Setting several SR values allows to observe the minimum SR required to detect the animal mobility states.

Moreover, we need to define the optimal window length (WL) to lower both the computation frequency and the energy required for processing the data to detect the mobility states. The window length should be wide enough to capture the full length of the mobility performed. Therefore, we trained the SOM with different WL ($\{2sec, 4sec, 6sec\}$) for SRs above 1 Hz, and WL ($\{4sec, 8sec\}$) for SRs below 1Hz. The number of epochs are set at 1000 for each training batch. Ti is the number of training instances from each class and it is used for training phase. In order to find the appropriate dimensions for the SOM neuron lattice, we conducted training phase with three different lattice size (LS): 2x2,3x3, 4x4 and 5x5 neurons. This will result into 208 different models, 16 for each window length.

Performance measures

In this subsection, we use the following evaluation metrics:

- Clustering analysis: Given that the original data-set from [12] is labeled, the clusters can be converted easily into classes. This is achieved by feeding the features set of the same class and observing the cluster it will fall into. This results in a confusion matrix $m \times n$, where m is the lattice size and n is the class number. Since the distribution classes are not balanced, the number of elements in the cluster are shown as the percentage of the class.
- Accuracy: The probability that a cluster C^n belongs to one of the three classes C_i^n is calculated as follows:

$$P(C^n) = \frac{C_i^n}{\sum_{i=1}^{3} (C_i^n)} \tag{6.9}$$

  The cluster is considered as a representative of a given class if the $P(C^n) > 0.5$, hence, the accuracy of each class Cl_i is calculated as

$$Acu(Cl_i) = \sum P(C_i) > 0.5 \tag{6.10}$$

  Thus, we can identify the clusters that belong to a class with a high level of probability. This method results in a better cluster distribution toward different activities that show similarities, such are *walking* and *running*. Once the accuracy is computed for all the parameters, we pick the maximum pair of accuracy for all the classes.

- True positive rate (TPR) and false detection rate (FDR): The purpose of this metric is to see how the misclassified data affect the overall classification. First we need to calculate the True Positive Rate (TPR) $\text{TPR} = \frac{\text{TP}}{P} = \frac{\text{TP}}{\text{TP}+\text{FN}}$. It is also important to know the False Detection Rate (FDR), i.e. the rate of falsely detecting the window as positive $\text{FDR} = \frac{\text{FP}}{\text{FP}+\text{TP}}$.
- Processing time: to evaluate the efficiency of the proposed classification algorithm, we record the average time required to complete one full task operation on our data-set for different input parameter values. Our proposed classification algorithm has a straight forward mechanism that starts with filling a buffer with sensor data, calculating features over that buffer, and normalizing the feature set followed by feeding the normalized feature set to the SOM model.
- Energy consumption: We evaluate the energy consumption by comparing the mobility driven mode with the conventional periodic BLE beaconing mechanism. The energy consumption per unit time is proportional to the ratio of active time to sleep-time. For the energy model, I_{tx} denotes the transmission current level. Thus, for both conventional periodic and mobility driven beacon transmission mechanisms, the energy consumed by a single AB beacon nodes is expressed as:

$$E_i = \begin{cases} P_{tx} \times \lceil T/T^+_{BC} \rceil \times \frac{ToA}{ToA+T^+_{BC}}, & \text{Periodically Cont.} \\ P_{tx} \times \Big(\underbrace{\lceil T/T^+_{sl,BOM} \rceil \times \frac{ToA}{ToA+T^+_{sl,BOM}} \times \rho}_{\text{BOM Mode}} + \underbrace{\lceil T/T^+_{sl,SM} \rceil \frac{ToA}{ToA+T^+_{sl,SM}} \times (1-\rho)}_{\text{SM Mode}} \Big), & \text{SOM \& K-Mean} \end{cases} \tag{6.11}$$

Thus the average network wide energy consumed is expressed as: $E = \frac{1}{N}\sum_{i=1}^{N} E_i$, for N-number of AB beacon nodes in the network. ρ is the percentage of mobility state dwell time that the AB node is in panic state, i.e. $\rho = 0.0237$ and $\rho = 0.057$ for SOM and k-mean algorithms respectively (Table. 6.2). $P_{tx} = I_{tx} \times V$, $ToA \approx 10$ms at 1MBs BLE data rate [155], $T^+_{sl,BOM} = WL/\alpha$, $\alpha \geq 1$ are the real-time mobility driven beacon interval adjusting factor, where $\alpha = 1$ is equivalent to the AB node in a continues periodic beacon advertising mode with a fixed $T^+_{BC} = 10$s value, which the maximum interval recommended for BLE beacon [6].

Note that in the periodic beacon, AB node's advertising interval (T^+_{BC}) is prefixed, so the sleep time is not optimally adjusted in real-time. However, as per our SOM and k-mean algorithm used, in the BOM mode, AB nodes send beacons at a rate equal to half the optimal WL determined (i.e. $T^+_{sl,BOM} = WL/2$), hence, $\alpha = 1/2$. In addition, since animals move occasionally, in the static mode (SM), AB nodes send beacons at $T^+_{sl,BOM} = 10$minutes. This would be practically enough to beacon a heart-beat data now and then.

6.3.5 Results and discussion

We first discuss the result for the accuracy of the clustering algorithm for each lattice size (LS), followed by the investigation of how much improvement is gained by increasing the epoch size. Finally, we observe the effect of window size (WL) in both data processing efficiency and beacon advertising energy consumption.

Clustering analysis

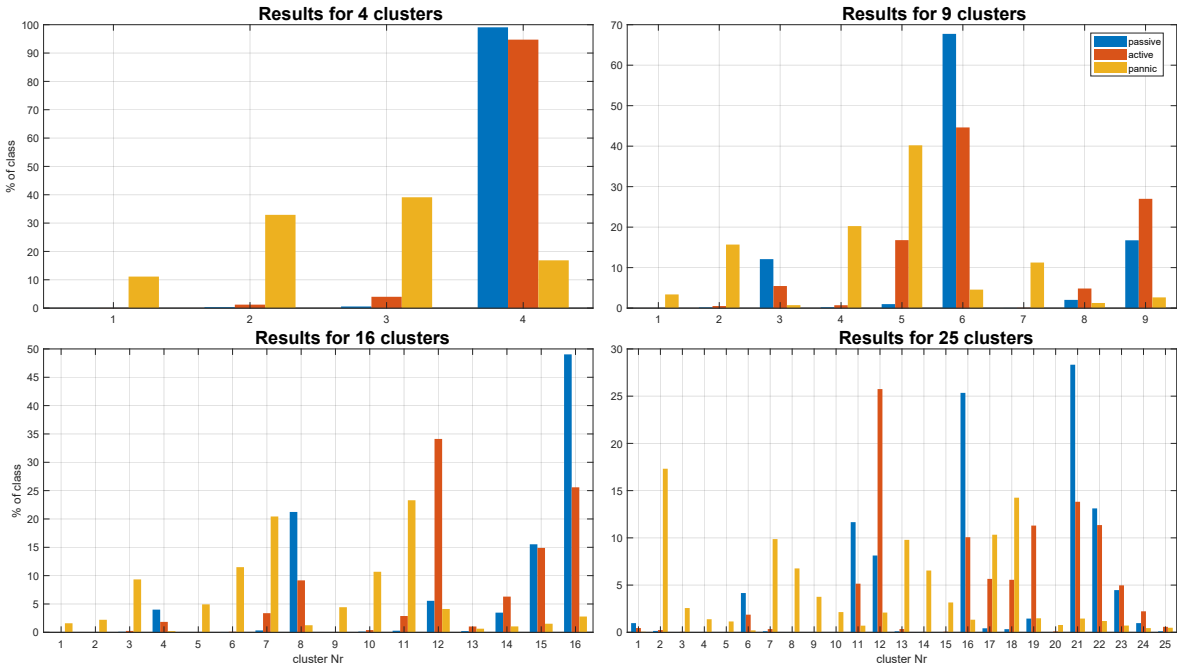

FIGURE 6.14: *Classification results of SOM algorithm for different lattice size m*

Figure 6.14 shows the results of different cluster sizes for SOM algorithm for data sampled at $SR = 10Hz$ and window legth $WL = 2sec$. We can see that *panic* class creates distinctive clusters with some overlapping with active state, which is expected as the walking and running activities only differ in frequencies when measured from the neck of the animal. The overlap is very small, however, it is more challenging to distinguish the *passive* and *active* classes with less clusters. Hence, we group the active and panic state into a generic Active state. *Active* class is only clustered distinctively for only 35% of instances in cluster Nr. 12 (4×4) SOM and cluster Nr.12&19 (5×5) SOM.

Accuracy

Figure 6.15 shows the accuracy SOM algorithm for different parameters of sampling rate (SR), window length (WL) and cluster size, when only accelerometer is used, or when both the accelerometer and gyroscope sensor data are used. It can be observed

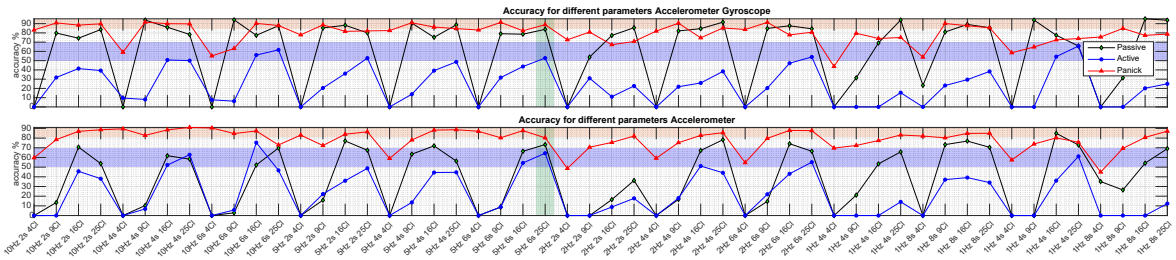

FIGURE 6.15: *Accuracy of SOM algorithm for different parameters*

that the magnitude of the rotation for the goat collar helps to better distinguish the running activity, when the animal does not rotate the neck that much, where most the accuracy levels are above 90% especially at $SR = 5Hz$ and $WL = 6s$. However, it brings uncertainties in distinguishing the active state with miss-classifications that result in low accuracy.

Processing time

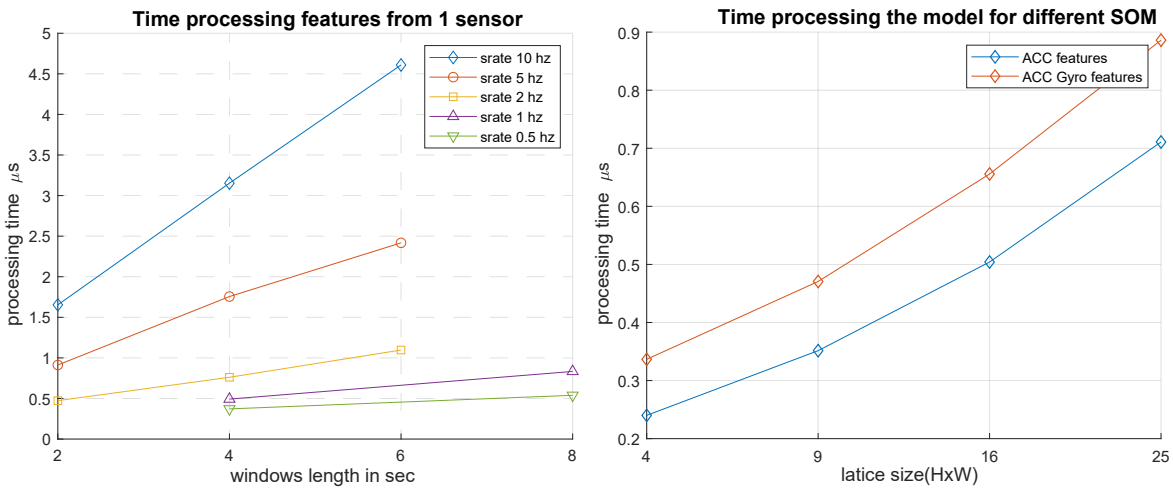

FIGURE 6.16: *Average processing time of SOM algorithm*

Figure 6.16 shows the average time required by the SOM algorithm to calculate the feature set for one sensor node for different WL and SR. The higher SR the higher the processing time, and the wider the WL the higher the processing time but the less frequent the number of processing. The average time required to normalize the feature set of length 5 features is $0.067\mu s$ if only accelerometer is used and $0.1\mu s$ for 10 features if both accelerometer and gyroscope sensors are used. Figure 6.16 shows the processing time required to apply SOM model over the feature set. As expected, less clusters will result in less weights, thus shorter processing time.

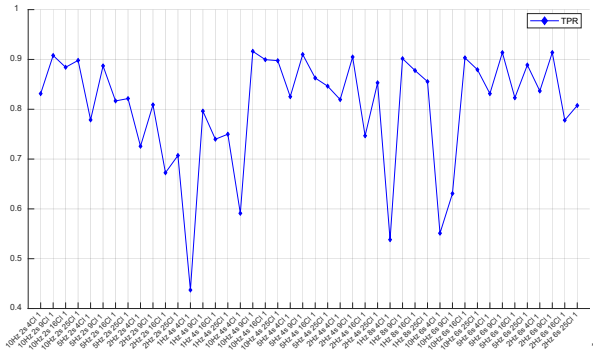

FIGURE 6.17: *SOM algorithm TPR from the classification results for different parameters with only accelerometer sensor*

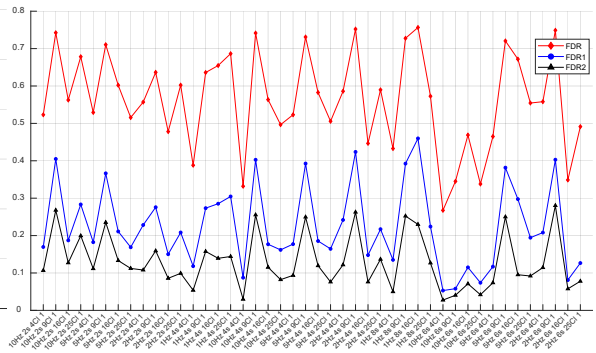

FIGURE 6.18: *SOM algorithm FDR when results with up to 2 and 3 consecutive detected windows are excluded from the results*

TPR and *FDR*

The TDR and FDR for SOM algorithm is shown in Figure 6.17 and Figure 6.18 respectively. The FDR is very high, nevertheless, most of the FDR are single misclassified windows. Furthermore, to establish the right ratio of detection before the panic flag is raised, the SOM algorithm requires n or more *true* consecutive detection before it decides to turn on the BLE radio and broadcast the activity with BLE beacon data. The rationale behind this reasoning is that the animals cannot go into panic state only for the duration of one WL. For instance, if an animal runs, naturally it will continue to run for some time longer than the window length (WL). Figure 6.18 shows the reduction of FDR where up-to 2 *consecutive windows* are excluded and detections with up-to 3 *consecutive windows* are excluded from the detection results. Given the half window overlap, the algorithm excludes detections that lasted for $1\frac{1}{2}WL$ or $2WL$, respectively.

Comparison to K-Mean

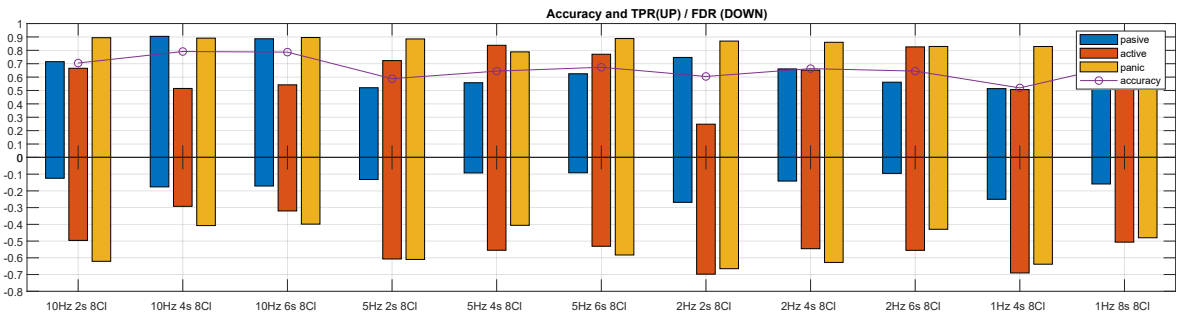

FIGURE 6.19: *Accuracy, TPR and FDR for K-Mean clustering*

To put the proposed SOM algorithm into a comparison with other types of unsupervised learning algorithms, we used the K-Mean algorithm as baseline to cluster the activities into distinctive clusters. The same training data set used for SOM is also

utilized for the K-Means clustering algorithm. In order to find the optimal number of clusters, in our case $k = 8$, the Calinski-Harabasz evaluation method is used as described in [172]. After training the clusters for each sampling rate and window length, we cluster the data while using the same methodology described in SOM, to calculate the accuracy, TPR and FDR.

The results are shown in Figure 6.19, we can see that although TPR is in the range of 80-90% for the pannic state, the FDR is very high, and the K-means fails to cluster well the active state. Moreover, the classification accuracy of the K-Mean algorithm is observed to be below $\approx$ 85%, which is way lower than the SOM algorithm. Regarding the k-mean clustering processing time complexity, the average computation time for an 8 centroid based k-mean is found to be 0.0644 μs and 0.121 μs for one sensor and two sensor nodes respectively, which is relatively longer than the SOM algorithm's processing time shown in Figure 6.16 This makes the K-Mean algorithm inappropriate for our particular scenario as the high FDR will have a counter indicative impact on energy consumption because the radio will have to transmit more frequently with false detections.

Energy consumption

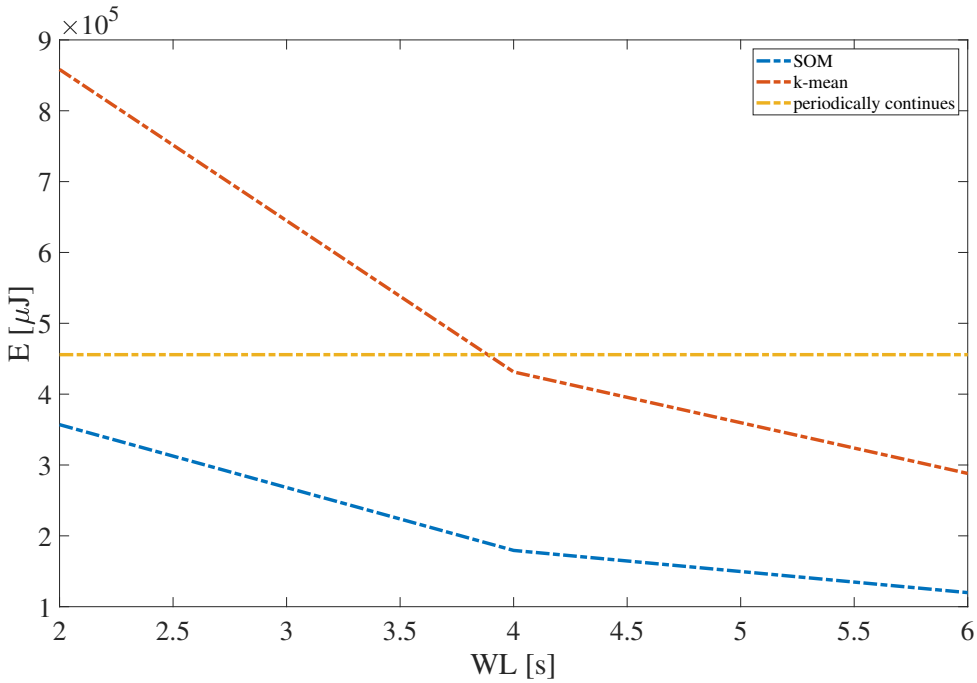

FIGURE 6.20: *Node energy consumption*

Figure 6.20, shows the node energy consumption for different window length (WL), i.e. 2 sec, 4 sec, 6 sec. For the mobility driven advertising depicts an decreasing energy consumption trend as WL increases. However, regardless of WL, the periodic beacon mode shows a steadily higher energy consumption level compared to the mobility driven advertising, as it often happens in wildlife monitoring applications. Overall, for higher WL, the mobility driven beacon advertising has lower energy

consumption compared to the conventional periodic advertising. This indicates the mobility driven beacon approach is more optimal than periodic beacon mode for animal monitoring, especially, where energy management is a challenge.

6.4 Conclusion

In this chapter, we discussed mobility aware communication protocols for wireless sensor network based wildlife monitoring. As commonly deployed, a fixed duty-cycle interval for dynamic network topology often leads to higher energy consumption. We presented HAMA protocol to cope with frequently changing network topology due to high node mobility. HAMA's feed-back stability controller analyzes the received and transmitted packets to determine an optimal sleep-time interval at run-time. To evaluate HAMA under in a dynamic network topology scenarios, we used two mobility scenarios based on Zebras activity and BonnMobility random way point. Our evaluation results show that compared to A-MAC and X-MAC, utilizing HAMA protocol the average network energy consumption is reduced by 22.28%-52.28%, providing an additional decrease in the average end-to-end latency by 11.65%-14.63%. The overall packet reliability is also up-to 16.3% increased. Moreover, we also presented a beacon advertising control scheme to monitor animals based on their mobility states. This approach utilizes a strategy that maximizes the accuracy of mobility state detection by using unsupervised learning SOM algorithm. To decrease the energy consumption, the proposed technique limits the number of beacons transmitted to the active state and only sending a heart beat of data in the stationary state. We have compared our solution to the continues beacon mode and k-mean algorithm by analyzing the energy consumption. Overall, for higher window length (WL), the proposed mobility driven data advertising approach has a higher network life-time than the continuously periodic advertising mode.

Chapter 7

Herd Aware Multi-hop Communication With Hybrid Tree Network

In this chapter, we present MANER, a herd aware multi-hop data dissemination scheme for WMS. In MANER, data forwarding is optimized with a replication function to control and prioritize data dissemination. In WMS scenario, wild animals show a sparsely con-specific mobility, which often results in a sporadic wireless link among nodes. Unlike existing opportunistic multi-hopping algorithms, MANER optimally makes data forwarding decisions by leveraging locally available information such hop count and amount of data replicated. Hence, the proposed algorithm adopts to dynamic network topology caused by the inherent intermittent connectivity among mobile herd of animals. We evaluated the performance of MANER by considering standard and real-life mobility models. Experimental results indicated that MANER decreases the average latency by up-to 65%, when compared to benchmark opportunistic routing algorithms. In addition MANER readily increased the network delivery ratio for various data traffic rates.

Part of this chapter has appeared in:
[25] *E. D. Ayele and N. Meratnia and P. J. M. Havinga, MANER: Managed Data Dissemination Scheme for IoT Enabled Wildlife Monitoring System, 2018 9th IFIP International Conference on New Technologies, Mobility and Security, Paris, Feb. 2018, pp. 1-7.*
[24] *E. D. Ayele and N. Meratnia and P. J. M. Havinga, Towards a New Opportunistic IoT Network Architecture for Wildlife Monitoring System, 2018 9th IFIP International Conference on New Technologies, Mobility and Security, Paris, 2018, Feb. 2018, pp. 1-5.*

7.1 Introduction

Wireless communication among sensor nodes in WMS deployment will facilitate local pre-processing and data sharing for collaborative decision making. Either the conventional multi-hopping protocol, (e.g DSR or AODV [151]), or an alternative opportunistic multi-hopping protocol could be used to develop a communication network protocol for WMS. Figure 7.1 illustrates the fundamental differences in the two communication paradigms.

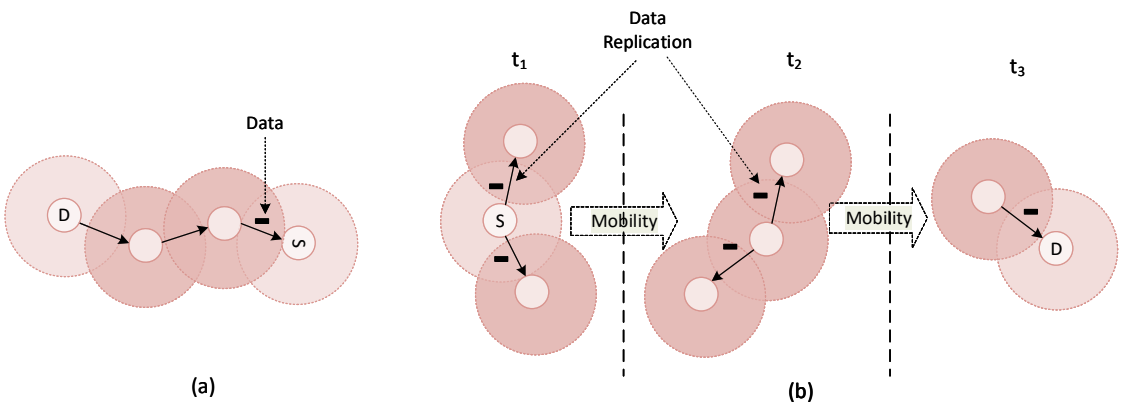

FIGURE 7.1: *(a) conventional multi-hopping networks via end-to-end paths and (b) opportunistic multi-hopping networks using data replications scheme. 'S'=source node and 'D'=destination.*

Conventional multi-hop network protocols typically employ the *store-and-forward* routing [70]. When a packet arrives, first it is buffered until it can be forwarded to a suitable path (Figure 7.1.a). One of the fundamental assumptions of these protocols are the availability of at least one end-to-end communication path between any source and destination node pairs [27, 153]. For example, in [173], multiple such paths are considered as backups, in case the primary path fails. Unfortunately, such communication link possibilities are rare in WMS applications where animals are often mobile. Hence, conventional multi-hop network protocols are less suitable for WMS applications, where wild animals depict sparse and con-specific movement behaviour, resulting in sporadic and unstable end-to-end connectivity among nodes.

To overcome such issues and constraints, data routing and collection could be addressed from an opportunistic multi-hop networking view point as used in [174], to cope with such node mobility and to provide interoperability among heterogeneous networks. Data multi-hopping in opportunistic networks follows the *store-carry-and-forward (SCF)* paradigm [70], where a node receives a data from another node and the former stores the data in its buffer (Figure 7.1.b). The receiver nodes can possibly move with while the data is stored in its buffer. Finally, when the node comes in contact with another node, it replicates the data with the hope that the receiver node can deliver the data to its corresponding destination. Data replication refers to the process where a transmitting node sends a copy of the data to the receiving node and itself retains the original data. Therefore, multiple copies of a data

can exist in the network. In opportunistic multi-hopping protocols such data replication is often utilized to enhance the chances of data delivery given the scarcity of communication link opportunities in mobile networks.

Even-though mobility is considered as the helpful for information dissemination in opportunistic multi-hop networks, recent researches have revealed that existing opportunistic multi-hop protocols perform less than expected for a sparsely mobile networks with non-deterministic movement [157]. For instance, Epidemic [157] and PRoPHET [152], offered a high data delivery ratio at the expense of high network overhead and latency. Spray and Wait (SnW) on the other hand resulted in low latency but high network overhead [157, 152]. As discussed in Chapter 2, several opportunistic multi-hopping network protocols have been used in wildlife monitoring projects for gathering sensor data, e.g. ZebraNet [13, 27], Rat Watch [153]. These works, often leverage an opportunistic multi-hop networks by utilizing a history based flooding, which are prone to low delivery ratio and high latency [157].

Fulfilling the overall WMS design requirements such as high reliability, low latency, and high energy efficiency, often requires a meta-heuristic approach, where each node makes a data forwarding decision locally. Therefore, in this chapter, we present MANER - managed data dissemination for herd aware multi-hop scheme for WMS. The characteristics that make MANER suitable for WMS scenario are: (i) there is no network topology limitation imposed, (ii) node mobility is easily supported, and (iii) intermediate nodes utilize a simple store-carry-and-forward (SCF) scheme for data dissemination with out relying on routing table information. MANER minimizes data latency while avoiding deterioration in data delivery ratio. To this end, the contributions of this chapter is to improve the existing opportunistic multi-hopping network protocols by managing the data replication decision through leveraging locally available routing parameters. Through simulation, the performance of the proposed protocol is compared and evaluated with the state-of-the-art data dissemination protocols based on opportunistic network protocols.

The rest of the chapter is organized as follows: Section 7.2 discusses a heuristic opportunistic multi-hop network protocol for WMS. Section 7.3 further presents the implementation and evaluation results. Section 7.4 discusses the simulation results. Finally, Section 7.5 outlines the concluding remarks.

7.2 Protocol design

In this section, we present the design overview of MANER followed by a discussion on its operation. The proposed scheme for managed opportunistic routing is based on store and carry technique. Here we present the contribution of our algorithm and outline the heuristics needed for the implementation of MANER protocol. Managing data forwarding decisions are made based on networking parameters such as: inter-contact time, hop-count, number of message replicated.

7.2.1 Scheme of MANER protocol

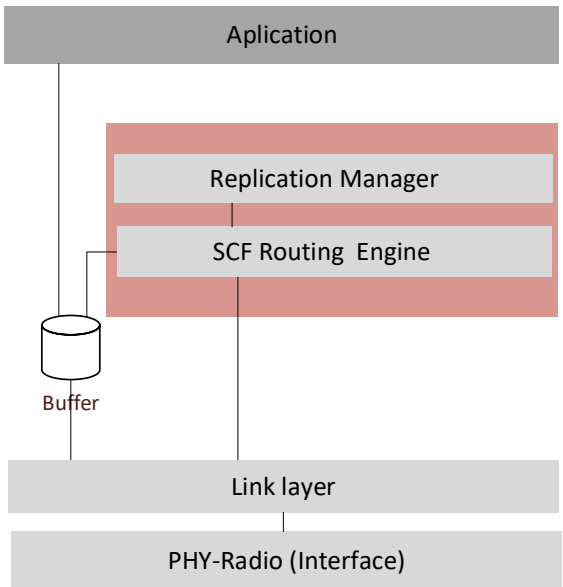

FIGURE 7.2: *MANER protocol stack*

Figure 7.2 shows MANER protocol with the SCF routing layer. When source nodes want to send data to sink node, it utilizes MANER, a simple opportunistic store-carry-forward (SCF) protocol. Below the link layer there is a BLE radio as the physical layer. Neighbor discovery is one of the key mechanisms of PHY/MAC to efficiently administer self-organizable opportunistic networks. Unlike other short-range wireless technologies, e.g. WiFi direct [175], the recently released specification for BLE - mesh v1.0 offers low-power and simple device discovery which easily enables opportunistic network deployment [176]. MANER can work on top of any MAC/PHY layer, however, to comply with the network architecture presented in Chapter 4 for BLE opportunistic multi-hop network, and abstract the MAC/PHY bearer as indicated in Section 7.3.

Unlike Epidemic protocol [115], the objective of MANER protocol is to provide a simple managed flooding scheme based on BLE mesh to accommodate herd mobility algorithms. As shown in Figure 7.3.b, when a source node S wants to send a data to destination node D, S passes data to its neighboring node and this process is repeated until data reaches D. We assume that nodes communicate only when they are within the transmission range of one another (Figure. 7.3.a and 7.3.b). If there is a disconnection of the link en route to D, it is likely that one or more node (s) come into contact with another node at a later time due to inherent animal movement. Thus data is spread throughout the entire network and will eventually be received by D. MANER enables node-to-node ($n : n$) or many-to-many ($m : m$) communication in WMS. Unlike conventional protocols, it does not require complex routing table management and it is inherently multi-path, while allowing neighboring nodes to communicate directly with one another to enable network level services such as proximity detection and peer-to-peer collaboration among nodes.

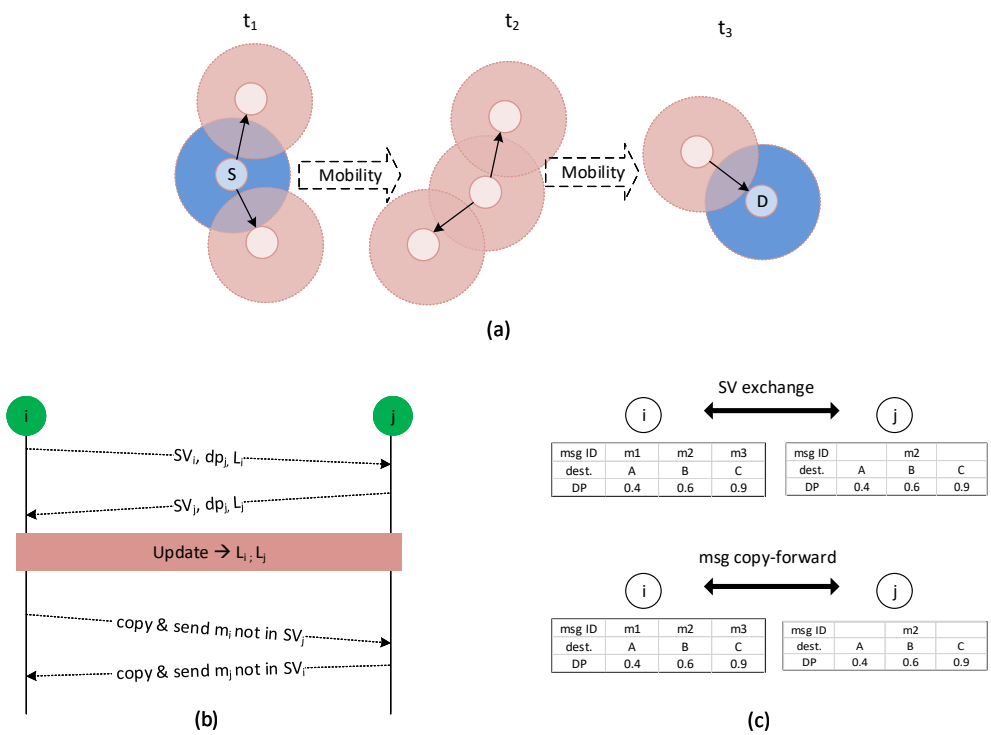

FIGURE 7.3: *(a) MANER protocol operation, (b) & (c) Summary Vector (SV) and inter-contact time (L) exchange between node i and j upon contact.*

7.2.2 Operation of MANER protocol

MANER adopts a simple store-carry-forward (SCF) algorithm involving the exchange of summary vectors (SVs) - a list of data IDs contained by a node in its buffer, and delivery probability (dp), similar to most opportunistic protocols [157] (Figure. 7.3.d). When a node receives an SV from another node, it learns the data that should not be replicated. MANER improves existing opportunistic algorithms by managing data replication decisions based on routing parameters such as: inter-contact time (L), hop-count ($Hc_{i,m}$), number of replication (n^r), and delivery probability (dp).

Algorithm 7.4 summarizes the operation of MANER carried out by a node, when an active forwarding event with another receiver is invoked. Consider that a forwarder node i is contemplating the replication of a data m to node j. The forwarding decision will depend on per-link replication cost (R_{cost}) computed based on L_i and $Hc_{i,m}$ (Algorithm. 7.4). Let $L_{i,j}$ be the time instant when the previous contact of node i with node j is terminated.

Then, at the next contact event with j at time instant (t), the exponential smoothed estimation of the next inter-contact time ($L_{i,j_{(t)}}$) value of node i is updated as $L_{i,j_{(t)}} = \alpha \times L_{0,i} + (1-\alpha) \times L_{i,j_{(t-1)}}$, where $L_{0,i}$ is the value at a time period (t), and $0 \leq \alpha \leq 1$ is the smoothing factor of $L_{i,j}$ [177]. Hence, the per-link replication cost (R_{cost}) of

Algorithm 7.4 MANER on node i replication started with node j event

Input: m_i: set of messages on node i, L, $Hc(i,m)$, n^r, dp.
Output: Decision to replicate message to node j, R_{cost}
for $m \in m_i$ **do**
  if $dp_i \geq dp_j$ *then* **then**
    // Sort receiver nodes
    // dp based neighborhood pruning
    continue
  end
  Compute L, $R_{cost}(m,i)$, $R_{cost}(m,j)$ using 7.1, 7.2
  $\delta R_{cost} = R_{cost}(m,j) - R_{cost}(m,i)$
  if $(\delta R_{cost} \leq 0)$ **then**
    replicate m to j
  end
end

having a data m at node i is expressed as according to [177]:

$$R_c(m,i) = L_{i,j_{(t)}} \times [1 + Hc_{i,m}] \tag{7.1}$$

The hop-count ($Hc_{i,m}$) is incremented by unity in order to prevent the cost function from becoming zero at the source of data. It may be observed that, if m is replicated to j, the hop-count of m at j increases by unity. In other words, the replication action will allow data to be spread to the next hop, while increasing the value of its routing cost. This is in line with other opportunistic routing algorithms [158]. Therefore, the replication function at receiver j is computed as:

$$R_c(m,j) = L_{j,i_{(t)}} \times [2 + Hc_{i,m}] \tag{7.2}$$

The steady state difference in the two cost functions is $\delta R_c = R_c(m,j) - R_c(m,i)$. Thus forwarder node i decides to replicate, if the $\delta R_{cost} \leq 0$. In other words, such a replication would help the data to flow from a higher cost state to a lower cost state. Algorithm 7.4 uses the local routing cost functions in Eq. 7.1 and 7.2 to initiate replication decision to the next hop.

7.2.3 Optimization of data replication decision

In addition, the forwarder node optimizes data replication decision by restricting the number of times (n^r) a data is replicated and pruning the receiving nodes according to (dp). To prevent the stored SV list for each data from becoming too long to overflow the buffer, number of replicated data is optimized by limiting n^r value. The n^r is decreased down to 1 after each successful forwarding to optimize the delivery ratio of data. All data originating from the same source have the same initial value of n^r.

As shown in Algorithm 7.4, when a forwarder node i encounters one or more nodes, the forwarder will collect and sort all active connections in descending order of the dp. When there are several nodes in communication range, a node will be selected as a forwarder node and remaining nodes as receiver nodes by applying some existing neighbor filtering mechanism, such as k-means clustering [158]. The receiver node, of which the dp is higher than that of others, will have higher priority to receive data from the forwarder. These requested messages are sorted by a message sorting method, such as, First In First Out ($FIFO$), before being pushed into the outgoing buffer. Due to the limited space, we will discuss the sorting schemes in more detail in journal.

Notice that MANER mimics an Epidemic routing by flooding the entire network with data copies, when n^r is set to $+\infty$ for all nodes. When n^r is finite value, a node will spread packets either like SnW ($-\infty \leq {n^r}_i \leq 1$) or DD (${n^r}_i = 1$) depending on the value set [158]. Thus, for a sparsely mobile network application, where herds of animals will often move randomly in con-specifics manner, n^r is set in the range ($1 \leq {n^r}_i \leq \infty$) depending on the expected optimal latency.

However, one of the easiest approach to determine the optimal n^r value for our WMS mobility use case is to solve the optimization equation as presented in [158], where the expected delay is related to optimal latency as $ED_{sw} = a \times ED_{opt}$, a is a factor for delay constraint set by an application. As per [158], $a = 5$, implying the average delay is up-to 5 times of the optimal latency.

$$n^r \approx \frac{n}{a \times k_n} \tag{7.3}$$

Assuming all nodes are mobile, this results in Equation. 7.3, where n is number of mobile nodes, which is consistent with the analysis done in [158]. We note that MANER requires *O(n)* storage for maintaining L, in accordance with PRoPHET, SnW, and DD protocols, however, in MANER the catch is temporarily occupied.

7.3 Evaluation

In this section, we discuss the simulation and experimental setup used to evaluate the performance of MANER for WMS applications.

7.3.1 Simulation set-up

We evaluated the performance of the proposed herd aware network protocol in **ONE** simulator [178], with movement models imported. We consider two mobility models: (i) the first is random way point (RWP) movement in which a mobile node moves in random trajectory. Naturally, animals do not just wander around randomly, they prefer to go somewhere for a purpose, often using the fastest path possible [13]. These destinations are driven by diverse reasons, ranging from ordinary points of interest (e.g. water, grazing, etc.) to a more distressing activity (e.g.

preying, running, etc.). (ii) we imported a second movement model from the ZebraNet GPS data to model the behavior of animal mobility [27]. The MAC/PHY layers are abstracted to transmission range and data rate in the ONE simulator. Since our proposed architecture considers BLE interface for short-range communication; all mobile nodes are set with a BLE radio at 250 kbps data rate with 200 m radio communication range.

TABLE 7.1: *Simulation parameters*

Grid area	1000mx1000m
Mobility model	RWP and ZebraNet
Simulation duration	15 hr
Data rate (DR)	BLE (250 kbps)
${T^+}_{BC}(sec.)$	$(25 \leq T_{mg} \leq 45)$
Tx range	BLE (200 m)
Number of nodes	70
Packet (PL)	31 bytes

Based on various animal species' empirically modeled data, it is known that the optimal average group or herd size is in the range of $(1 \leq n \leq 400)$ [179]. For instance, impala and zebra have a mean herd density of $(\leq 70/km^2)$ [180]. In both mobility models, we simulate a herd moving in a defined trajectory in a grid area of 1000mx1000m, which is practical area size to simulate the animal herd interaction. The network is set-up to run in a varying message generation rate (${T^+}_{BC}(sec.)$). The data replication number is set to $n^r = 13$ for optimal trade-off between latency and average reliability in our scenario, as reported in [158], which is in agreement with $n^r \approx 12.5$ (for $a = 5$ and $n = 400$ mobile nodes in Equation. 7.3).

The network is set-up to operate in a varying data generation rate (${T^+}_{BC}(sec.)$). The source nodes randomly generate data with 31 bytes payload at $(25 \leq {T^+}_{BC} \leq 45)$ for a relatively high data traffic, and $(400 \leq {T^+}_{BC} \leq 1500)$ for a relatively low data traffic settings. We remark that 31 bytes suffice for recording animal activity features (e.g. type and duration of activity), such as running, grazing, or walking. In this aspect, one of the influential network parameters is time-to-live (TTL) and it highly impacts network performance. Table 7.1 summarizes the simulation parameters set. We consider data to be generated from all AB nodes towards to an AS node initially located at the center of grid area, however, through time all nodes move based on the mobility trajectory model supplied. We recorded the packet generation time as well as the time when they are received at the sink node.

7.3.2 Benchmark opportunistic multi-hop protocols

The proposed network protocol is investigated under the following commonly used benchmark opportunistic multi-hop protocols to characterize their application for WMS applications [157, 158]:

- Direct delivery (DD), where a source node directly delivers its data to the destination node (s).
- Epidemic, it is modeled after the spreading of epidemic diseases, i.e. a source node spreads data through the entire network until it reaches she destination nodes.
- ProPHET, it estimates delivery predictability for each known destination at each node before forwarding a data. The estimation relies on the history of encounters between nodes.
- Spray and Wait (SnW), it imposes a maximum limit on the number of possible replications of a data.

7.4 Results and discussion

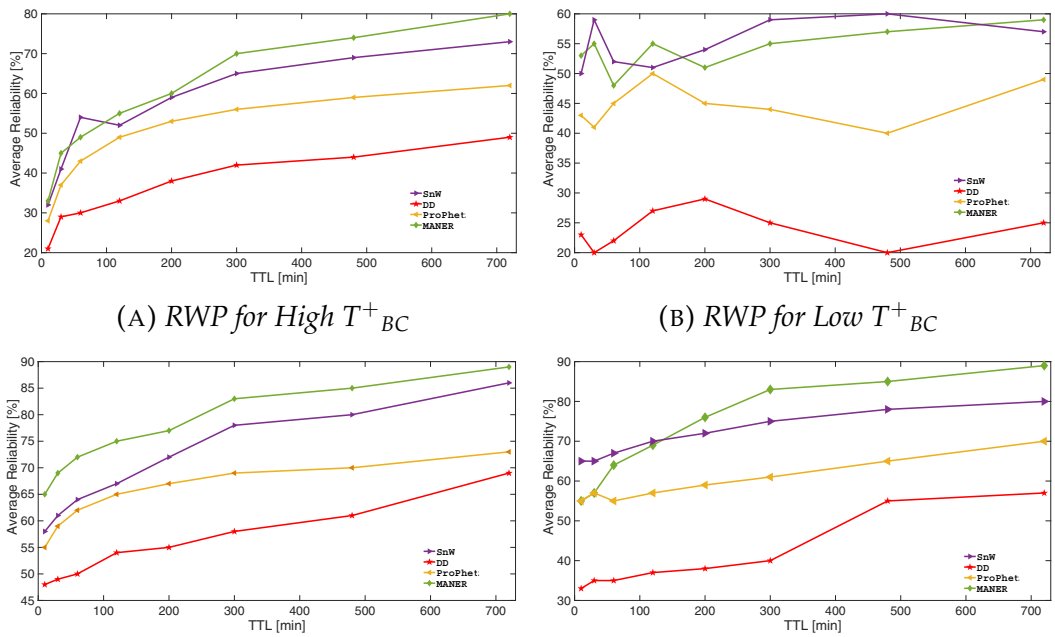

(A) *RWP for High* $T^{+}{}_{BC}$ (B) *RWP for Low* $T^{+}{}_{BC}$

(C) *ZebraNet for High* $T^{+}{}_{BC}$ (D) *ZebraNet for Low* $T^{+}{}_{BC}$

FIGURE 7.4: *Average reliability for RWP and ZebraNet mobility models*

In monitoring applications events are relayed with high priority. In this aspect, one of the influential network parameters is time-to-live (TTL) and it highly impacts network average reliability and latency. However, it is not thoroughly studied in previous works [157]. Figure 7.4 shows that, an increase in TTL of a data improved the trend of average reliability in both $T^{+}{}_{BC}$ cases for all the protocols. High TTL value is expected to increase the overall average reliability and vise versa [157].

In case of ZebraNet for higher TTL, MANER in particular, shows a relatively high average reliability compared to benchmark protocols. DD, PRoPHET and SnW show high average reliability with increasing TTL value, this is as expected, since for higher TTL, the chance of data reaching the intended destination would be higher.

For both RWP and ZebraNet mobility model, the average reliability plot shows a pronounced change when the $T^{+}{}_{BC}$ is high. This is mainly due to the inherent data replication properties of the routing protocols. MANER, SnW and PRoPHET are multi-copy, thus the number of duplicated data increases exponentially with higher TTL [157].

DD results in a lower average reliability due to the allowed one copy of data to be made, however, as can be seen from the latency plot, DD scores low latency (Fig. 7.5). The minimum observed average reliability for DD protocol is 20% and 45% respectively for RWP and ZebarNet mobility models at high $T^{+}{}_{BC}$. MANER showed a maximum average reliability of approximately 90%, this is because MANER leverages managed data replication to optimize the number of data duplication.

Overall, packet average reliability of MANER is at least 12.3% (for ZebraNet) and 16.3% (for RWP) higher than of that of benchmark protocols. Furthermore, one can see that increasing packet generation rate leads to decreased difference between the average reliability performance of all protocols. In general, since data is replicated to all nodes in a network, the overall storage requirements for probabilistic routing becomes high, reducing the routing performance. Therefore, MANER routing is more suitable for wildlife opportunistic sensing.

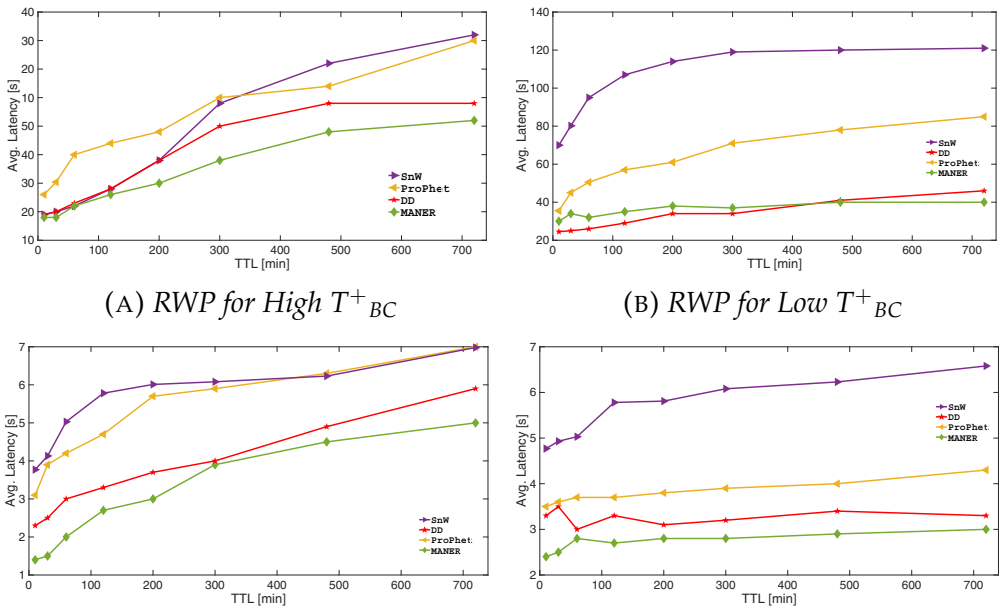

(A) *RWP for High* $T^{+}{}_{BC}$ (B) *RWP for Low* $T^{+}{}_{BC}$

(C) *ZebraNet for High* $T^{+}{}_{BC}$ (D) *ZebraNet for Low* $T^{+}{}_{BC}$

FIGURE 7.5: *Average latency for RWP and ZebraNet mobility models*

Moreover, data average latency is lower for MANER, when compared to other protocols. Figure 7.5 shows the latency against TTL for both mobility models with $T^{+}{}_{BC}$. Generally, the plot depicts that as the data TTL increases the overall message latency shows an increasing trend, this is in accordance with previous works [157]. However, MANER shows shortest average delay of ≈17s and ≈1.5s respectively for ZebarNet and RWP mobility models. Overall SnW and PRoPHET have relatively higher average latency as shown in Figure. 7.5. This is due to the replication of data based on probability of contact, resulting in unnecessary flooding of data through

out the entire network without optimization. ZebraNet model shows shorter average latency than RWP, supporting the hypothesis that opportunistic networks are applicable to wild life monitoring scenarios (Figure. 7.5). Overall, the average latency is decreased by up-to 65% when MANER is used.

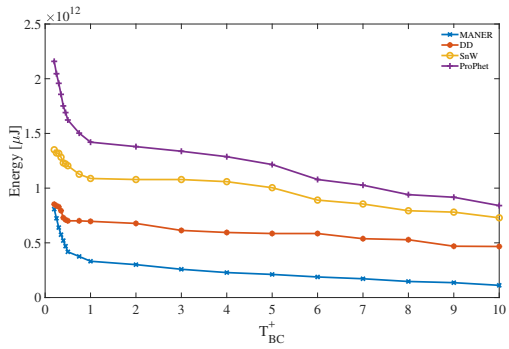

(A) *ZebraNet*

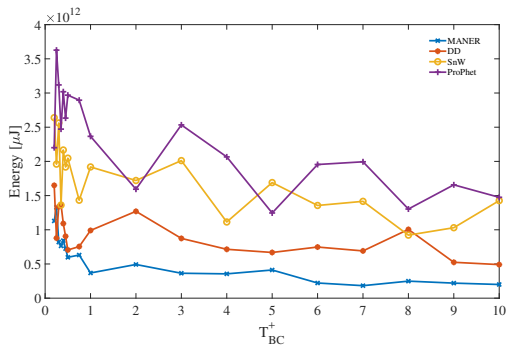

(B) *RWP*

FIGURE 7.6: *Average average energy consumption*

Figure 7.6 shows that an increase in $T^{+}{}_{BC}$ increases the trend of average energy consumption in both mobility models. Longer $T^{+}{}_{BC}$ interval is expected to increase the overall energy consumption as reported in [157]. The benchmark protocols in particular, showed a relatively high average energy in case of ZebraNet for the specified range of $T^{+}{}_{BC}$. In general, DD, PRoPHET and SnW show a trend of decreasing average energy with $T^{+}{}_{BC}$ value. This is as expected, since for higher $T^{+}{}_{BC}$ the AB nodes send data less frequently, resulting in lower energy consumption. For both RWP and ZebraNET mobility pattern, the average energy plot indicates a higher energy for SnW and ProPhet compared to MANER when the $T^{+}{}_{BC}$ is high. This is mainly attributed to inherent data replication properties associated with routing protocols. In particular, SnW and PRoPHET are multi-copy, thus the number of duplicated data increases exponentially with higher $T^{+}{}_{BC}$ [157].

7.5 Conclusion

In this chapter, we presented, MANER, an opportunistic multi-hopping protocol for wildlife monitoring. This approach facilitates optimal data communication between

sensor devices to be used for wildlife monitoring. In MANER, a node solely makes its decision for data forwarding based on local observations. In practice, it is near impossible, to determine a dissemination protocol for mobile network of wildlife monitoring systems. However, when subjected to diverse mobility patterns and traffic generation rate, MANER protocol showed an improved performance than existing protocols. The evaluation results showed that the proposed protocol outperforms the traditional algorithms. On average, our approach reduced the average latency by up-to 65%. In addition the architecture improved network delivery ratio by up-to 16% for various packet traffic rates in the network.

Chapter 8

Animal Spatial Social Network Analysis

In ecology and wildlife conservation, animal spatial social network analysis (ASSNA) is used for investigating the social interaction among animals in their natural habitat. Such analysis helps determine how animal population density changes according to certain environmental disturbances and how the animals react to each other and to their environment. These changes are often considered as early warning signs for animal population fragmentation, which will influence the animal encounter rates, such as mate choice and anti-predatory behaviour. Hence, biologists and ecologists, in particular, highly benefit from ASSNA by analyzing animals proximity and their close interaction to study animals behavioural patterns. Existing ASSNA solutions often record social interaction measurements either using GPS or proximity sensors through bio-logging or bio-telemetry techniques. However, nowadays most off-the-shelf animal monitoring/tracking tags have built-in wireless modules such as BLE, which is known for its low energy consumption compared to the power hungry GPS module. The aim of this chapter is to investigate the utilization of BLE radios for relative ranging as an alternative solution to the existing application of GPS for ASSNA. The potential of BLE radio and its performance in the context of ASSNA is explored using a simulation tool based on path-loss model and various graph theory and social network analysis metrics. The evaluation outcomes show that BLE radios are comparable solutions to GPS based solutions. In addition, in this chapter, the application of opportunistic BLE network is demonstrated for inferring the movement patterns of wild-animals.

[26] *H. Coen, Inferring animal social interaction using proximity based on BLE and LoRa, Essay (Master), EEMCS: Electrical Engineering, Mathematics and Computer Science, August 2018.*
[Under review] *E. D. Ayele and H. Coen and N. Meratnia and P. J. M. Havinga, Animal Spatial Social Network Analysis Through Utilizing BLE, ACM Transactions on Internet of Things (TIOT), 2019.*

8.1 Introduction

The application of social network analysis techniques to study the social contact and interaction among animals are well researched in [181, 182]. In general, animal spatial social network analysis (ASSNA) can help ecologists understand social and ecological interactions among animals. Existing ASSNA research mainly focus on inter-herd analyses of: (i) social structures, (ii) causes and consequences of the different behaviour of individual animals, (iii) social processes, e.g. for information or disease spreading, and (iv) relationship between environment and social network structure [182].

Applications of ASSNA in wild-life conservation will provide an understanding and detection of the overall changes in animal social interaction [181]. One in five mammal species is threatened with extinction, due to not only poaching but also other causes such as deforestation, habitat changes, or decreasing territory size [183, 184]. Hence, in wildlife conservation, ASSNA can be used to quantify social structures in a group of animals, helping to predict how animal population will respond to certain environmental disturbances that could cause a population to fragment or crash.

For instance, drastic change of spatial proximity (connectivity) among individual animals could be caused by habitat fragmentation, which in-turn influences encounter rates and will likely influence animal social interaction, e.g. mate selections and anti-predatory behaviour. Consequently, all of these can influence the fitness of individual animals [181]. Monitoring and learning these social structures can help in planning solutions related to the herds' health problems, for example, by identifying which animals should be strategically vaccinated to stop the fast spreading of diseases or to see what happens when a group of animals is relocated to a new location [181].

In ASSNA, proximity data is often collected by utilizing GPS bio-logging and/or occupancy sensors with ultra-high-frequency (UHF) transceivers to register when animals are in proximity of each other. However, conventional power hungry GPS units regularly need to download and configure satellite data, and relay it (e.g. through a GSM network) to a central system before the animal location can be derived, resulting in high energy consumption compared to low power radio based solutions (e.g. Bluetooth Low Energy (BLE) technology) [185].

Moreover, existing animal tracking or monitoring tags on the market are often already embedded with a built-in BLE radio module. Biologists often recommend to use sensor tags smaller than 5% of the body weight of the animal, in order to minimize its effect on the survival and living behaviour of the animal [37]. Thus utilizing BLE radio module, that already exist on the tags and currently only used for wireless communication, as alternative solutions for GPS location data, eliminates the need for additional hardware, resulting in a smaller overall tag size and lower power consumption.

The rest of this chapter is structured as follows: Section 8.2 details the methodology and simulation tool models used for investigating the utilization of BLE radio

for proximity estimation in a temporally stationary movement model. Section 8.3 further discuses the potential application of BLE network architecture for animal movement pattern identification. Section 8.4 concludes this research work.

8.2 Leveraging BLE for spacial proximity estimation

The main aim of this section is to investigate the application of BLE for relative ranging as an alternative solution for GPS data to infer information about the social interaction of animals. Moreover, we performed animal social interaction analysis through simulation.The challenge here relates to the difficulty in using radio signal strength for distance estimation. Due to phenomena like path-loss, reflection and scattering, the received signal strength is not a precise rendition of the true distance between the radios, but rather a rough estimation.

8.2.1 Methodology and implementation

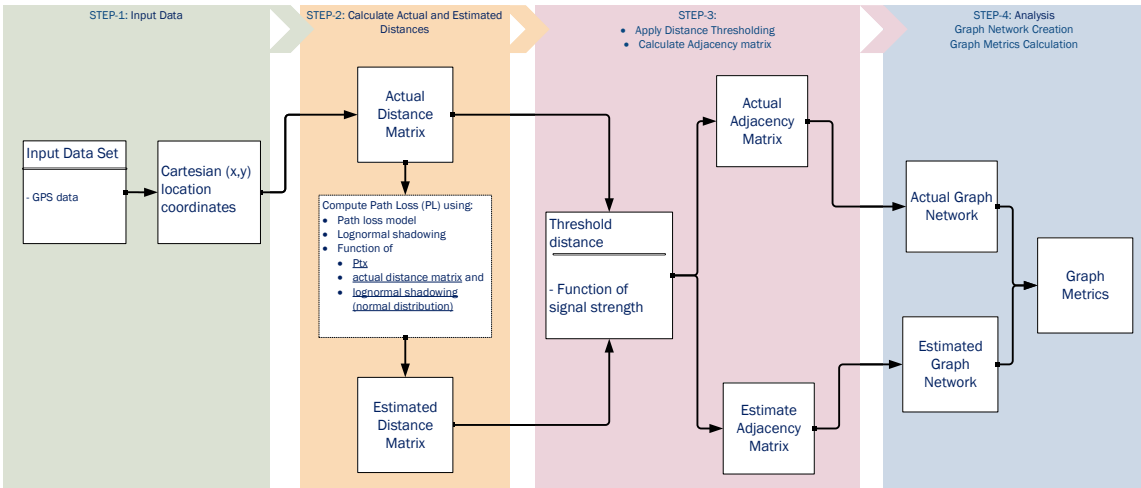

FIGURE 8.1: *Overview of the various steps involved in the ASSNA approach*

In this section, we present our approach in evaluating applicability of BLE for proximity information to analyze animal spatial social network.

Figure 8.1 shows the steps taken in our approach, which are also directly implemented in our simulation tool developed in Matlab (See Appendix A and B). We perform the following step-by-step activities:

1. The raw input data, the actual animal's GPS data is used from the ZebraNet project, where actual GPS data is collected from collared Zebras [160]. We adopted the supplementary Python script [160] provided by the ZebraNet project, to convert these GPS data to (x,y) coordinates to be used in our Matlab simulation tool.

2. Both the actual and estimated distances are computed for all animals. The euclidean distance is derived using the (x,y) coordinates for all possible animal node pairs per time-frame and stored in an *actual distance matrix* variable. The *actual distance matrices* are calculated for two purposes. First, they will be used in the next step to check if the nodes are within the range of each other. Second, they are used for finding the *estimated distances* between nodes and logged in an *estimated distance matrix* variable. The *estimated distance matrix* is calculated based on the actual distances by utilizing the path-loss models in combination with the log-normal shadowing, as described in Section 6.2.3, Equation 4.9 [145].
3. The *actual distance* and the *estimated distance* matrices are used to generate the *actual adjacency matrix*, and *estimated adjacency matrix* respectively, by applying a simple distance thresholding technique (i.e. the critical distance using the theoretical maximum radio coverage of BLE, Equation. 4.9). If the distance between the nodes is shorter than the critical distance, then animals are assumed to be in range of each other, hence, the graph edge would be represented by a '1' in the corresponding adjacency matrix. Otherwise it would be '0'. The *actual adjacency matrix* and the *estimated adjacency matrix* are in-turn used to create the *actual graph network* and *estimated graph network*, respectively.
4. From the distance matrix we generate the (x,y)-coordinate using *mdscal* function that will transform the distance matrix to a relative cartesian coordinates by performing a multidimensional scaling and returns a configuration points [186].
5. Finally the animal social network indicators, as presented in the following section, are computed and compared for both the actual and the estimated graphs.

8.2.2 Animal social network indicators

Animal social network analysis is currently carried out based on range and proximity information derived from GPS or proximity sensors. The range and proximity information is then used to calculate animal social interaction indicators, such as *betweenness centrality, density, number of communities, number of components* and *node degree* based on graph theory concepts [32, 181](See Appendix A). Thus, since the graph theory concepts and animal social network indicators are essential for our methodology, in what follows we explain them.

Graph theory based metrics

The graph theory is in the heart of social network analysis. A graph basically consists of vertices (also called nodes) (V) and edges (E) connecting those vertices. A graph G contains the sets (V,E) with the vertices labelled as V = v_1,...,v_n, and the pair of edges labelled as E = (v_1,v_n), often also labelled as E = e_1,...,e_m,. A graph is also represented by an adjacency matrix, consisting of a $|V|X|V|$ matrix $A = (a_{ij})$, where a_{ij} = 1 if $(i, j) \in E$, otherwise $a_{ij} = 0$ [187].

An important feature in animal social network analysis is the animal social connectivity, which covers the fragmentation and distribution of animals population in their habitat. A problem is that there is no exact definition of habitat connectivity, since it can be measured at a patch or landscape scale and can be structurally or functionally defined [181]. Graph theory provides a solution to this problem by providing a framework to quantify connectivity and flow in social networks [188].

Some important indicators used for graphs in the context of social network analysis are explained hereafter.

- *Node degree* is the number of edges connecting to a node [187]. For example, node A and B in Figure 8.2, both have a degree of four, since there are four edges connecting to those nodes. In ASSNA, node degree is used to identify nodes with more connections to other nodes to model, for instance, disease spreading. The higher the degree, the more connections the node has.

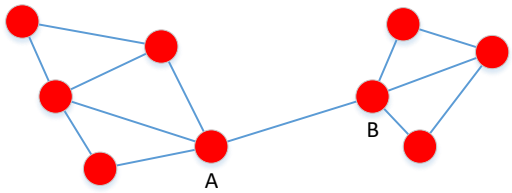

FIGURE 8.2: *Example a graph network*

- *Network density* of a graph is defined by the number of edges in a network divided by the total possible edges or in case of a weighted graph, the sum of edge weights divided by the number of possible edges [182].

$$D = \frac{2E}{V(V-1)} \tag{8.1}$$

  The density calculation for an undirected graph is shown in Equation 8.1, where E is the number of edges and V the number of vertices in the graph. The maximum density is 1 for a fully connected graph and the minimum density is 0 for an unconnected graph [189]. In ASSNA, network density is used for the analysis of movement patterns, e.g. the connectivity in a herd of animals [190].

- *Betweenness centrality* is a measure of the importance of a node in a graph indicating the flow-potential of information or diseases dissemination in the context of ASSNA [181]. It shows the number of shortest paths between all possible pairs of nodes in the graph that traverse the node. An example is shown in Figure 8.2, the edge between nodes A and B has the highest betweenness in this graph because it connects the left community with the community on the right. Thus all the links connecting the nodes in the left community with those in the right community pass through the edge between A and B, resulting in a high betweenness value for nodes A and B [191]. Nodes with a high betweenness are likely to connect largely independent communities [182].

- *Number of communities* represents number of densely connected nodes in a graph. In the context of animal social network analysis, it indicates inter-herd movement strategies [32].
- *Number of components* is used to measure the number of groups in a graph with at least more than one node, with no connections to other nodes. In the context of ASSNA, it is an indication of fragmentation in the animal population.
- *Number of isolated nodes* is the number of nodes that are completely isolated from the rest by checking the node degree. If the degree of a node is 0, the node is completely disconnected or isolated [187].
- *Isomorphism* is used to check if two graphs are the same. The graphs G and G′ are isomorphic if the vertices of G can be relabelled to to be vertices of G′, while maintaining the same edges in G and G′ [187].

An overview of the above-mentioned indicators and their application to ASSNA is provided in Table 8.1.

TABLE 8.1: *Animal social network indicators*

Metrics	Purpose	Indications	Ref.
Node degree	Measures the number of edges connected to a node	e.g. insight in disease spreading	[32]
Network density	Measures the number of connections	Connectivity in a network	[32] [181]
Betweenness centrality	Indication for flow potential (e.g. of information/diseases) in a network	The importance of individuals in a network	[32] [181]
Number of communities	Measures the number of communities and their membership in a population	Strength of social integration inside the population	[32] [181]
Number of components	Measures the number of communities in a network that are entirely disconnected	An indication of population fragmentation	[181]
Number of Isolated nodes	check if a node is completely disconnected	Indicates animal separation from its herd	[181]
Isomorphism	To check if two graphs are the same	An indication of population similarity	[181]

Supplementary indicators

In this paper, we also use a supplementary statistical measures, such as *normalized mutual information (NMI)*, *mean absolute deviation (MAD)*, *off-set*, and *same node score* in-order to evaluate the potential of BLE for community detection and animal social network analysis. In what follows we provide what each of these measures represents.

- *Normalized mutual information (NMI)* is used to evaluate whether the communities found in the estimated graph are the same as in the actual graph. The mutual information $I(X : Y)$ is defined in Equation 8.2, where $H(X|Y)$ and

$H(Y|X)$ represent the non-mutual information (or variation of information), $H(X)$ is the information in X where $H(Y)$ is the information in Y [192]. The authors in [193], use the concept of NMI to evaluate community structures using Equation 8.3. The algorithm creates a confusion matrix N, with rows corresponding to real communities the columns corresponding to the found communities. Matrix N_{ij} represents the nodes in the actual community i that are present in the estimated community j.

$$I(X:Y) = \frac{1}{2}[H(X) - H(X|Y) + H(Y) + H(Y|X)] \tag{8.2}$$

$$I(A,B) = \frac{-2\sum_{i=1}^{c_A}\sum_{j=1}^{c_B} N_{ij} log(N_{ij}N/N_iN_j)}{\sum_{i=1}^{c_A} N_i log(N_i/N) + \sum_{j=1}^{c_B} N_j log(N_j/N)} \tag{8.3}$$

c_A is the number of communities in graph A, and c_B is the number of communities in graph B. N_i is the sum over row i of matrix N_{ij} and N_j is the sum over column j of the matrix. *I(A,B)* is 1 when the two partitions (i.e. the actual and estimated communities) are identical to each other. When both partitions are totally independent of each other, *I(A,B)* equals 0 [193].

- *Mean absolute deviation (MAD)* is the average distance between each data point in the set and the mean, giving an idea of the variability. The MAD value is calculated by finding the mean of the data set, then calculating the absolute deviation (the absolute distance to the mean) of each data-point, summing the deviations and dividing them by the number of data-points, as shown in Equation 8.4.

$$MAD = \frac{\sum |x_i - \bar{x}|}{n} \tag{8.4}$$

- *Offset Value* is the difference between values of a node in one graph and its corresponding value in a second graph per time-frame, defined as ($Offset = (Value)_1 - (Value)_2$). This parameter shows the comparison value between actual and estimated data, providing insight into closeness values of two nodes. A high positive or negative value indicates high deviation between two values.

- *Same node score* indicates how many of the nodes are the same in both actual and estimated graphs. For example, let us assume that nodes with a high betweenness in the actual graph are node 1, 2 and 3 and the nodes with a high betweenness in the estimated graph are nodes 3, 4 and 5. This means that there is one overlapping node (node 3), so the node score is (1/3 = 0.33). Hence, the same node score is equal to the ratio of the number of overlapping nodes (with the same node number) and the number of nodes with high betweenness in the actual graph.

- *Energy consumption* indicates how much energy is consumed in each type of radio technology used. For the energy analysis model, the network graph

is assumed to have n nodes and are complete (fully connected) undirected graph, in which every pair of distinct nodes are connected by a unique radio link. This kind of graph topologies are useful to investigate the maximum energy consumed. Therefore, the total network energy overhead with periodic transmission (E_{BLE}) in each link is given by:

$$E_{BLE} = \lceil t/IPI \rceil \times E \times (n \times (n-1)) \tag{8.5}$$

, where t is total simulation duration, IPI inter-packet interval in seconds, (t/IPI) and $t/(IPI + T_{offsubBand})$ are the total number of packets sent in BLE case. E is the energy per packet for BLE radio as expressed in Equation. 4.1.

8.2.3 Simulation setup

For simulation and anlaysis, we adopted the mobility model from the ZebraNet GPS data set to emulate animal behaviour [27] The generated data set includes 8000 time-frames. Every time-frame includes the (x,y) location coordinates of 50 nodes, representing 50 animals. The simulation uses this data to calculate the *actual distance* among individual nodes, i.e. formally the euclidean distance. This is procedure is repeated across all time-frames. Tables 8.2 shows the input simulation parameters used. It includes the parameters for the path-loss models used. The communication covers a disk area with radius limited by the receiver sensitivity, $BLEP_{sen}$ and received signal power ($P_{Rx}(d)$). To demonstrate the utilization of BLE radio, we selected two extreme radio communication range of BLE at near and far (critical) distances (see Figure 8.3).

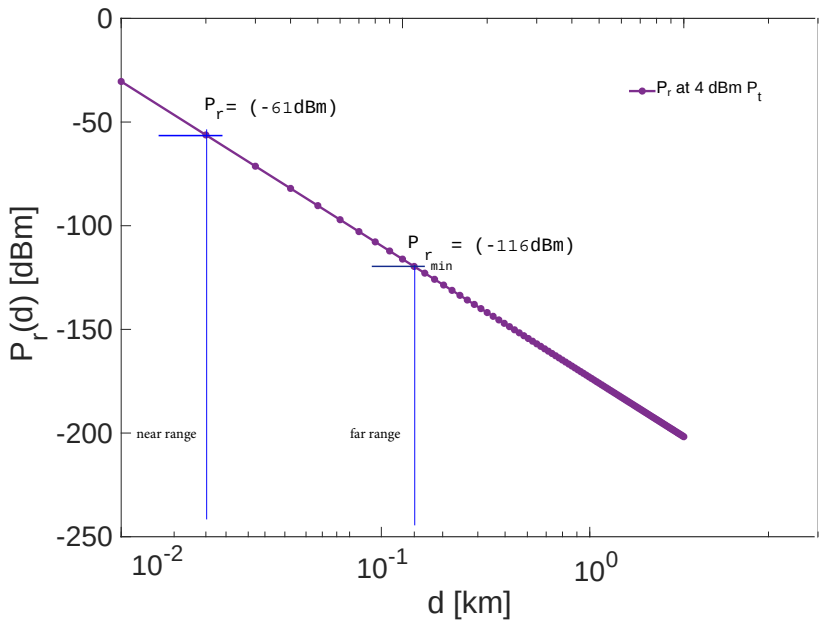

FIGURE 8.3: *Received power ($P_{Rx}(d)$) values are based on simplified path loss model with log-normal shadowing for BLE radio, indicating the near ($\leq$ 20m) and far (critical) ($\leq$ 200m) region of the radio communication range (d).*

TABLE 8.2: *Simulation input parameters*

P_t	4 dBm
$BLEP_{sen}$	-116 dBm
γ	2.7
d_0	1 m
$\sigma_{\psi_{dB}}$	3.65
$f_{c,BLE}$	2.4 GHz
h_t	50m
h_r	2m
C_m	0

8.2.4 Results and discussion

Following our approach outlined in Section 8.2.1, we calculated the *betweenness centrality, density, number of communities, number of components* and *node degree*, for both the actual graph (i.e. based on Zebranet GPS data) and estimated graph (i.e. based on BLE). In what follows we present and discuss the simulation results.

Betweenness

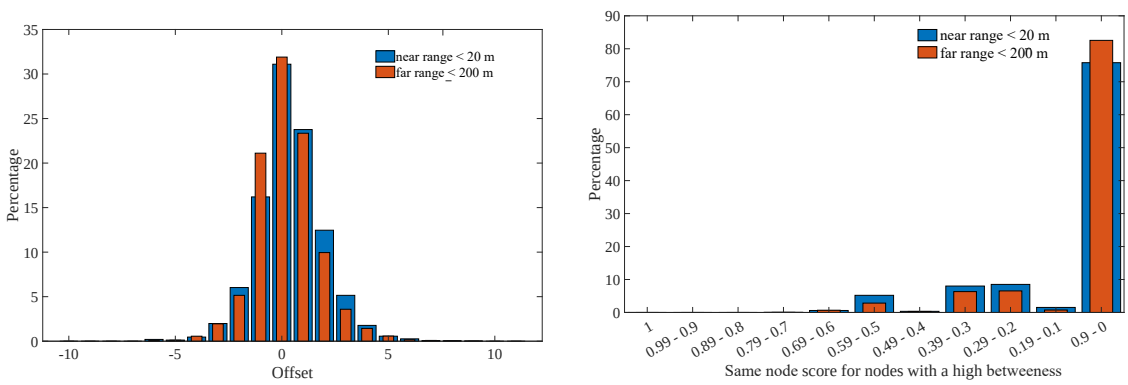

(A) (B)

FIGURE 8.4: *Offset and similarity score comparison for betweeness of the actual and estimated graphs, (a) Offset of the number of nodes with high betweenness, (b) same node score for nodes with high betweeness*

Figure 8.4a shows the offset comparison of nodes with high betweenness for the actual and estimated graphs. It shows that the betweeness offset is almost the same for most of the time-frames (i.e. 31.9% and 32.5% for near and far BLE range respectively). There are almost no common node with high betweenness in both graphs. As it can be seen in Figure 8.4b, 82.6% and 75.8% of the nodes showing almost no similarity (i.e. 0 to 0.9 score) in near and far BLE range respectively.

Generally, one may note that BLE is a better indicator of betweenness. Both BLE ranges are able to identify the relative number of nodes with a high betweenness because the '0', '-1' and '+1' offset values are quite close to each other (Figure 8.4a).

The estimation of the betweeness is influenced by the radio transmission channel environment. If two animals are either at the border or out of the radio communication range, they may be incorrectly identified as being in range, thus influencing the betweenness calculation.

Node degree

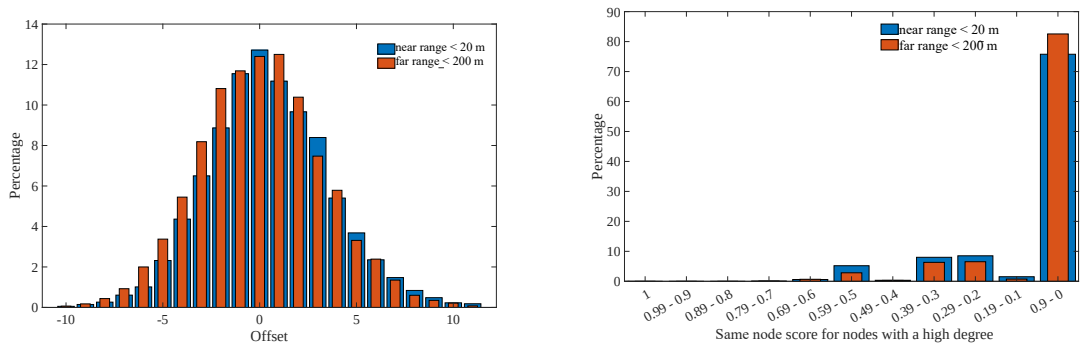

(A) (B)

FIGURE 8.5: *Offset and similarity score comparison for node degree of the actual and estimated graphs: (a) Offset of the number of nodes with high degree, (b) Same node score*

Figure 8.5a shows the offset comparison between the actual and estimated graph, showing that offset values of '0', '-1' '+1', represent over 10% of the total distribution and these offsets are likely to differ between the actual and estimated graphs. Figure 8.5b shows the overlapping same node scores for the above average degree and high degree nodes. In most cases, less than 50% of the nodes in the estimated graph show overlap with the actual graph. This means that the node degree is very hard to be determined using near or far BLE range.

This is mainly due to the wireless environment causing a path-loss and shadowing phenomena. If nodes are either at the border or out of the communication range, it is possible that nodes can receive their broadcast data. If all animals are close to each other, the node degree is easier to be determined. This is because shadowing and path-loss have a higher influence when the transmission range is larger.

Network density

tno Figure 8.6 shows the density offset between the actual and estimated density of different time-frames. In most time-frames the offset is between [-0.001,-0.0019] (i.e. 46.6% and 50.4% for near and far distance BLE radio respectively), followed by [-0.02,-0.029] (37.8% and 32.6% for near and far BLE range radio respectively). For near BLE range, the average density in the actual graphs is 0.1125 with MAD of 0.0058, and in the estimated graphs is 0.1245 with MAD of 0.0065. For far BLE range, the average density in the actual graphs is 0.0957 with MAD of 0.0081, and in the estimated graphs is 0.1134 with MAD of 0.0091.

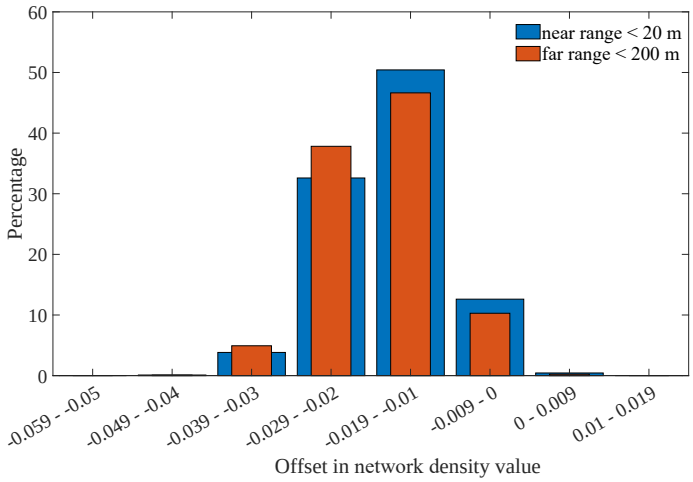

FIGURE 8.6: *Comparing network density offset for the actual and estimated graphs*

Since network density is measured in a value between 0 and 1 and the measured difference between the actual and estimated density values is small, the results are considered to be good. Thus both near and far BLE ranges are applicable for calculating the graph density, with far range BLE performing better than near distance BLE. It should be noted that the estimated network density value is higher than the actual network density.

Number of isolated nodes

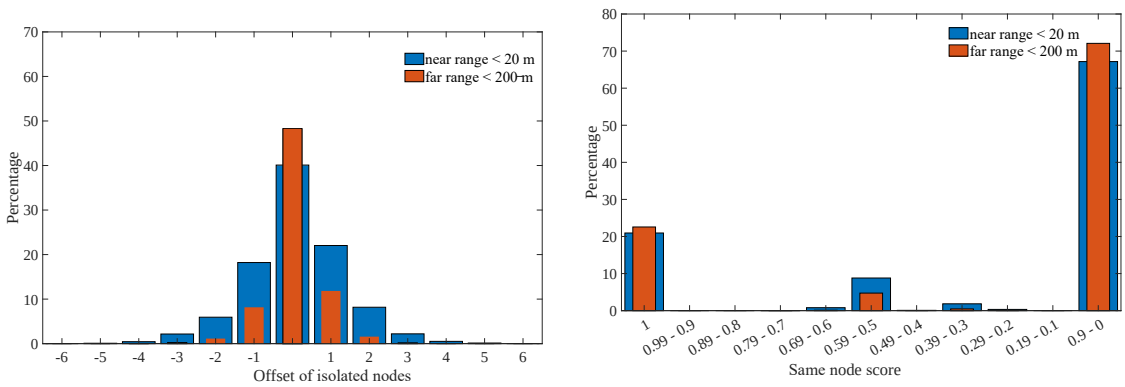

(A) (B)

FIGURE 8.7: *Comparing number of detected isolated nodes in the actual and estimated graphs: (a) Offset, (b) Same node score*

Figure 8.7a illustrates the offset of number of isolated nodes observed in the actual and estimated graphs. It can be seen that the number of isolated nodes in both graphs is over 65% and 40% for near and far ranges BLE radio respectively. In over 11.4% of the time-frames, the offset is less than one isolated node for near range BLE radio. The same node score value is '0' in 72.1% and 67.2% for near and far range, respectively. Figure 8.7b shows the same node score for the isolated nodes. It shows

that the time-frames with similarity score of '1' is greater than 20% for both near and far range BLE radio. The same node score is '0' in 72.1% and 67.2% for BLE radio. There is at least one isolated node in the estimated graph, while there is no isolated node in the actual graph in 12% of the time-frames and no isolated nodes in both graphs in 57.2% for near and far ranges.

This means that near distance BLE performs better interms of isolated nodes, especially, for identifying correct number of isolated nodes. It should be taken into account that there is a possibility that both BLE ranges used can miss or falsely identify a link between nodes, resulting in a node appearing to be disconnected. One reason for this is that even-though two animals are within the theoretical radio range, BLE signal between pair of nodes is not detected due to, for example, trees blocking the signal. On the other hand, the signal can be transmitted further than expected due to reflections, leading to the situation that, even though a node is in reality isolated, other nodes are still able to receive the broadcast of the isolated nodes. Both BLE ranges seem to be suitable for the detection of nodes in a network, but it is often hard to identify the isolated node.

Number of components

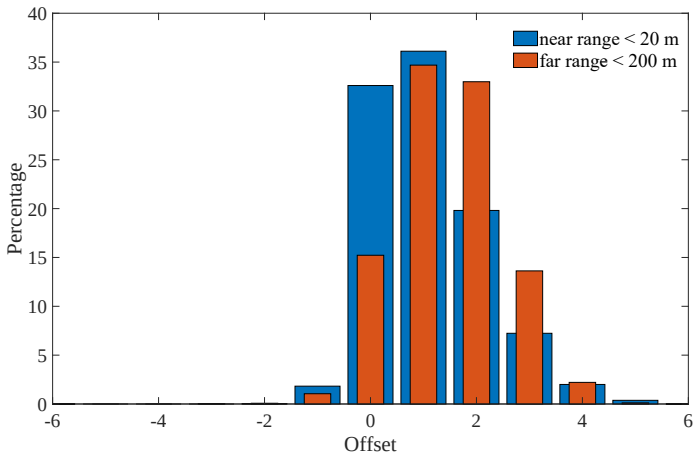

FIGURE 8.8: *Comparing Offset values of the number of detected components for the actual and estimated graphs*

As shown in Figure 8.8, the number of detected components indicates that 15.2% of the time-frames have an offset of '0'. An offset of '+1' and '+2' have occurred in 34.7% and 33% of the time-frames, respectively for far range BLE radio. An offset of '+3' and '+4' is seen in 13.6% and 2.2% respectively for far range. While this was 36.1% and 19.8% for near range BLE radio. Again it can be concluded that far range BLE performs better in terms of number of detected components, however, it shows a large offset. This is because BLE wrongly identifies important links among nodes, resulting in more components in the estimated graph than in the actual graph. The cause for this is that some animals are out of range of the theoretical distance and due to the signal blockage and/or path loss, this results in missing actual links between group of animals.

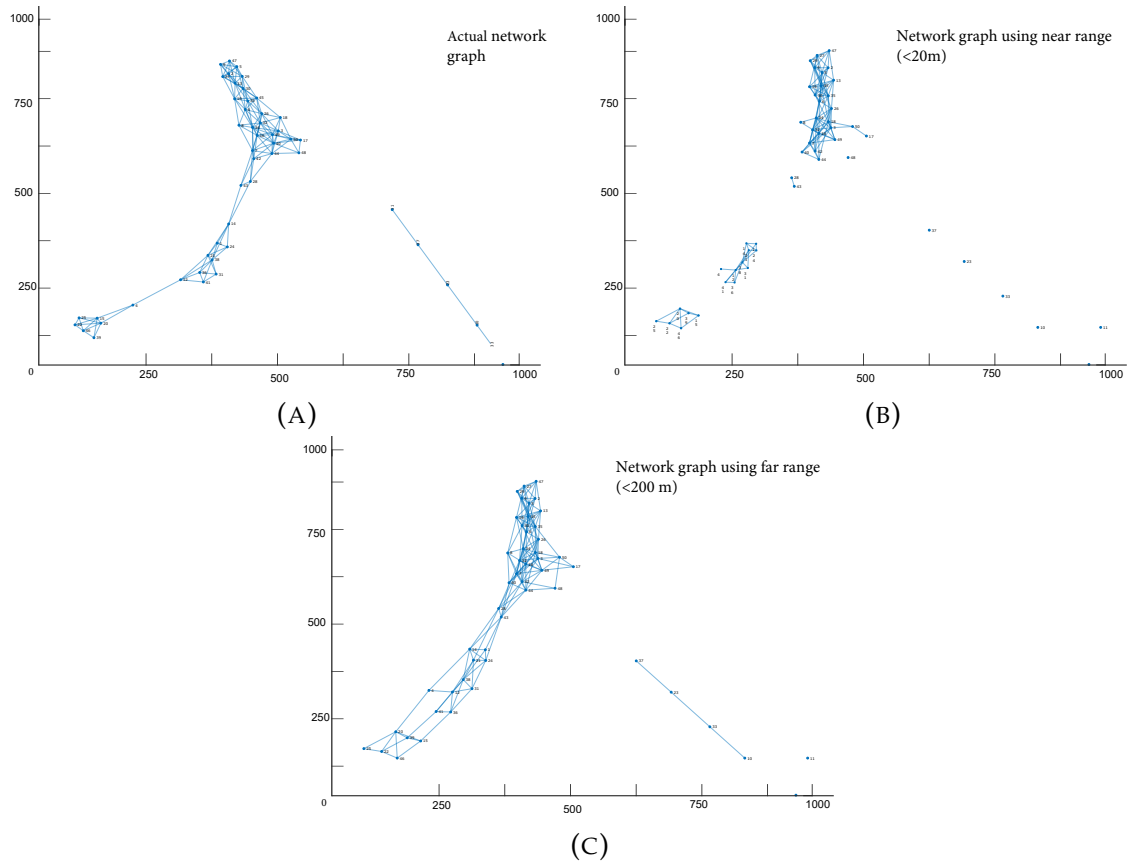

FIGURE 8.9: *Comparing number of detected components in (a) actual graph, (b) estimated graph based on near range, and (c) estimated graph based on far range for one sample time-frame*

Since number of detected component metric is used to give an insight into the fragmentation of a network, thus near range BLE is suitable only when it is taken into account that the actual number is lower than the detected number of isolated components and this only gives an estimation.

Figure 8.9 shows the actual and estimated graphs for one time frame. Note that the nodes are displayed in a random manner, ignoring their actual coordinates. The number of components detected is two for the actual and far range BLE graph, but three components are detected using near range BLE graph. However, the near range estimated graph also includes more than one disconnected node, which is not considered as a component, thus both graphs contain three components.

Number of communities

Figure 8.10 depicts the NMI values for number of communities. The results show that the average NMI value is 0.8846 and 0.8324 for near and far BLE range respectively. Majority of the entries (i.e 51.5% for near range, and 49.8% for far range) score an NMI value between 0.80 and 0.89 for near and far BLE ranges respectively. For near BLE range, 9.28% of the entries score the maximum NMI value of 1, for near BLE range this is 5.52%. A score between 0.90 and 0.99 is obtained in 29.76% and

9.88% of the time-frames for near and far BLE ranges respectively. Finally, 9.44% (near range) obtained a score between 0.70 and 0.79, as can be seen in Figure 8.10.

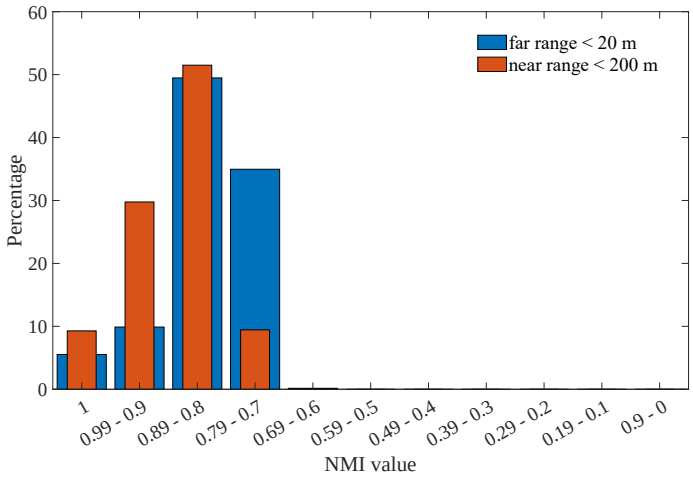

FIGURE 8.10: *Comparing the NMI values for the number of detected communities between the actual and estimated graphs*

The results show that near distance BLE is more suitable for detecting the number of communities. This can be explained by the same reasoning for the other metrics. Both techniques miss important links or edges among nodes due to shadowing and path-loss phenomena. Especially, far distance BLE suffers from shadowing and path loss because of the larger link distances among nodes. However, both ranges show quite good results and seem to be useful for the estimation of community structures. Information about the exact community structure is not likely to be achieved.

We further elucidate, the performance of community detection algorithm combined with NMI, by discussing detecting the number of communities in two different sample time-frames (i.e. time frame-1 and time frame-2). In the first example comparing the actual communities (inferred from the actual graph) and estimated communities (inferred from the estimated graph) with an NMI of 1. The actual and estimated communities are detected in the same time-frame. In the second example, the actual and estimated communities have an NMI value of 0.95. Again, the actual and the estimated communities were found in the same time-frame.

Figure 8.11 shows the communities detected in time-frame-1 for the actual and the estimated graphs. It should be noted that the node locations in the graph do not represent the actual locations. Calculating the NMI gives a value of 1 for the two communities detected, which indicates that both communities are similar. Figure 8.12 shows the communities detected for time-frame-2 for the actual and the estimated graphs. Calculating the NMI for the two communities gives a value of 0.95, which indicates that both communities are almost similar, but not completely the same. For instance, node 26 is a member of community 2 in the actual graph, but it is found in community 3 in the estimated graph.

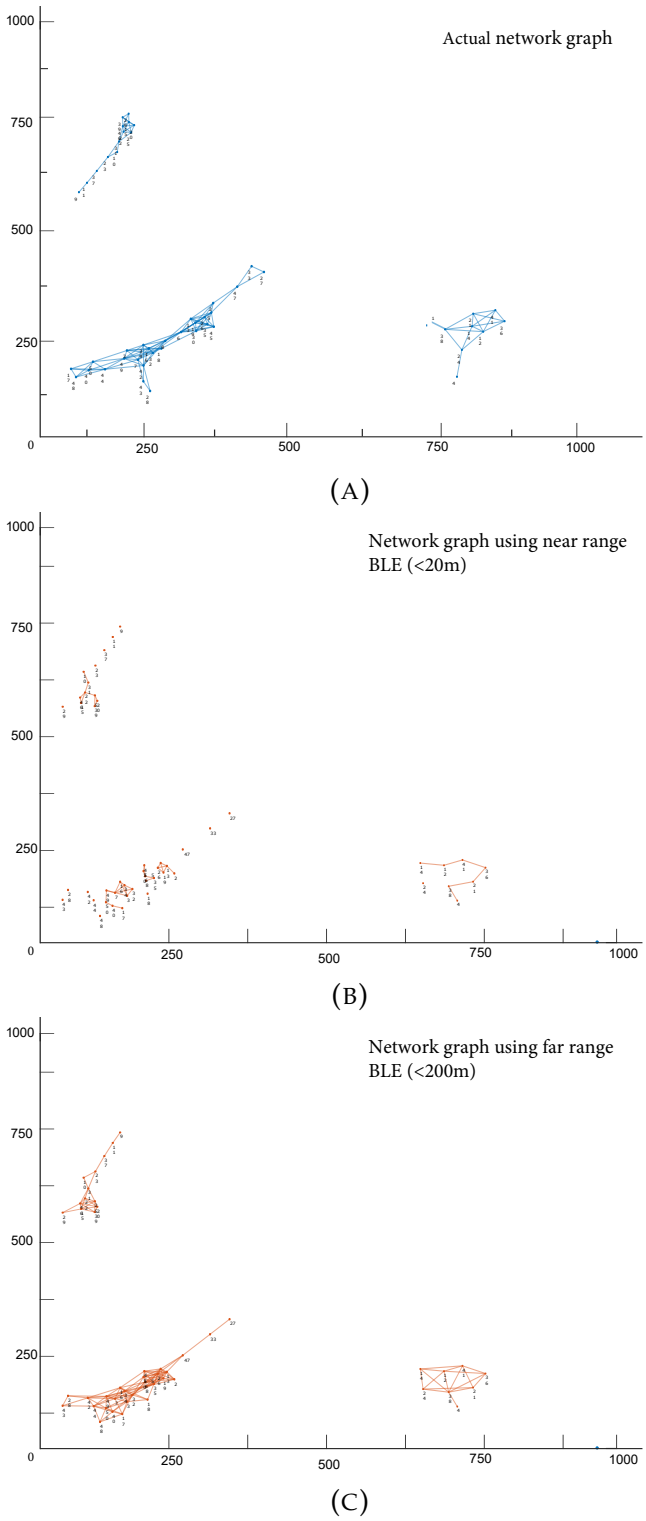

FIGURE 8.11: *Time frame-1: number of detected communities in the (a) actual graph, (b) estimated graph (based on near range), and (c) estimated graphs (based on far range)*

Isomorphishm

None of the graphs displayed isomorphic behaviour, indicating that there is no time-frame in which the actual graph and the estimated graph are exactly the same. Since

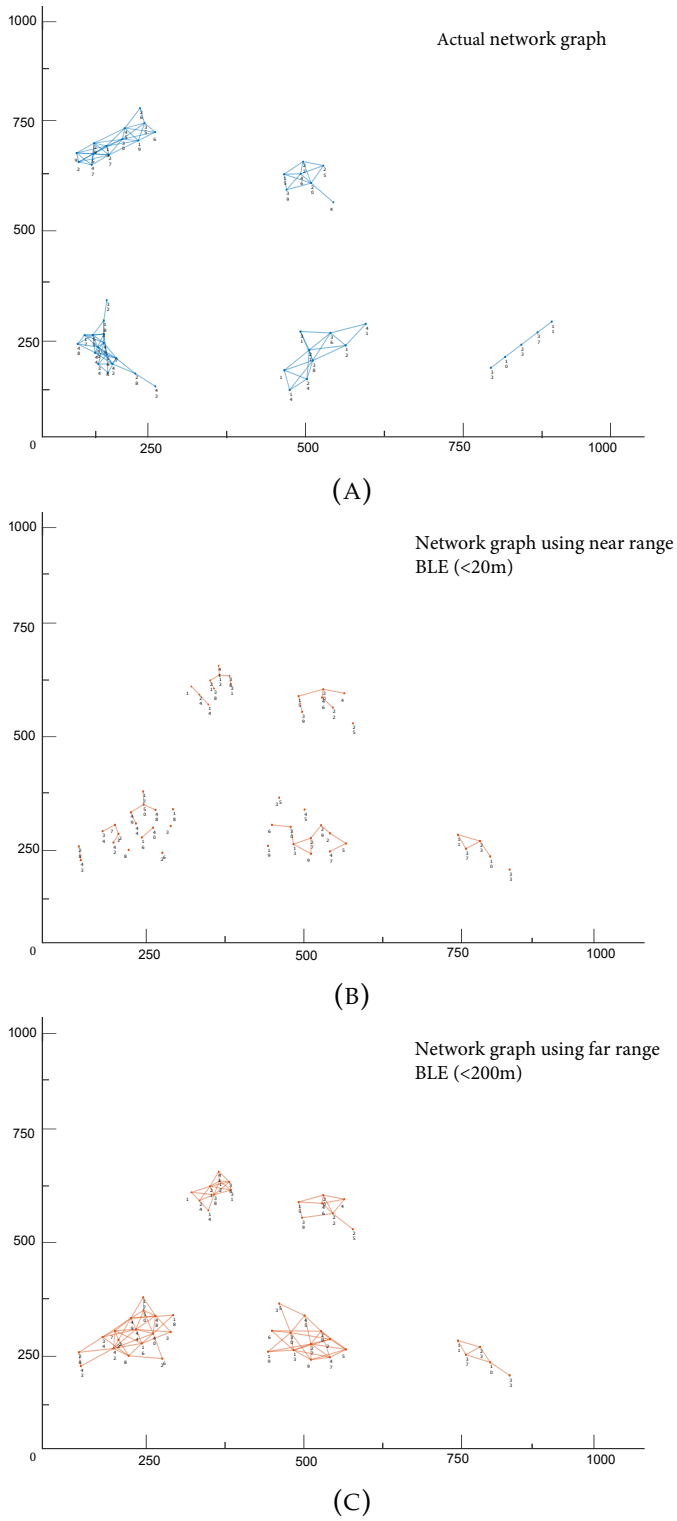

FIGURE 8.12: *Time-frame-2: number of communities in the (a) the actual graph, (b) estimated graphs (based on near range), and (c) estimated graphs (based on far range)*

isomorphism gives a binary output indicating whether (two graphs are exactly the same or different), it is unclear to what extent the graphs differ. It might be that only one edge is different but there is also a possibility that both graphs are completely

different and have no similarity at all.

Energy consumption

In this section, we compare the energy consumption required in case of the actual (based on GPS data) and the estimated (based on far range BLE radio) graphs. For energy consummation modelling, the number of nodes (n) is inclusively varied between 2 and 400, while the other parameters are kept similar as before.

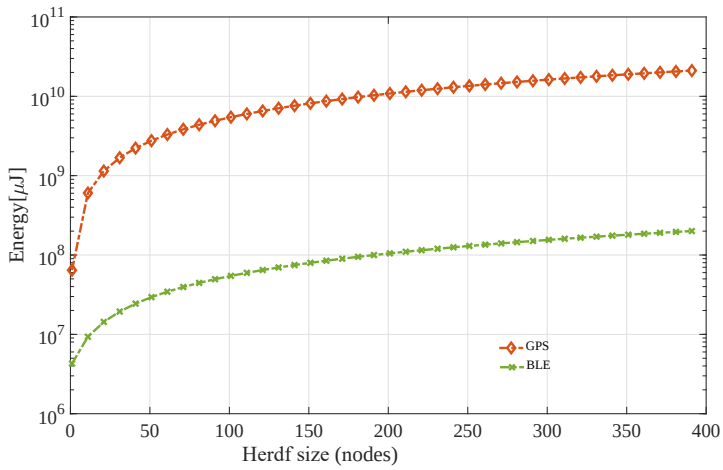

FIGURE 8.13: *Impact of node density on energy consumption*

As shown in Figure 8.13, the energy consumption increases as the number of nodes increases, and as expected the BLE network saves more energy than GPS based approaches. This is mainly due to the fact that ToA duration for BLE is relatively shorter and because of higher modulation bit rate of BLE (1 Mbps). It is clear from Figure 8.13 that in case of GPS, a higher number of node density will contribute to more pronounced energy consumption. The GPS under performs in terms of energy consumption, indicating that it is less suitable for data collection where energy source is very limited. However, the utilization of GPS would be more beneficial for monitoring area, where BLE are incapable of reaching.

8.2.5 Summary

Our research showed that BLE radio could be used for inferring animal social network information. However, a fine grained social behavioural structure can be inferred using near range BLE to the extent that it is only possible to identify how many animals are important in the network. Detecting accurate number of components is often hard because most of the time there will be an high estimation offset. Taking this into account, it is possible to estimate the number of components. Both near and far range are suitable for identifying which animals have a high betweenness. Furthermore, we performed a network wide energy consumption comparison for BLE and GPS to demonstrate that BLE is a potential alternative solution to GPS. BLE is especially accurate in indicating the network density within a herd.

TABLE 8.3: *Summary of overall performance of near and far range BLE for different graph metrics*

Metric	BLE	Notes
Isomorphism	n/a	No isomorphism
Number of isolated nodes	✓	Near range BLE is suitable
Betweenness	✓	Both near and far range BLE are suitable
Node degree	×	Both near and far range BLE are not suitable
Network density	✓	Both near and far range BLE are suitable
Number of components	✓	Far range BLE is suitable
Number of communities	✓	Near range BLE is suitable

8.3 Utilization of opportunistic BLE network for animal mobility pattern identification

In the previous sub-section (i.e. Section 8.2, we utilized a stationary data set per time-frame from the ZebarNet project to characterise the behaviour of animal movement. However, practically, animals move in clusters with a specific aim such as grazing or running from a prey. Thus, in this section, we present a mobility aware network analysis that focuses on the utilization of an opportunistic BLE beacon network for animal mobility behaviour indication. We present a framework to systematically analyze the animal mobility pattern. As shown in Figure 8.14, the framework focuses on the following key aspects: mobility models, the metrics for mobility and connectivity graph characteristics, and the potential relationship between the opportunistic BLE network and the analysis of its impact on animal movement pattern. The framework utilizes several standard mobility models that captures the fundamental characteristics of animal movement behaviours.

Therefore, the main aim of this sub-section is to utilize received signal information that is logged from the opportunistic network simulation tool as presented in Section 5.2, to estimate the animal movement pattern and compare with the actual trajectory of the animal mobility. These approach will helps us to answer the research question such as: *how similar is the estimated movement pattern with the actual movement pattern? is it possible to differentiate between several movement patterns or models given the actual mobility?*. Addressing the above questions will enable to answer the core question of the this thesis work.

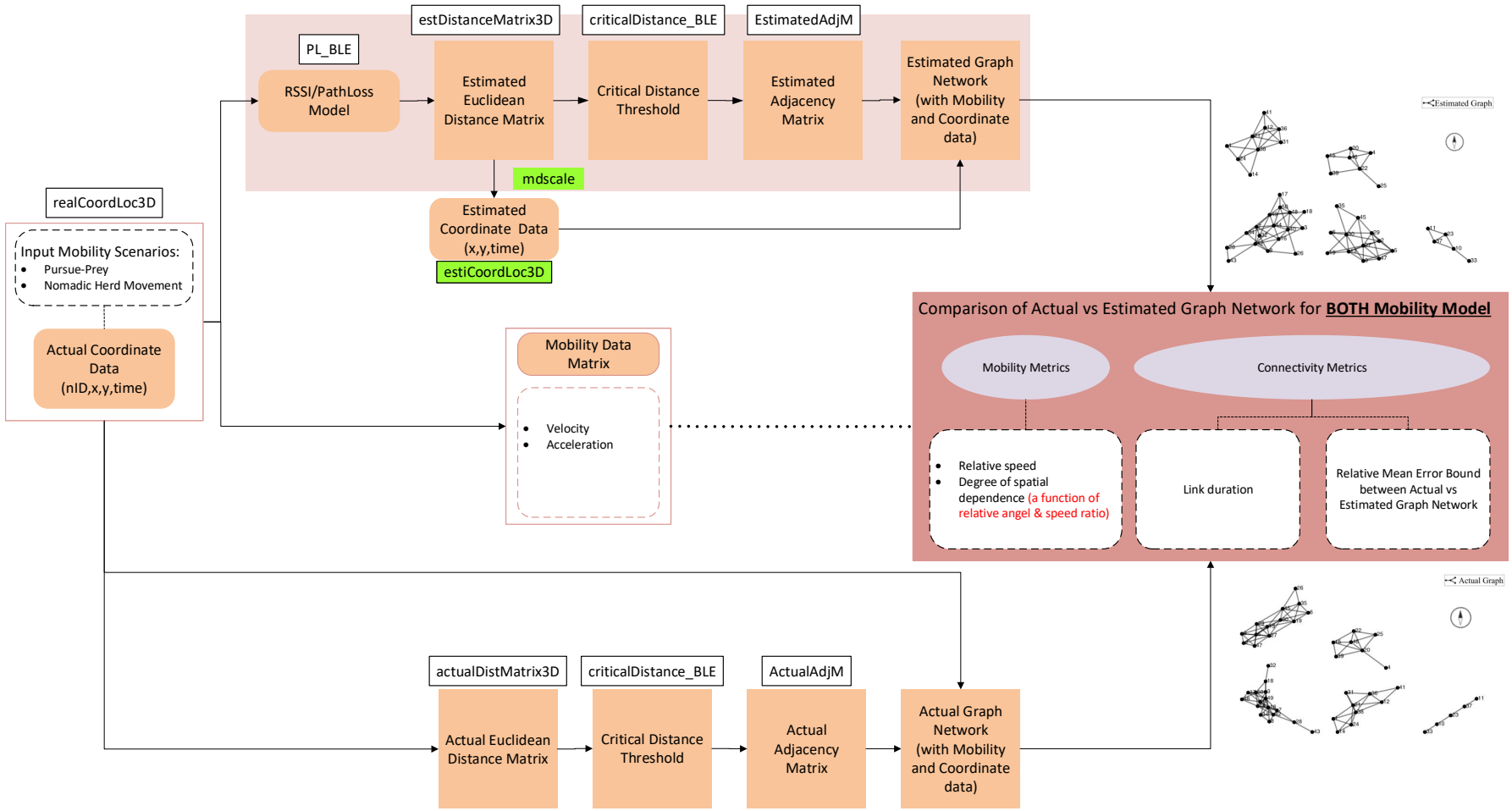

FIGURE 8.14: *Movement pattern analyses framework*

8.3.1 Methodology

The following step-by-step activities are carried out by the movement pattern analysis framework:

- We used the same NS3 simulation parameters as in Section 5.2.4, except that we introduce three more input mobility models such as such as pursue, nomadic, and random way-point (RWP); to define the movement behaviour of animals across the grazing area as described in Section 1.6 [28]. In the simulation, the opportunistic BLE network is used to advertise beacons with AB nodes and store the BLE RSSI values as seen by the AS nodes in the network. NS3 registers the RSSI for every beacons data received on the AS nodes.
- The actual graph is constructed using the actual coordinate tuples (nID, x, y, t) from the input movement model data set.
- For the estimated graph, we first estimate the euclidean distance matrix for the peer to peer nodes from the RSSI information collected by utilizing the distance and path-loss models in combination with the log-normal shadowing [145] (Equation 4.11).
- From the euclidean distance matrix we generate the (x,y)-coordinate using *mdscal* function that will transform the distance matrix to a relative Cartesian coordinates.
- The *actual distance* and the *estimated distance* matrices are then used to generate the *actual adjacency matrix* and *estimated adjacency matrix* respectively, by applying a simple distance thresholding technique (i.e. using the theoretical maximum radio coverage of BLE) (Equation 4.9). If the distance between pair of nodes is shorter than the far BLE radio range (i.e. the critical (threshold) range, then animals are assumed to be in range of each other, hence, the existent of the graph edge would be represented by a '1' in the corresponding adjacency matrix. Otherwise it would be '0'.
- The *actual adjacency matrix* and the *estimated adjacency matrix* are in-turn used to create the *actual graph network* and *estimated graph network*, respectively.
- Thus, once we have the (nID, x, y, t) values for the *actual adjacency matrix* and the *estimated adjacency matrix* corresponding to the estimated and actual graph topology, then we can compute the mobility metrics and error bound difference for both actual and estimated network topologies.

8.3.2 Mobility specific indicators

We utilize mobility and connectivity metrics such as relative speed and link duration to differentiate the various mobility patterns introduced as a result of herd movement. The basis of differentiation is the extent to which a given mobility pattern captures the characteristics of spatial and temporal dependence. In addition to these metrics, we also use the error bound metric that is able to capture the relative

similarity between the actual and estimated graphs in-terms of distance distribution [30].

Terminology

Before formally defining the metrics, we introduce some basic terminology that will be used later in this sub-section:

- $x_i(t)$: X coordinate of node i at time t.
- $y_i(t)$: Y coordinate of node i at time t.
- $V(t)$: velocity vector of node i at time t in relative to the previous time frame t'. $V(t) = (\sqrt{(x_i(t') - x_i(t))^2 + (y_i(t') - y_i(t))^2})/(t' - t)$.
- $v_i(t) = |V_i(t)|$: speed of node i at time t in relative to the previous time slot.
- $E_{i,j}(t)$: Euclidean distance between nodes i and j at time t.
- $RD(A(t), B(t'))$: the relative direction (RD) (or cosine of the angle between two vectors A(t) and B(t') given by

  $$RD(A(t), B(t')) = \frac{A(t).B(t')}{|A(t)| * |B(t')|}$$

  . (i.e. change in angel between a pair of nodes which is a dot product of two vectors).
- $SR(A(t), B(t'))$: the speed ratio (SR) between two vectors A(t) and B(t') given by

  $$SR(A(t), B(t')) = \frac{min(|A(t)|, |B(t')|)}{max(|A(t)|, |B(t')|)}$$

  .
- R: maximum transmission range of a mobile node.
- N: number of mobile nodes.
- T: simulation time.
- $G = (v, E)$-Graph network: a graph $G = (v, E)$; where V is the nodes and E is the edges, such that $|V| = N$ and at time t, a link $(i, j) \in E$ iff the euclidean distance $E_{i,j}(t) \leq R$. Let $X(i, j, t)$ be an indicator random variable which has a value 1 iff there is a link between nodes i and j at time t. $X(i, j) = max_{t=1}^{T} X(i, j, t)$ be an indicator of random variable which is 1 if a link existed between nodes i and j at any time during the simulation, 0 otherwise.

Metrics

Relative speed (RS): We use the standard definition for speed, i.e.

$$RS(i, j, t) = |V_i(t) - V_j(t)| \tag{8.6}$$

Average relative speed: It is the value of $RS(i,j,t)$ averaged over node pairs and time instants. Expressed as:

$$RS(Avg) = \frac{\sum_{i=1}^{N}\sum_{j=1}^{N}\sum_{t=1}^{T} RS(i,j,t)}{P} \tag{8.7}$$

, where P is the number of tuples (i,j,t), such that $RS(i,j,t) \neq 0$.

Degree of spatial dependence (D_S): It is a pair-wise measure of the extent of similarity of the velocities of two nodes, i.e the relative speed a node with respect to its linked node. D_S also includes the relative angle or direction information of the nodes. Defined as:

$$D_S(i,j,t) = RD(v_i(t), v_j(t)) * SR(v_i(t), v_j(t)) \tag{8.8}$$

The value of $D_S(i,j,t)$ is high when the nodes i and j travel in more or less the same direction and at almost similar speeds. However, $D_S(i,j,t)$ decreases if the relative direction or the speed ratio decreases. As it is rare for a nodes motion to be spatially dependent on a far off node, we add the condition that if the euclidean distance between pair of nodes is less-than the transmission range of the radio, if $E_{i,j}(t) \geq R \Rightarrow D_S(i,j,t) = 0$.

Average Degree of Spatial Dependence: It is the value of $D_s(i,j,t)$ averaged over node pairs and time instants. Expressed as:

$$D_S(Avg) = \frac{\sum_{t=1}^{T}\sum_{i=1}^{N}\sum_{j=i+1}^{N} D_S(i,j,t)}{P} \tag{8.9}$$

where P is the number of tuples (i,j,t), such that $D_S(i,j,t) \neq 0$. Thus, if mobile nodes move independently of one another, then the mobility pattern is expected to have a smaller value for $D_S(Avg)$. On the other hand, if the node movement is coordinated by a central entity, or influenced by nodes in its neighborhood, such that they move in similar directions and at similar speeds, then the mobility pattern is expected to have a higher value for $D_S(Avg)$.

Link duration (LD): Since opportunistic beacon network protocol is affected by the network topology dynamics, it is useful to have a metrics that analyzes the effect of mobility on the connectivity graph between the mobile nodes. The the link duration metric aims to address this effect. For two nodes i and j, at time t, duration of the link (i,j) is the length of the time interval $[t,t']$ during which the two nodes are within the transmission range of each other. Formally,

$$LD(i,j,t,t') = t' - t \tag{8.10}$$

Average link duration: It is the value of $LD(i,j,t,t')$ averaged over all existing links for node pairs. Formally,

$$LD(Avg) = \frac{\sum_{t=1}^{T}\sum_{i=1}^{N}\sum_{j=i+1}^{N} LD(i,j,t,t')}{P} \tag{8.11}$$

where P is the number of node pairs (i, j, t, t') such that $LD(i, j, t, t') \neq 0$.

8.3.3 Evaluation

We used the NS3 simulation parameters as in Section 5.2.4, except that the AB nodes' advertising interval is set to $T_{BC}^{+} = 1000$ ms for a controlled and uniform data generation across the various input mobility models used. The AB and AS nodes operates as per the operation scheme described in Section 5.2. We introduce mobility models such as the nomadic, pursue, and RWP mobility models. When the simulator is in action, the AB nodes transmit BLE beacon data periodically to AS nodes, then AS nodes record the RSSI values for every received packets, which will be used to estimate the euclidean distance.

Input mobility models

Nomadic and pursue movement models are used as an input mobility scenarios with actual coordinate data tupils $(nID, x, y, time)$ as shown in (Figure 8.15. The Nomadic cluster model represents groups of mobile nodes that collectively move from one point to another [29, 30]. As shown in Figure 8.15a, within each cluster or group of mobile nodes, individual animals maintain their own personal proximity where they move in random ways. For example, consider a herd of animals wondering around a land for grazing. The herd would move from one location of interest to another together; however, the animals within the herd would roam around a within the cluster individually with leaving the cluster.

As the name implies, the pursue mobility model attempts to represent mobile nodes tracking a particular target [29, 30]. For example, this model could represent predators or poachers attempting to catch a prey animal. Figure 8.15b gives an illustration of pursing nodes moving with the Pursue mobility model. The white node represents the node being pursued and the solid black nodes represent the pursuing nodes.

Each mobile node deviate its velocity (both speed and direction) randomly from that of the cluster leader. The movement in group/herd mobility can be characterized as follows: $|V_{member}(t)| = |V_{leader}(t)| + random() * SDR * |V_{max}|$; $|\theta_{member}(t)| = |\theta_{leader}(t)| + random() * ADR * |\theta_{max}|$ where $0 \leq SDR, ADR \leq 1$. SDR is the speed deviation ratio and ADR is the angle deviation ratio. SDR and ADR are used to control the deviation of the velocity (magnitude and direction) of group members from that of the leader. $|V_{max}|$ and $|\theta_{max}|$ are used to specify the maximum deviation a group member can take. For pursue model, the random vector value is obtained via an entity mobility model (e.g., the Random Walk Mobility Model); the amount of randomness for each mobile node is limited in order to maintain effective tracking of the node being pursued. In our simulation, we set $|V_{max}|$ for the group leader as the max speed and set $|\theta_{max}| = 180^o$ as the max angle as outlined in [29]. Since the group leader mainly decides the mobility of group members, group mobility pattern is expected to have high spatial dependence for small values of SDR and ADR.

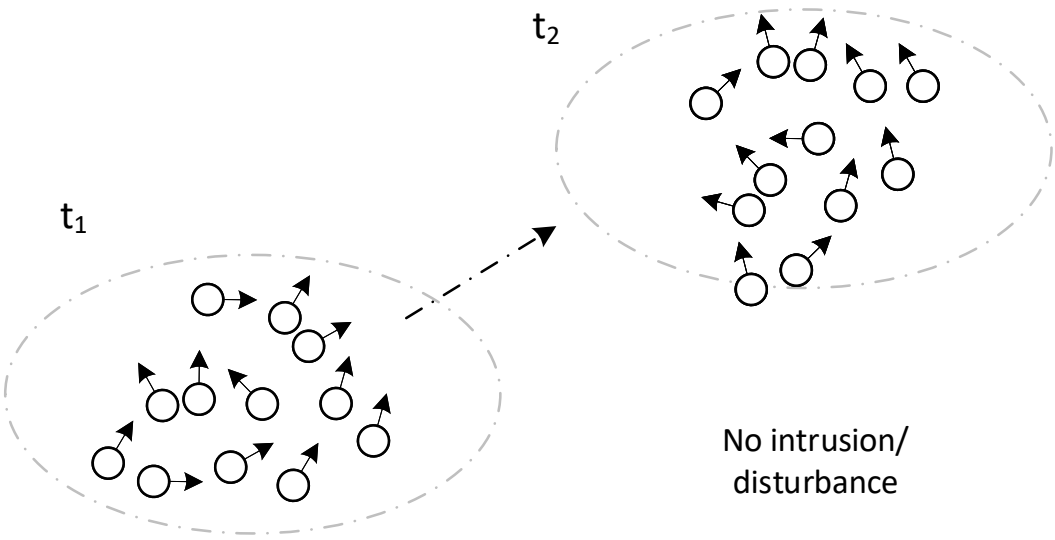

(A) *Nomadic movement scenario, emulating a clustered movement behaviours e.g. grazing, walking etc.*

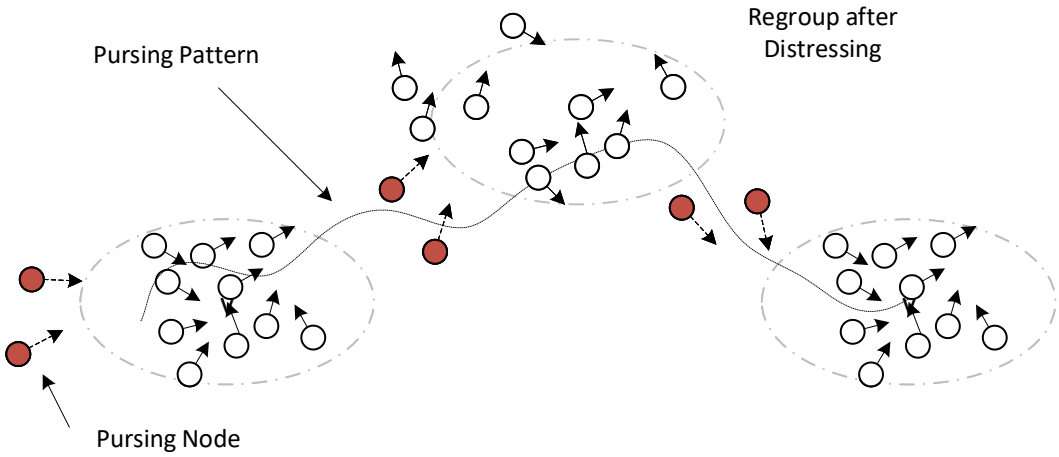

(B) *Pursue/prey-predator scenario: the white node represents the node being pursued/preys and the solid red nodes represent the pursuing/predator nodes.*

FIGURE 8.15: *Mobility models*

Moreover, we also use the RandomWay Point (RWP) mobility model a the generic baseline reference mobility model for evaluation purposes.

The mobility scenario generator produced the mobility patterns following the Nomadic, Pursue and RWP models according to the format required by NS3 simulator. In all these patterns, 50 mobile nodes moved in an area of 1000mx1000m for a period of T=8000 time frames. Random Waypoint mobility pattern was generated using the

setdest tool which is a part of the NS3 distribution. For nomadic, we used 5 groups of 10 nodes each moving independently of each other and in an overlapping fashion. For pursue, the 50 mobile nodes were placed in a similar way as nomadic model, and two extra pursuing nodes are introduced randomly to emulate predatory distressing behaviour. Their movement was controlled as per the specifications of each models. If a pursing node moves beyond the boundary of the defined area, it is re-inserted at the beginning position in a randomly chosen coordinate in the area. The maximum speed V_{max} was set to 1, 5, 15, 25, 35, 45, 55 and 65 m/sec to generate multiple movement for each mobility model.

8.3.4 Results and discussion

While evaluating the results with the mobility metrics, we observed that the measurement metrics were able to differentiate between the different mobility models.

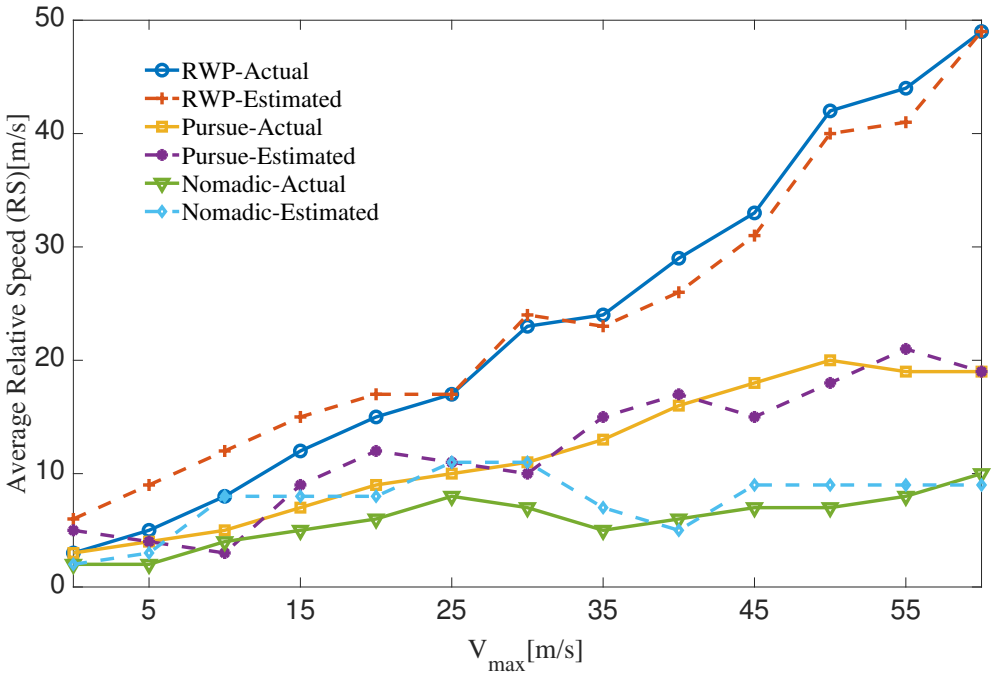

FIGURE 8.16: *Relative speed (RS)*

As shown in Figure 8.16, the relative speed (RS) is able to distinctly identify between the various mobility patterns and their actual and estimated graphs. As illustrated, the more coordinated they are the smaller RS value. Thus, RS follows a trend such that $RS_{Nomadic} \leq RS_{Pursue} \leq RS_{RWP}$ for both estimated and actual graphs. RS has the lowest value for Nomadic (multiple group mobility) as the nodes move together in a coordinated fashion with little deviation from the cluster head, while RS has a medium value for pursue mobility where group nodes disperse in a random way. For both actual and estimated network, RS value for the RWP mobility model patterns is the highest and almost twice that for nomadic. This high value is due to the mobile modes moving relatively faster in a random direction for RWP mobility patterns.

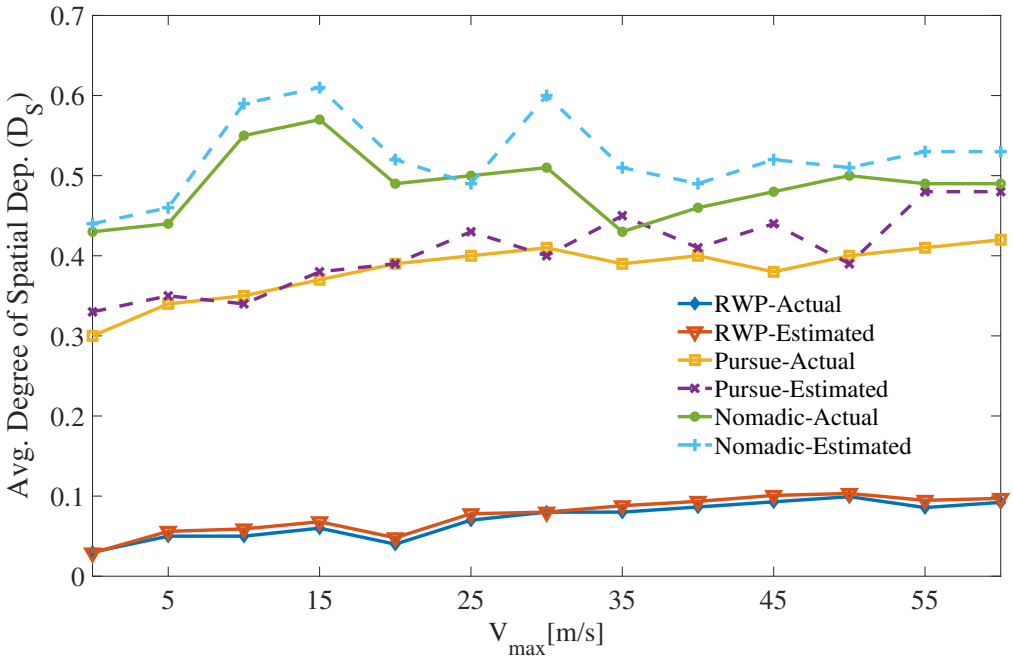

FIGURE 8.17: *Degree of spatial dependence (D_S)*

As shown in Figure 8.17, D_s is also able to differentiate between the different mobility patterns but not as clearly as RS. D_s has a higher value for nomadic mobility (around 0.5) than that of pursue mobility (about 0.35). However, for the RWP, its value is close to 0. Intuitively, this is because in nomadic model, the cluster/group head leads the movement of the mobile nodes and thus the mobility pattern has a high spatial dependence than RWP or Pursue model. In RWP, due to the random movement direction of nodes, the positive degree of spatial dependence of a node with nodes in the same direction cancels the negative degree of spatial dependence of the nodes with nodes traveling in the opposite direction. Initially, we expected the Pursue mobility patterns to have a high spatial dependence as a node's movement is influenced by nodes pursuing the other nodes, hence, creating a disturbance.

On the other hand, as shown in Fig. 8.18, LD has a higher value for nomadic groups than the Purseu and RWP. For the RWP its value is similar to Pursue. Since nodes in a group move at velocities that are deviated by a small fraction from the group leader, an already existing link between two nodes is expected to have a higher duration (Figure 8.18). The highly low value for the RWP is again related to node's randomness in movement direction of motion and relative speeds. Thus, the more random they are the smaller LD, i.e. $LD_{Nomadic} \geq LD_{Pursue} \geq LD_{RWP}$.

In addition, a *distance error bounds value* is used to show the difference between the distance values for actual and estimated graphs per time-frame, defined as ($ErrBnds = abs(estDistanceMatrix3D - actualDistMatrix3D)$). This value indicates the comparison value between actual and estimated graphs, providing answer on how closesly similar the two graphs are. This parameter is determined for all mobility model types. Figure 8.19 shows the distance error bound histogram for the actual and estimated graphs. Since the sample size and bin width of the error bound data are

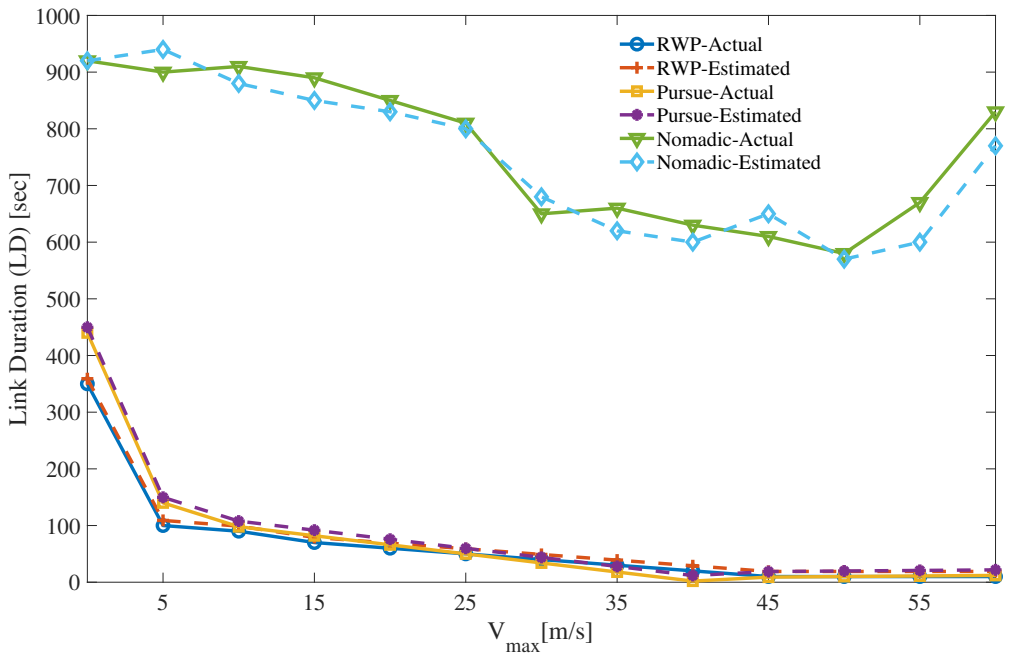

FIGURE 8.18: *Link duration (LD)*

different, it is difficult to compare them. Therefore, we normalized the histograms so that all of the bar heights add to 1 and it uses a uniform bin-width. A larger distance error bound indicates a high deviation between the actual and estimated graphs for each mobility models. The discrepancy is highly exaggerated especially for RWP and Pursue mobility. For Nomadic movement model, most of the distance errors are highly frequent around average range less than 50m. For RWP and Pursue, the error bound is in the range of around 200m and 150m respectively.

8.4 Conclusion

In this chapter, we investigated the application of BLE for determining spatial proximity between nodes to be used for animal spatial social network analysis. The research was motivated by the high energy consumption of GPS and the fact that BLE radio is already used for wireless communication.

We applied graph theory concepts to estimate and analysis the social interaction among animals. A path-loss model are simulated to measure the performance of BLE radio. The overall observation is that, as expected, BLE radio is more energy efficient than GPS. Additionally, near range BLE outperforms far range BLE in terms of all graph theory indicators, except in number of detected components. Thus BLE may be used as an alternative for GPS for animal spatial social network analysis. Moreover, as expected from dynamic radio signal property, determining the exact proximity values are not possible using BLE radio.

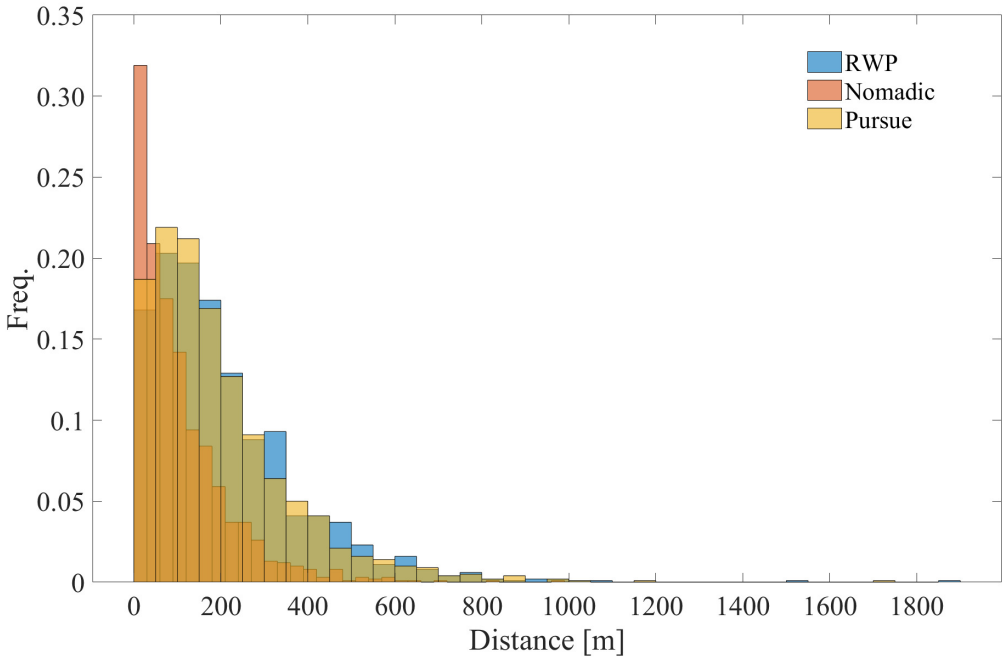

FIGURE 8.19: *Error Bounds (RMS):root-mean-square deviation (RMSD) or root-mean-square error (RMSE)*

One of the limitations of this work is that it is not yet verified in a real large scale network topology. Another issue worthwhile to investigate is how BLE performs using different node density levels. This might influence the performance of certain metrics. In future work, it is interesting to investigate if multiple time-frames are used to construct one graph.

This might increase the estimation accuracy, for example, a graph is constructed from ten time-frames and the broadcast of one node is received only in two of the ten time-frames by other nodes, this node can be filtered out of the graph because it can be assumed that it was an error due to the path-loss and shadowing. On the other hand, this might also lead to the loss of information. At the hardware level, it is interesting to see if Bluetooth Mesh can be used for animal social network applications. While there has already been research to Bluetooth mesh networks, to the best of knowledge of the authors, there is no research in applying Bluetooth Mesh protocol for animal social network analysis applications.

Moreover, we presented a movement pattern analysis framework for several mobility models using generic movement metrics introduced for this specific scenario. Overall, the link duration (*LD*) is found to be the more useful metric to differentiate the connectivity graphs arising from the different mobility patterns used in the study.

Chapter 9

Conclusions and Future Works

In this thesis, we focused on developing an energy efficient and reliable wireless communication network protocol suitable for wildlife monitoring. In this chapter, we outline our research contributions, conclusions derived from our work, and future research challenges for wireless wildlife monitoring system design.

9.0.1 Research hypothesis

We tackle the outlined research questions, with the following accompanying hypothesis.

To answer research question 1,
Hypothesis 1 (H1): A hybrid tree network topology, which is a combination of inter-cluster with short-range (BLE) and intra-cluster with long-range (LoRa) wireless link, is more optimal than simple star network topology based on short-range or long-range only wireless communication.

To answer research question 2,
Hypothesis 2 (H2): A light-weight single-hop based communication network architecture will significantly reduce the energy consumption of end-nodes while at the same time achieving very low latency and high reliability for WMS.

We also addressed other alternative approaches to address the research question 2, such as
Hypothesis 3 (H3): A multi-hop network with a data traffic adaptiveness for the wildlife monitoring.

Hypothesis 4 (H4): Movement adaptiveness could be complemented with beacon transmission mode, where the sensor nodes would be aware of the nodes' mobility states by utilizing real sensor data such as accelerometer.

To answer research question 3,
Hypothesis 5 (H5): It is possible to implement an opportunistic multi-hop network network architecture with a data replication scheme to control and prioritize data dissemination in WMS. Hence, the communication routing algorithm will adapt to dynamic network topology due to the inherent lack of full-connectivity between herd of animals.

9.1 Summary of the research

The prime research objective of this thesis is to provide a network communication protocol ensuring energy-efficiency, high reliability and low latency, and handled the WMS challenges in node mobility and herd sparsity (clustered) for wildlife monitoring applications (Section 1.4). Furthermore, we investigated the research issues such as (i) Can the effect of sporadic animal movement be utilized for optimal communication network architecture design while achieving the network requirements? and (ii) How to address the lack of full network connectivity by leveraging the animals' conspecific or clustering behaviour? (Section 1.4). We addressed these fundamental research questions and hypothesis with the following contributions:

Contribution 1: Leveraging BLE and LoRa radio for WMS
In Chapter 2, to answer research question 1 and H1, we did an extensive literature review on the existing wireless technologies for wildlife monitoring, we identified

the weakness and strength of each technology for the WMS design (Section 1.4). Following the literature review, in Chapter 4, we presented an analyses and comparison of a hybrid tree based network topologies to the conventional star based networks. From the evaluation results, we identified and modelled a suitable wireless communication model for wildlife monitoring technique. We demonstrated that hybrid tree topologies are more optimal in-terms of energy consumption than the conventional star network topology for WMS.

Contribution 2: Single-hop communication with hybrid tree network
In Chapter 5, to look into the research question 2 and H2, we presented the design and implementation of light-weight asynchronous beacon network (Section 1.4). We evaluated the performance of the protocol in comparison with the conventional opportunistic systems under actual animal movement scenarios. The key advantage of this network architecture is that nodes achieve wider control on the trade-off between total energy consumption and latency. The evaluation results indicated that the proposed architecture outperforms the traditional opportunistic networks. On average, our protocol improved the data delivery radio and latency incured by up-to 60% and 75% respectively. In addition, the architecture improved the network energy consumption considerably, especially, at faster packet traffic rates in the network. Our protocol is found to be more optimal than utilizing only conventional opportunistic multi-hop network. Moreover, we presented a movement pattern analysis framework for several mobility models using movement metrics defined for this specific purpose.

Contribution 3: Multi-hop communication with hybrid tree network
In Chapter 6, to further explore research question 2 with hypothesis H3 and H4, we presented a herd-movement driven asynchronous duty-cycling communication protocol suitable for mobile sensor nodes (Section 1.4). The protocol is demonstrated to adapt to the specific animal movement patterns to make the wireless communication more energy-efficient and reliable. As commonly implemented, a fixed duty-cycle interval for mobile network topology often leads to low reliability, high energy consumption, and latency. We identified that the WMS protocol is able to cope with highly frequently changing network topologies occurring due to high mobility. We presented a feed-back stability controller, to analyze the received and transmitted packets to determine an optimal sleep-time interval at run-time. Our evaluation results showed that, compared to A-MAC and X-MAC, utilizing the protocol on average network energy consumption is reduced by 22.28%-52.28%, providing an additional decrease in the average end-to-end latency by 11.65%-14.63%. The overall packet reliability is also up-to 16.3% increased. In addition, we also discussed an alternative approach based on a beacon advertising control scheme to based on their mobility states. This approach utilizes a strategy that maximizes the accuracy of mobility state detection by using unsupervised learning algorithm to decrease the energy consumption. We have compared our solution to the continues beacon advertising mode and k-mean algorithm by analyzing the network energy consumption. Overall, for high activity window length, the proposed mobility state driven approach has demonstrated to decrease the network energy consumption by up-to six fold lower than the continuously periodic mode.

Contribution 4: Opportunistic multi-hop communication in hybrid tree radio network
In Chapter 7, alternatively to answer research question 2 and H5, we identified that conventional multi-hop routing algorithms often perform poorly in scenarios where the communication link is sporadic due to node mobility (Section 1.4). To overcome this problem, in Chapter 6 we explored the existing opportunistic multi-hop protocols that are the recent evolution of the traditional wireless sensor networks (WSN). In addition, we presented an optimized opportunistic multi-hop protocol utilized to provide communication facilities among devices in sparse and mobile network scenarios, as in WMS applications. We observed that opportunistic multi-hop networks are suitable for WMS scenario as there is no network topology limitation, node mobility is supported, and intermediate nodes utilize a simple store-carry-and-forward (SCF) scheme for data dissemination with out relying on routing tables. This will effectively minimize data latency while avoiding deterioration in data reliability.

Contribution 5: Animal spatial social network analysis
Moreover, to address the research question 3 on handle animal behaviour, animal spatial social network analysis is used for investigating the social interaction among animals in their natural habitat (Section 1.4). Such analysis helps determine how animal population density changes according to certain environmental disturbances and how the animals react to each other and their environment. In this thesis, we demonstrated that wireless communication protocols could be utilized in inferring the movement patterns of animals. In Chapter 5 and Chapter 9, the application of BLE radio based WMS protocol is discussed for analyzing animal social behaviour. This approach makes possible to use proximity ranging as an alternative solution to the existing application of GPS for studying the animal movement behaviours.

9.2 Lessons learned

During our research we learned the following lessons:

- *No ultimate solution for animal protection:* Wireless communication technologies are evolving continuously to encompass several application scenarios. The existing technologies cannot always be directly applied to satisfy the specific application requirements. Investigating wireless communication technologies to determine their limitation is very crucial in developing an energy efficient and reliable wireless monitoring system for wildlife protection efforts. Most of the solutions utilizing single type of technology are noted to have a relatively high latency and high energy consumption, mainly due to the dynamic network topology. This will make them not suitable for wildlife monitoring where energy resources are very limited. Based on our study, we suggested to utilize a hybrid wireless solution by collaboratively combining short-range sensor network with long range low power technology for providing efficient WMS. It is our believe that the long term solution for the animal poaching crisis is to remove the drivers of demand. People in the demanding countries should be educated and made aware of the poaching crisis. Until these kind of actions take effect, there will be a continuous and urgent need for effective

wireless based WMS solutions that assure the survival of endangered animals such as rhinoceros and elephant species.

- *Dealing with the effect of sporadic animal movement pattern is essential for developing a suitable wireless monitoring technology:* The effectiveness of a wireless communication is largely influenced by the sensor node movement and the physical radio channel environment. Therefore, it is essential to understand the impact of animal mobility pattern on the wireless link in more detail such as radio propagation, path-loss, and to address their limitation on the design of the communication protocol.
- *Detecting node mobility:* The way mobility should be captured and handled requires a careful consideration. Most of the discussed wireless sensor network protocols encompassing multi-hopping and opportunistic protocols, implicitly assume that the number of static nodes is significantly larger than the number of mobile animals. Experiment and simulation results indicate that accurate animal mobility estimation is essential to avoid unnecessary oscillation in link establishment. However, the results also indicate the existence of a strong trade-off between estimation accuracy, estimation time, and signal processing cost (both in terms of energy consumption and computing resources). Therefore, WMS protocols should integrate with a mobility estimation techniques that optimizes the required trade-off. Moreover, estimation techniques that are based only on RSSI values are found to less accurate leading to frequent oscillations even when nodes are not mobile. Therefore, using accelerometer sensor data for further identifying the mobility pattern of animals will significantly reduce both false positives and false negatives.
- *Data processing is much more cheaper than transmission:* Transmission of raw data over the wireless communication link is found to more costly than processing data locally on the node. To ensure overall energy consumption efficiency, a light-weight data concatenation scheme is used to aggregate incoming data.
- *Run-time mobility adaption is beneficial for wireless sensor network based wildlife monitoring:* As commonly implemented setting, a fixed duty-cycle interval for mobile network topology often leads to low reliability, high energy consumption and latency. This is especially the case for high mobility networks as in WMS. Introducing a mechanism to cope with highly frequently changing network topologies can be beneficial. One important criteria for this kind of approach is to decrease the energy consumption by limiting the number of data transmitted in the active state.
- *Sensor node should make data forwarding decision locally:* To facilitate optimal data communication between sensor devices to be used for wildlife monitoring, a node can make its decision for data forwarding based on local observations. In practice, it is near impossible, to determine a unique dissemination protocol for mobile network. However, when subjected to diverse mobility patterns and traffic generation rate, communication protocol should an improved performance than existing protocols.

- *Proximity range information is important for inferring animal mobility behaviour:* The application of BLE radio for determining the spatial proximity between pairs of nodes is found to be essential for social network analysis of animal herds. Once the spacial information is retrieved, it is possible to determine the temporal network topology of the network at specific time. This will provide an efficient alternative solution to GPS.

9.3 Future work

- We have evaluated several wireless communication based solutions for WMS. However, they are mainly investigated based on simulation tools currently available. One of the limitations of this work is that it is not yet verified in a large scale real network set-up. While the performance of the WMS is tested using small scale network, it is actually deployed in a controlled scenarios without the use of actual animal subjects. More real tests using hardware and larger groups are needed to validate the results in this work. Another issue worthwhile to investigate is how WMS will perform for different node density levels. This might influence the performance of certain evaluation metrics, thus, in the future, it is interesting to investigate WMS in a practical scenario specific to real animal species.
- In our research, we used an openly available animal mobility data sets generated from a limited actual animals for designing and validating the wildlife monitoring system. However, any further validation of our proposed solution using another real animal data set was not possible due to the limited availability of similar data sets. This problem could be overcome if the research community is open about sharing their data set. This will significantly help in fine tuning the results and reproduce it for collective knowledge among the research community. As a future research, it would also be important to deploy prototype sensor collar devices on the animal in actual game park to collect real mobility pattern of wild animals.
- We implemented and analysed several adaptive schemes to make the WMS more energy efficient. However, the limitation and feasibility of these techniques could be studied in more practical mobility model scenarios and design of these algorithms could be substantially improved.
- WMS is responsible to relay monitored animal activities between the sensor nodes, gateway, and the central system. The data could be sniffed out at any point of the communication system by malicious entity. The WMS could be extended with highly robust security features such data encryption, at the physical or cross layer level for the data forwarded.

Appendix A

Implementation of Opportunistic Beacon Network in NS3

A.1 NS3 simulator dual interface network implementation

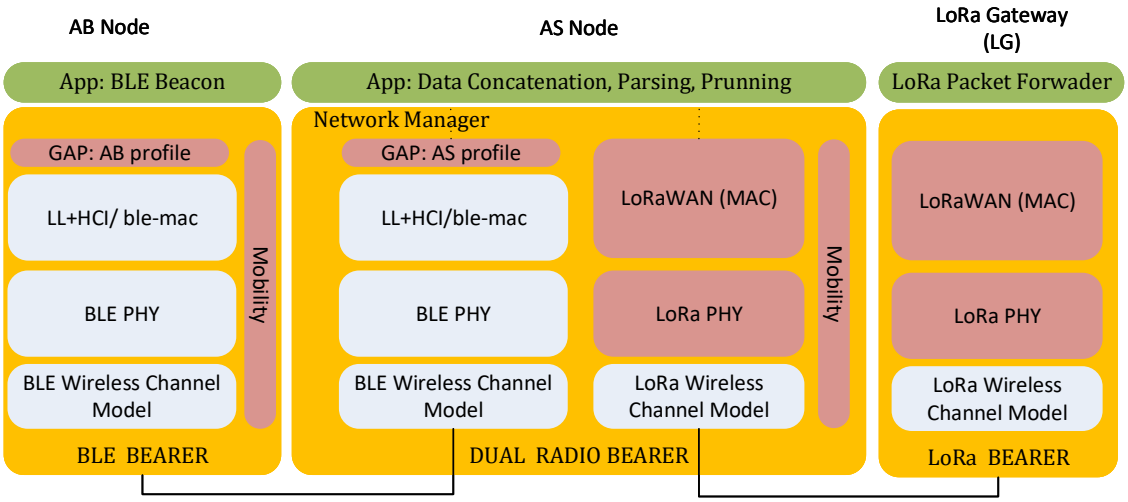

FIGURE A.1: *Dual interface implementation in NS3. AB node utilizes only BLE bearer while AS node can switch between BLE and LoRa interface.*

In this section we introduce the implementation of dual radio in NS3. This module provides an NS3 modules of BLE AS-AB beacon modes integrated with LoRaWAN network module [194]. The simulator includes a propagation channel model, PHY and MAC layers of both BLE and LoRa protocols. The BLE and LoRa use different PHY interfaces to transmit packets (Figure. A.1). Due to the intrinsic complexity of the BLE specification and the various operation modes for BLE devices, it makes hard to only use analytical methods for studying BLE beacon networks as noted in [195]. At the time of writing this work, to the best of the authors' knowledge, there is no openly available network level simulation tools that support BLE beacons. This motivated us to develop a complete BLE simulation tool, for investigating the networking aspects of the protocol. Once validation and documentation is finalized,

we plan to place the tool in the public domain. The event-based simulator uses C++ NS3 framework as the basis for the tool (v26.1) and it comprises of nearly 115 classes. It provides a basis for further extensions as well as the development of a complete tool in the future. We implemented the BLE module with the existing NS3 helpers and models.

It includes the channel loss model, physical layer, LL layer, GAP and network devices. In addition to those classes representing the network protocol layer in the stack (BLEPhy, BLEMac and LoraMac), other classes are used to model aspects of the system such as Netdevices, and path-loss model. Figure A.2 shows the summarised UML diagram of the most important classes that compose the module. It is important to remark that the diagram only reports the most important data members and functions. Some details about the relationship among classes have been omitted due to space limitations. The basic modules utilized by AS and AB nodes are presented in this section.

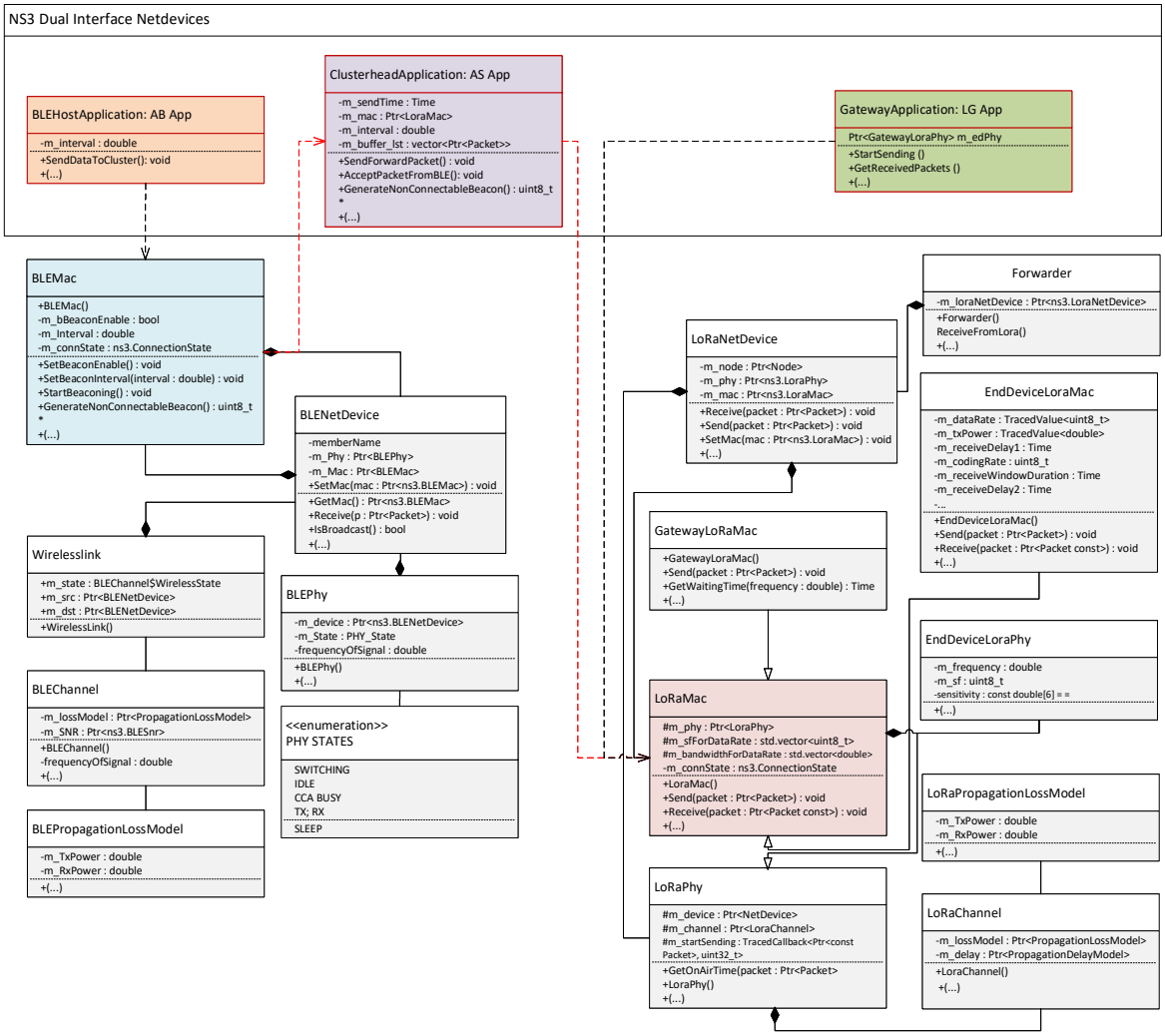

FIGURE A.2: *Summarised NS3 UML class relations diagram.*

A.2 BLE beacon nework module

A.2.1 Overview of BLE protocol stack

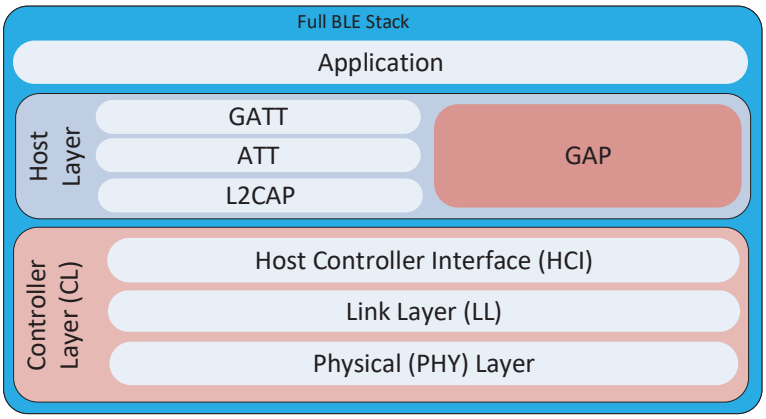

FIGURE A.3: *BLE protocol stack as per BLE 5 specification [5]*

BLE beacon mode is a broadcasting technique, through which the small pieces of information is broadcasted in the network. Any type of information can be broadcasted through BLE beacon, e.g. environmental data (e.g. temperature, humidity etc.), location aware data (asset tracking, retail etc.) and orientation data (rotation, acceleration etc.). Usually, the nature of transmitted data is typically static, however, dynamic data can also be transmitted using BLE beacons. It is designed to operate for many years on a single coin cell battery. The architecture of BLE protocol stack is depicted in Figure A.3.

Similar to the classic Bluetooth protocol stack, BLE's protocol stack is also comprised of two components: a BLE Host and a BLE Controller (see Fig. A.3). These two components can either operate on the same or different physical devices. The link layer (LL) and physical (PHY) layer is controlled by a BLE controller, which is a logical entity [5]. The upper layer functionalities which defines different connectivity roles i.e. GAP and GATT, are implemented by BLE Host entity [5]. We implement the controller and a simplified GAP layer roles of the protocol stack in accordance with the specification of BLE 5 [5]. This implementation is enough to simulate the beacon network features.

A.2.2 BLE PHY and Channel models

The *BLEPhy*, *BLEChannel*, and *BLEPropagationLossModel* classes represent the physical layer of BLE and its channel model as shown in Figure. A.2. *BLEPhy* class includes the methods for BLE physical layer (PHY) features and models the physical layer parameters for the Nordic nRF BLE device [196]. After receiving the packets from the BLE MAC layer, the main role of the *BLEPHY* class is to deliver the packets to the channel class. Furthermore, based on the received values of power and

interference for specific device signal, this class makes a decision about the obtained packet's correct reception. This class also represents the current state of the desired RF chip by utilizing the pre-defined *m_state:PHY_State* attribute. Transmission of packet through RF chip is represented by *TX* while *RX* is used to denote that RF chip is receiving an incoming packet. *IDLE* status represents the listening mode of RF chip for incoming packets whereas, low power consumption mode is represented by *SLEEP* status (Figure. A.2). We can link the above status of the RF chip with a different value of voltage and current, consumed by the*energy model*. This energy model provides an estimate of the lifetime of the given device by taking note of the energy expenditure of the desired device.

BLEPhy provides support to the *BLEMac* layer and translates the raw data into digital symbols to transmit it over the air. 2.4 GHz ISM band is used in the physical layer to transmit the data. This frequency band is divided into 40 frequency sub-channels. There is a 2 MHz frequency space between each channel and it ranges from 2.4000 GHz to 2.4835 GHz, starting at 2402 MHz. From the 40 frequency sub-channels, the number of advertising channels are 3 and the associated channel numbers are 37, 38, 39, while the rest of the 37 sub-channels are used for data communication and the associated channels range from 0-36. The simulator performs the beacon data discovery (scanning or observing), connection establishment, broadcast transmissions (advertising or beaconing) with the help of advertising channels. *BLEPhy* radio is set to transmit at 1 Mbps with 1 bit per symbol. As per the Nordic BLE devices data sheet, the output power of the radio ranges from -20dBm to +4dBm for the BLE and the receiver sensitivity of the RF chip is set to the level of -117dBm for the same mode [196]. *BLEPhy* layer is implemented in *ble_phy.h* and *ble_phy.cc* module. After receiving the signal the PHY layer decides whether to accept or drop the signal, based on its frequency components. Hence, NS3's BLE module can operate in scenarios where multiple interfaces are involved including Wifi frequency range.

The propagation loss model proposed for the BLE bearer combines environment path loss and shadowing model, which are implemented in the classes *BLEChannel*, *BLEPropagationLossModel* class. The wireless channel for the transmission of BLE packets is modelled through the *BLEChannel* class. The main responsibility of this class is to transmit the BLE packets coming from the *BLEPhy* layer to the set of other *BLEPhy* objects, over the wireless interface. After the signal is received, the RSSI is determined by *ns3::PropagationLossModel Class*.

Channel objects register the *BLEPhy* objects in the list during the configuration phase. Two different methods can be used to interconnect registered *BLEPhy* in the *BLEChannel* class. This method can either be *Send* or *Receive*. A message can be sent to the channel by simply calling the *Send* function with the data. Along with this data, the information about the duration of packet, the transmission power of packet and the associated channel number is also included. After the function is invoked, BLEchannel checks the list of ADV channels. After getting the list of listening nodes for the specific communication channel, it schedules a *Receive* event for them. PropagationDelayModel is used to calculate the schedule time for a given Receive event. The receiver and transmitter can determine the latency based on the information given in MobilityModel (i.e., the node positions). we use *ns3::PropagationLossModel Class*'s delay model, which helps in the computation of the RSSI in dBm by using the value

of signal's transmit power (dbm). The position of source and destination is found using the mobility model, since our *AB-AS* device nodes are assumed to be mobile we adopt this loss model as shown in Figure. A.1.

A.2.3 BLE Network Devices

In our simulator, a BLE device is modeled by the *BLENetDevice* class, and is based on the abstract NetDevice class provided by the NS3. This class contains and manages the Link Layer in the BLE protocol stack, in addition to all other common functionalities specific to BLE end devices. In NS3 this NetDevice can be attached to an AB or AS NS3 node i.e. each device can use the BLE module for the transmission and reception of data from other BLE devices. *BLENetDevice* is a generalized device class and it contains all the BLE objects necessary for the BLE packet transmission i.e. a *BLEPhy* and *BLEMac*.

BLEMac class models the link layer of a BLE beacon devices. This class works above the *BLEPhy* layer, and is responsible for waking up the RF radio chip from the sleeping mode, when it senses an incoming received packet. The BLE timing parameters such as advertising interval (T^{+}_{BC}), scan interval (T^{+}_{sc}), and scan window (T^{+}_{sW}) are configured in *BLEMac* logic. Setting these parameters correctly drastically impact the performance of the overall BLE beacon communication. For instance, the *SetBeaconInterval*() method is utilized to set how fast the AB node can transmit BLE beacons on the shared channel (i.e. T^{+}_{BC}). To this end, *BLEMac* is primarily concerned with channel management, packets discovery, and connection procedures. According to the BLE specification [5], it defines the three role pairs in accordance with BLE LL i.e. broadcaster-observer (AB-AS mode), slave-master, advertiser-scanner (initiator). The roles exist and evolve during various phases of discovery or connections. Connections are defined in the two modes i.e. connection based or unicast (P2P) and connectionless (BLE beacon). Note that in this work, BLE beacon is used for validating *WISE*, based on connectionless mode (broadcaster-observer AB-AS) pair role.

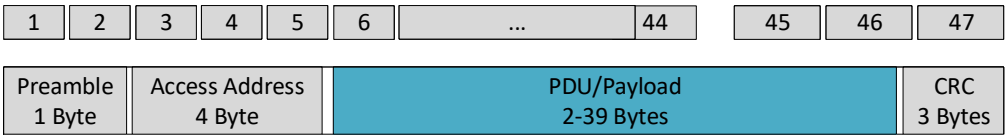

FIGURE A.4: *BLE Packet structure in BLE Beacon Network implementation.*

At *BLEMac* layer, AB beacon packets are created and broadcasted through advertising channels by *GenerateNonConnectableBeacon()* method. BLE beacons follow the one-way communication i.e. they are either sent in one-to-many (1-to-m) or many-to-many (m-to-m) scheme. The formatting of the transmitted data from a AB BLE device follows the pre-defined BLE specifications and the composition of this packet is shown in Figure A.4. in case of connection mode of BLE, the synchronization and timing estimation at the receiver is done by defining the preamble, which is a 1

byte value. It will always be *0xAA* for AB generated broadcast beacons. Unlike, the connection based BLE communication, in *AB-AS* beacon mode there is a chance of collision, where a AS (receiver) could listen for a BLE beacons from multiple AB nodes. On advertising channels, this is not a problem as communication is expected to be unreliable. Hence, in NS3 the access address for AB node is set to a fixed address i.e. *0x8E89BED6*.

TABLE A.1: *Advertising Channel PDU Types*

Packet Name	PDU Type	**Type of Advertising Supported**
ADV_IND	0000	Connectable Undirected Advertising
ADV_NONCONN_IND	0010	Non-Connectable Undirected Advertising
ADV_SCAN_IND	0110	Scannable Undirected Advertising

In the simulator, header and the payload completes the BLE packet for transmission. The packet type is defined by the header, while the payload is include in the PDU. As shown in Table A.1, *ADV_SCAN_IND* and *ADV_IND* packets are used for connection based data, whereas in the connectionless BLE beacons, *ADV_NONCONN_IND* advertising PDU data is used. In the simulator the initialization file defines BLE communication constant parameters (e.g. advertisement channels, *ADV_PDU* types, advertising and scanning intervals). This has been implemented correctly as in shown in Figure A.4 and A.5. In *BLEMac*, *GenerateNonConnectableBeacon* method creates BLE beacon message for each connection state. Figure A.5 shows the logic that has been implemented for setting an unconnectable undirected BLE advertising event (*ADV_NONCONN_IND*).

```
147 /**
148  * Generate non-connectable beacon message.
149  */
150 uint8_t *BLEMac::GenerateNonConnectableBeacon()
151 {
152     BLEPacket *connectablePacket = new BLEPacket;
153     connectablePacket->premable = 0x01;
154     connectablePacket->address = 0x8E89BED6;
155     connectablePacket->payload_header = ADV_NONCONN_IND;
156     memset (connectablePacket->payload, 0, 37);
157     strcpy (connectablePacket->payload, strdup ("payload"));
158     memset (connectablePacket->CRC, 0, 3);
159     strcpy (connectablePacket->CRC, strdup ("CRC"));
160     return (uint8_t*)connectablePacket;
161 }
162
```

FIGURE A.5: *BLE beacon structure implementation to simulate the BLE data*

A.2.4 Periodic Beacon Sender

The BLE Beacon application layer, *BLEHostApplication* class, is used by AB nodes to send beacon to AS nodes (Figure. A.2). It includes various methods such as

SendDataToCluster to send beacon data to AS device. Beacon generator creates the dummy packets having random size. Note that the simulation results will not be enhanced by using the 'realistic' payload contents, as the payload contents are not used in the link layer model. The application transmission period *m_interval* (T^{+}_{BC}) is set up as an attribute of this class and time of *'random packet transmission'* event, scheduled after a sender is defined in this class. It should be noted that, beacon sending is defined at the NS3 application level as a simple packet forwarding from application layer to the *BLEMac* layer. During the transmission of one data, the application also schedules the sending of another beacon, therefore, consecutive data will be sent by the application unless a specific function is called to stop scheduling. Thus β_{Bd} is the random delay before the transmission of first packet and is set by the application, when it is started on a AB node.

A.3 AS Beacon Processing Application

ASScannerApplication class is utilized by AS nodes to perform processing of the received data from AB nodes. It include methods to receive and relay data to LG. For instance, *SendForwardPacket()* sends a packet using the LoraNetDevice's *Send* method. *SetSendTime* sets the time at which this application will send a packet. *AcceptPacketFromBluetooth*($Ptr < Packet > packet$) received beacons from AB nodes. $Ptr < LoraMac > m\_mac$ is a link pointer to BLEMac layer of AS node. The AS application sends LoRa packet every *m_interval* equal to T^{+}_{sc}. The AS data forwarding scheme is set to uniform processes with mean $m\_interval = T^{+}_{sc}$. At the application level, the packet forwarding from the AS BLEMac to the LoRaMac is performed at LoRa end-device (Figure. 5.3). Moreover, the AS nodes will deffer from accessing the LoRa channel for a period of at least $T_{offsubBand} = 99 \times ToA$ seconds due to the restriction of 1% duty-cycle on LoRa transmission. Hence, the AS node stops scanning for BLE beacons while relaying LoRa packet, after sending LoRa packets, AS switches back to listening mode for AB beacons using the BLEPhy interface.

A.4 LoRaWAN Module

The LoRaWAN module is based on the existing LoRa/LoRaWAN NS3 implementation, for more details please refer to the work by [179]. Here, we only provide an overview of the NS3 LoRaWAN module adapted to our work.

A.4.1 LoRa PHY and Channel models

It includes *LoRaPhy* class, *LoRaChannel*, *LoRaPropagationLossModel* classes. The propagation loss model proposed for the LoRa bearer is made up of hata-cost path loss and shadowing, which are implemented respectively using the classes *LoRaChannel*, *LoRaPropagationLossModel* class[145].

A.4.2 LoRa Network Devices

The LoRa device, modeled by the *LoRaNetDevice* class, implements the abstract NetDevice class provided by the NS3. It also includes *LoRaMac*, *GatewayLoRaMac*,*Forwarder* classes. The MAC layer of a LoRa end device is modeled by the LoRaMAC class. This class contains LogicalLoraChannelHelper object which is responsible for the tracking of the available network channels. It is also responsible for the implementation of the duty-cycle limitations i.e. to not forward the message to the PHY layer, coming from the upper layers, by queuing them for the transmission after the end of duty cycle restriction. More specifically, the LoRa end device and LoRa gateway behaviors are implemented by the two subclasses EndDeviceLoraMac and GatewayLoraMac respectively. EndDeviceLoraMac defines the LoRa end device class and replicate the physical layer behavior of LoRa end device. Currently, only Class A devices are supported by the LoRa module. As compared to the EndDeviceLoRaMac, only a simple, forward-only MAC layer is implemented in the GatewayLoraMac class. The interpretation of multiple MAC layer commands are also the responsibility of these classes. Basic packet class was extended to support the LoRa packets with their specific structure.

A.5 BLE Module Validation

We performed multiple small scale simulation runs to validate the NS3 BLE module, and results are then compared with real-world prototype findings. BLE beacon data reception depends on the environmental factors and packet collisions. Therefore, we formulated an experiment to analyze the number of received beacons by varying the beacon transmission interval and number of beacon sending devices.

A.5.1 Small scale validation setup

TABLE A.2: *Validation input parameters for BLE module*

Mobility	M: Static
Freq.	2.4GHz (BLE)
Data Rate (DR)	BLE (1Mbps)
P_t	4dBm
AB Node Density (N)	N: 15
AS size (N_{AS})	N:1
Simulation Area (S_A)	S: 10mx10m
Packet (PL)	31 bytes (Max for ADV)
T^+_{BC}	[100∼600]ms in 100ms steps
T^+_{sc}	700ms, 800ms, 1000ms
T^+_{sW}	600ms, 700ms
Simulation duration (hr)	15

We simulated one AS node and 15 AB nodes, fixed in a randomly defined grid area of 10mx10m in both simulation and real-world experiment (Fig. A.6). The summarized simulation parameters are shown in the Table A.2. BLE beacon payloads of 31 bytes are generated by the AB nodes for data communication at various T^+_{BC}, T^+_{sc}, and T^+_{sW} settings. The time taken to generate a packet along with the time when AS node receives these packets are recorded in the both simulation and real-world tests.

We set the measurement to run for 15 hours. Since animals do not move continuously, rather intermittently for fixed duration, AB nodes are set to send beacons in a uniform beacon transmission distribution with mean T^+_{BC} to simulate stationary mode (SM) and beacon-on-motion (BOM) modes of beacon operation. Moreover, $T^+_{BC} = 100$ms is minimum advertising interval allowed in BLE, thus the broadcasted event duration or time-on-air at data rate of 1Mb is $ToA \approx 0.352ms$ for each adv channel [5, 21].

We deployed a prototype, as shown in Figure A.6b, based on Ruuvi BLE tags built on nRF52832 Nordic system-on-Chip. The Real-world experiment consist of 15 Ruuvi BLE tags that are situated in range of each other. We used (3v,1000mAh) CR2477 lithium battery to power up beacons prototype. For the transmission of link layer packet with 31-byte payload, the current consumed by the real BLE transceiver hardware is compared with the simulated device. We followed the data-sheet of nRF52832 Ruuvi BLE transceiver for this purpose and the values of peak current consumption of these nodes is set for multiple states, i.e. transmit (13mA), receive (13mA) and sleep (10μA).

The Ruuvi tag current consumption during advertising is measured with the DCDC disabled and transmit power set to +4dBm transmission power. We stored the received data on the phone, this log data includes the MAC address, RSSI and the advertising channel number on which the packet is received, i.e. 37, 38 or 39. Ruuvi BLE open firmware and nRF connect app is used to collect the beacon data [196]. All tests are performed under no mobility, thus, it is aimed to discover the accuracy of the simulated protocol when mobility effect is not present, i.e. when it is static, because we want to make a controlled validation for NS3 module.

A.5.2 Validation Discussion

We run several experiments where AB transmits at varying T^+_{BC} and an AS device performs scans with a particular T^+_{sc}, and T^+_{sW}. For each T^+_{BC}, we use the values in steps of 100ms in [100$\sim$600]ms. To make sure that AS and AB timing overlap, we follow the BLE timing guide line, i.e. for T^+_{sc} values of setting 700ms, 800ms, 1000ms and T^+_{sW} values of setting $T^+_{sW} \gg T^+_{BC} + 10$ms [5].

However, this setting is not optimal for power, but it is useful to test the packet collision and delivery of the BLE beacon network. Therefore, we measure the number of beacons received at the AS compared to the number of beacons transmitted from the AB, by computing the delivery ratio, i.e. the ratio of total number of received beacons at AS to total number of transmitted beacons from ABs, for both real-world and simulated tests.

Figure A.7 shows the delivery ratio for different T_{BC}^{+} values. For both real-world and simulated tests, the delivery ratio indicates an increasing trend as network packet generation rate, i.e. T_{BC}^{+}, decreases. However, for higher T_{BC}^{+}, real-world prototype has a relatively lower delivery compared to the simulation at shorter T_{sW}^{+} duration. This is mainly due to the higher environment influence in case of real-world test compared to the simulation. Overall, however, both tests demonstrated a the similar trend. This shows how the developed simulator follows the prototype approach.

Moreover, Figure A.8 depicts the influence of AB devices on the number of received packets, especially, at high rates. For all network settings, the simulation results are in line with the real-world test results. Nevertheless, minor deviations are notable, the received packets values obtained in the simulations are from 5 to 10% higher than the values obtained in the real-world setups. Especially for number of AB node ≥ 10, there is a high difference between the real-world and simulated results. This could be as a result of either due to less extensive real-world tests or to channel environment influences that is not considered affecting the link layer of BLE.

In addition, Figure A.9, shows the current consumption for the simulated and real-world values for AB and AS devices separately. Nordic power profiler kit is used to measure the current on a a ruuvi device [5]. The profiler gives information about the different components in a BLE event as well as the average current over a specified interval. All data is based on actual measurements conducted on the nRF52, and they are correlated with the BLE power profiles found in the SoftDevice specification to set the current levels in the simulator.

Hence, the typical peak current consumed in RX (scanner) mode is found to be 13 mA, and for the broadcasting event TX mode consumes 16mA current. It can be seen from the results that the simulation also shows approximately similar results of current consumption of the simulated device as compared to the hardware current consumption values, however, the current consumption of the micro-controller (CPU) for packet processing and generation is not taken into consideration in the simulated device. In general, from the presented validation results, it can be observed that the BLE module is able to simulating various levels of BLE beacon protocol.

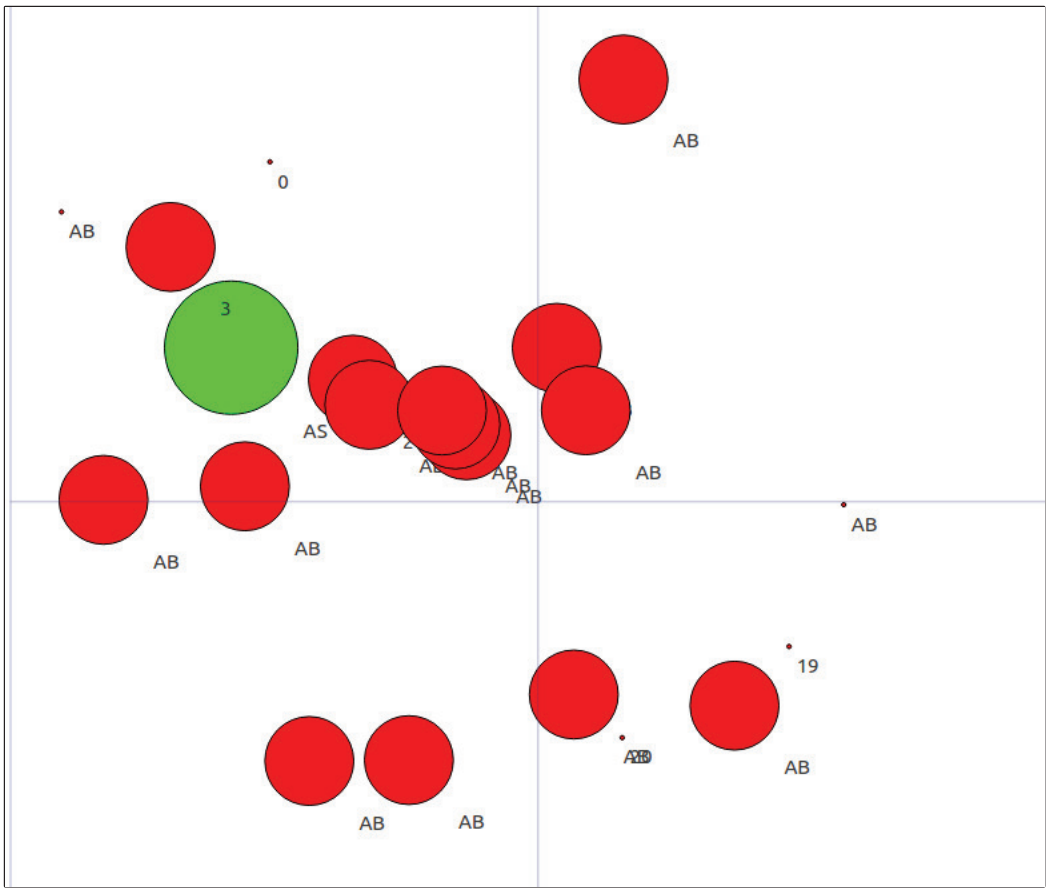

(A)

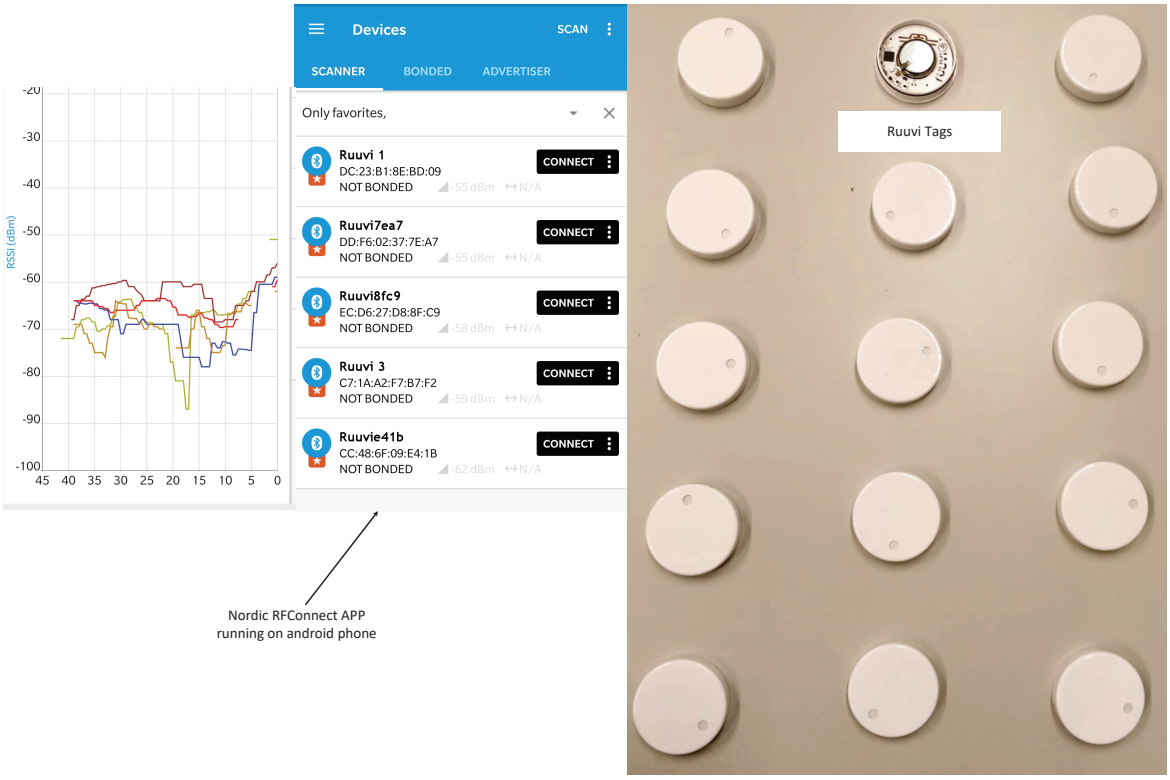

(B)

FIGURE A.6: *Small scale validation test: (a) simulation set-up, (b) AB-AS mode real-world prototyping.*

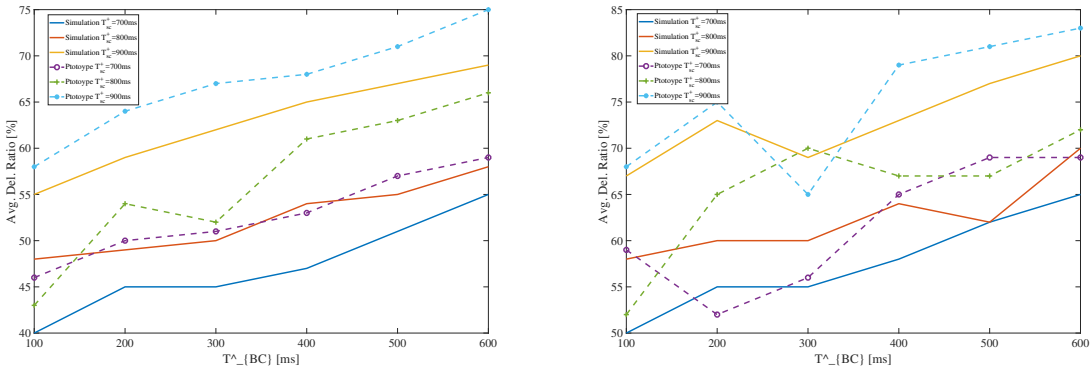

(A) (B)

FIGURE A.7: *Impact of AB T^{+}_{BC} timing parameter on packet delivery ratio, (a) for $T^{+}_{sW} = 600ms$, (b) for $T^{+}_{sW} = 700ms$.*

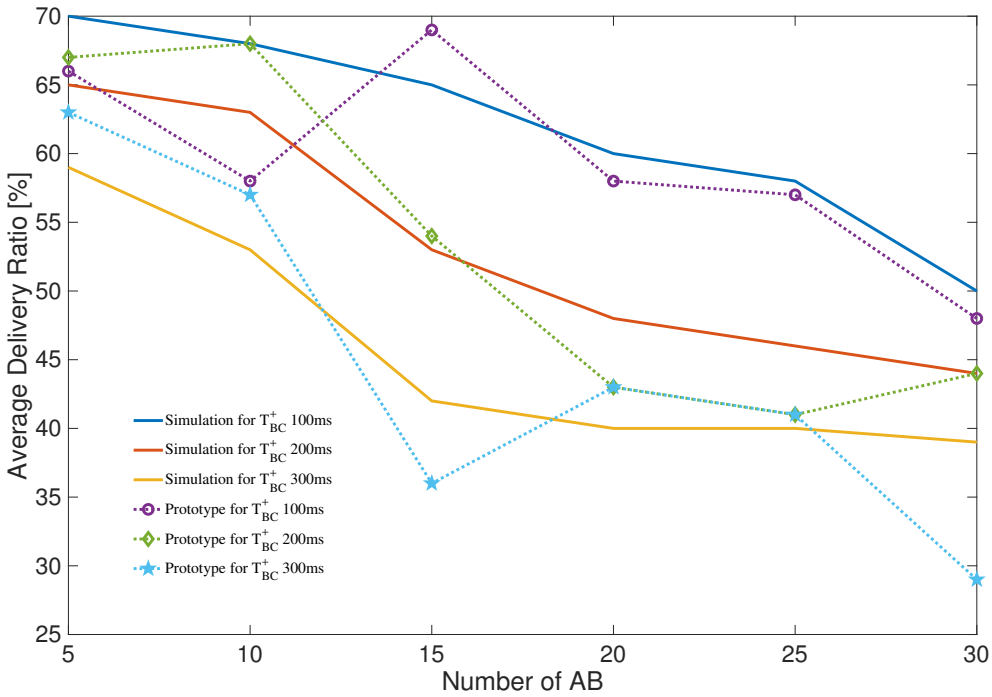

FIGURE A.8: *Impact of number of AB nodes on packet delivery ratio for $T^{+}_{sW} = 600ms$.*

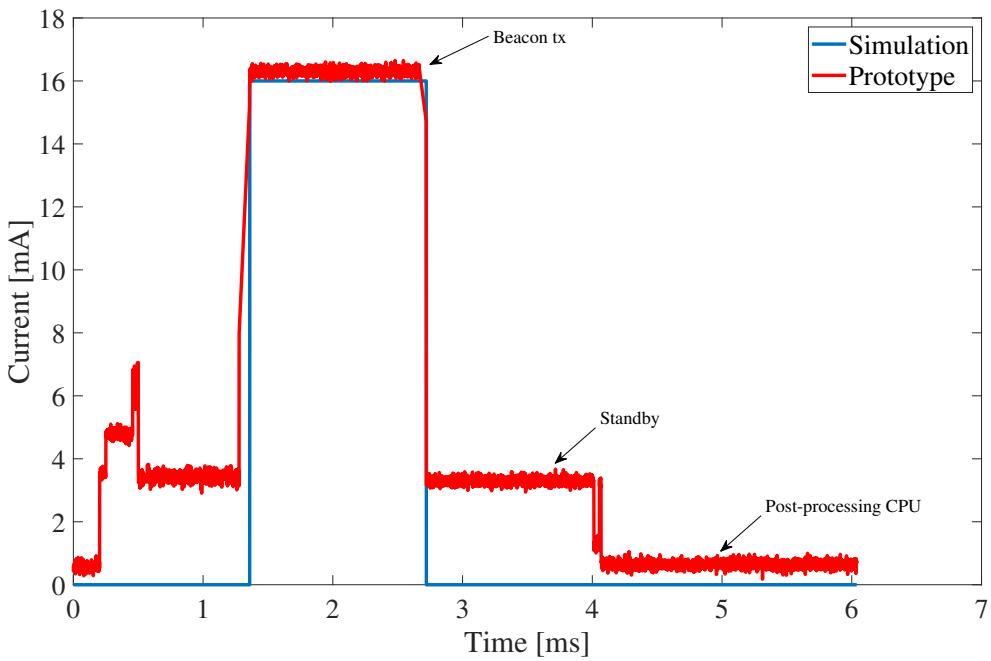

FIGURE A.9: *AB Beacon advertising mode peak current consumption profile for real-world and simulation.*

Appendix B

Algorithms used for animal social network analysis

In this appendix, we outline the main animal social interaction indicators' algorithms adopted from [181], used in our ASSNA analysis and evaluation model.

Betweenness: nodes with a high betweenness are nodes of interest in an ASSNA. However, the definition of "high" is not defined in the literature, so the choice has been made to define nodes as high when the betweenness of a node is 0.85 times the highest betweeness value in the graph *and* it is above average, where the higher the betweeness, the more important a node is [181]. Algorithm 2.5 shows the high betweeness analysis for one time-frame.

Node degree: generally, a node degree is defined to be **high** when the measured degree is 0.85 times the highest degree in the graph [182]. In the same way as in betweenness calculation, the approach is to identify, per time-frame, the nodes with a high degree in the actual and estimated network. Nodes with a high degree are defined when their degree is 0.85 times the highest degree in the graph *and* it is above the average overall degree. This is summarized in algorithm 2.6. For the validation purpose, the number of high degree nodes per time-frame and same score nodes are checked in both actual and estimated graph networks.

Network density: Equation B.1 is used to calculate the density in both graphs per single time-frame, as can be seen in algorithm 2.7. For evaluation, the offset between actual and estimated density value is calculated per time-frame, defined by ($OffsetDensity = ActualDensity - EstimatedDensity$). The maximum density is 1 for a fully connected graph and the minimum density is 0 for an unconnected graph [189]. In ASSNA, graph density is used in the analysis of movement patterns, e.g. the connectivity in a herd of animals [190, 32].

$$D = \frac{2E}{V(V-1)} \tag{B.1}$$

Community detection algorithm uses betweenness to identify the edges that need to be removed because this method has the best performance [197]. Without betweenness recalculation the performance of the algorithm drops drastically [197]. For the detection of the optimal community structure, each entry in the dataset is checked

Algorithm 2.5 High betweenness check (for one time-frame)

```
Result: High betweenness check (for one time-frame)
G = graph actual distances
 GE = graph estimated distances
 BetweennessG = centrality(G,'betweenness',Cost,G.Edges.Weight)
 BetweennessGE = centrality(GE,'betweenness',Cost,GE.Edges.Weight)
 SumBetweennessG = sum(BetweennessG)
 SumBetweennessGE = sum(BetweennessGE)
 MeanBetweennessG = mean(BetweennessG)
 MeanBetweennessGE = mean(BetweennessGE)
 HighBetweennessG = max(BetweennessG)*0.85
 HighBetweennessGE = max(BetweennessGE)*0.85
 NumHighBetweennessNodesG = 0
 NumHighBetweennessNodesGE = 0
 i = 1
 while i smaller than 51 do
    if G.betweenness(i) >MeanBetweennessG & G.betweenness(i) ≥ HighBetweennessG
     then
        NumHighBetweennessNodesG = NumHighBetweennessNodesG + 1
    end
    if GE.betweenness(i) >MeanBetweennessGE & GE.betweenness(i) ≥ HighBetween-
     nessGE then
        NumHighBetweennessNodesGE = NumHighBetweennessNodesGE + 1
    end
    i = i + 1
end
```

for its optimal number of communities (k) based on its number of connected components (stored in vectors Vtemp and VEtemp) as input, as can be seen in algorithm 2.8.

Component detection is similar to the community detection, whereas component in a graph is defined as a group in a network with at least more than one node, with no connections to other groups. It is used to measure the number of components, showing signs of fragmentation in the population. In the evaluation, Algorithm 2.9 checks if the number of components are the same in both graphs. If not, it calculates for the $offset$. For example, if the actual network has *three* components, but the estimated network contains *two* components, the offset would be -1. For the evaluation, it is checked if the amount of components are the same in both graphs. If not, it checks what the offset is. For example, if the actual network has three components, but the estimated network contains two components, the offset is -1.

Isolated nodes algorithm 2.10 checks the number of nodes with a degree of '0' in the actual network and the estimated network. For the evaluation, it checks if the isolated nodes are the same, resulting in a score between '0' and '1'. If there are no

Algorithm 2.6 High degree check (for one timeframe)

```
Result: High degree check (for one time-frame)
G = graph actual distances
 GE = graph estimated distances
 DegreeG = centrality(G,'degree',Importance,G.Edges.Weight)
 DegreeGE = centrality(GE,'degree',Importance,GE.Edges.Weight)
 SumDegreeG = sum(DegreeG)
 SumDegreeGE = sum(DegreeGE)
 MeanDegreeG = mean(DegreeG)
 MeanDegreeGE = mean(DegreeGE
 HighDegreeG = max(DegreeG)*0.85
 HighDegreeGE = max(DegreeGE)*0.85
 NumHighDegreeNodesG = 0
 NumHighDegreeNodesGE = 0
 i = 1
 while i smaller than 51 do
    if G.Degree(i) >MeanDegreeG & G.Degree(i) ≥ HighDegreeG then
       NumHighDegreeNodesG = NumHighDegreeNodesG + 1
    end
    if GE.Degree(i) >MeanDegreeGE & GE.Degree(i) ≥ HighDegreeGE then
       NumHighDegreeNodesGE = NumHigDegreeNodesGE + 1
    end
    i = i + 1
end
```

Algorithm 2.7 Density calculation (for one timeframe)

```
Result: Density calculation (for one timeframe)
G = Actual graph
 GE = Estimated graph
 NumEdgeG = numedges(G)
 NumEdgeGE = numedges(GE)
 NumNodesG = numnodes(G)
 NumNodesGE = numnodes(GE)
 DensityG = (2*NumEdgeG) / (NumNodesG*(NumNodesG - 1))
 DensityGE = (2*NumEdgeGE) / (NumNodesGE*(NumNodesGE - 1))
```

isolated nodes in both graphs, the score is '1', otherwise, their offset is calculated. If there are '0' isolated nodes in the graph based on the actual distances, but at least one in the graph based on the estimated distances, the score would be '0'. For example, if the number of isolated nodes in the actual network is '0' and '1' in the estimated network, then the offset will be '+1'.

Isomorphism: the *isisomorphic* function returns a '1' when the two graphs are isomorph, otherwise '0'. Algorithm 2.11 shows the procedure for checking isomorphic

Algorithm 2.8 Community detection

```
Result: Community detection
G = Actual graph
 GE = Estimated graph
 Q = 0
 Qtemp = 0
 k = 0
 i = 1
 while i smaller than 51 do
    commdetreal = GirvanNewman(G,i)
     commdetEstimated = GirvanNewman(GE,i)
     Vtemp = connectedcomponents(commdetreal)
     VEtemp = connectedcomponents(commdetEstimated)
     Qtemp = NMI(Vtemp,VEtemp)
     if Qtemp bigger than Q then
        Q = Qtemp
    end
    i = i + 1
end
```

Algorithm 2.9 Component detection (for one timeframe)

```
Result: Component detection (for one time-frame)
G = graph real locations
 GE = graph estimated locations
 ConnCompG = conncomp(G)
 ConnCompGE = conncomp(GE)
 NumIsolatedNodesG = 0
 NumIsolatedNodesGE = 0
 i = 1
 while i smaller than 51 do
    if G.degree(i) == 0 then
        NumIsolatedNodesG = NumIsolatedNodesG + 1
    end
    if GE.degree(i) == 0 then
        NumIsolatedNodesGE = NumIsolatedNodesGE + 1
    end
    i = i + 1
end
NumSubgroupsG = (ConnCompG - NumIsolatedNodesG) NumSubgroupsGE =
 (ConnCompGE - NumIsolatedNodesGE)
```

for one timeframe.

Algorithm 2.10 Isolated node calculation per time-frame

```
Result: Isolated node calculation (for one time-frame)
G = Actual graph
 GE = Estimated graph
 NumIsolatedNodesG = 0
 NumIsolatedNodesGE = 0
 N = total nodes in garph

i = 1
 while i smaller than N do
    if G.degree(i) == 0 then
        NumIsolatedNodesG = NumIsolatedNodesG + 1
    end
    if GE.degree(i) == 0 then
        NumIsolatedNodesGE = NumIsolatedNodesGE + 1
    end
    i = i + 1
end
```

Algorithm 2.11 Isomorphism computation

```
Result: Isomorphism check (for one time-frame)
G = Actual graph
 GE = Estimated graph
 N = total nodes in garph

i = 1
 while i smaller than N do
    IsomorphismCheck = isisomorphic(G,GE)
     i = i + 1
end
```

Bibliography

[1] *Poaching: The Statistics*. [online] https://www.savetherhino.org/rhino_info/poaching_statistics. 2015. URL: https://www.savetherhino.org/rhino_info/poaching_statistics.

[2] Yasar Guneri Sahin. "Animals as Mobile Biological Sensors for Forest Fire Detection". In: *Sensors* 7 (2007), pp. 3084–3099. ISSN: 1424-8220. DOI: 10.3390/s7123084.

[3] Jin He et al. "Demo Abstract : Mote-Scale Human-Animal Classification via Micropower Radar". In: *SenSys*. 2014, pp. 328–329. ISBN: 9781450331432.

[4] Steve Piper. *New Invention Could Drive Poaching Towards Extinction*. http://www.hsi.org/world/united_kingdom/news/releases/2015/07/protect-rapid-072015.html Accessed: 15-10-2015. 2015.

[5] Shahid Raza et al. "Building the Internet of Things with bluetooth smart". In: *Ad Hoc Networks* 57 (2017). Special Issue on Internet of Things and Smart Cities security, privacy and new technologies, pp. 19 –31. ISSN: 1570-8705. DOI: https://doi.org/10.1016/j.adhoc.2016.08.012. URL: http://www.sciencedirect.com/science/article/pii/S1570870516302050.

[6] *BLE Core Specifications*. [online] https://www.bluetooth.com/specifications/bluetooth-core-specification. 2018.

[7] Asian Rhino et al. "African and Asian Rhinoceroses – Status , Conservation and Trade". In: *Africa* 230.December 2007 (2009), pp. 1–18.

[8] R. H. Emslie. "African Rhinoceroses – Latest trends in rhino numbers and poaching". In: *African indaba, e-newsletter* 51 (2013), pp. 11–12. URL: http://www.rhinoresourcecenter.com/index.php?s=1{\&}act=refs{\&}CODE=ref{_}detail{\&}id=1368137474.

[9] Michael J. Chase et al. "Continent-wide survey reveals massive decline in African savannah elephants". In: *PeerJ* 4 (Aug. 2016), e2354. ISSN: 2167-8359. DOI: 10.7717/peerj.2354. URL: https://doi.org/10.7717/peerj.2354.

[10] WWF-Dalberg. "Fighting Illicit Wildlife Trfficking". In: (2012), p. 32. DOI: 10.1057/978-1-349-95085-0_5.

[11] WildAid. *WildAid*. online:http://wildaid.org/ Accessed: 14-6-2017. 2017.

[12] Jacob W. Kamminga et al. "Robust Sensor-Orientation-Independent Feature Selection for Animal Activity Recognition on Collar Tags". In: *UBiCOm* 2.1 (Mar. 2018), 15:1–15:27. ISSN: 2474-9567. DOI: 10.1145/3191747.

[13] Paul O'Donoghue and Christian Rutz. "Real-time anti-poaching tags could help prevent imminent species extinctions". In: *Journal of Applied Ecology* 53.1 (2016), pp. 5–10. DOI: 10.1111/1365-2664.12452.

[14] E. D. Ayele, N. Meratnia, and P. J. M. Havinga. "HAMA: A Herd-Movement Adaptive MAC Protocol for Wireless Sensor Networks". In: *NTMS*. 2016, pp. 1–7. DOI: 10.1109/NTMS.2016.7792456.

[15] W.E. Cooper and D.T. Blumstein. *Escaping From Predators: An Integrative View of Escape Decisions*. Cambridge University Press, 2015. DOI: 10.1017/CBO9781107447189.

[16] Julie K Petersen. *Understanding Technologies Surveillance Spy Devices, Their Origins & Applications*. CRC Press, 2002. ISBN: 0849322987.

[17] J. Polastre et al. "Analysis of wireless sensor networks for habitat monitoring". In: *Wireless Sensor Networks*. Springer, 2004, pp. 399–423. DOI: 10.1007/978-1-4020-7884-2_18.

[18] C. Jones et al. "Potential applications of wireless sensor networks for wildlife trapping and monitoring programs". In: *Wildlife Society Bulletin* 39.2 (2015), pp. 341–348. DOI: 10.1002/wsb.543.

[19] Anupriya K et al. "Integrating ZigBee and Sub GHz devices". In: *2016 ICGET*, pp. 1–5. DOI: 10.1109/GET.2016.7916826.

[20] "LoRa Alliance". In: (2015). [online] https://www.lora-alliance.org/What-Is-LoRa/Technology. URL: https://www.lora-alliance.org/What-Is-LoRa/Technology.

[21] E. D. Ayele et al. "Leveraging BLE and LoRa in IoT network for wildlife monitoring system (WMS)". In: *2018 IEEE 4th World Forum on Internet of Things (WF-IoT)*. 2018, pp. 342–348. DOI: 10.1109/WF-IoT.2018.8355223.

[22] E. D. Ayele, N. Meratnia, and P. J. M. Havinga. "An Asynchronous Dual Radio Opportunistic Beacon Network Protocol for Wildlife Monitoring System". In: *2019 10th IFIP International Conference on New Technologies, Mobility and Security (NTMS)*. 2019, pp. 1–7. DOI: 10.1109/NTMS.2019.8763854.

[23] E. D. Ayele, N. Meratnia, and P. J. M. Havinga. "HAMA: A Herd-Movement Adaptive MAC Protocol for Wireless Sensor Networks". In: *2016 8th IFIP International Conference on New Technologies, Mobility and Security (NTMS)*. 2016, pp. 1–7. DOI: 10.1109/NTMS.2016.7792456.

[24] E. D. Ayele, N. Meratnia, and P. J. M. Havinga. "Towards a New Opportunistic IoT Network Architecture for Wildlife Monitoring System". In: *2018 9th IFIP International Conference on New Technologies, Mobility and Security (NTMS)*. 2018, pp. 1–5. DOI: 10.1109/NTMS.2018.8328721.

[25] E. D. Ayele, N. Meratnia, and P. J. M. Havinga. "MANER: Managed Data Dissemination Scheme for LoRa IoT Enabled Wildlife Monitoring System (WMS)". In: *2018 9th IFIP International Conference on New Technologies, Mobility and Security (NTMS)*. 2018, pp. 1–7. DOI: 10.1109/NTMS.2018.8328701.

[26] C. Hazekamp. *Inferring animal social interaction using proximity based on BLE and LoRa*. 2018. URL: http://essay.utwente.nl/76529/.

[27] P. Juang et al. "ZebraNet". In: *ACM SIGARCH* 30.5 (2002), pp. 96–107. DOI: 10.1145/635508.605408.

[28] Nils Aschenbruck et al. "BonnMotion: a mobility scenario generation and analysis tool". In: *Proceedings of the 3rd International ICST Conference on Simulation Tools and Techniques*. ICST (Institute for Computer Sciences, Social-Informatics and Telecommunications Engineering). 2010, p. 51.

[29] Per Johansson et al. "Scenario-based Performance Analysis of Routing Protocols for Mobile Ad-hoc Networks". In: *Proceedings of the 5th Annual ACM/IEEE International Conference on Mobile Computing and Networking*. MobiCom '99. Seattle, Washington, USA: ACM, 1999, pp. 195–206. ISBN: 1-58113-142-9. DOI:

10.1145/313451.313535. URL: http://doi.acm.org/10.1145/313451.313535.

[30] Fan Bai, Narayanan Sadagopan, and Ahmed Helmy. "IMPORTANT: A framework to systematically analyze the Impact of Mobility on Performance of RouTing protocols for Adhoc NeTworks". In: *INFOCOM*. 2003. DOI: 10.1109/INFCOM.2003.1208920.

[31] Jacob Kamminga et al. "Poaching detection technologies—a survey". In: *Sensors* 18.5 (2018), p. 1474. DOI: 10.3390/s18051474.

[32] Davind Jacoby and Robin Freeman. "Emerging Network-Based Tools in Movement Ecology". In: *Trends in Ecology and Evolution* 31.4 (2016), pp. 301 –314. DOI: 10.1016/j.tree.2016.01.011.

[33] Roland Kaysa et al. "Monitoring wild animal communities with arrays of motion sensitive camera traps". In: *arXiv preprint arXiv:1009.5718* (2010).

[34] Daniel J Mennill et al. "Field test of an affordable, portable, wireless microphone array for spatial monitoring of animal ecology and behaviour". In: *Methods in Ecology and Evolution* 3.4 (2012), pp. 704–712. DOI: 10.1111/j.2041-210X.2012.00209.x.

[35] Marieke Lettink and Doug P Armstrong. "An introduction to using mark-recapture analysis for monitoring threatened species". In: *Department of Conservation Technical Series A* 28 (2003), pp. 5–32.

[36] Steven J Cooke. "Biotelemetry and biologging in endangered species research and animal conservation: relevance to regional, national, and IUCN Red List threat assessments". In: *Endangered species research* 4.1-2 (2008), pp. 165–185. DOI: 10.3354/esr00063.

[37] Roland Kays et al. "Terrestrial animal tracking as an eye on life and planet". In: *Science* 348.6240 (2015). ISSN: 0036-8075. DOI: 10.1126/science.aaa2478.

[38] Daniel T Blumstein et al. "Acoustic monitoring in terrestrial environments using microphone arrays: applications, technological considerations and prospectus". In: *Journal of Applied Ecology* 48.3 (2011), pp. 758–767. DOI: 10.1111/j.1365-2664.2011.01993.x.

[39] Kenji Inomata and Takashi Hirai. "Microwave Back-Projection Radar for Wide-area Surveillance System". In: *Radar Conference, 2004. EURAD. First European*. 2004, pp. 89–92.

[40] Christoph Neumann et al. "Ground surveillance with mmw radar for border control and camp protection applications". In: *Proceedings of the 37th European Microwave Conference, EUMC*. Munich, 2007, pp. 700–703. ISBN: 9782874870033. DOI: 10.1109/EUMC.2007.4405288.

[41] Youngsoo Kim et al. "Design of a fence surveillance system based on wireless sensor networks". In: *Autonomic Computing and Communication Systems. Proceedings of the 2nd International Conference on* (2008), pp. 1–7. DOI: 10.4108/ICST.AUTONOMICS2008.4592. URL: http://dl.acm.org.ezproxy.lib.monash.edu.au/citation.cfm?id=1487652.1487656.

[42] Tian He et al. "Energy-efficient surveillance system using wireless sensor networks". In: *Proceedings of the 2nd international conference on Mobile Systems, Applications, and Services (MobiSys)* (2004), pp. 270–283.

[43] Tian He et al. "VigilNet: An integrated sensor network system for energy-efficient surveillance". In: *ACM Trans. Sen. Netw.* 2.1 (2006), pp. 1–38. ISSN: 1550-4859. DOI: 10.1145/1138127.1138128.

[44] a. Arora et al. "A line in the sand: A wireless sensor network for target detection, classification, and tracking". In: *Computer Networks* 46.5 (2004), pp. 605–634. ISSN: 13891286. DOI: 10.1016/j.comnet.2004.06.007.

[45] R Keith Harman and NAM Mackay. "GUIDAR: An intrusion detection system for perimeter protection". In: *Proceedings, 1976 Carnahan Conference on Crime Countermeasures*. 1976.

[46] J Leon Poirier. "Leaky Coaxial Cable Resource Protection Sensor Performance Analysis". In: *Aerospace and Electronic Systems, IEEE Transactions on* AES-18.3 (1982), pp. 275–285. DOI: 10.1109/TAES.1982.313319.

[47] Keith Harman and Bill Hodgins. "Next Generation of Guidar Technology". In: *Security Technology*. IEEE, 2004, pp. 169–176. ISBN: 0-7803-8506-3. DOI: 10.1109/CCST.2004.1405387.

[48] Kenji Inomata, Wataru Tsujita, and Takashi Hirai. "Pattern analysis for human intrusion detection with Leaky Coaxial Cables". In: *2014 IEEE MTT-S International Microwave Symposium (IMS2014)* (2014), pp. 1–4. ISSN: 0149645X. DOI: 10.1109/MWSYM.2014.6848298.

[49] Kenji Inomata et al. "Wide-area Surveillance Sensor with Leaky Coaxial Cables". In: *SICE-ICASE, 2006. International Joint Conference*. IEEE, 2006, pp. 959–963. ISBN: 89-950038-4-7. DOI: 10.1109/SICE.2006.315652.

[50] Yurong Xu et al. "Mobile Anchor-free Localization for Wireless Sensor Networks". In: *Proceedings of the 3rd IEEE International Conference on Distributed Computing in Sensor Systems*. DCOSS'07. Santa Fe, NM, USA: Springer-Verlag, 2007, pp. 96–109. ISBN: 978-3-540-73089-7. DOI: 10.5555/1769087.1769094.

[51] Mark E Cambron et al. "Poacher Detection at Fence Crossing". In: *Southeast-Con 2015*. Fort Lauderdale, FL: IEEE, 2015, pp. 1–2. ISBN: 9781467373005. DOI: 10.1109/SECON.2015.7132898.

[52] Georg Wittenburg et al. "Fence monitoring–experimental evaluation of a use case for wireless sensor networks". In: *EWSN'07 Proceedings of the 4th European conference on Wireless sensor networks* (2007), pp. 163–178. DOI: 10.1007/978-3-540-69830-2_11.

[53] Ali Yousefi et al. "Intelligent fence intrusion detection system: detection of intentional fence breaching and recognition of fence climbing". In: *2008 IEEE Conference on Technologies for Homeland Security* (2008), pp. 620–625. DOI: 10.1109/THS.2008.4635057.

[54] Senstar Stellar. *Intelli-FLEX Microphonic Cable Fence Disturbance Sensor*. Tech. rep. Senstart, 2015.

[55] Mel Maki. "Fiber Optic Fence Sensor Developments". In: *Proceedings - International Carnahan Conference on Security Technology* (2007), pp. 163–168. ISSN: 10716572. DOI: 10.1109/CCST.2007.4373484.

[56] M.C. Maki, I.A. Newcomb, and J.W. Robotham. "Cost effective security system integration". In: *Proceedings IEEE 32nd Annual 1998 International Carnahan Conference on Security Technology (Cat. No.98CH36209)* (1998), pp. 140–146. DOI: 10.1109/CCST.1998.723779.

[57] Southwest Microwave. *MicroPoint Cable A New Fence Sensor Technology*. Tech. rep. Micropoint, 2015, pp. 1–10.

[58] A.J. Backx and R.K. Harman. "Intrepid MicroPoint system - European fence experienc". In: *36th Annual International Carnahan Conference onSecurity Technology*. 2002, pp. 80–86. DOI: 10.1109/CCST.2002.1049230. arXiv: arXiv:1011.1669v3.

[59] Jared D. Tuinstra. *Perimeter Security and Intruder Detection Using Gravity Gradiometry: a Feasability Study*. Thesis. DTIC Document, 2011.

[60] Zhi Sun et al. "BorderSense: Border patrol through advanced wireless sensor networks". In: *Ad Hoc Networks* 9.3 (2011), pp. 468–477. ISSN: 15708705. DOI: 10.1016/j.adhoc.2010.09.008.

[61] Jamali Firmat Banzi. "A Sensor Based Anti-Poaching System in Tanzania". In: *International Journal of Scientific and Research Publications* 4.4 (2014), pp. 1–7.

[62] Mariano R. Recio et al. "Lightweight GPS-Tags, One Giant Leap for Wildlife Tracking? An Assessment Approach". In: *PLoS ONE* 6.12 (2011), e28225. ISSN: 1932-6203. DOI: 10.1371/journal.pone.0028225.

[63] W R Langbauer et al. "African Elephants Respond To Distant Playbacks of Low-Frequency Conspecific Calls". In: *Journal of Experimental Biology* 157 (1991), pp. 35–46.

[64] Matthias Zeppelzauer and Angela S. Stoeger. "Establishing the fundamentals for an elephant early warning and monitoring system". In: *BMC Research Notes* 8.1 (2015), p. 409. ISSN: 1756-0500. DOI: 10.1186/s13104-015-1370-y. URL: http://www.biomedcentral.com/1756-0500/8/409.

[65] Ben Jones et al. "The development of a methodology for the evaluation of Wide Area Detection Systems (WADS)". In: *IEEE International Carnahan Conference on Security Technology (ICCST)*. IEEE, 2011, pp. 1–5. DOI: 10.1109/CCST.2011.6095893.

[66] Philo Juang et al. "Energy-efficient computing for wildlife tracking". In: *ACM SIGOPS Operating Systems Review* 36.5 (2002), p. 96. ISSN: 01635980. DOI: 10.1145/635508.605408.

[67] Olaf Landsiedel et al. "Rat watch: Using sensor networks for animal observation". In: *ACM REALWSN* (2006).

[68] J Schiller, A Liers, and H Ritter. "ScatterWeb: A wireless sensornet platform for research and teaching". In: *Computer Communications* 28.13 (2005), pp. 1545–1551. ISSN: 01403664. DOI: 10.1016/j.comcom.2004.12.044.

[69] Norman Dziengel et al. "Deployment and evaluation of a fully applicable distributed event detection system in Wireless Sensor Networks". In: *Ad Hoc Networks* 000 (2015), pp. 1–23. ISSN: 15708705. DOI: 10.1016/j.adhoc.2015.08.017. URL: http://linkinghub.elsevier.com/retrieve/pii/S1570870515001833.

[70] Chung-Ming Huang, Kun-chan Lan, and Chang-Zhou Tsai. "A survey of opportunistic networks". In: *22nd International Conference on Advanced Information Networking and Applications-Workshops (aina workshops 2008)*. IEEE. 2008, pp. 1672–1677. DOI: 10.1109/WAINA.2008.292.

[71] Peter Rothenpieler et al. "FleGSens - secure area monitoring using wireless sensor networks". In: *Proceedings of the International Conference on Sensor Networks, Information, and Ubiquitous Computing (ICSNIUC 2009), Singapore* 3.8 (2009), pp. 1635–1646. DOI: 10.5281/zenodo.1059497.

[72] Mohammed Aseeri et al. "Peer Trust based Trust and Reputation Model for Wireless Sensor Networks to Protect Border". In: 14.8 (2014), pp. 14–21.

[73] Daeyoung Kim et al. "ANTS : An Evolvable Network of Tiny Sensors". In: *Embedded and Ubiquitous Computing – EUC 2005* (2005), pp. 142 –151. ISSN: 03029743. DOI: 10.1007/11596356.

[74] The samraksh company. *The samraksh company*. https://samraksh.com Accessed: 7-12-2015. 2015.

[75] J De Vries. "A low cost fence impact classification system with Neural Networks". In: *AFRICON*. IEEE, 2004.

[76] A. Mainwaring et al. "Wireless sensor networks for habitat monitoring". In: *Proceedings of the 1st ACM international workshop on Wireless sensor networks and applications*. Acm. 2002, pp. 88–97.

[77] Éfren L. Souza, Richard W. Pazzi, and Eduardo F. Nakamura. "A prediction-based clustering algorithm for tracking targets in quantized areas for wireless sensor networks". In: *Wireless Networks* (2015), pp. 2263–2278. ISSN: 1022-0038. DOI: 10.1007/s11276-015-0914-3. URL: http://link.springer.com/10.1007/s11276-015-0914-3.

[78] Weipeng Zhang and Ting Jiang. "Intrusion Detection and Classification in Forest Area Using Inter-Sensor Communication Signals and SVM". In: *Communication Problem-Solving (ICCP), 2014 IEEE International Conference on*. 2014, pp. 401–404.

[79] Ting Jiang and Minglei You. "New method for target identification in a foliage environment using selected bispectra and chaos particle swarm optimisation-based support vector machine". In: *IET Signal Processing* 8.April 2013 (2014), pp. 76–84. ISSN: 1751-9675. DOI: 10.1049/iet-spr.2012.0389. URL: http://digital-library.theiet.org/content/journals/10.1049/iet-spr.2012.0389.

[80] Ian Jolliffe. *Principal component analysis*. Wiley Online Library, 2002. DOI: 10.1002/9781118445112.stat06472.

[81] Corinna Cortes and Vladimir Vapnik. "Support-vector networks". In: *Machine learning* 20.3 (1995), pp. 273–297.

[82] Thierry Antoine-Santoni et al. "AMBLoRa: a Wireless Tracking and Sensor System Using Long Range Communication to Monitor Animal Behavior". In: July 2018, pre–print.

[83] Carlos Trasviña-Moreno et al. "Unmanned aerial vehicle based wireless sensor network for marine-coastal environment monitoring". In: *Sensors* 17.3 (2017), p. 460. DOI: 10.3390/s17030460.

[84] *IRNAS*. [online] https://www.irnas.eu/animal-conservation-with-lorawan-turtles-fish-and-more/. 2019.

[85] *The Things Network (TTN)*. [online] https://www.thethingsnetwork.org/. 2019.

[86] *Smart Parks Org.* [online] https://www.smartparks.org/. 2019.

[87] *Lacuna.* [online] http://lacuna.space/what-is-lacuna/. 2019.

[88] Shyla A Hatch et al. "Performance of implantable satellite transmitters in diving seabirds". In: *Waterbirds* 23.1 (2000), pp. 84–94.

[89] Rory P Wilson et al. "Remote-sensing systems and seabirds: their use, abuse and potential for measuring marine environmental variables". In: *Marine Ecology Progress Series* 228 (2002), pp. 241–261.

[90] Michael R Miller et al. "Spring migration of Northern Pintails from California's Central Valley wintering area tracked with satellite telemetry: routes, timing, and destinations". In: *Canadian Journal of Zoology* 83.10 (2005), pp. 1314–1332.

[91] Kevin P Kenow et al. "Use of satellite telemetry to identify Common Loon migration routes, staging areas and wintering range". In: *Waterbirds* 25.4 (2002), pp. 449–459.

[92] Steven J Cooke et al. "Biotelemetry: a mechanistic approach to ecology. Trends in Ecology". In: *Evolution*. Citeseer. 2004. DOI: 10.1016/j.tree.2004.04.003.

[93] *GPS Collar*. [online] http://www.awt.co.za/. 2015.

[94] Intel. *Anti-Poaching Technology: Wearables are Helping Save Rhinos*. http://blogs.intel.com/csr/2014/08/rhino/ Accessed: 14-12-2015. 2015.

[95] Yuping Dong et al. "Energy aware routing algorithm for WSN applications in border surveillance". In: *2010 IEEE International Conference on Technologies for Homeland Security, HST 2010* (2010), pp. 530–535. DOI: 10.1109/THS.2010.5654979.

[96] Majid Nabi et al. "MCMAC: An optimized medium access control protocol for mobile clusters in wireless sensor networks". In: *Sensor Mesh and Ad Hoc Communications and Networks (SECON), 2010 7th Annual IEEE Communications Society Conference on*. IEEE. 2010, pp. 1–9. DOI: 10.1109/SECON.2010.5508200.

[97] M. Ali, T. Suleman, and Z. A. Uzmi. "MMAC: a mobility-adaptive, collision-free MAC protocol for wireless sensor networks". In: *PCCC 2005. 24th IEEE International Performance, Computing, and Communications Conference, 2005.* 2005, pp. 401–407. DOI: 10.1109/PCCC.2005.1460597.

[98] Antonio Gonga, Olaf Landsiedel, and Mikael Johansson. "MobiSense: Power-efficient micro-mobility in wireless sensor networks". In: *Distributed Computing in Sensor Systems and Workshops (DCOSS), 2011 International Conference on*. IEEE. 2011, pp. 1–8. DOI: 10.1109/DCOSS.2011.5982172.

[99] Arshad Jhumka and Sandeep Kulkarni. "On the Design of Mobility-tolerant TDMA-based Media Access Control (MAC) Protocol for Mobile Sensor Networks". In: *Proceedings of the 4th International Conference on Distributed Computing and Internet Technology*. ICDCIT'07. Bangalore, India: Springer-Verlag, 2007, pp. 42–53.

[100] Joseph Polastre, Jason Hill, and David Culler. "Versatile Low Power Media Access for Wireless Sensor Networks". In: (). DOI: 10.1145/1031495.1031508.

[101] Eyuel D Ayele et al. "Adaptive Sleep-Time Management Model for WSNs". In: *Computer Communication and Networks (ICCCN), 2015 24th International Conference on*. IEEE. 2015, pp. 1–7. DOI: 10.1109/ICCCN.2015.7288372.

[102] Michael Buettner et al. "X-MAC: A Short Preamble MAC Protocol for Duty-cycled Wireless Sensor Networks". In: *Proceedings of the 4th International Conference on Embedded Networked Sensor Systems*. SenSys '06. Boulder, Colorado, USA: ACM, 2006, pp. 307–320. ISBN: 1-59593-343-3. DOI: 10.1145/1182807.1182838. URL: http://doi.acm.org/10.1145/1182807.1182838.

[103] Prabal Dutta et al. "Design and evaluation of a versatile and efficient receiver-initiated link layer for low-power wireless". In: *Proceedings of the 8th ACM Conference on Embedded Networked Sensor Systems*. ACM. 2010, pp. 1–14.

[104] Jiliang Wang et al. "Sleep in the Dins: Insomnia therapy for duty-cycled sensor networks". In: *INFOCOM, 2014 Proceedings IEEE*. IEEE. 2014, pp. 1186–1194. DOI: 10.1109/INFOCOM.2014.6848050.

[105] Marco Zimmerling et al. "pTunes: runtime parameter adaptation for low-power MAC protocols". In: *Proceedings of the 11th international conference on Information Processing in Sensor Networks*. ACM. 2012, pp. 173–184. DOI: 10.1109/IPSN.2012.6920955.

[106] Geoffrey Werner Challen, Jason Waterman, and Matt Welsh. "IDEA: Integrated distributed energy awareness for wireless sensor networks". In: *Proceedings of the 8th international conference on Mobile systems, applications, and services*. ACM. 2010, pp. 35–48. DOI: 10.1145/1644038.1644112.

[107] Zhenjiang Li, Mo Li, and Yunhao Liu. "Towards energy-fairness in asynchronous duty-cycling sensor networks". In: *ACM Transactions on Sensor Networks (TOSN)* 10.3 (2014), p. 38. DOI: 10.1145/2490256.

[108] Heejung Byun and Jungmin So. "Queue-based adaptive duty cycle control for wireless sensor networks". In: *Algorithms and Architectures for Parallel Processing*. Springer, 2011, pp. 205–214.

[109] A. Gonga, O. Landsiedel, and M. Johansson. "MobiSense: Power-efficient micro-mobility in wireless sensor networks". In: *2011 International Conference on Distributed Computing in Sensor Systems and Workshops (DCOSS)*. 2011, pp. 1–8. DOI: 10.1109/DCOSS.2011.5982172.

[110] Joseph Polastre, Jason Hill, and David Culler. "Versatile low power media access for wireless sensor networks". In: *Proceedings of the 2nd international conference on Embedded networked sensor systems*. ACM. 2004, pp. 95–107. DOI: 10.1145/1031495.1031508.

[111] Prabal Dutta et al. "Design and evaluation of a versatile and efficient receiver-initiated link layer for low-power wireless". In: *Proceedings of the 8th ACM Conference on Embedded Networked Sensor Systems*. ACM. 2010, pp. 1–14.

[112] Huan Pham and Sanjay Jha. "An adaptive mobility-aware MAC protocol for sensor networks (MS-MAC)". In: *Mobile Ad-hoc and Sensor Systems, 2004 IEEE International Conference on*. IEEE. 2004, pp. 558–560.

[113] Qian Dong and Waltenegus Dargie. "A survey on mobility and mobility-aware MAC protocols in wireless sensor networks". In: *Communications surveys & tutorials, IEEE* 15.1 (2013), pp. 88–100.

[114] Gertjan P Halkes, Tijs van Dam, and KG Langendoen. "Comparing energy-saving MAC protocols for wireless sensor networks". In: *Mobile Networks and Applications* 10.5 (2005), pp. 783–791.

[115] Amin Vahdat, David Becker, et al. "Epidemic routing for partially connected ad hoc networks". In: (2000).

[116] Zygmunt J Haas and Tara Small. "A new networking model for biological applications of ad hoc sensor networks". In: *IEEE/ACM Transactions on Networking* 14.1 (2006), pp. 27–40.

[117] Xiaolan Zhang et al. "Performance modeling of epidemic routing". In: *Computer Networks* 51.10 (2007), pp. 2867–2891.

[118] Y. Li et al. "Evaluating the Impact of Social Selfishness on the Epidemic Routing in Delay Tolerant Networks". In: *IEEE Communications Letters* 14.11 (2010), pp. 1026–1028. ISSN: 1089-7798. DOI: 10.1109/LCOMM.2010.093010.100492.

[119] P. Mundur, M. Seligman, and G. Lee. "Epidemic routing with immunity in Delay Tolerant Networks". In: *MILCOM 2008 - 2008 IEEE Military Communications Conference*. 2008, pp. 1–7. DOI: 10.1109/MILCOM.2008.4753334.

[120] T. Matsuda and T. Takine. "(p,q)-Epidemic routing for sparsely populated mobile ad hoc networks". In: *IEEE Journal on Selected Areas in Communications* 26.5 (2008), pp. 783–793. ISSN: 0733-8716. DOI: 10.1109/JSAC.2008.080605.

[121] Thrasyvoulos Spyropoulos, Konstantinos Psounis, and Cauligi S Raghavendra. "Spray and wait: an efficient routing scheme for intermittently connected mobile networks". In: *Proceedings of the 2005 ACM SIGCOMM workshop on Delay-tolerant networking*. ACM. 2005, pp. 252–259.

[122] T. Spyropoulos, K. Psounis, and C. S. Raghavendra. "Efficient Routing in Intermittently Connected Mobile Networks: The Single-Copy Case". In: *IEEE/ACM Transactions on Networking* 16.1 (2008), pp. 63–76. ISSN: 1063-6692. DOI: 10.1109/TNET.2007.897962.

[123] Eyuel D Ayele, Nirvana Meratnia, and Paul JM Havinga. "Towards A New Opportunistic IoT Network Architecture for Wildlife Monitoring System". In: *NTMS*, IEEE. 2018, pp. 1–5.

[124] Thrasyvoulos Spyropoulos, Konstantinos Psounis, and Cauligi S. Raghavendra. "Efficient Routing in Intermittently Connected Mobile Networks: The Multiple-copy Case". In: *IEEE/ACM Trans. Netw.* 16.1 (Feb. 2008), pp. 77–90. ISSN: 1063-6692. DOI: 10.1109/TNET.2007.897964. URL: http://dx.doi.org/10.1109/TNET.2007.897964.

[125] Anders Lindgren, Avri Doria, and Olov Schelén. "Probabilistic routing in intermittently connected networks". In: *ACM International Symposium on Mobilde Ad Hoc Networking and Computing, MobiHoc 2003: 01/06/2003-03/06/2003*. 2003.

[126] T. Huang, C. Lee, and L. Chen. "PRoPHET+: An Adaptive PRoPHET-Based Routing Protocol for Opportunistic Network". In: *2010 24th IEEE International Conference on Advanced Information Networking and Applications*. 2010, pp. 112–119. DOI: 10.1109/AINA.2010.162.

[127] Na Li and Sajal K. Das. "A trust-based framework for data forwarding in opportunistic networks". In: *Ad Hoc Networks* 11.4 (2013), pp. 1497 –1509. ISSN: 1570-8705. DOI: https://doi.org/10.1016/j.adhoc.2011.01.018.

[128] Samo Grasic et al. "The Evolution of a DTN Routing Protocol - PRoPHETv2". In: *Proceedings of the 6th ACM Workshop on Challenged Networks*. CHANTS '11. Las Vegas, Nevada, USA: ACM, 2011, pp. 27–30. ISBN: 978-1-4503-0870-0. DOI: 10.1145/2030652.2030661. URL: http://doi.acm.org/10.1145/2030652.2030661.

[129] S. C. Nelson, M. Bakht, and R. Kravets. "Encounter-Based Routing in DTNs". In: *IEEE INFOCOM 2009*. 2009, pp. 846–854. DOI: 10.1109/INFCOM.2009.5061994.

[130] Sujata Pal and Sudip Misra. "Contact-based Routing in DTNs". In: *Proceedings of the 9th International Conference on Ubiquitous Information Management and Communication*. IMCOM '15. Bali, Indonesia: ACM, 2015, 3:1–3:6. ISBN: 978-1-4503-3377-1. DOI: 10.1145/2701126.2701145. URL: http://doi.acm.org/10.1145/2701126.2701145.

[131] Vijay Erramilli et al. "Delegation Forwarding". In: *Proceedings of the 9th ACM International Symposium on Mobile Ad Hoc Networking and Computing*. MobiHoc '08. Hong Kong, Hong Kong, China: ACM, 2008, pp. 251–260. ISBN: 978-1-60558-073-9. DOI: 10.1145/1374618.1374653. URL: http://doi.acm.org/10.1145/1374618.1374653.

[132] Andreas F Molisch et al. "IEEE 802.15. 4a channel model-final report". In: *IEEE P802* 15.04 (2004), p. 0662.

[133] Shahin Farahani. *ZigBee wireless networks and transceivers*. Newnes, 2011.

[134] M. Centenaro et al. "Long-range communications in unlicensed bands: the rising stars in the IoT and smart city scenarios". In: *IEEE Wireless Communications* 23.5 (2016), pp. 60–67. ISSN: 1536-1284. DOI: 10.1109/MWC.2016.7721743.

[135] N. Sornin et al. "LoRaWAN^{TM} Specifications". In: *LoRa^{TM} Alliance* (2015).

[136] Sakshi Popli, Rakesh Kumar Jha, and Sanjeev Jain. "A Survey on Energy Efficient Narrowband Internet of Things (NBIoT): Architecture, Application and Challenges". In: *IEEE Access* 7 (2019), pp. 16739–16776.

[137] *Weightless*. [online] http://http://www.weightless.org/. 2017.

[138] Konstantin Mikhaylov, Juha Petaejaejaervi, and Tuomo Haenninen. "Analysis of capacity and scalability of the LoRa low power wide area network technology". In: *European Wireless 2016; 22th European Wireless Conference*. VDE. 2016, pp. 1–6.

[139] E. D. Ayele et al. "Performance analysis of LoRa radio for an indoor IoT applications". In: *IoTGC*. 2017, pp. 1–8. DOI: 10.1109/IoTGC.2017.8008973.

[140] Min H. and Xue T. "Wetlands study in China: creating a database using GPS and GIS technology". In: *IEEE Instrumentation Measurement Magazine* 8.4 (2005), pp. 40–43. ISSN: 1094-6969. DOI: 10.1109/MIM.2005.1518621.

[141] ZigBee Alliance. "ZigBee and Wireless Radio Frequency Coexistence, June 2007". In: *White Paper* ().

[142] Q. Wang, M. Hempstead, and W. Yang. "A realistic power consumption model for wireless sensor network devices". In: *Sensor and Ad Hoc Communications and Networks, 2006. SECON'06. 2006 3rd Annual IEEE Communications Society on*. Vol. 1. IEEE. 2006, pp. 286–295. DOI: 10.1109/SAHCN.2006.288433.

[143] Douglas Brent West et al. *Introduction to graph theory*. Vol. 2. Prentice hall Upper Saddle River, NJ, 1996.

[144] S. Ganeriwal, R. Kumar, and Mani B Srivastava. "Timing-sync protocol for sensor networks". In: *Proceedings of the 1st conf. ENSS* (2003). DOI: 10.1145/958491.958508.

[145] Andrea Goldsmith. *Wireless communications*. Cambridge university press, 2005.

[146] K. Zhang et al. "MobiBone: An energy-efficient and adaptive network protocol to support short rendezvous between static and mobile wireless sensor nodes". In: *ICNC 2017*. 2017, pp. 1024–1030. DOI: 10.1109/ICCNC.2017.7876275.

[147] R. Jovani and R. Mavor. "Group size versus individual group size frequency distributions". In: *Animal Behaviour, Elsevier,* 82.5 (2011), pp. 1027 –1036. ISSN: 0003-3472. DOI: http://dx.doi.org/10.1016/j.anbehav.2011.07.037. URL: http://www.sciencedirect.com/science/article/pii/S0003347211003344.

[148] *MultiTech*. [online] http://www.multitech.com/. 2016.

[149] TR ETSI. "TR 102-313 v1. 1.1,"" in: *Electromagnetic compatibility and Radio spectrum Matters (ERM), pp8* ().

[150] *SX1276*. [online] http://www.semtech.com/wireless-rf/rf-transceivers/sx1276/. 2016.

[151] Shih-Lin Wu and Yu-Chee Tseng. *Wireless ad hoc networking: personal-area, local-area, and the sensory-area networks*. CRC Press, 2007.

[152] S. Pathak, N. Gondaliya, and N. Raja. "A survey on PROPHET based routing protocol in DTN". In: *ICEI*. 2017, pp. 110–115. DOI: 10.1109/ETIICT.2017.7977020.

[153] O. Landsiedel et al. "Rat watch: Using sensor networks for animal observation". In: *ACM REALWSN* (2006).

[154] and. "Wetlands study in China: creating a database using GPS and GIS technology". In: *IEEE Instrumentation Measurement Magazine* 8.4 (2005), pp. 40–43. ISSN: 1094-6969. DOI: 10.1109/MIM.2005.1518621.

[155] E. D. Ayele et al. "Leveraging BLE and LoRa in IoT network for wildlife monitoring system (WMS)". In: *WF-IoT*. 2018, pp. 342–348. DOI: 10.1109/WF-IoT.2018.8355223.

[156] *NS3 Network Simulator*. [online] https://www.nsnam.org/. 2019.

[157] Payal J. and Rachna S. "A Survey on Opportunistic Routing Protocols for Wireless Sensor Networks". In: *Procedia Computer Science* 79 (). ICCCV 2016, pp. 603 –609. ISSN: 1877-0509. DOI: http://dx.doi.org/10.1016/j.procs.2016.03.076. URL: http://www.sciencedirect.com/science/article/pii/S1877050916002076.

[158] A. Al-Hinai et al. "TB-SnW". In: *The Journal of Supercomputing* 69.2 (2014), pp. 593–609. ISSN: 1573-0484. DOI: 10.1007/s11227-014-1095-z. URL: https://doi.org/10.1007/s11227-014-1095-z.

[159] SA Hameed et al. "Mobility-aware MAC protocol for delay-sensitive wireless sensor networks". In: *Ultra Modern Telecommunications & Workshops, 2009. ICUMT'09. International Conference on*. IEEE. 2009, pp. 1–8.

[160] Philo Juang et al. "Energy-efficient Computing for Wildlife Tracking with ZebraNet". In: *SIGARCH* 30 (Oct. 2002), pp. 96–107.

[161] Jeremiah F Hayes and Thimma VJ Ganesh Babu. *Modeling and analysis of telecommunications networks*. John Wiley & Sons, 2004.

[162] Hugo V Bitencourt, Adriano B da Cunha, and Diogenes C da Silva. "Simulation domains for networked embedded systems". In: *Student Forum on Microelectronics, SForum*. 2012.

[163] Tracy Camp, Jeff Boleng, and Vanessa Davies. "A survey of mobility models for ad hoc network research". In: *Wireless communications and mobile computing* 2.5 (2002), pp. 483–502.

[164] Omprakash Gnawali et al. "Collection Tree Protocol". In: *Proceedings of the 7th ACM Conference on Embedded Networked Sensor Systems*. SenSys '09. Berkeley, California: ACM, 2009, pp. 1–14. ISBN: 978-1-60558-519-2. DOI: 10.1145/1644038.1644040. URL: http://doi.acm.org/10.1145/1644038.1644040.

[165] Michael Buettner et al. "X-MAC: a short preamble MAC protocol for duty-cycled wireless sensor networks". In: *Proceedings of the 4th international conference on Embedded networked sensor systems*. ACM. 2006, pp. 307–320.

[166] Teuvo Kohonen. *Self-Organization and Associative Memory*. Vol. 8. Springer Series in Information Sciences. Berlin, Heidelberg: Springer Berlin Heidelberg, 1989. ISBN: 978-3-540-51387-2 978-3-642-88163-3.

[167] Teuvo Kohonen˙. "The self-organizing map". In: *Proceedings of the IEEE* 78.9 (1990), pp. 1464–1480.

[168] David Arthur and Sergei Vassilvitskii. "K-means++: The Advantages of Careful Seeding". In: *Proceedings of the Eighteenth Annual ACM-SIAM Symposium on Discrete Algorithms*. SODA '07. New Orleans, Louisiana: Society for Industrial and Applied Mathematics, 2007, pp. 1027–1035. ISBN: 978-0-898716-24-5. URL: http://dl.acm.org/citation.cfm?id=1283383.1283494.

[169] Kui Zhang et al. "MobiBone: An energy-efficient and adaptive network protocol". In: *ICNC*, IEEE. 2017, pp. 1024–1030. DOI: 10.1109/ICCNC.2017.7876275.

[170] T. H. Lim and I. Bate. "An Opportunistic Transmission Protocol for Body Sensor Networks using RSSI and on-board accelerometer". In: *2015 IEEE Tenth International Conference on Intelligent Sensors, Sensor Networks and Information Processing (ISSNIP)*. 2015, pp. 1–6. DOI: 10.1109/ISSNIP.2015.7106936.

[171] A. Perez and R. C. Gonzalez. "An Iterative Thresholding Algorithm for Image Segmentation". In: *IEEE Transactions on Pattern Analysis and Machine Intelligence* PAMI-9.6 (1987), pp. 742–751. DOI: 10.1109/TPAMI.1987.4767981.

[172] T. Caliński and J Harabasz. "A dendrite method for cluster analysis". In: *Communications in Statistics* 3.1 (1974), pp. 1–27. URL: https://www.tandfonline.com/doi/abs/10.1080/03610927408827101.

[173] Barun Kumar Saha et al. "Pre-emptive dynamic source routing: a repaired backup approach and stability based DSR with multiple routes". In: *Journal of computing and information technology* 16.2 (2008), pp. 91–99.

[174] P Siva Kumar and B Muthu Kumar. "Location Tracking and Position Detection for Non-GPS Mobile users". In: *Asian Journal of Research in Social Sciences and Humanities* 6.cs1 (2016), pp. 368–379.

[175] A. Al-Fuqaha et al. "Internet of things: A survey on enabling technologies, protocols, and applications". In: *IEEE Communications Surveys & Tutorials* 17.4 (2015), pp. 2347–2376.

[176] P. Kindt and S. Chakraborty. "Neighbor discovery latency in BLE-like duty-cycled protocols". In: *CoRR* abs/1509.04366 (2015). URL: http://arxiv.org/abs/1509.04366.

[177] B. K. Saha, S. Misra, and S. Pal. "SeeR". In: *TMC* 16.10 (2017), pp. 2876–2888. ISSN: 1536-1233. DOI: 10.1109/TMC.2017.2673842.

[178] A. Keränen, J. Ott, and T. Kärkkäinen. "The ONE Simulator for DTN Protocol Evaluation". In: *IC*. ICST, 2009.

[179] Brecht Reynders, Qing Wang, and Sofie Pollin. "A LoRaWAN Module for Ns-3: Implementation and Evaluation". In: *Proceedings of the 10th Workshop on Ns-3*. WNS3 '18. Surathkal, India: ACM, 2018, pp. 61–68. ISBN: 978-1-4503-6413-3. DOI: 10.1145/3199902.3199913. URL: http://doi.acm.org/10.1145/3199902.3199913.

[180] R. Jovani and R. Mavor. "Group size versus individual group size frequency distributions". In: *Animal Behaviour, Elsevier,* 82.5 (2011), pp. 1027 –1036. ISSN: 0003-3472. DOI: http://dx.doi.org/10.1016/j.anbehav.2011.07.037. URL: http://www.sciencedirect.com/science/article/pii/S0003347211003344.

[181] Lysanne Snijders et al. "Animal Social Network Theory Can Help Wildlife Conservation". In: *Trends in Ecology and Evolution* 32.8 (2017), pp. 567 –577.

[182] Damien R Farine and Hal Whitehead. "Constructing, conducting and interpreting animal social network analysis". In: *Journal of Animal Ecology* 84.5 (2015), pp. 1144–1163. DOI: 10.1111/1365-2656.12418.

[183] *Er zijn 25.000 bedreigde diersoorten, welke verliezen we als eerst? Retrieved May 29, 2018 from [Online]*. 2018. URL: https://nos.nl/op3/artikel/2235445-er-zijn-25-000-bedreigde-diersoorten-welke-verliezen-we-als-eerst.html.

[184] *'Mens veroorzaakt wereldwijde uitstervingsgolf'. Retrieved May 20, 2018 from [Online]*. 2015. URL: https://nos.nl/op3/artikel/2042853-mens-veroorzaakt-wereldwijde-uitstervingsgolf.html.

[185] Christopher C Wilmers et al. "The golden age of bio-logging: how animal-borne sensors are advancing the frontiers of ecology". In: *Ecology* 96.7 (2015), pp. 1741–1753. DOI: 10.1890/14-1401.1.

[186] *Matworks website*. [online] https://nl.mathworks.com/help/stats/mdscale.html. 2019.

[187] Thomas H Cormen. *Introduction to algorithms*. third. MIT press, 2009.

[188] Emily S Minor and Dean L Urban. "A graph-theory framework for evaluating landscape connectivity and conservation planning". In: *Conservation biology* 22.2 (2008), pp. 297–307.

[189] Thomas F Coleman and Jorge J Moré. "Estimation of sparse Jacobian matrices and graph coloring blems". In: *SIAM journal on Numerical Analysis* 20.1 (1983), pp. 187–209.

[190] Kilian M Stehfest et al. "Network analysis of acoustic tracking data reveals the structure and stability of fish aggregations in the ocean". In: *Animal behaviour* 85.4 (2013), pp. 839–848. DOI: 10.1016/j.anbehav.2013.02.003.

[191] K Ruohonen. "Graph theory; 2008". In: *Tampere University of Technology* ().

[192] Aaron F McDaid, Derek Greene, and Neil Hurley. "Normalized mutual information to evaluate overlapping community finding algorithms". In: *arXiv preprint arXiv:1110.2515* (2011).

[193] Leon Danon et al. "Comparing community structure identification". In: *Journal of Statistical Mechanics: Theory and Experiment* 2005.09 (2005), P09008. DOI: 10.1088/1742-5468/2005/09/P09008.

[194] D. Magrin, M. Centenaro, and L. Vangelista. "Performance evaluation of LoRa networks in a smart city scenario". In: *2017 IEEE International Conference on Communications (ICC)*. 2017, pp. 1–7. DOI: 10.1109/ICC.2017.7996384.

[195] G. Shan et al. "Design and implementation of simulator for analysis of BLE broadcast signal collision". In: *2017 International Conference on Information Networking (ICOIN)*. 2017, pp. 448–452. DOI: 10.1109/ICOIN.2017.7899533.

[196] *nRF51822 Bluetooth low energy and 2.4GHz proprietary SoC Active*. [online] https://www.nordicsemi.com/eng/Products/Bluetooth-low-energy/nRF51822. 2017.

[197] Mark EJ Newman and Michelle Girvan. "Finding and evaluating community structure in networks". In: *Physical review E* 69.2 (2004), p. 026113.

[198] *Internet of Wild Animals (IoWA) – Leveraging BLE and LoRa in IoT Network*. [online] https://research.utwente.nl/en/prizes/second-best-poster-award-at-the-ctit-symposium-2017. 2017.

About The Author

Eyuel D. Ayele is a PhD researcher in the Pervasive Systems Research Group at the University of Twente. Prior to beginning the PhD program, Eyuel received his M.Sc. from the Technology University of Delft faculty of Mathematics and Electrical Engineering. Before that, he received a B.Sc. in Electrical Engineering from Hawassa University, Ethiopia. He served as a telecom engineer at the Ethiopian telecom corporation. Before joining the research group he was a research assistant at the Technology University of Dresden, Germany. The topic of his research project is "Smart Parks: Internet of Wild animals by leveraging IoT network technologies". His primary research interests lie in resource management for Internet of Things (IoT) networks, including medium access control and routing, intelligent wireless sensor networks, adaptive algorithm and protocol design.

His list of publications and awards are as follows:

- ***Best paper in the category of WSN and IoT***:
  Fatjon Seraj, E. D. Ayele and N. Meratnia, Unsupervised learning of wildlife behaviour for activity-driven opportunistic beacon networks, in proceedings of the 13th International Conference on Sensing Technology (ICST), 2 December, 2019, Sydney, Australia;.

- ***Second Best Poster Award at the CTIT Symposium 2017*** [198]:
  Ayele, E. D., "Internet of Wild Animals (IoWA) – Leveraging BLE and LoRa in IoT Network".

- Ayele, E. D., and Fatjon Seraj, "Highly Energy Efficient Animal Mobility Driven BLE Beacon Advertising Control for Wildlife Monitoring", Best paper in the category of WSN and IoT, in proceedings of the 13th IEEE SysCon April, 2020*(accepted and presented)*.

- Ayele, E. D. , Havinga, P. J. M. , and Meratnia, N. Asynchronous Dual Radio Opportunistic Beacon Network Protocol for Wildlife Monitoring System. In NTMS'2019 - Mobility Wireless Networks Track.

- Kamminga, J. , Ayele, E. , Meratnia, N. , and Havinga, P. (2018). Poaching Detection Technologies - A Survey. Sensors (Switserland), 18(5).

- Ayele, E. D. , Meratnia, N. , and Havinga, P. J. M. (2018). Towards A New Opportunistic IoT Network Architecture for Wildlife Monitoring System. Paper presented at 2018 9th IFIP International Conference on New Technologies, Mobility and Security (NTMS), Paris, France.

- Ayele, E. D. , Meratnia, N. , and Havinga, P. J. M. (2018). MANER: Managed Data Dissemination Scheme for LoRa IoT Enabled Wildlife Monitoring System (WMS). Paper presented at 2018 9th IFIP International Conference on New Technologies, Mobility and Security (NTMS), Paris. France.
- Ayele, E. D., Hakkenberg, C. , Meijers, J. P., Zhang, K. , Meratnia, N. , and Havinga, P. J. M. (2017). Performance analysis of LoRa radio for an indoor IoT applications. In Internet of Things for the Global Community, IoTGC 2017 - Proceedings [8008973] IEEE.
- Zhang, K. , Ayele, E. D. , Meratnia, N. , Havinga, P. J. M., Guo, P., and Wu, Y. (2017). MobiBone: An energy-efficient and adaptive network protocol to support short rendezvous between static and mobile wireless sensor nodes. In 2017 International Conference on Computing, Networking and Communications, ICNC 2017 (pp. 1024-1030).
- Ayele, E. D. , Das, K. , Meratnia, N. , and Havinga, P. J. M. (2016). Leveraging BLE and LoRa in IoT Network for Wildlife Monitoring System (WMS). In 2016 IEEE 3rd World Forum on Internet of Things (WF-IoT) Piscataway, NJ: IEEE.
- Karuppiah Ramachandran, V. R. , Ayele, E. D. , Meratnia, N. , and Havinga, P. J. M. (2016). Potential of Wake-Up Radio-Based MAC Protocols for Implantable Body Sensor Networks (IBSN)—A Survey. Sensors (Switserland), 16(12), 2012.
- Ayele, E. D. , Meratnia, N. , and Havinga, P. J. M. (2016). HAMA: A Herd-Movement Adaptive MAC Protocol for Wireless Sensor Networks. 1-7. Paper presented at 8th IFIP International Conference on New Technologies, Mobility and Security, NTMS 2016.
- Ayele, E. D., Wen, J., Ansar, Z., and Dargie, W. (2015). Adaptive sleep-time management model for WSNs. In 24th International Conference on Computer Communications and Networks, ICCCN 2015, IEEE.
- Ansar, Z., Wen, J. , Ayele, E. D., and Dargi, W. (2015). An efficient burst transmission scheme for wireless sensor networks. In MSWiM 2015 - Proceedings of the 18th ACM International Conference on Modeling, Analysis and Simulation of Wireless and Mobile Systems (pp. 151-155). Association for Computing Machinery (ACM).

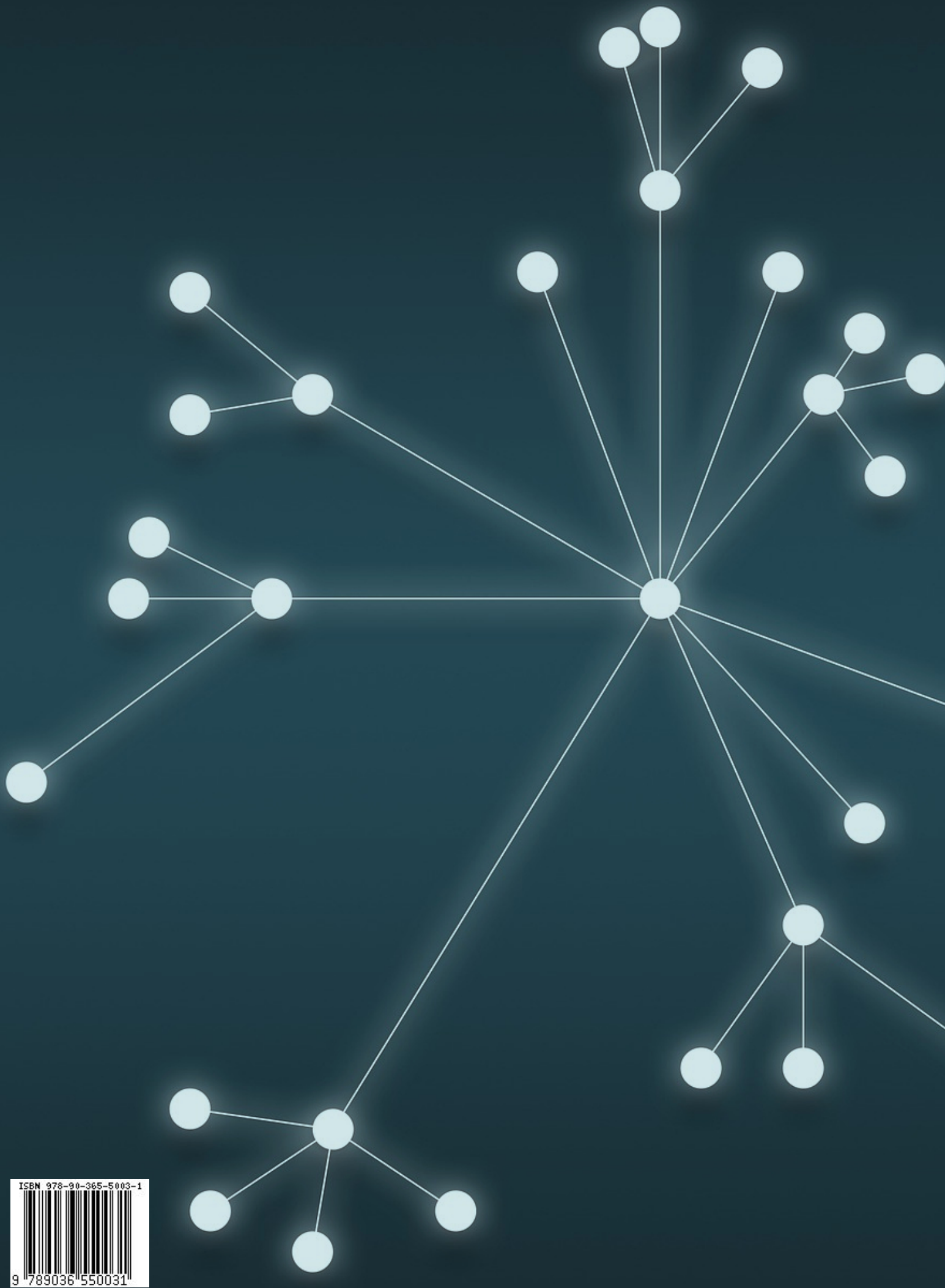

ISBN 978-90-365-5003-1
9 789036 550031